# Structural investigations, cellular imaging and radiolabelling of neutral, polycationic and polyanionic functional metalloporphyrin conjugates

Valeria Ciaffaglione[1#], Philip A. Waghorn[2#], Rüdiger M. Exner[1#], Fernando Cortezon-Tamarit[1#], Samuel P. Godfrey[1], Sophia Sarpaki[1], Helena Quilter[3,4], Ruggero Dondi[3], Haobo Ge[1], Stanley W. Botchway,[5] Gabriele Kociok-Kohn[1,6], Ian Eggleston[3] *, Jonathan R. Dilworth[2] * and Sofia I. Pascu[1,4] *

**Addresses:**
1. Department of Chemistry, University of Bath, Claverton Down, Bath, BA2 7AY, email: s.pascu@bath.ac.uk
2. Chemistry Research Laboratory, University of Oxford, 12 Mansfield Road, Oxford, OX1 3TA, email: jon.dilworth@chem.ox.ac.uk
3. Department of Pharmacy and Pharmacology, University of Bath, Claverton Down, Bath, BA2 7AY, email: ie203@bath.ac.uk
4. Centre for Sustainable and Circular Technologies, University of Bath, Bath BA2 7AY UK
5. Material and Chemical Characterisation (MC2), University of Bath, BA2 7AY
6. Research Complex at Harwell, STFC Rutherford Appleton Laboratory, Harwell Oxford, Didcot, OX11 0QX.

## Table of contents

## 1. General Experimental

All reagents were purchased from Sigma-Aldrich, Merck Chemicals, Fluorous Technologies or Alfa-Aesar and were used as supplied without prior purification unless otherwise stated.

Thin layer chromatography was performed on Merck Kiesegel 60 $F_{254}$ 0.25 mm precoated aluminium plates. Product spots were visualized under UV light ($\lambda_{max}$ = 254 nm) and/or by staining with ceric ammonium molybdate or potassium permanganate. Flash chromatography was performed using silica gel 60 (0.043-0.063 mm, VWR) using head pressure by means of head bellows.

$^{1}$H NMR spectra were recorded on a Varian Mercury VX300 (300 MHz) spectrometer or a Varian Unity (500 MHz) spectrometer or a Bruker AVC 500 (500 Hz) spectrometer at 298 K and referenced to residual non-deuterated solvent peaks. Chemical shifts are quoted in ppm with resonances denoted as singlet (s), doublet (d), triplet (t), quartet (q), quintet (qt) and multiplet (m). Coupling constants, *J*, are measured to the nearest 0.1 Hz and are presented as observed. $^{13}$C NMR spectra were recorded on a Varian Mercury VX300 (300 MHz) spectrometer or a Varian Unity (500 MHz) spectrometer or a Bruker AVC 500 (500 Hz) spectrometer at 298 K and were referenced to the solvent peak [1]. NMR spectra were processed using Mestrelab software [2].

Mass spectrometry was performed using a Bruker Micromass LCT instrument. Mass spectra were recorded by Mr Colin Sparrow at the Chemistry Research Laboratory, University of Oxford, on a Micromass LCT time-of-flight mass spectrometer under conditions of electrospray ionization (ESI-MS). Accurate masses are reported to four decimal places using tetraoctylammonium bromide (466.5352 Da) as an internal reference. Values are reported as a ratio of mass to charge in Daltons.

HPLC characterization (analytical HPLC) of compounds was performed by one of the following methods.

**Method A** was performed using a Waters C-18 column (4.6 x 250 mm) with UV-Vis detection at $\lambda_{obs}$ = 410 nm with a 0.9 mL/min gradient elution method (Solvent A: THF with 0.1 % TFA *v/v*, Solvent B: water with 0.1% TFA *v/v*): start 5 % A, gradient over 12 min reaching 95 % A, hold to 15 min at 95 % A, reverse gradient till 18 min reaching 5 % A, then hold to 20 min at 5 % A.

**Method B** was performed using a Waters C-18 column (4.6 x 250 mm) with UV-Vis detection at $\lambda_{obs}$ = 410 nm with a 1.0 mL/min gradient elution method (Solvent A: acetonitrile, Solvent B: water with 0.1% $NH_4OAc$ *v/v*): start 5 % A, gradient over 12 min reaching 65 % A, hold to 15 min at 65 % A, reverse gradient till 18 min reaching 5 % A, then hold to 20 min at 5 % A.

**Method C** was performed using a Waters C-18 column (4.6 x 250 mm) with UV-Vis detection at $\lambda_{obs}$ = 410 nm with a 1.0 mL/min gradient elution method (Solvent A: acetonitrile with 0.1 % TFA *v/v*, Solvent B: water with 0.1% TFA *v/v*): start 5 % A, gradient over 12 min reaching 65 % A, hold to 15 min at 65 % A, reverse gradient till 18 min reaching 5 % A, then hold to 20 min at 5 % A.

**Method D** was performed using a Waters C-18 column (4.6 x 250 mm) with UV-Vis detection at $\lambda_{obs}$ = 410 nm with a 1.0 mL/min gradient elution method (Solvent A: acetonitrile with 0.1 % TFA *v/v*, Solvent B: water with 0.1% TFA *v/v*):

start 5 % A, gradient over 23 min reaching 95 % A, hold to 25 min at 95 % A, reverse gradient till 27 min reaching 5 % A, then hold to 30 min at 5 % A.

**Method E** was performed on a Hamilton-PRP1 reverse phase column, (4.1 mm x 150 mm, particle size 5 µm, SN 10843) with UV-Vis detection at $\lambda_{obs}$ = 495 nm using a 0.9 mL/min gradient elution method (Solvent A: acetonitrile with 0.1 % TFA *v/v*, Solvent B: water with 0.1% TFA *v/v*): start 5 % A, gradient till 15 min reaching 95 % A, hold to 16 min at 95 % A, reverse gradient till 18 min reaching 5 % A, then hold to 20 min at 5 % A.

**Method F** was performed on a Dionex UltiMate 3000 system, equipped with a Phenomenex Gemini 5 µm C-18 (150 x 4.6 mm) with UV detection at 214, 220, 245 and 280 nm using a 1.0 mL/min gradient elution method (Solvent A: acetonitrile with 0.1 % TFA *v/v*, Solvent B: water with 0.1% TFA *v/v*): start 5 % A, gradient till 10 min reaching 95 % A, hold to 15 min at 95 % A, reverse gradient till 15.1 min reaching 5 % A, then hold to 18 min at 5 % A.

**Preparative HPLC** purification was performed on one of the following systems:

Gilson instrument (C18 column) with UV-Vis detection at $\lambda_{obs}$ = 410 nm at a flow rate of 10 mL/min with the following gradiant (Solvent A: acetonitrile with 0.1 % TFA *v/v*, Solvent B: water with 0.1% TFA *v/v*) or (Solvent A: THF, Solvent B: water with 0.1% $NH_4OAc$ *v/v*) : start 5 % A hold until 2 min, gradient till 30 minutes reaching 95 % A, hold to 50 min at 95 % A, reverse gradient till 60 min to 5 % A, hold to 70 min at 5 % A.

Dionex system with a Phenomenex Gemini 5 µm C-18 (250 x 10 mm) column. with UV detection at 214, 220, 245 and 380 nm using a 2.5 mL/min gradient elution method (Solvent A: acetonitrile with 0.1 % TFA *v/v*, Solvent B: water with 0.1% TFA *v/v*): start 5 % A, gradient till 25 min reaching 95 % A, hold to 35 min at 95 % A, reverse gradient till 35.1 min reaching 5 % A.

Elemental analyses were performed either by the microanalysis service at the Inorganic Chemistry Department, University of Oxford, or by Mr. S. Boyer, at London Metropolitan University.

UV-Vis spectroscopy was carried out using a PerkinElmer Lambda 25 spectrometer running UV WinLab software. Samples of porphyrin precursors and bombesin conjugates were prepared as 2.0 µM solutions in DMSO. Spectra were recording using quartz cuvettes with a path length of 1.0 cm. Absorption was measured between 200-900 nm.

Fluorescence spectra were recorded in 1.00 cm quartz cuvettes using a Hitachi F-4500 fluorescence spectrometer, running FL Solutions software.

Cyclic voltammetry experiments were performed on a CH instruments 600A electrochemical analyser with Chi600 software, using a platinum working electrode, a platinum wire supporting electrode and a Ag|AgNO3 reference electrode. Scans were internally referenced to ferrocene (+0.53 V vs SCE).3,4 Solutions of the respective complexes were prepared to approximately 2.5 mM in degassed DMF containing 0.1 M TBA[$BF_4$] and scans run between +1.6 and -1.8 V (vs SCE) at a scan rate of 100 mV/s unless otherwise stated. All samples were iR compensated and deoxygenated with nitrogen purging for at least 15 minutes prior to each scan.

X-ray crystal structure analyses were performed using the synchrotron radiation source ($\lambda$ = 0.84570 Å) at the CCLRC Daresbury Laboratory, Warrington, UK, or measured using an Enraf-Nonius Kappa CCD diffractometer (monochromated Mo-Kα radiation, $\lambda$ = 0.71073 Å).

Density functional theory (DFT) and time dependent density functional theory (TDDFT) calculations were performed using the Amsterdam Density Functional (ADF) suite [3]. All calculations were performed applying the continuous solvation model COSMO (conductor like screening model) [4]. It was used to model DMSO as the solvent (dielectric constant $\varepsilon = 46.7\ F \cdot m^{-1}$, radius of the rigid-sphere solvent molecules = 3.04 Å). Following the findings by Rydberg et al., the generalized gradient approximation (GGA) functional BP86 was employed [5]. All calculations were performed utilizing the TZ2P basis set, to accurately describe the metal centers [6]. No frozen cores were applied. In the case of indium chloride, scalar relativistic corrections were applied using the ZORA (zero order regular approximation) formalism and MAPA (minimum of neutral atomical potential approximation) [6-8]. Geometries were optimized and analytical frequencies calculated [9-11], before allowed singlet-singlet transitions were modelled at the TD-DFT level of theory using the Davidson algorithm (lowest Eigenvalues) [12-14].

***General Radiolabelling Procedures:***

The ligand or complex was prepared as a 1.0 mg/mL solution in DMSOor distilled water. For $^{11}$In labeling of water soluble porphyrins 10 µL of the stock porphyrin solution was diluted with 90µL of pH 4.5 sodium acetate buffered solutionand heated at 115 °C for 30 min in an Eppendorf tube in the presence of 20 µL 111InCl3(< 10 MBq per experiment). For the $^{111}$Indium labeling of tetraphenyl porphyrin derivatives 10 µL of the stock solution was diluted with 90µL of AcOH and heated at 120 °C for 1 hin the presence 10 µL of a 0.1 M NaOAc (aq.) solution and 20 µL 111InCl3(< 10 MBq per experiment). AcOH was then driven off under nitrogen and the residue resuspended in 50 µL of CHCl3. The CHCl3 layer was washed repeatedly with 100 µL aliquots of distilled water until no further activity was associated with the aqueous washings. For copper-64 radiolabelling10 µL of the stock porphyrin solution was diluted with 40µL of DMSO and 50 µL $^{64}Cu(OAc)_2$ was added (< 10 MBq per experiment) and the reaction stirred for 20 min at room temperature. On reaction completionan aliquot (20 µL) was removed via syringe, and analysed by HPLC (radio and UV detection, in series). In all cases the 20 min HPLC gradient methods A, B and C were used for the porphyrin labeling experiments.

Measurement of LogP: The indium-111complex (15 µL, <1MBq) was added to a mixture of octan-1-ol (0.5 mL) and H2O (0.5 mL). The mixture was shaken for 1 min, then centrifuged for 5 min at 2000 rpm. A 50 µL sample of each layer was taken and counted using a gamma counter. The measurements were performed in triplicate. Log Pwas calculated using the formula:log P= log(counts(octanol)/counts(H2O))

***General $^{68}$Ga Radiochemistry Methodology***

The positron emitting radiotracer [$^{68}$Ga]$GaCl_3$ was extracted from a $^{68}$Ge/$^{68}$Ga generator (Department of Surgery and Cancer of Imperial College in London) using a 0.6 M HCl solution. The eluted gallium-68 was subsequently trapped on a 30 mg/mL Strata X-C cartridge, which was preactivated with 1 mL of HCl solution 0.1 M and washed with 10 mL of water. Then [$^{68}$Ga]$GaCl_3$ was eluted from the cartridge with 0.8 mL of a THF/HCl (0.02 M) solution (98%) or Acetone/HCl (0.02 M) solution (98%) and dried for 15 minutes under a stream of nitrogen at 110 °C.

## 2. Synthesis

Porphyrin-based building blocks **3**, **4** and **6** were synthesized in order to allow a variety of coupling reactions. The synthesis of compound **1**, free base TPP, was accomplished following one of the most frequently used protocols for synthesizing *meso*-substituted porphyrins, the Adler-Longo method [15], via condenzation of pyrrole and benzaldehyde in propanoic acid under reflux. Esters **2** and **5** were also prepared under Adler-Longo conditions with methyl-4-formylbenzoate or 4-pyridinecarboxaldehyde, respectively. Carboxylic acids **3** and **6** and amine **4** (TPP-$NH_2$) were then obtained as templates to prepare more challenging structures (Schemes 1-6). Compounds **3** and **6** were synthesized through the hydrolysis of the corresponding methyl esters **2** and **5**, as described in the literature [16]. The hydrolysis was carried out in aqueous potassium hydroxide solution, followed by acidification with HCl solution to pH 5 and extraction with dichloromethane. For **2**, the product proved very soluble in aqueous solution and hence extraction into chlorinated solvent was unsuccessful. In this case, an $NH_2$ functionalized solid phase extraction (SPE) cartridge was used to extract the product into organic solvent and the desired product was obtained as purple crystals in 70% yield. The synthesis of mono-amino TPP **4** was achieved through a modification of the method of Luguya et al. [17] as reported by Dondi et al. [18]. Briefly, TPP was taken forward to sequential nitration (with sodium nitrite in TFA) and reduction (with sodium borohydride and Pd/C 5% catalyst). After column chromatography, the mono-amine product **4** was isolated in 17 % yield, over two steps. Intermediate **3.2** was synthesized from carboxylic acid **3** by activation with NHS and DCC [19] and used as starting building block for obtaining the functionalized porphyrins **3.3-3.24** (Schemes 1-4).

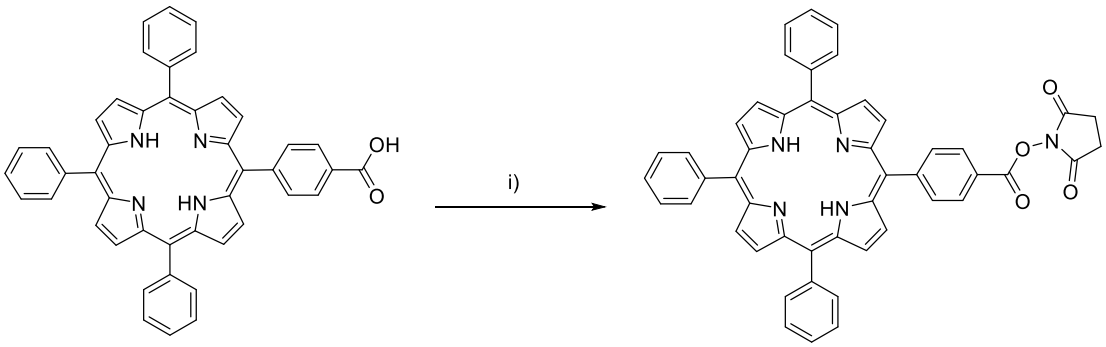


**3** **3.2**

**Scheme S1.** Reagents and conditions: i) NHS, DCC, THF, 12 h [19].

Nitroimidazole derivatives **3.3**, **3.4** were obtained in 71 and 79 % yield, respectively, by coupling the respective amine hydrochlorides **7**, **8** (obtained according to the literature [20, 21]) with activated *N*-hydroxysuccinimide ester **3.2** in DMF and in the presence of DIPEA (Scheme 2). Metal complexation was successfully achieved by heating the porphyrin ligands **3.3** and **3.4** under reflux in presence of $GaCl_3$ or $InCl_3$ and NaOAc in AcOH, with $^{1}H$, $^{13}C$ NMR, ESI-MS and HPLC supporting the formation of complexes **3.5**, **3.6**, **3.8** and **3.9**. For the insertion of copper, $Cu(OAc)_2 \cdot H_2O$ was heated with the porphyrin under reflux in DMF, with ESI-MS and HPLC supporting the production of **3.7** and **3.10** as single species. Sulphonamide analogues **3.16-3.21** were prepared following a similar route to that employed for the nitroimidazole conjugates (Scheme 3).

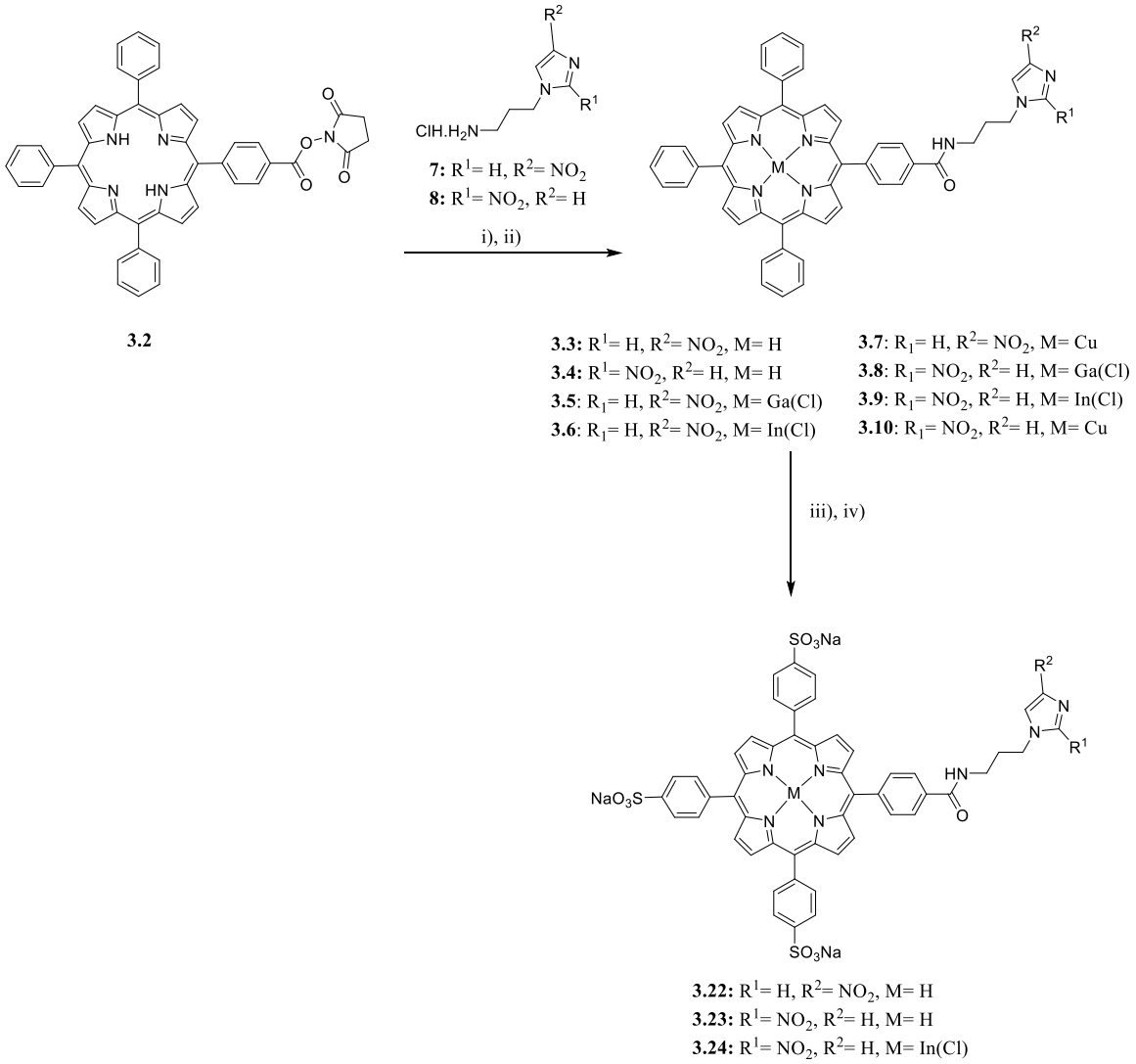


**Scheme S2.** Reagents and conditions: i) **7**/**8**, DIPEA, DMF; ii) $GaCl_3/InCl_3/Cu(OAc)_2H_2O$, NaOAc, AcOH/DMF; iii) conc. $H_2SO_4$; iv) $InCl_3$, pH 4.5 buffer.

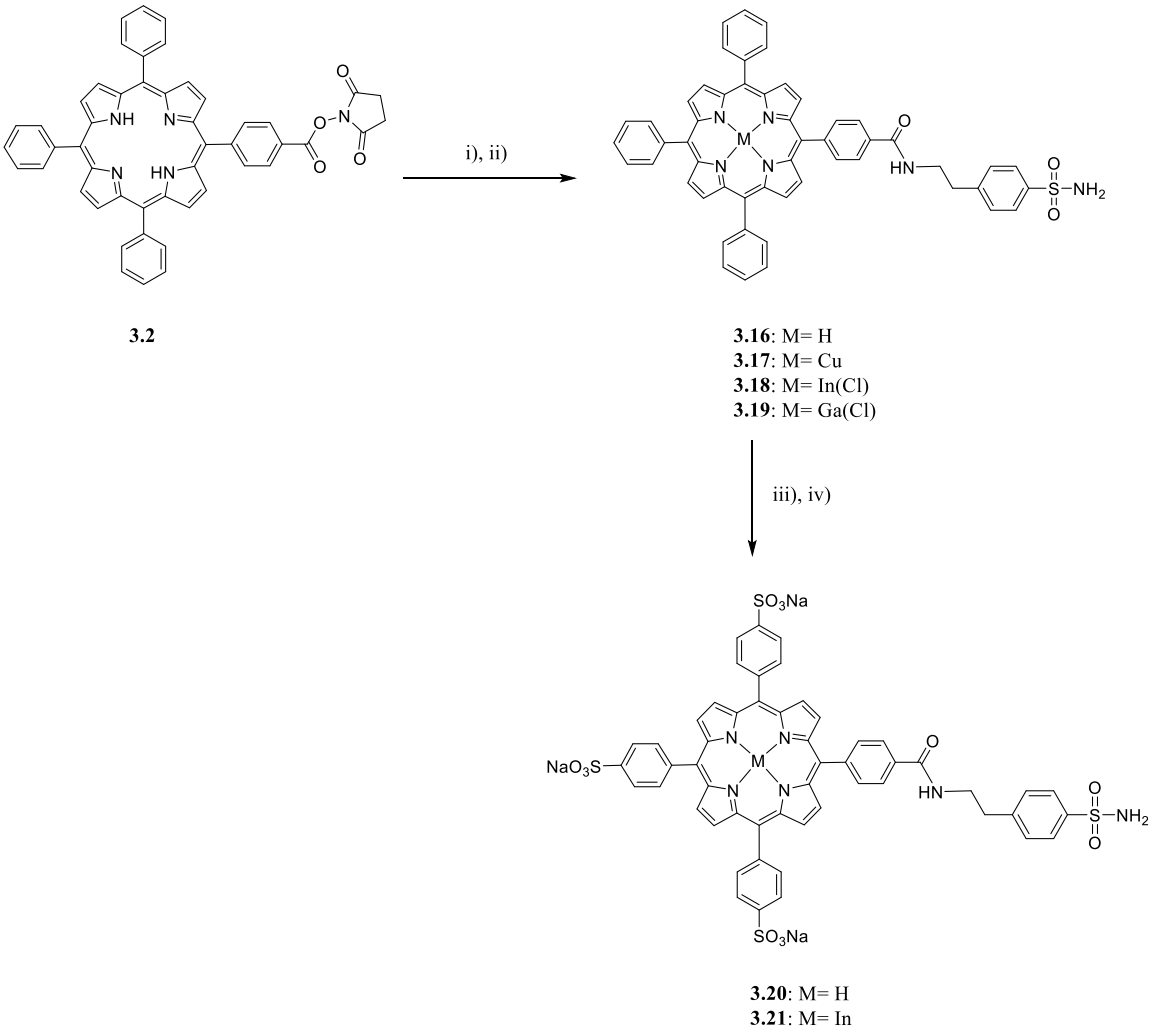


**3.2**

**3.16**: M= H
**3.17**: M= Cu
**3.18**: M= In(Cl)
**3.19**: M= Ga(Cl)

**3.20**: M= H
**3.21**: M= In

**Scheme S3.** Reagents and conditions: i) $NH_2$-$(CH_2)_2$-p-$C_6H_4$-$SO_2NH_2$, DIPEA, DMF; ii) $Cu(OAc)_2$/ $InCl_3$/ $GaCl_3$, NaOAc, AcOH; iii) $H_2SO_4$, 2M NaOH; iv) $InCl_3$, AcOH.

Tri-sulfonated porphyrins without nitroimidazole moiety **3.11-3.15** were synthesized according to Scheme 4. Compound **3.11** was obtained from the activated *N*-hydroxysuccinimide ester **3.2** and propylamine in 89% yield, followed by the reaction with $InCl_3$ in acetic acid to synthesise the indium complex **3.12** and with $Cu(OAc)_2 \cdot H_20$ in MeOH to obtain the copper complex **3.13**. Compound **3.14** was synthesized from **3.11** in conc. $H_2SO_4$ and then metallated with $InCl_3$.

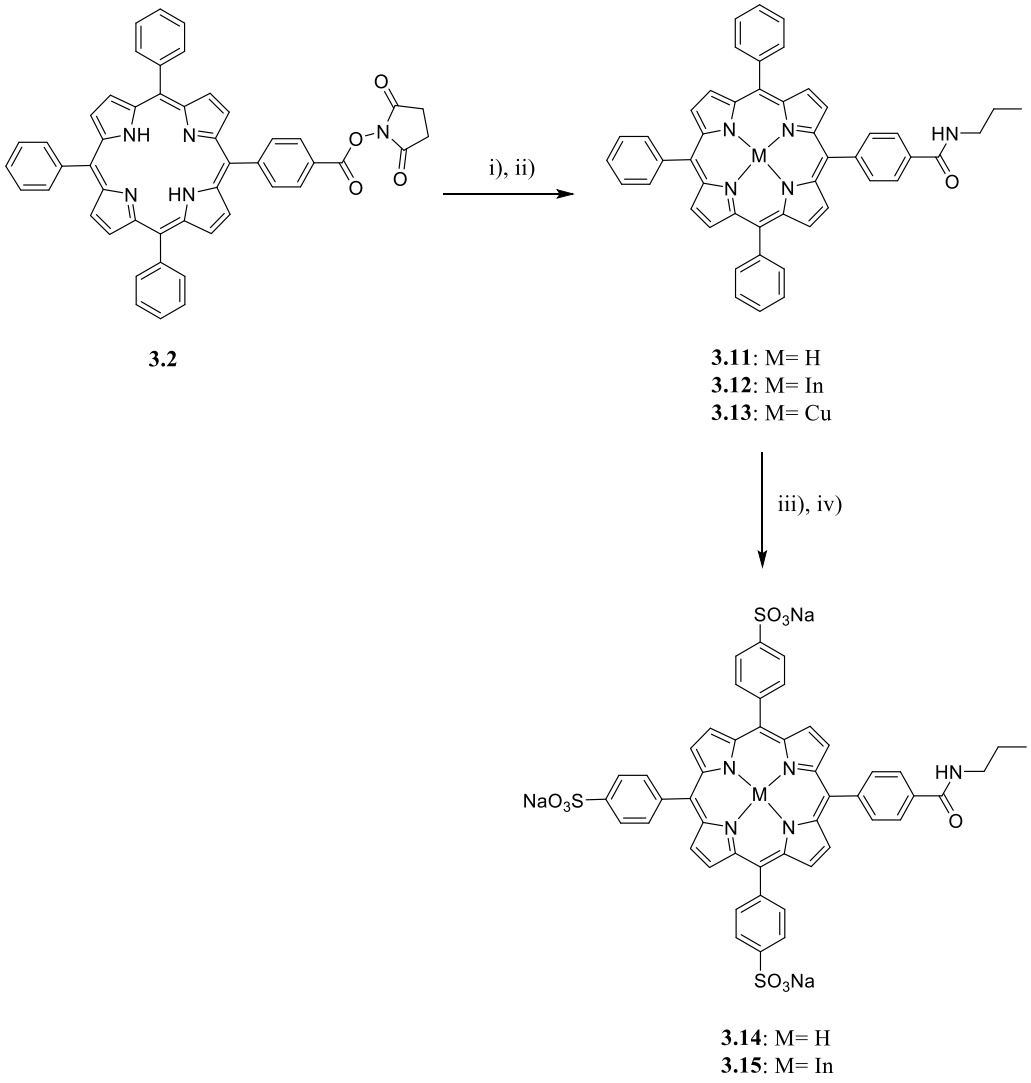


**3.2**

**3.11**: M= H
**3.12**: M= In
**3.13**: M= Cu

**3.14**: M= H
**3.15**: M= In

**Scheme S4.** Reagents and conditions: i) propylamine, DCM; ii) $InCl_3$, AcOH; iii) $H_2SO_4$, 2M NaOH; iv) $InCl_3$, AcOH.

Coupling reactions starting from pyridyl porphyrin **6** were carried out directly using BOP, followed by alkylation of the coupled products with methyl iodide (MeI) and complexation with $InCl_3$ in pH 4.5 NaOAc buffer (Scheme 5).

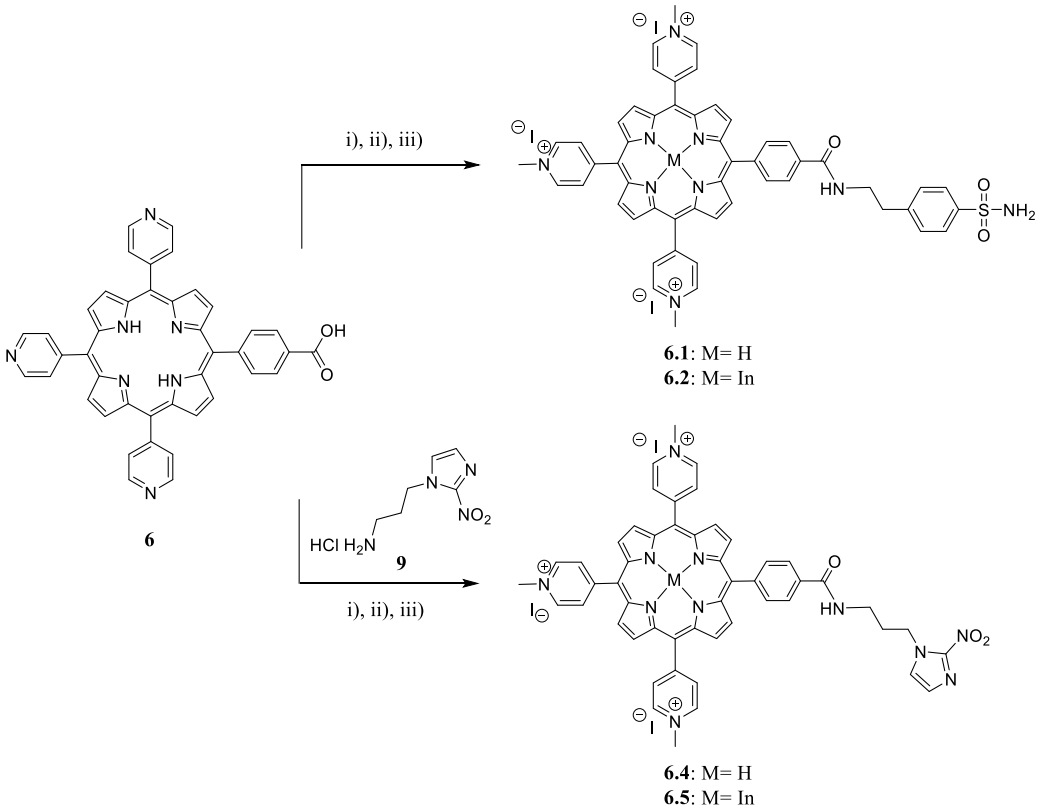


**Scheme S5.** Reagents and conditions: i) $NH_2$-$(CH_2)_2$-p-$C_6H_4$-$SO_2NH_2$/ **9**, DIPEA, BOP, DMF; ii) MeI, DMF; iii) $InCl_3$, NaOAc.

Finally, Scheme 6 describes the coupling of 2- and 4-nitroimidazoles **10**/ **11** to compound **4.** An aliphatic linker was introduced to obtain a new amine group with increased nucleophilicity. Porphyrin **4.3** was obtained through the reaction of the commercially available NHS activated alanine linker in ten-fold excess in DCM with DMAP, followed by TFA deprotection and basic workup and it was used as precursor to the porphyrins **4.4-4.8.** The coupling between porphyrin **4.3** and either 2- or 4-nitroimidazoles **10/ 11** in DMF gave the desired product after stirring at room temperature overnight in yields of 74 and 79 %, respectively. Both products, **4.4** and **4.5**, were purified by silica gel chromatography (5 % MeOH in DCM). The obtained ligands were then labelled with $GaCl_3$ and $Cu(OAc)_2 \cdot H_2O$. The metalation reactions were confirmed by $^1H$ NMR, ESI-MS and HPLC analysis.

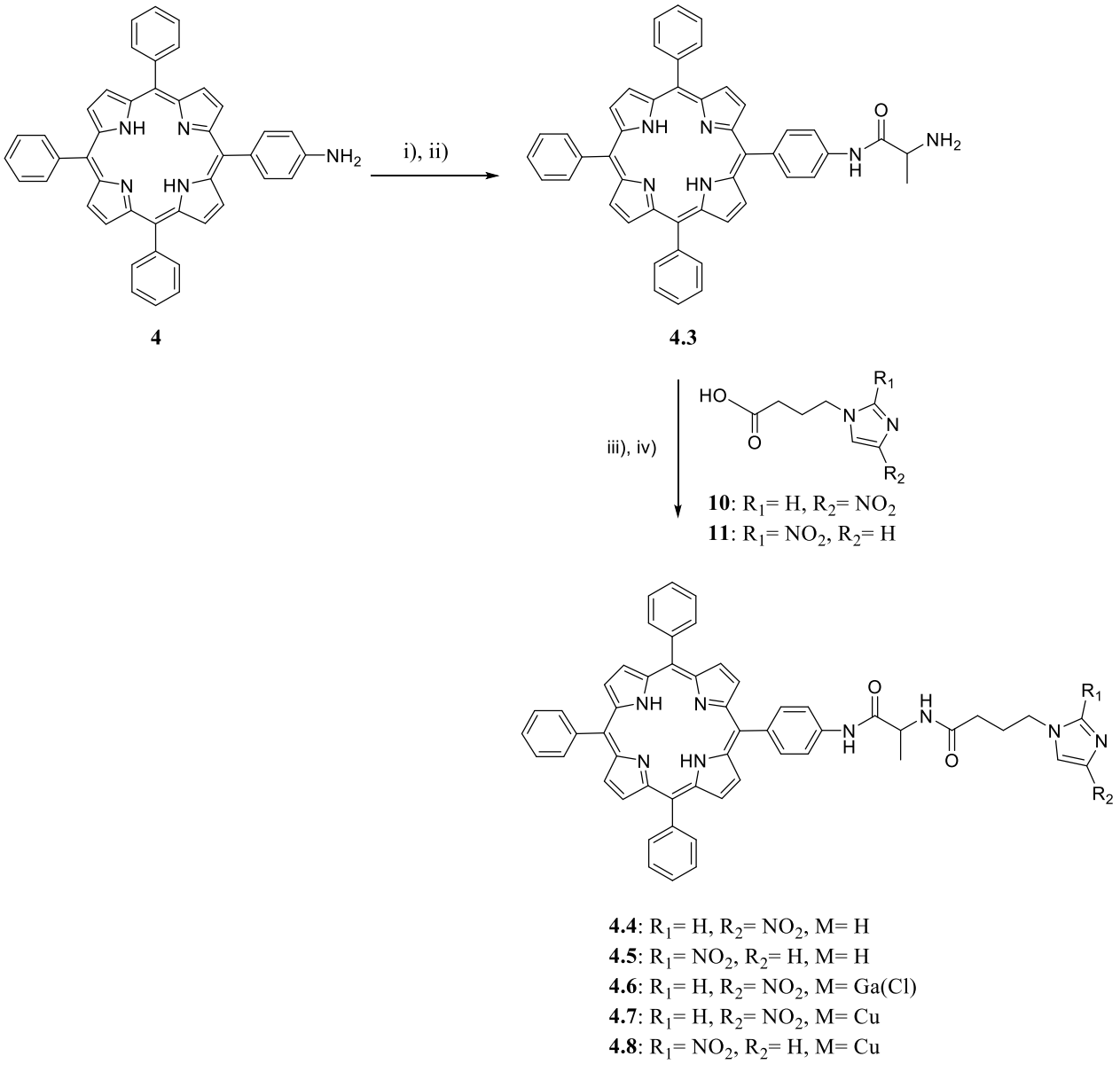


**Scheme S6.** Reagents and conditions: i) Boc-ala-NHS, DMAP,DMF; ii) TFA, $CHCl_3$; iii) $NEt_3$, DMF; iv) $GaCl_3$/$Cu(OAc)_2$ $2H_2O$, NaOAc, AcOH.

**5,10,15,20-*meso*-Tetraphenylporphyrin (TPP) (1)**

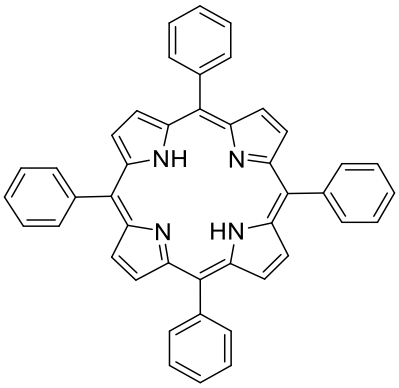


A mixture of propanoic acid (20 mL) pyrrole (5.6 mL, 80 mmol) and benzaldehyde (8.0 mL, 0.08 mol) was heated at reflux and stirred for 30 min. The resulting suspension was filtered to give a purple solid. This was washed with cold methanol and water and dried in air (1.96 g, 4 %).

**$^{1}$H NMR (300 MHz, CDCl$_3$)**: δ 8.85 (s, 8H, C*H*$_{pyrr}$), 8.30–8.13 (m, 8H, *o*-Ph), 7.86–7.66 (m, 12H, *m, p*-Ph), -2.77 (s, 2H, ring N*H*) ppm.

**$^{13}$C NMR (126 MHz, CDCl$_3$)**: δ 142, 134, 130 (broad), 127, 126, 120 ppm.

Data are in agreement with those previously reported [22].

**Methyl 4-(10,15,20-triphenylporphyrin-5-yl)benzoate (2)**

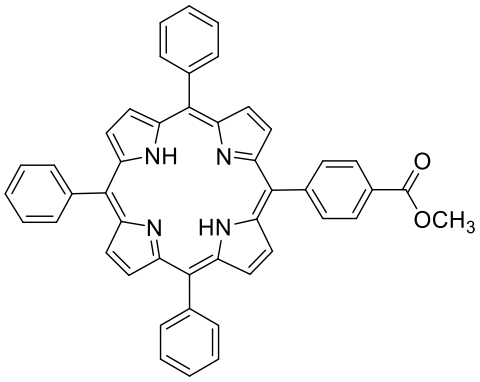


A solution of anhydrous DCM (1000 mL), benzaldehyde (1.86 mL, 18.2 mmol), methyl-4-formylbenzoate (1000 mg, 6.09 mmol), pyrrole (1.69 mL, 24.4 mmol) and ethanol (10 mL) was bubbled with nitrogen gas for 10 min. Boron trifluoride diethyl etherate (0.5 mL, 4.05 mmol) was added and the solution was stirred at ambient temperature for 1 h. 2,3-Dichloro-5,6-dicyano-1,4-benzoquinone (DDQ, 4140 mg, 18.2 mmol) was added, the solution was exposed to air and stirred for 1 h. Triethylamine (10 mL) was added and the solution was reduced in volume *in vacuo* to an oily black tar. The crude was filtered over silica and eluted with DCM, before it was purified by flash column chromatography (DCM/n-hexane 1:1) to give a purple solid (125.4 mg, 6 %).

**$^1$H NMR (500 MHz, $CDCl_3$)**: δ 8.85 (m, 8H, C$H_{pyrr}$), 8.45 (d, J=8.1 Hz, 2H, *m*-Ar*H*), 8.30 (d, *J* = 8.1 Hz, 2H, *o*-Ar*H*), 8.20 (d, *J* = 7.2 Hz, 6H, *m, o*-Ph), 7.75 (m, 9H, *m-, p*-Ph), 4.20 (s, 3H, OC$H_3$), -2.55 (s, 2H, ring N*H*) ppm.

Data are in agreement with those previously reported [23].

**4-(10,15,20-Triphenyl-porphyrin-5-yl)-benzoic acid (3)**

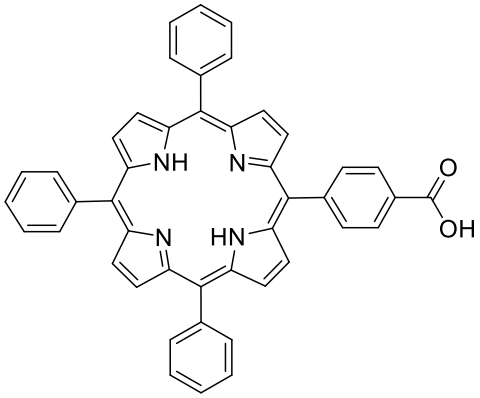


4-(10,15,20-Triphenyl-porphyrin-5-yl)-benzoic acid was synthesized according to literature methods [24], with analytical data in accord with the literature values.

A solution of ethanol (50 mL), methyl 4-(10,15,20-triphenylporphyrin-5-yl)benzoate (**2**) (21.6 mg, 0.032 mmol) and aqueous potassium hydroxide (1 M, 25 mL) was stirred at ambient temperature until the starting material was no longer visible by TLC, showing only the product spot. A minimum amount of THF (*ca.* 15 mL) was added to dissolve the solid product and the solution was acidified to pH 5 with HCl (aq, 1 M). The solution was loaded onto an $NH_2$ functionalized Solid Phase Extraction (SPE) cartridge. The cartridge was washed with water (30 mL) before liberating the product with acetic acid in diethyl ether solution (5 %, v/v). Removal of solvent *in vacuo* afforded purple crystals (14.7 mg, 70 %).

**$^1$H NMR (300 MHz, $CDCl_3$)**: δ 8.93-8.74 (m, 8H, C$H_{pyrr}$), 8.50 (d, *J* = 7.9 Hz, 2H, *m*-Ar*H*), 8.35 (d, *J* = 7.8 Hz, 2H, *o*-Ar*H*), 8.22 (dd, *J* = 7.3, 2.0 Hz, 6H, *o*-Ph), 7.77 (d, *J* = 6.6 Hz, 9H, *m, p*-Ph), -2.77 (s, 2H, ring N*H*) ppm.

**Mass spec:** ESI-MS calculated for $C_{44}H_{31}N_5$ [M - H]$^-$: 657.2296, found: 657.2314 [M - H]$^-$. Deviation: 2.74 ppm.

Data are in agreement with those reported [25].

**4-(10,15,20-Triphenyl-porphyrin-5-yl)-benzoic acid zinc complex (3.1)**

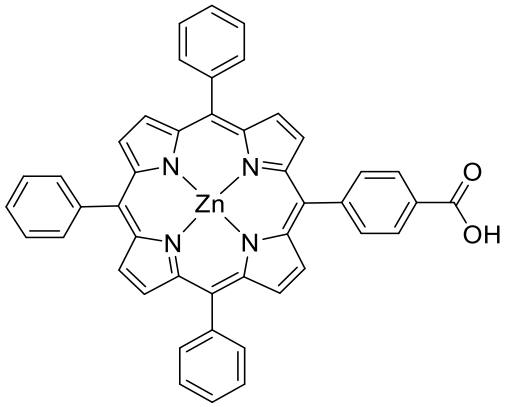


Porphyrin **2.1** was dissolved in THF (24 mL) and heated to reflux. KOH (aq, 2 M, 6 mL) was added and the resulting solution was stirred at reflux for 16h. THF was removed *in vacuo* and water (80 mL) was added. The resulting suspension was acidified to pH 4 with HCl (aq, 2 M, *c.a.* 15 mL). Chloroform (100 mL) was added and the organic layer was extracted, washed with water (2 x 50 mL) and dried over $MgSO_4$. Solvent was removed *in vacuo* affording a purple solid, (215 mg).

**$^1$H NMR (300 MHz, DMSO-$d_6$)** δ 13.23 (s, 1H, COO*H*), 8.82–8.71 (m, 8H, C$H_{pyrr}$), 8.35 (d, *J* = 8.3 Hz, 2H, *m*-Ar*H*), 8.29 (d, *J* = 8.3 Hz, 2H, *o*-Ar*H*), 8.22–8.11 (m, 6H, *o*-Ph), 7.86–7.71 (m, 9H, *m*-*p*-Ph).

**5-(4-aminophenyl)-10,15,20-triphenylporphyrin (4)**

5-(4-Aminophenyl)-10,15,20-triphenylporphyrin was synthesized according to the literature procedure of Kruper et al., with analytical data in accordance with the literature values [22].

Synthesis of 5-(4-nitrophenyl)-10,15,20-triphenylporphyrin

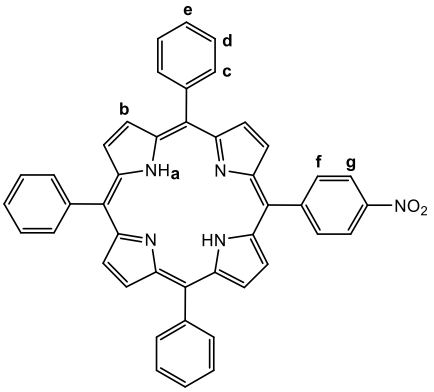

Tetraphenylporphyrin (TPP; 200mg, 325 µmol) was added to 4 mL TFA. $NaNO_2$ (40.4 mg, 586 µmol) was added to the mixture and stirred for 3 min. The reaction was quenched with water. The mixture was extracted with DCM (4 x 10 mL) and the organic layer collected and washed with saturated $NaHCO_3$ (10 mL) then water (10 mL). The organic layer was dried over $Na_2SO_4$, filtered and the solvent removed under vacuum. The mixture was purified using column chromatography on a gradient of 1:1 to 6:4 DCM/hexane (v/v). 23.6 mg (21 %) was obtained as a purple solid.

**$^1$H NMR (500 MHz, $CDCl_3$, 298 K)**: δ 8.90–8.74 (m, 8H, Hb), 8.64 (d, *J* = 8.6 Hz, 2H, Hg), 8.40 (d, *J* = 8.5 Hz, 2H, Hf), 8.22–8.21 (m, 6H, Hc), 7.80–7.75 (m, 9H, Hd/He), -2.77 (s, 2H, Ha).

**$^{13}$C NMR:** δ 116.55, 120.64, 121.83, 121.95, 126.75, 126.81, 127.86, 134.50, 135.08, 141.86, 141.90, 147.72.

**Mass spec:** $ESI^-$ $TOF^+$ mode m/z calculated for $C_{44}H_{30}N_5O_2$ $[M+H]^+$: 660.2394, found: 660.2395 $[M+H]^+$. Deviation: 0.15 ppm

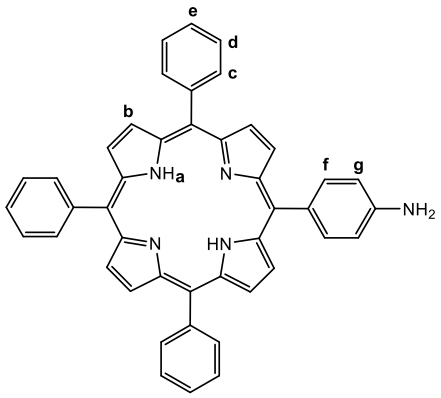


80 mg of 5-(4-nitrophenyl)-10,15,20-triphenylporphyrin (80 mg, 0.121 mmol) 10 mL DCM/MeOH (4:1, v/v). 10 % Pd/C (9 mg) was added with care under stirring. $NaBH_4$ (64.0 mg, 1.69 mmol) was added portion-wise over 10 min. After stirring for 15 min, 8 mL water was added, and a gas produced. After the evolution of the gas, the reaction mixture was filtered over celite then washed with brine. The mixture was dried over $Na_2SO_4$, filtered and the solvent removed under vacuum to give a green powder. 60.9 mg (80 %) was obtained.

**Mass Spec:** $ESI^+$ $TOF^+$ m/z calculated for $C_{44}H_{32}N_5$ $[M+H]^+$:630.2652 , found: 630.2684 $[M+H]^+$. Deviation: 5.08 ppm

**$^1$H NMR (500 MHz, $CDCl_3$, 298 K):** δ 8.97–8.83 (m, 8H, H**b**), 8.25–8.23 (m, 6H, H**c**), 8.01–8.00 (m, 2H, H**f**), 7.81–7.74 (m, 8H, H**d**/H**e**), 7.04–7.03 (m, 2H, H**g**), -2.71 (2H, s, H**a**).

**$^{13}$C NMR (500MHz, $CDCl_3$):** δ 113.44, 126.62 (β-C), 127.62, 134.53 (β-C), 135.68, 142.27.

Data are in agreement with those previously reported [22].

**5-(4-aminophenyl)-10,15,20-triphenylporphyrin zinc complex (4.1)**

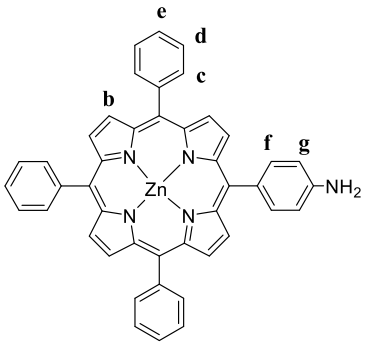


5-(4-aminophenyl)-10,15,20-triphenylporphyrin **4** (17 mg, 0.0269 mmol) was dissolved in $CDCl_3$ in a nmr tube. $Zn(CH_3CO_2)_2$ (5.43 mg, 0.0295 mmol) dissolved in MeOD was added and heated for 1 h. The mixture ($CDCl_3$/MeOD, 9:1) was washed with water (3 times) and the organic layer was dried under vacuum. A purple powder was obtained (13.7 mg, 74 %).

$^1$H NMR data are in agreement with those previously reported [26].

**$^{13}$C NMR (500 MHz, $CDCl_3$):** δ 142.44, 135.84, 134.71, 127.80, 126.80, 120.12, 113.59.

**Mass spec:** ESI-MS m/z calculated for $C_{44}H_{29}N_5Zn$ $[M]^+$ 691.1709, found: 691.1707 $[M]^+$. Deviation: 0.28 ppm

**Synthesis of 5-(4-aminophenyl)-10,15,20-triphenylporphyrin gallium complex (4.2)**

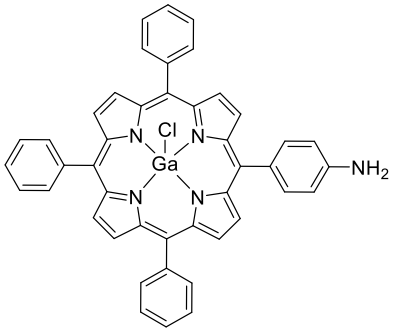


$GaCl_3$ (4.40 mg, 0.025 mmol) was added to a suspension of 5-(4-aminophenyl)-10,15,20-triphenylporphyrin zinc complex **4.1** (18 mg, 0.025 mmol) in MeOH (4 mL) under reflux for 4 h. The solvent was removed under vacuum. A green powder was obtained (20.6 mg).

**Mass spec:** ESI-MS m/z calculated for $C_{44}H_{30}ClGaN_5$ $[M + H]^+$ 732.1445, found: 732.1262. Deviation: 24.99 ppm

**HPLC:** (Method E) Rt (min): 19.21.

**Methyl 4-(10,15,20-tri(pyridin-4-yl)benzoate (5)**

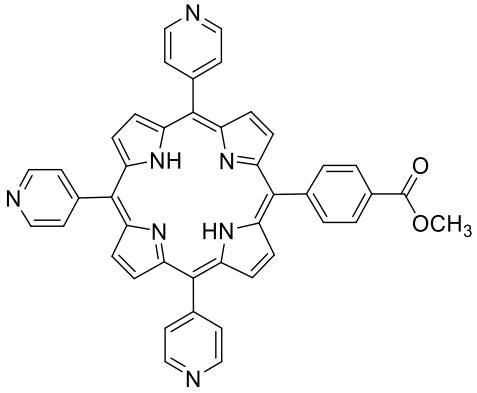


A mixture of propanoic acid (120 mL), methyl-4-formyl benzoate (1130 mg, 6.88 mmol) and 4-pyridine carboxaldehyde (2.0 mL, 20.7 mmol) was heated to reflux whilst shielded from light. Pyrrole (1.94 mL, 27.5 mmol) was added over 10 min, the resulting solution was stirred for 2 h and reducing in volume (to *ca.* 50 mL) *in vacuo*. MeOH (30 mL) and ethylene glycol (30 mL) were added and the solution was kept at -18 °C for 12 h before vacuum filtering over a frit, affording purple crystals. These were washed with cold ethanol and dried in air (224.8 mg). Purification by flash chromatography eluting at a gradient from 10-100 % EtOAc in DCM afforded the product (90 mg, 20 %)

**$^1$H NMR (300 MHz, $CDCl_3$)**: δ 9.06 (m, 6H, *m*-pyr*H*), 8.91–8.80 (m, 6H, C$H_{pyrr}$), 8.47 (d, *J* = 8.2 Hz, 2H, *m*-Ar*H*), 8.21–8.12 (m, 6H, *m*-pyr*H*), 4.13 (s, 3H, OC$H_3$), -2.88 (s, 2H, ring N*H*) ppm.

Data are in agreement with those previously reported [27].

**5-(4-carboxyphenyl)-10,15,20-tripyridylporphyrin (6)**

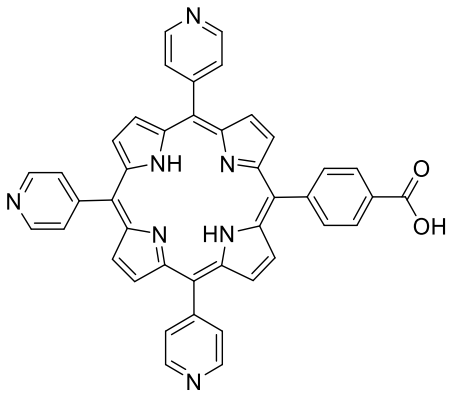

Porphyrin **5** (130 mg, 0.19 mmol) was suspended in EtOH (100 ml) and the reaction vessel shielded from light. 5M KOH (50 ml) was added and the solution brought to reflux until analysis by TLC showed no presence of **5**. The resulting red solution was acidified to pH 5 with 1M HCl and the desired product was extracted into $CH_2Cl_2$ and washed with water (3 x 50 ml). No further purification was required (112 mg, 88%).

**$^1$H NMR (400 MHz, DMSO-*d*$_6$, 298 K)**: δ 9.04–9.07 (6H, m, *2,6*-Py), 8.85–8.94 (8H, m, β-pyrr), 8.25–8.30 (8H, m, *3,*5-Py and *o*-Ph), 8.07–8.11 (2H, m, *m*-benzoate), -3.07 (s, 2H, ring N*H*) ppm.

**Mass spec:** ESI-MS m/z calculated for $C_{42}H_{28}N_7O_2$ $[M + H]^+$: 662.2305, found: 662.2345. Deviation: 6.19 ppm

Data are in agreement with those previously reported [28].

**Ni 5-(4-carboxymethylphenyl)-10,15,20-tripyridylporphyrin (12)**

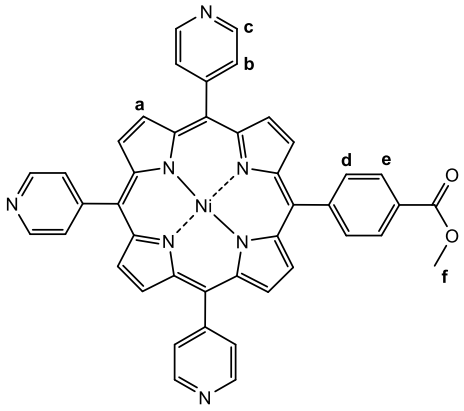

4-Pyridinecarboxaldehyde (4 mL, 57.7 mmol) and methyl-4-formyl benzoate (2.21 g, 13.5 mmol) were added to 240 mL propionic acid and stirred. Pyrrole (4 mL, 42.5 mmol) was added dropwise and the mixture shielded from light and refluxed at 150 °C for 2 hours. The reaction mixture was allowed to cool to room temperature and concentrated to approx. 80 mL before adding 60 mL MeOH and 60 mL ethylene glycol. The mixture was stored overnight at -18 °C. The propionic acid was removed under vacuum and the remaining liquid was suspended in MeOH/$CHCl_3$. The $CHCl_3$ layer was collected and run through silica before being suspended in water/$CHCl_3$. The $CHCl_3$ layer was collected and solvent

removed under vacuum to produce a black powder. The crude product was dissolved in 40 mL DMF and treated with 8 g nickel acetate tetrahydrate at 150 °C under reflux for 4.5 hours. The mixture was cooled to room temperature and DMF was removed under vacuum to leave a black solid. The solid was suspended in MeOH, filtered and washed with $CHCl_3$ before being purified by flash chromatography. It was dry loaded and eluted with a gradient of DCM to DCM/MeOH 85:15 (v/v). 15 mg (0.15 %) was obtained.

**$^1$H NMR (500 MHz, $CDCl_3$):** δ 8.75–8.70 (m, 8H, H**a**), 8.40–8.36 (m, 4H, H**d**/H**e**) 8.11–8.09 (m, 6H, H**c**), 8.03–7.92 (m, 6H, H**b**), 4.28 (s, 3H, H**f**).

**$^{13}$C NMR (500 MHz, $CDCl_3$):** δ 57.74 (COO**Me**), 111.66, 114.99, 128.17, 128.70, 129.42, 129.82, 133.66, 136.47, 142.56 (aromatic **c**), 167.07 (**C**OOMe).

**Mass Spec:** $ESI^-$ $TOF^+$ mode m/z calculated for $C_{43}H_{28}N_7O_2Ni$ $[M+H]^+$: 732.1658, found: 732.1672 [M+H]. Deviation: 1.91 ppm

**3-(4-Nitroimidazol-1-yl)-propylamine hydrochloride (7)**

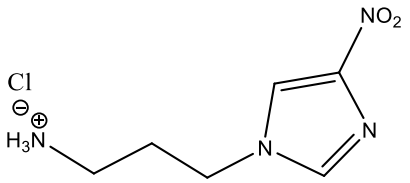


3-(4-Nitroimidazol-1-yl)-propylamine hydrochloride **7** was synthesized according to a literature method [29]. Hydrazine monohydrate (0.20 mL, 4.33 mmol) was added to a stirred suspension of 3-(4-nitroimidazol-1-yl)-propylphthalamide (0.75 g, 2.50 mmol) in ethanol (20 mL) and was heated under reflux for 2 h. The resulting suspension was cooled to 0 °C, filtered and the filtrate concentrated under reduced pressure. The residue was dissolved in 1 M HCl (1 mL), filtered, and the solvent removed under reduced pressure to yield **2.12** as an off-white solid after recrystallization (MeOH:EtOAc (1:1)). Yield: 345 mg, 1.62 mmol, 66 %.

**$^1$H NMR (300 MHz, DMSO-*d*$_6$, 25 ºC )**: δ 8.45 (d, 1H, *J* =1.4, C*H*$_{imid}$), 7.82 (d, 1H, *J* = 1.5, C*H*$_{imid}$), 4.41 (t, 2H, *J* = 6.8, $NH_3CH_2CH_2C\mathit{H}_2N_{imid}$), 2.74 (t, 2H, *J* = 6.4, $NH_3C\mathit{H}_2CH_2CH_2N_{imid}$), 2.10 (m, 2H, $NH_3CH_2C\mathit{H}_2CH_2N_{imid}$).

**$^{13}$C NMR (75.5 MHz, DMSO-*d*$_6$, 25 ºC )**: δ 149.7, 137.8, 121.5, 44.7, 35.8, 27.3.

**Mass spec:** ESI-MS calculated for $C_6H_{11}N_4O_2$ $[M - Cl]^-$ 171.0877, found: 171.0889.

**3-(2-Nitroimidazol-1-yl)-propylamine hydrochloride (8)**

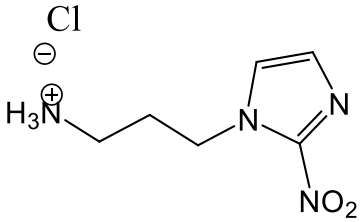


Compound **8** was synthesized analogous to compound **7**. 3-(2-nitroimidazol-1-yl)-propylphthalamide (500 mg, 1.67 mmol), hydrazine monohydrate (0.134 mL, 2.90 mmol), EtOH (15 mL). Yield: 248 mg, 1.20 mmol, 72 %.

**$^1$H NMR (300 MHz, DMSO-*d*$_6$, 25 ºC)**: δ 7.86 (s, 1H, C*H*$_{imid}$), 7.27 (s, 1H, C*H*$_{imid}$), 4.45 (t, 2H, *J* = 6.8, $NH_3CH_2CH_2C\mathit{H}_2N_{imid}$), 2.78 (t, 2H, *J* = 6.4, $NH_3C\mathit{H}_2CH_2CH_2N_{imid}$), 2.12 (m, 2H, $NH_3CH_2C\mathit{H}_2CH_2N_{imid}$).

**$^{13}$C NMR (75.5 MHz, DMSO-*d*$_6$, 25 ºC )**: δ 144.7, 128.4, 127.9, 45.2, 36.1, 28.1.

**5-[4-(*N*-3-(4-Nitroimidazol-1-yl)-propyl benzamide)]-10,15,20-triphenyl-porphyrin [$H_2$TPP-4Nitim] (3.3)**

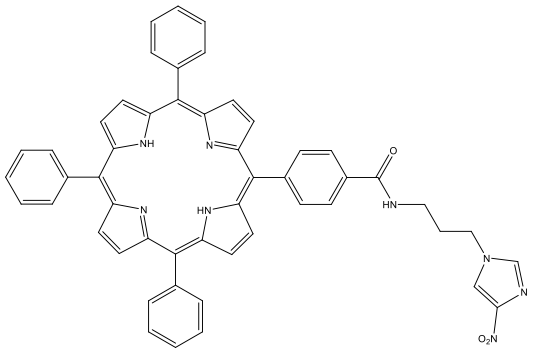

Compound **3.3** was synthesized employing general amide coupling procedure A. 5-[4-(Succinimidyloxycarbonylphenyl]-10,15,20-triphenylporphyrin (250 mg, 0.331 mmol), **7** (100 mg, 0.484 mmol), DIPEA (64.6 mg, 87.1 µL, 0.500 mmol), DMF (10 mL). Silica gel chromatography (5 % MeOH in $CHCl_3$). Yield: 191 mg, 0.235 mmol, 71 %.

**$^1$H NMR (500 MHz, DMSO-*d*$_6$, 25 ºC)**: δ 8.93 (t, 1H, *J* = 5.6, CON*H*), 8.81 (m, 8H, C*H*$_{pyrr}$), 8.58 (d, 1H, *J* = 1.5, C*H*$_{imid}$), 8.30 (d, 1H, *J* = 8.5, Ar*H*) , 8.26 (d, 1H, *J* = 8.3, Ar*H*) , 8.17 (m, 6H, *o-Ph*), 8.01 (d, 1H, *J* = 1.4, C*H*$_{imid}$), 7.76 (m, 9H, *m,p-Ph*), 4.25 (t, 2H, *J* = 6.9, CONHCH$_2$CH$_2$C*H*$_2$N$_{imid}$), 3.44 (m, 2H, CONHC*H*$_2$CH$_2$CH$_2$N$_{imid}$), 2.18 (m, 2H, CONHCH$_2$C*H*$_2$CH$_2$N$_{imid}$), -2.90 (s, 2H, ring N*H*).

**$^{13}$C NMR (125 MHz, DMSO-*d*$_6$, 25 ºC)**: δ 166.5, 147.1, 144.0, 141.2, 137.6, 134.3, 134.0, 132-131(broad), 128.2, 128.0, 127.1, 126.9, 125.9, 121.9, 120.1, 119.0, 45.5, 36.4, 30.3.

**Mass spec**: ESI-MS calculated for $C_{51}H_{39}N_8O_3$ $[M+H]^+$ 811.3145, found: 811.2841.

**HPLC:** (Method A) $R_t$ = 10.49 min.

**Elem. Anal.**: Found: C; 76.1 %, H; 4.8 %, N; 13.6 %. Calc.: C; 75.5 %, H; 4.7 %, N; 13.8 %.

**5-[4-(*N*-3-(2-Nitroimidazol-1-yl)-propyl benzamide)]-10,15,20-triphenyl-porphyrin, [$H_2$TPP-2Nitim] (3.4)**

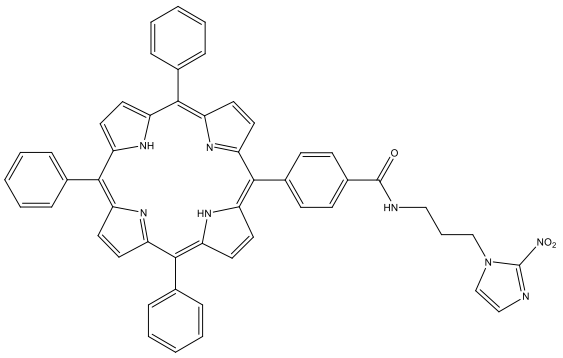

Compound **3.4** was synthesized employing general amide coupling procedure A. 5-[4-(Succinimidyloxycarbonylphenyl]-10,15,20-triphenylporphyrin (122 mg, 0.161 mmol), **8** (40.0 mg, 0.194 mmol), DIPEA (32.3 mg, 43.5 µL, 250 mmol), DMF (2 mL). Silica gel chromatography: 5% MeOH in $CHCl_3$. Yield: 0.103 mg, 0.127 mmol, 79 %.

**$^1$H NMR (500 MHz, DMSO-$d_6$, 25 ºC)**: δ 8.96 (t, 1H, *J* = 5.9, CON*H*), 8.85 (br. s, 8H, C$H_{pyrr}$), 8.34 (d, 2H, *J* = 7.9, Ar*H*), 8.29 (d, 2H, *J* = 7.8, Ar*H*), 8.19–8.25 (m, 6H, *o*-Ph), 7.86 (s, 1H, C$H_{imid}$), 7.86–7.79 (m, 9H, *m-p-Ph*) 7.26 (s, 1H, C$H_{imid}$), 4.55 (t, 2H, *J* = 7.1, CONHCH$_2$CH$_2$C$H_2$N$_{imid}$), 3.45 (m, 2H, CONHC$H_2$CH$_2$CH$_2$N$_{imid}$), 2.17 (m, 2H, CONHCH$_2$C$H_2$CH$_2$N$_{imid}$), -2.98 (s, 2H, ring N*H*).

**$^{13}$C NMR (125 MHz, DMSO-$d_6$, 25 ºC)**: 166.5, 144.7, 144.0, 141.2, 134.22, 134.17, 134.1, 131.3 (broad), 128.1, 128.0, 127.9, 127.0, 125.9, 120.3, 120.2, 119.0, 47.6, 36.5, 30.0.

**Mass spec:** ESI-MS calculated for $C_{51}H_{38}NaN_8O_3$ $[M + Na]^+$ 833.2959, found: 833.2958.

**HPLC** (Method A): $R_t$ = 10.73 min.

**Elem. Anal.**: Found: C; 75.8 %, H; 4.6 %, N; 14.1 %. Calc.: C; 75.5 %, H; 4.7 %, N; 13.8 %.

**Synthesis of 5-[4-(*N*-3-(4-Nitroimidazol-1-yl)-propyl benzamide)]-10,15,20-triphenyl-porphyrin gallium (III) chloride, [Ga(Cl)TPP-4Nitim] (3.5)**

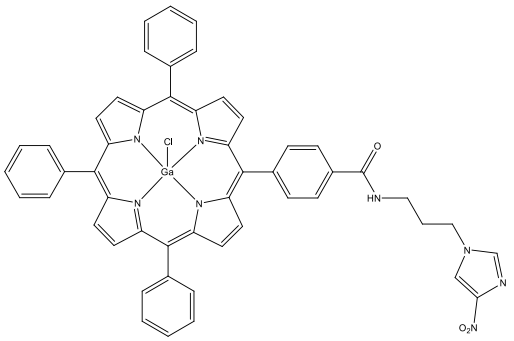


Compound **3.5** was synthesized employing general metal complexation method A. **3.3** (100 mg, 0.123 mmol), NaOAc (61.0 mg, 0.744 mmol), $GaCl_3$ (26.0 mg, 0.148 mmol), AcOH (10 mL). A maroon colored solid was obtained. Yield: 87.5 mg, 0.096 mmol, 78 %.

**$^1$H NMR (300 MHz, DMSO-$d_6$, 25 ºC )**: δ 9.00 (br. s, 8H, C$H_{pyrr}$), 8.59 (t, 1H, *J* = 5.9, CON*H*), 8.40 (s, 1H, C$H_{imid}$), 8.26 (m, 4H, Ar*H*), 8.20 (m, 6H, *o*-Ar*H*), 7.90 (s, 1H, C$H_{imid}$), 7.88–7.76 (m, 9H, *m-p*-Ar*H* ), 4.28 (t, 2H, *J* = 6.9, CONHCH$_2$CH$_2$C$H_2$N$_{imid}$), 3.48 (m, 2H, CONHC$H_2$CH$_2$CH$_2$N$_{imid}$), 2.22 (m, 2H, CONHCH$_2$C$H_2$CH$_2$N$_{imid}$).

**$^{13}$C NMR (125 MHz, DMSO-$d_6$, 25 ºC)**: δ 147.9 (broad), 147.0, 141.0 (broad), 137.6, 137.3 (broad), 134.1 (broad), 132.0 (broad), 128.2 (broad), 127.1 (broad), 121.7, 120.2 (broad). Peaks missing, spectrum shows strong broadening.

**Mass spec:** ESI-MS calculated for $C_{51}H_{37}ClGaN_8O_3$ $[M +H]^+$ 913.1933, found: 913.1954.

**HPLC:** (Method A) $R_t$ = 9.57 min.

**Elem. Anal.**: Found: C; 67.5 %, H; 4.2 %, N; 11.5 %. Calc.: C; 67.1 %, H; 4.0 %, N; 12.3 %.

**5-[4-(*N*-3-(4-Nitroimidazol-1-yl)-propyl benzamide)]-10,15,20-triphenyl-porphyrin indium (III) chloride, [In(Cl)TPP-4Nitim] (3.6)**

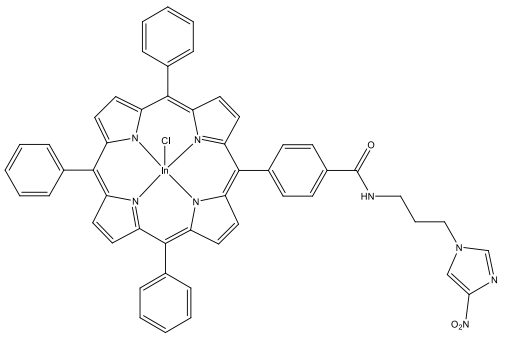

Compound **3.6** was synthesized employing general metal complexation method B. **3.3** (100 mg, 0.123 mmol), NaOAc (56.7 mg, 0.691 mmol), $InCl_3$ (55.0 mg, 0.247 mmol), AcOH (15 mL). A purple colored solid was obtained. Yield: 84.9 mg, 0.089 mmol, 72 %.

**$^1$H NMR (300 MHz, DMSO-$d_6$, 25 ºC)**: δ 8.96 (m, 9H, C*H*$_{pyrr}$, CON*H*), 8.62 (d, 1H, *J* = 1.2, C*H*$_{imid}$), 8.35 (s, 4H, Ar*H*), 8.25 (m, 6H, *o*-Ar*H*), 8.05 (d, 1H, *J* = 1.2, C*H*$_{imid}$), 7.90 (m, 9H, *m*-,*p*-Ar*H*), 4.31 (t, 2H, CONHCH$_2$CH$_2$C*H*$_2$N$_{imid}$), 3.48 (m, 2H, CONHC*H*$_2$CH$_2$CH$_2$N$_{imid}$), 2.22 (qt, 2H, CONHCH$_2$C*H*$_2$CH$_2$N$_{imid}$).

**$^{13}$ C NMR (125 MHz, DMSO-$d_6$, 25 ºC)**: δ 166.5, 147.9, 147.8, 147.5, 147.1, 144.3, 141.5, 137.7, 134.5, 134.4, 134.0, 132.7, 132.6, 132.5, 132.3, 128.2, 127.0, 125.9, 121.9, 121.4, 121.3, 120.1, 45.5, 36.5, 30.3.

**Mass spec:** ESI-MS calculated for $C_{51}H_{36}InN_8O_3$ $[M - Cl]^+$ 923.1949, found 923.1922.

**HPLC:** (Method A) $R_t$ = 9.86 min.

**5-[4-(*N*-3-(4-Nitroimidazol-1-yl)-propyl benzamide)]-10,15,20-triphenyl-porphyrin copper (II), [CuTPP-4Nitim] (3.7)**

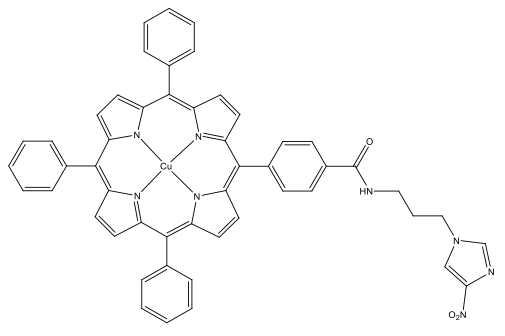

Compound **3.7** was synthesized employing general metal complexation method B. **3.3** (50 mg, 0.062 mmol), $Cu(OAc)_2 \cdot H_2O$ (24.6 mg, 0.123 mmol), DMF (10 mL). A red colored solid was obtained. Yield: 35.9 mg, 0.040 mmol, 65 %.

**Mass spec:** ESI-MS calculated for $C_{51}H_{37}CuN_8O_3$ $[M + H]^+$ 872.2279, found: 872.2296.

**HPLC:** (Method A) $R_t$ = 10.37 min.

**Elem. Anal.**: Found: C; 70.5 %, H; 4.7 %, N; 12.8 %. Calc.: C; 70.2 %, H; 4.2 %, N; 12.9 %.

**5-[4-(*N*-3-(2-Nitroimidazol-1-yl)-propyl benzamide)]-10,15,20-triphenyl-porphyrin gallium (III) chloride, [Ga(Cl)TPP-2Nitim] (3.8)**

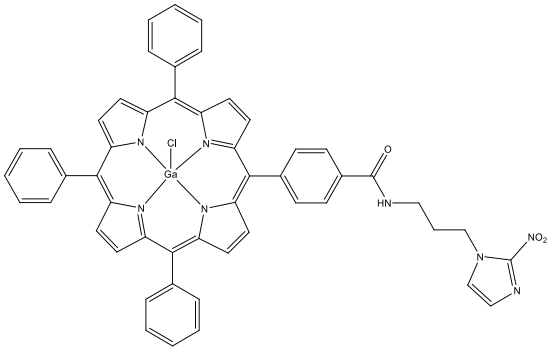

Compound **3.8** was synthesized employing general metal complexation method A. **3.4** (85 mg, 0.105 mmol), NaOAc (51.6 mg, 0.629 mmol), $GaCl_3$ (36.9 mg, 0.210 mmol), AcOH (10 mL). A maroon colored solid was obtained. Yield: 77.8 mg, 0.085 mmol, 81 %.

**$^1$H NMR (300 MHz, DMSO-$d_6$, 25 ºC)**: δ 8.89 (br. s, 8H, C$H_{pyrr}$), 8.53 (t, 1H, $J$ = 6.1, CON$H$), 8.31 (m, 4H, Ar$H$), 8.15 (m, 6H, *o-Ph*), 7.95 (s, 1H, C$H_{imid}$), 7.77 (m, 9H, *m-p*-Ar$H$), 7.22 (s, 1H, C$H_{imid}$), 4.36 (t, 2H, $J$ = 6.5, CONHCH$_2$CH$_2$C$H_2$N$_{imid}$), 3.41 (m, 2H, CONHC$H_2$CH$_2$CH$_2$N$_{imid}$), 2.31 (quin, 2H, $J$ = 6.4, CONHCH$_2$C$H_2$CH$_2$N$_{imid}$).

**Mass spec:** ESI-MS calculated for $C_{51}H_{36}GaN_8O_3$ $[M - Cl]^+$ 877.2166, found: 877.2145.

**HPLC:** (Method A) $R_t$ = 9.64 min.

**Elem. Anal.**: Found: C; 67.8 %, H; 4.2 %, N; 12.1 %. Calc.: C; 67.1 %, H; 4.0 %, N; 12.3 %.

**5-[4-(*N*-3-(2-Nitroimidazol-1-yl)-propyl benzamide)]-10,15,20-triphenyl-porphyrin indium (III) chloride, [In(Cl)TPP-2Nitim] (3.9)**

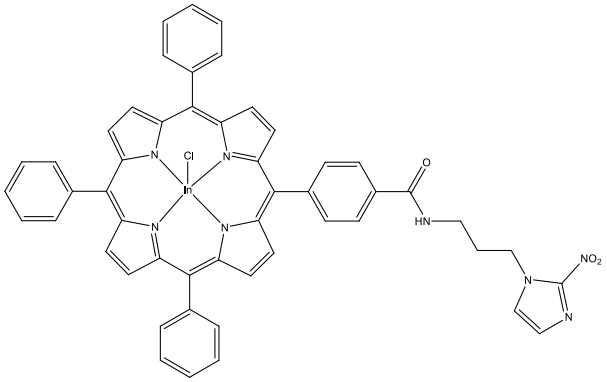

Compound **3.9** was synthesized employing general metal complexation method B. **3.4** (50mg, 0.062 mmol), NaOAc (28.3 mg, 0.345 mmol), $InCl_3$ (27.5 mg, 0.124 mmol), AcOH (10 mL). A purple colored solid was obtained. Yield: 51.1 mg, 0.053 mmol, 86 %.

**$^1$H NMR (300 MHz, DMSO-$d_6$, 25 ºC)**: δ 9.01 (m, 9H, C$H_{pyrr}$, CON$H$), 8.31 (m, 4H, Ar$H$), 8.24 (m, 6H, *o*-Ar$H$) 7.85 (m, 10H, *m-,p*-Ar$H$ C$H_{imid}$), 7.31 (s, 1H, C$H_{imid}$), 4.31 (t, 2H, $J$ = 6.8, CONHCH$_2$CH$_2$C$H_2$N$_{imid}$), 3.56 (m, 2H, CONHC$H_2$CH$_2$CH$_2$N$_{imid}$), 2.25 (qt, 2H, $J$ = 6.5, CONHCH$_2$C$H_2$CH$_2$N$_{imid}$).

**$^{13}$C NMR (125 MHz, DMSO-$d_6$, 25 ºC)**: δ 166.7, 148.1, 148.0, 147.6, 147.0, 144.9, 144.2, 143.4, 134.5, 134.4, 134.2, 132.7, 132.5, 132.4, 128.2, 127.9, 127.7, 127.0, 125.9, 121.4, 121.3, 120.2, 44.9, 36.3, 31.0.

**Mass Spectrum:** ESI-MS calculated for $C_{51}H_{36}InN_8O_3$ $[M - Cl]^+$ 923.1949, found: 923.1965.

**HPLC:** (Method A) $R_t$ = 9.52 min.

**Elem. Anal.**: Found: C; 64.4 %, H; 4.1 %, N; 11.4 %. Calc.: C; 63.9 %, H; 3.8 %, N; 11.7 %.

**5-[4-(*N*-3-(2-Nitroimidazol-1-yl)-propyl benzamide)]-10,15,20-triphenyl-porphyrin copper (II), [CuTPP-2Nitim]. (3.10)**

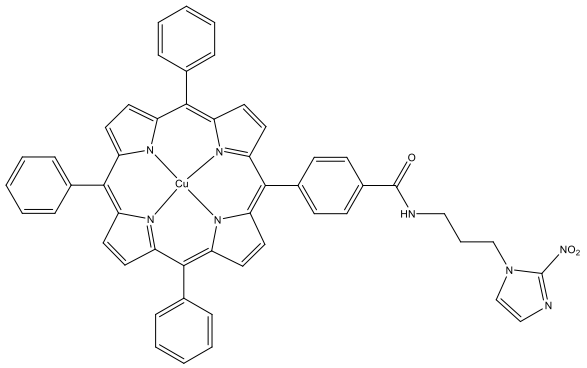


Compound **3.10** was synthesized employing general metal complexation method B. **3.4** (40 mg, 0.049 mmol), $Cu(OAc)_2 \cdot H_2O$ (19.6 mg, 0.098 mmol), DMF (5 mL). A red colored solid was obtained. Yield: 36.7 mg, 0.042 mmol, 86 %.

**Mass spec:** ESI-MS calculated for $C_{51}H_{36}CuNaN_8O_3$ $[M + Na]^+$ 894.2104, found: 894.2115.

**HPLC:** (Method A) $R_t$ = 10.21 min.

**Elem. Anal.**: Found: C; 70.5 %, H; 4.3 %, N; 13.1 %. Calc.: C; 70.2 %, H; 4.2 %, N; 12.9 %.

**5-[4-(*N*-propyl benzamide)],10,15,20-triphenyl-porphyrin [$H_2$TPP-propyl] (3.11)**

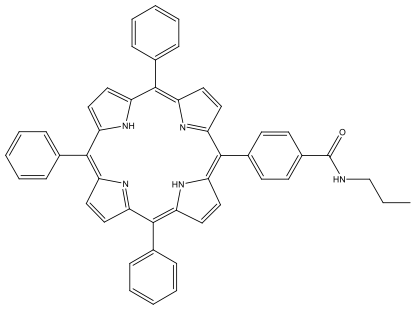

Compound **3.11** was synthesized employing general amide coupling procedure A. 5-[4-(Succinimidyloxycarbonylphenyl]-10,15,20-triphenylporphyrin (130 mg, 0.198 mmol), propylamine (58.6 mg, 59.1 µL, 0.992 mmol), $CHCl_3$ (in place of DMF) (5 mL). **3.11** was purified *via* silica gel chromatography (1% MeOH in $CHCl_3$). Yield: 123 mg, 0.176 mmol, 89 %.

**$^1$H NMR (300 MHz, $CDCl_3$, 20 ºC)**: δ 8.93–8.54 (m, 8H, C$H_{pyrr}$), 8.21–7.95 (m, 8H, *o*-Ph, Ar*H*), 7.84 (d, 2H, *J* = 8.1, Ar*H*), 7.61 (m, 9H, *m-,p-Ph*), 6.31 (t, 1H, *J* = 5.2, CON*H*), 3.43 (m, 2H, CONHC$H_2$$CH_2$$CH_3$), 1.47–1.76 (m, 2H, CONHCH$_2$C$H_2$$CH_3$), 0.96 (t, 3H, *J* = 7.1, CONHCH$_2$CH$_2$C$H_3$), -2.87 (br. s, 2H, ring N*H*).

**$^{13}$C NMR (75.5 MHz, $CDCl_3$, 20 ºC)**: δ 167.7, 145.4, 142.1, 134.7, 134.6, 134.2, 131.2, 127.8, 126.7, 125.3, 120.6, 120.4, 118.7, 42.0, 23.1, 11.6.

**Mass spec:** ESI-MS calculated for $C_{48}H_{38}N_5O$ $[M + H]^+$ 700.3071, found 700.3060.

**HPLC** (Method A): $R_t$ = 10.97 min.

**5-[4-(*N*-propyl benzamide)],10,15,20-triphenyl-porphyrin indium(III) chloride [In(Cl)TPP-propyl] (3.12)**

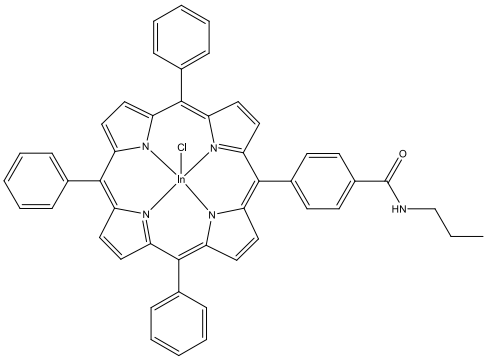

Compound **3.12** was synthesized employing general metal complexation method A. **3.11** (50.0 mg, 0.072 mmol), NaOAc (35.0 mg, 0.429 mmol), $InCl_3$ (32.0 mg, 0.143 mmol), AcOH (10 mL). Yield: 51.2 mg, 0.061 mmol, 84 %.

**$^1$H NMR (500 MHz, DMSO-$d_6$, 25 ºC )**: δ 8.99 (s, 8H, C$H_{pyrr}$), 8.50 (t, 1H, *J* = 5.4, CON*H*), 8.31 (2xd, 2x2H, Ar*H*), 8.22 (m, 6H, *o*-Ph), 7.85 (m, 9H, *m-,p-Ph*), 3.43 (m, 2H, CONHC$H_2$$CH_2$$CH_3$), 1.75 (m, 2H, CONHCH$_2$C$H_2$$CH_3$), 1.02 (t, 3H, *J* = 7.6, CONHCH$_2$CH$_2$C$H_3$).

**$^{13}$C NMR (125 MHz, DMSO-$d_6$, 25 ºC)**: δ 166.0, 147.3, 147.0, 143.6, 140.8, 134.2, 132.3, 132.2, 128.4, 127.2, 126.2, 126.1, 120.4, 120.3, 119.4, 43.1, 23.4, 11.5.

**Mass spec:** ESI-MS calculated for $C_{48}H_{36}InN_5O$ $[M - Cl]^+$ 812.1875, found: 812.1855.

**HPLC** (Method A): $R_t$ = 10.64 min.

**5-[4-(*N*-propyl benzamide)],10,15,20-triphenyl-porphyrin copper (II), [CuTPP-propyl] (3.13)**

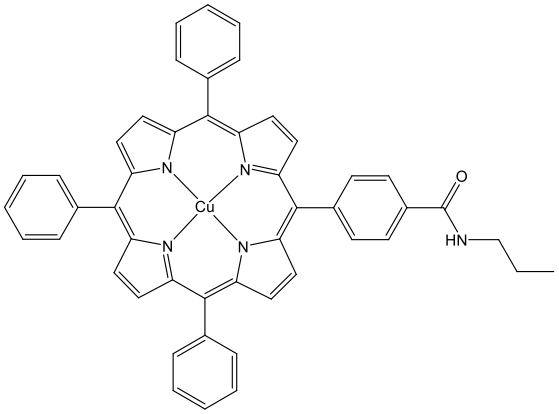


$Cu(OAc)_2 \cdot H_20$ (8.3 mg, 0.042 mmol) in MeOH (1 mL) was added with stirring at rt to a $CHCl_3$ (1 mL) solution of **3.11** (30 mg, 0.04 mmol). After 5 min the solvent was removed under reduced pressure and the residue re-dissolved in $CHCl_3$. The $CHCl_3$ layer was washed with water and brine and dried over anhydrous magnesium sulfate. The solvent was removed under reduced pressure to give a red solid. Yield: 27.8 mg, 0.036 mmol, 96 %.

**Mass spec:** ESI-MS calculated for $C_{45}H_{34}CuN_5O$ $[M - H]^-$ 759.2059, found: 759.2071.

**HPLC:** (Method A) $R_t$ = 10.81 min.

**5-[4-( *N*-propyl benzamide)]-10,15,20-tri-(4-sulfonylphenyl)-porphyrin [$H_2$TSPP-propyl] (3.14)**

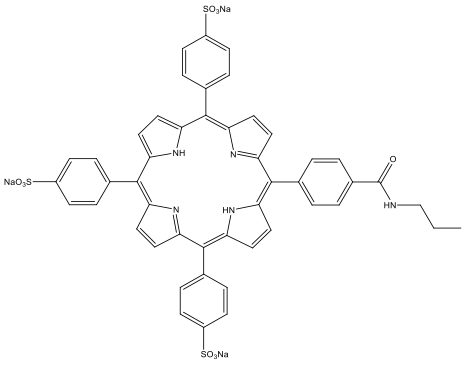


**3.14** was synthesized according to the general sulphonation method with **3.11** (80.0 mg, 0.114 mmol) in conc. $H_2SO_4$ (2 mL). Yield: 81.4 mg, 0.081 mmol, 71 %.

**$^1$H NMR (500 MHz, DMSO-$d_6$, 25 ºC)**: δ 8.96 (t, 1H, *J* = 5.7, CON*H*), 8.82 (m, 8H, C$H_{pyrr}$), 8.33 (d, 2H, *J* = 8.0, Ar*H*), 8.22 (d, 2H, *J* = 7.9, Ar*H*), 8.15 (d, 6H, *J* = 8.0, Ar$H_{SO3Na}$), 8.03 (d, 6H, *J* = 8.1, Ar$H_{SO3Na}$).

**$^{13}$C NMR (125 MHz, DMSO-$d_6$, 25 ºC)**: δ 166.5, 147.6, 144.1, 141.3, 134.5, 133.8, 133.7, 132.4, 126.2, 124.8, 119.9, 119.7, 119.3, 45.2, 24.6, 11.8.

**Mass spec:** ESI-MS calculated for $C_{48}H_{34}N_5O_{10}S_3$ $[M - 3Na]^{3-}/3$, 312.0495, found: 312.0511.

**HPLC** (Method B): $R_t$ = 11.42 min.

**5-[4-( *N*-propyl benzamide)]-10,15,20-tri-(4-sulfonylphenyl)-porphyrin [$H_2$TSPP-propyl] indium(III) chloride, [In(Cl)TSPP-propyl] (3.15)**

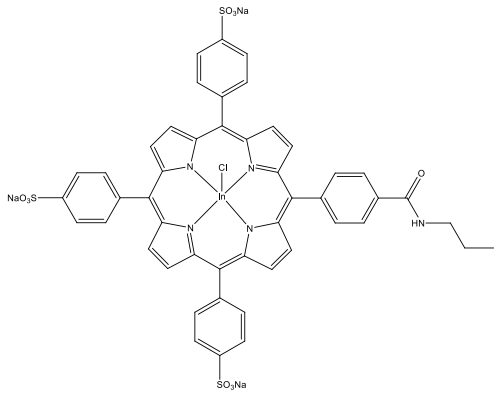


Compound **3.15** was synthesized employing general metal complexation method C. **3.14** (40.0 mg, 0.031 mmol), $InCl_3$ (17.5 mg, 0.080 mmol) in pH 4.5 NaOAc buffer (5 mL). Yield: 36.0 mg, 0.081 mmol, 78 %.

**$^1$H NMR (500 MHz, DMSO-$d_6$, 25 ºC)**: 8.99 (m, 8H, C$H_{pyrr}$), 8.79 (t, 1H, *J* = 5.4, CON*H*), 8.33 (d, 2H, *J* = 8.2, Ar*H*), 8.29 (d, 2H, *J* = 8.2, Ar*H*), 8.17 (d, 6H, *J* = 8.0, Ar$H_{SO3Na}$), 8.11 (d, 6H, *J* = 8.0, Ar$H_{SO3Na}$), 3.39 (m, 2H, CONHC$H_2$CH$_2$CH$_3$), 1.67 (m, 2H, CONHCH$_2$C$H_2$CH$_3$), 0.99 (t, 3H, *J* = 7.4, CONHCH$_2$CH$_2$C$H_3$).

**$^{13}$C NMR (75.5 MHz, DMSO-$d_6$, 25 ºC)**: δ 166.2, 148.22, 148.19, 148.0, 147.7, 144.0, 141.6, 134.4, 133.9, 132.6, 132.4, 125.9, 124.2, 121.0, 120.5, 46.1, 24.1, 11.2.

**Mass spec:** ESI-MS calculated for $C_{48}H_{32}InNaN_5O_{10}S_3$ $[M - 2Na - Cl]^+$ 1072.0247, found: 1072.0400.

**HPLC** (Method B): $R_t$ = 10.64 min.

**5-[4-(N-(4-Sulphamoylphenethyl)benzamide)]-10,15,20-triphenyl-porphyrin, [$H_2$TPP-ABS] (3.16)**

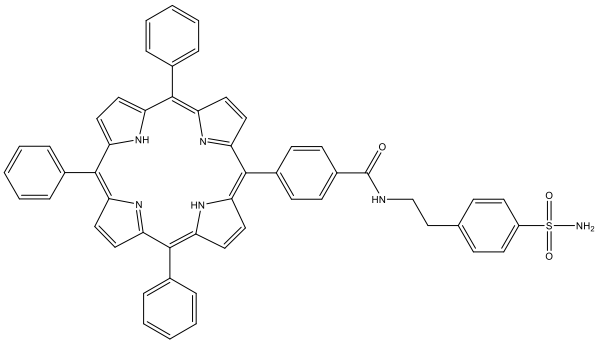

Compound **3.16** was synthesized employing general peptide coupling method A. **2.11** (250 mg, 0.331 mmol), 4-(2-aminoethyl) benzene sulphonamide (100 mg, 0.500 mmol), DIPEA (64.6 mg, 87.1 µL, 0.500 mmol), DMF (10 mL). **3.16** was purified by silica gel chromatography (5 % MeOH in CHCl3). Yield: 236 mg, 0.281 mmol, 85 %.

**$^1$H NMR (300 MHz, DMSO-$d_6$, 25 ºC)**: 8.99 (t, 1H, *J* = 5.5, CON*H*), 8.81 (m, 8H, C$H_{pyrr}$), 8.29 (d, 2H, *J* = 8.1, Ar*H*), 8.23 (d, 2H, *J* = 8.4, Ar*H*), 8.17 (m, 6H, *o*-Ar*H*), 7.84 (d, 2H, *J* = 8.4, Ar*H*), 7.77 (m, 9H, *m,p*-Ar*H*), 7.55 (d, 2H, *J* = 8.4 Ar*H*), 7.37 (s, 2H, $SO_2NH_2$), 3.69 (m, 2H, CONHC$H_2CH_2$), 3.06 (t, 1H, *J* = 7.2, $CONHCH_2CH_2$).

**$^{13}$C NMR (125 MHz, DMSO-$d_6$, 25 ºC)**: 166.3, 144.0, 143.9, 142.2, 141.2, 134.2, 134.1, 131.0 (bs), 129.3, 128.1, 127.0, 125.9, 120.3, 120.2, 119.1, 34.9, 25.3.

**Mass spec:** ESI-MS calculated for $C_{53}H_{40}N_6O_3S$ [M + H]+ 841.2961, found: 841.2768.

**HPLC:** (Method A) Rt =11.81 min.

**Elem. Anal.**: Found: C; 75.2 %, H; 4.9 %, N; 10.1 %. Calc.: C; 75.7 %, H; 4.8 %, N; 10.0 %.

**5-[4-(N-(4-Sulphamoylphenethyl)benzamide)]-10,15,20-triphenyl-porphyrin copper (II), [CuTPP-ABS] (3.17)**

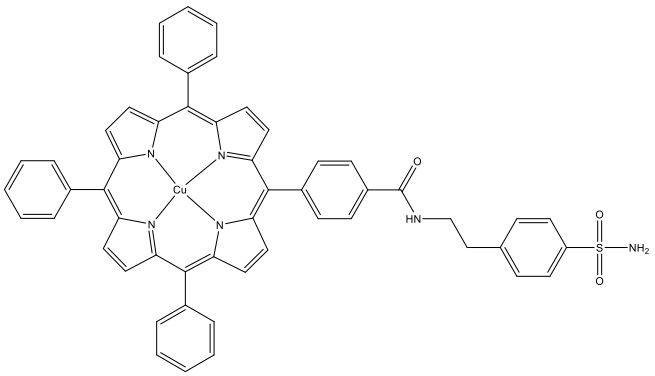

Compound **3.17** was synthesized employing general metal complexation method B. **3.16** (25 mg, 0.030 mmol), $Cu(OAc)_2{\cdot}H_2O$ (11.9 mg, 0.060 mmol), DMF (2 mL). A red colored solid was obtained. Yield: 17.9 mg, 0.020 mmol, 66 %.

**Mass spec:** ESI-MS calculated for $C_{53}H_{38}CuNaN_6O_3S$ $[M + Na]^+$ 924.1920, found: 924.1946.

**HPLC:** (Method A) Rt = 11.43 min.

**Elem. Anal.**: Found: C; 71.0 %, H; 4.1 %, N; 9.7 %. Calc.: C; 70.6 %, H; 4.2 %, N; 9.3 %.

**5-[4-(N-(4-Sulphamoylphenethyl)benzamide)]-10,15,20-triphenyl-porphyrin indium (III) chloride, [In(Cl)TPP-ABS] (3.18)**

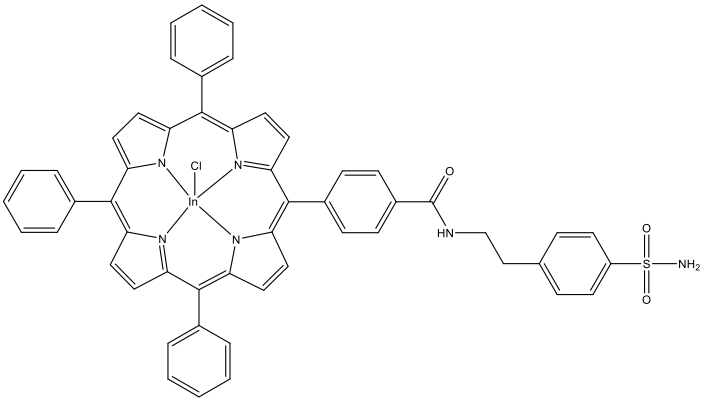


Compound **3.18** was synthesized employing general metal complexation method A. **3.16** (74.5 mg, 0.087 mmol), NaOAc (43.6 mg, 0.532 mmol), $InCl_3$ (39.2 mg, 0.177 mmol), AcOH (10 mL). A maroon colored solid was obtained. Yield: 69.7 mg, 0.070 mmol, 81 %.

**$^1$H NMR (300 MHz, DMSO-$d_6$, 25 ºC)**: 9.11 (t, 1H, *J* = 5.6, CON*H*), 9.13–9.01 (m, 8H, C$H_{pyrr}$), 8.26 (d, 2H, *J* = 7.8, Ar*H*), 8.19 (m, 8H, *o*-Ph, Ar*H*), 7.95 (d, 2H, *J* = 8.2, Ar*H*), 7.89 (m, 9H, *m,p*-Ph), 7.51 (d, 2H, *J* = 8.0, Ar*H*), 3.71 (m, 2H, CONHC$H_2$CH$_2$), 3.04 (t, 2H, *J* = 7.6, CONHCH$_2$C$H_2$).

**$^{13}$C NMR (75.5 MHz, DMSO-$d_6$, 25 ºC)**: 166.1, 148.0, 147.8, 147.7, 147.4, 144.5 144.1, 141.9, 141.3, 134.4, 134.2, 133.9, 132.54, 132.51, 132.4, 130.5, 128.1, 127.1, 125.9, 125.8, 121.5, 121.3, 120.1, 38.2. 27.4.

**Mass spec:** ESI-MS calculated for $C_{53}H_{38}InN_6O_3S$ $[M - Cl]^+$ 953.1765, found: 953.1789.

**HPLC:** (Method A) Rt = 10.12 min.

**Elem. Anal.**: Found: C; 63.9 %, H; 4.0 %, N; 8.7 %. Calc.: C; 64.4 %, H; 3.9 %, N; 8.5 %.

**5-[4-(N-(4-Sulphamoylphenethyl)benzamide)]-10,15,20-triphenyl-porphyrin gallium (III) chloride, [Ga(Cl)TPP-ABS] (3.19)**

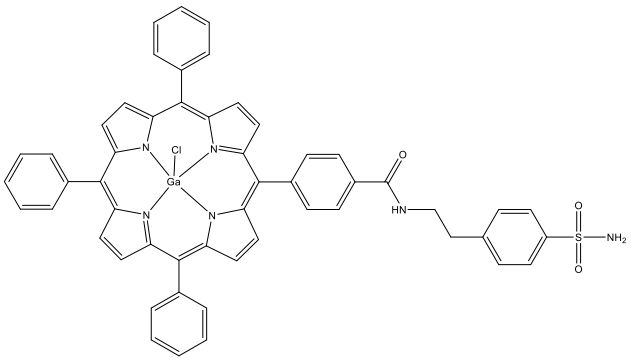


Compound **3.19** was synthesized employing general metal complexation method A. **3.16** (68.5 mg, 0.082 mmol), NaOAc (40.1 mg, 0.489 mmol), $GaCl_3$ (28.7 mg, 0.163 mmol), AcOH (10 mL). A maroon colored solid was obtained. Yield: 57.3 mg, 0.061 mmol, 74 %.

**$^1$H NMR (500 MHz, DMSO-$d_6$, 25 ºC)**: 8.92 (m, 8H, C$H_{pyrr}$), 8.76 (t, 1H, $J$ = 5.5, CON$H$), 8.32 (d, 2H, $J$ = 7.6, Ar$H$), 8.21 (d, 2H, $J$ = 7.7, Ar$H$), 8.26 (m, 6H, *o*-Ph), 7.88 (d, 2H, $J$ = 8.1, Ar$H$), 7.85 (m, 9H, *m,p*-Ph), 7.49 (d, 2H, $J$ = 7.9, Ar$H$), 3.75 (m, 2H, CONHC$H_2$CH$_2$), 3.15 (t, 2H, $J$ = 7.3, CONHCH$_2$C$H_2$).

**Mass Spectrum:** ESI-MS calculated for $C_{53}H_{38}GaN_6O_3S$ $[M - Cl]^+$ 907.1982, found: 907.1965.

**HPLC:** (Method A) Rt = 10.05 min.

**Elem. Anal.**: Found: C; 67.8 %, H; 4.3 %, N; 8.7 %. Calc.: C; 67.5 %, H; 4.1 %, N; 8.9 %.

**5-[4-(N-(4-Sulphamoylphenethyl)benzamide)]-10,15,20-tri(4-sulphonylphenyl)- porphyrin, [$H_2$TSPP-ABS] (3.20)**

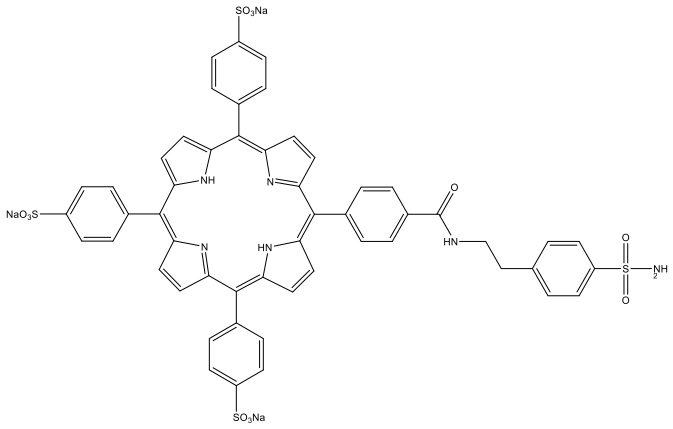


Compound **3.20** was synthesized employing the general sulphonation method. **3.16** (70.0 mg, 0.083 mmol), conc. $H_2SO_4$ (2 mL). Yield : 66.6 mg, 0.058 mmol, 70 %.

**$^1$H NMR (500 MHz, DMSO-$d_6$, 25 ºC)**: 9.05 (t, 1H, *J* = 5.7, CON*H*), 8.82 (m, 8H, C$H_{pyrr}$), 8.29 (d, 2H, *J* = 8.0, Ar*H*), 8.21 (m, 6H, Ar*HSO$_3$Na*), 8.17 (d, 2H, *J* = 8.1 Hz, Ar*H*), 8.05 (m, 6H, Ar*HSO$_3$Na*), 7.87 (d, 2H, *J* = 8.1, Ar*H*), 7.61 (d, 2H, *J* = 7.8, Ar*H*), 7.37 (s, 2H, SO$_2$N$H_2$), 3.71 (m, 2H, CONHC$H_2$CH$_2$), 3.14 (t, 1H, *J* = 7.5, CONHCH$_2$C$H_2$).

**$^{13}$C NMR (75.5 MHz, DMSO-$d_6$, 25 ºC)**: 166.1, 147.8, 144.1, 143.8, 142.5, 141.1, 134.24, 134.16, 133.7, 131.4 (broad), 131.2, 129.1, 125.9, 124.6, 120.1, 119.8, 118.9, 35.6, 26.4.

**Mass spec:** ESI-MS calculated for $C_{53}H_{37}N_6O_{12}S_4$ $[M - 3Na]^{3-}$ /3 359.0451, found: 359.0467.

**HPLC:** (Method B) Rt = 15.20 min.

**5-[4-(*N*-(4-Sulphamoylphenethyl)benzamide)]-10,15,20-tri(4-sulphonylphenyl)- porphyrin indium (III) chloride, [In(Cl)TSPP-ABS] (3.21)**

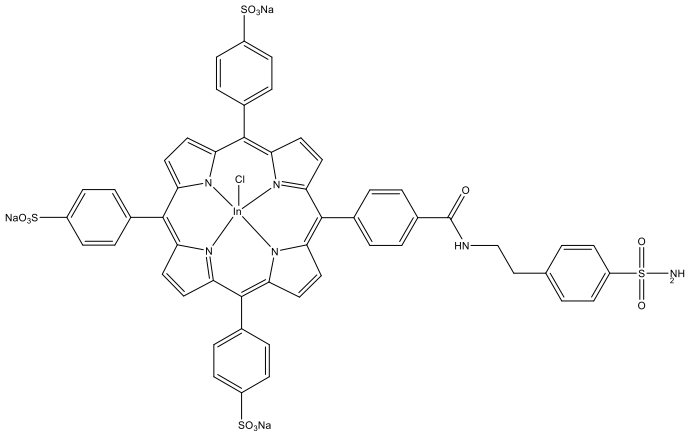


Compound **3.21** was synthesized employing general metal complexation method C. **3.20** (40.0 mg, 0.035 mmol), $InCl_3$ (15.5 mg, 0.070 mmol) in pH 4.5 NaOAc buffer (5 mL). Yield: 29.9 mg, 0.023 mmol, 66 %.

**$^1$H NMR (300 MHz, DMSO-$d_6$, 25 ºC)**: 9.07 (t, 1H, *J* = 5.4, CON*H*), 8.94 (s, 8H, C$H_{pyrr}$), 8.29 (s, 4H, Ar*H*), 8.18 (d, 6H, *J* = 8.0, Ar*HSO$_3$Na*), 8.08 (d, 6H, *J* = 8.2, Ar*HSO$_3$Na*), 7.60 (d, 2H, *J* = 8.0, Ar*H*), 7.32 (d, 2H, *J* = 8.0, Ar*H*), 3.65 (m, 2H,CONHC$H_2$CH$_2$), 3.00 (t, 2H, *J* = 7.4, CONHCH$_2$C$H_2$).

**$^{13}$C NMR (75.5 MHz, DMSO-$d_6$, 25 ºC)**: 166.3, 147.72, 147.69, 147.5, 147.4, 145.9, 144.1, 141.7, 140.3, 134.2, 134.0, 132.6 (broad), 128.1, 125.9, 125.7, 124.2, 120.8, 120.4, 35.0, 25.0.

**Mass spec:** ESI-MS calculated for $C_{53}H_{35}ClInN_6O_{12}S_4$ $[M - 3Na]^{3-}$/3 408.3313, found: 408.3345.

**HPLC:** (Method B) Rt = 13.23 min.

**5-[4-(*N*-3-(4-Nitroimidazol-1-yl)-propyl benzamide)]-10,15,20-tri(4-sulfonylphenyl)-porphyrin [$H_2$TSPP-4Nitim] (3.22)**

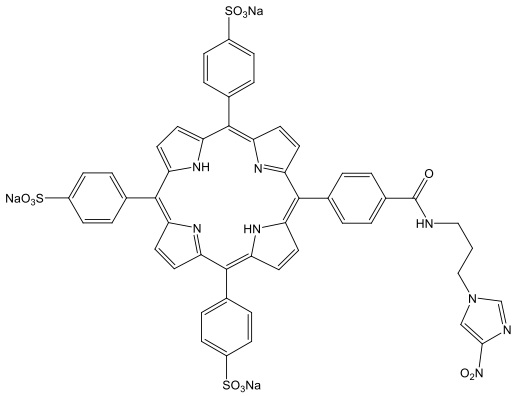


Compound **3.22** was synthesized employing the general sulfonation method. **3.3** (100 mg, 0.123 mmol), $H_2SO_4$ (2 mL). Yield: 92.1 mg, 0.082 mmol, 67 %.

**$^1$H NMR (500 MHz, DMSO-$d_6$, 25 ºC)**: δ 8.95 (t, 1H, *J* = 5.6, CONH), 8.83 (m, 8H, C$H_{pyrr}$), 8.59 (d, 1H, *J* = 1.4, C$H_{imid}$), 8.33 (d, 2H, *J* = 8.2, Ar*H*), 8.28 (d, 2H, *J* = 8.2, Ar*H*), 8.18 (d, 6H, *J* = 8.1, Ar$H_{SO3Na}$), 8.04 (d, 6H, *J* = 8.1, Ar$H_{SO3Na}$), 8.02 (d, 1H, *J* = 1.4, C$H_{imid}$), 4.27 (t, 2H, *J* = 6.8, CONHCH$_2$CH$_2$C$H_2$N$_{imid}$), 3.43 (m, 2H, CONHCH$_2$CH$_2$CH$_2$N$_{imid}$), 2.17 (qt, 2H, *J* = 6.7, CONHCH$_2$C$H_2$CH$_2$N$_{imid}$), -2.95 (s, 2H, ring N*H*).

**$^{13}$C NMR (125 MHz, DMSO-$d_6$, 25 ºC)**: δ 166.6, 147.9, 147.0, 144.0, 141.2, 137. 7, 134.2, 133.7, 133.7, 131.7, 125.9, 124.2, 121.9, 119.9, 119.8, 119.1, 45.43, 36.37, 30.32.

**Mass spec:** ESI-MS calculated for $C_{51}H_{35}N_8O_{12}S_3$ $[M - 3Na]^{3-}$/3 349.0525, found: 349.0518.

**HPLC:** (Method B) $R_t$ = 11.24 min.

**5-[4-(*N*-3-(2-Nitroimidazol-1-yl)-propylbenzamide)]-10,15,20-tri(4-sulfonylphenyl)-porphyrin [$H_2$TSPP-2Nitim] (3.23)**

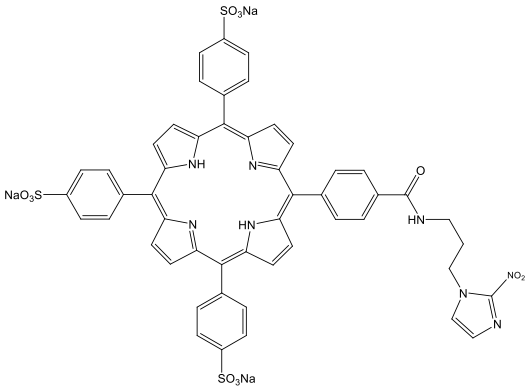


Compound **3.23** was synthesized employing the general sulfonation method. **3.4** (75 mg, 0.093 mmol), $H_2SO_4$ (2 mL). Yield: 66.5 mg, 0.017 mmol, 64 %.

**$^1$H NMR (500 MHz, DMSO-$d_6$, 25ºC)**: δ 8.95 (t, 1H, *J* = 5.6, CON*H*), 8.85 (m, 8H, C$H_{pyrr}$), 8.33 (d, 2H, *J* = 8.1, Ar*H*), 8.26 (d, 2H, *J* = 8.2, Ar*H*), 8.17 (d, 6H, *J* = 8.0Hz, Ar$H_{SO3Na}$), 8.03 (d, 6H, *J* = 8.0, Ar$H_{SO3Na}$), 7.86 (d, 1H, *J* = 0.8, C$H_{imid}$), 7.24 (d, 1H, *J* = 0.8, C$H_{imid}$), 4.57 (t, 2H, *J* = 7.0, CONHC$H_2$C$H_2$C$H_2$N$_{imid}$), 3.46 (m, 2H, CONHC$H_2$C$H_2$C$H_2$N$_{imid}$), 2.18 (qt, 2H, CONHC$H_2$C$H_2$C$H_2$N$_{imid}$), -2.95 (s, 2H, ring N*H*).

**$^{13}$C NMR (125 MHz, DMSO-$d_6$, 25 °C)**: δ 166.6, 147.9, 144.7, 144.0, 141.2, 134.2, 133.7, 133.7, 131.5, 128.1, 127.9, 125.9, 124.2, 119.9, 119.8, 199.1, 47.6, 36.5, 30.0.

**Mass spec:** ESI-MS calculated for $C_{51}H_{35}N_8O_{12}S_3$ $[M - 3Na]^{3-}$ 1049.1699, found: 1049.1647.

**HPLC** (Method B) $R_t$ = 11.14 min.

**Elem. Anal.**: Found: C; 54.3 %, H; 3.4 %, N; 10.2 %. Calc.: C; 54.8 %, H; 3.2 %, N; 10.0 %.

**5-[4-(*N*-3-(2-Nitroimidazol-1-yl)-propyl benzamide)]-10,15,20-tri(4-sulfonylphenyl)-porphyrin indium (III) chloride, [In(Cl)TSPP-2Nitim] (3.24)**

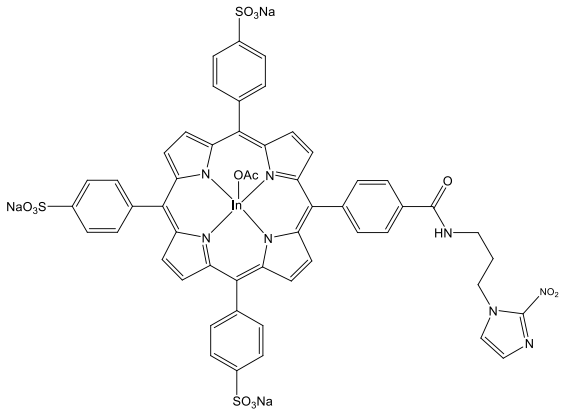

Compound **3.24** was synthesized employing general metal complexation method C. **3.23** (50.0 mg, 0.045 mmol), $InCl_3$ (19.8 mg, 0.090 mmol) in pH 4.5 NaOAc buffer (5 mL). Yield: 44.1 mg, 0.034 mmol, 76 %.

**$^1$H NMR (500 MHz, DMSO-*d*$_6$, 25 ºC)**: δ 9.05 (s, 1H, CON*H*), 8.95 (m, 8H, C*H*$_{pyrr}$), 8.32 (br s, 4H, Ar*H*), 8.18 (d, 6H, *J* = 8.0, Ar*H*$_{SO3Na}$), 8.07 (d, 6H, *J* = 7.9, Ar*H*$_{SO3Na}$), 7.90 (s, 1H, C*H*$_{imid}$), 7.24 (br s, 1H, C*H*$_{imid}$), 4.59 (t, 2H, *J* = 6.9, $CONHCH_2CH_2CH_2N_{imid}$), 2.19 (m, 2H, $CONHCH_2CH_2CH_2N_{imid}$). 1 peak obscured by water peak.

**Mass spec:** ESI-MS calculated for $C_{53}H_{37}InN_8O_{14}S_3$ $[M - 3Na+AcOH]^{2-}/2$ 610.03207, found: 610.03212.

**HPLC** (Method B) $R_t$ = 10.12 min.

**Benzyl diphenylsulphonium tetrafluoroborate**

Benzyl diphenylsulphonium tetrafluoroborate was synthesized according to a literature procedure with data in accord with the literature values [30].

***N*-Benzyl-5-[4-(*N*-propyl benzamide)],10,15,20-triphenyl-porphyrin, [N-Bz-HTPP-propyl] (benzyl-3.11)**

Benzyl diphenylsulphonium tetrafluoroborate (57.3 mg, 0.157 mmol) is added to a $CHCl_3$ (5 mL) solution of **3.11** (100 mg, 0.143 mmol) and stirred for 18 h at rt. The solution was neutralized with 1 M aqueous $NH_3$ (10 mL) and the $CHCl_3$ layer washed with water. The $CHCl_3$ is reduced to minimum volume and the crude material purified by basic alumina chromatography (2 % MeOH in DCM) to yield a green solid on removal of solvent. Yield: 97.1 mg, 0.123 mmol, 86 %.

**$^1$H NMR (500 MHz, DMSO-*d*$_6$, 25 ºC)**: δ 8.93–8.81 (m, 3H, CON*H*, C*H*$_{pyrr}$), 8.59–8.53 (m, 2H, C*H*$_{pyrr}$), 8.41–8.38 (m, 4H, C*H*$_{pyrr}$), 8.30–8.14 (m, 6H, *o*-Ph), 8.04–7.90 (m, 4H, Ar*H*), 7.84–7.78 (m, 9H, *m,p*-Ph), 6.79–6.73 (m, 1H, C*H*Bz), 6.58–6.53 (m, 2H, C*H*Bz), 4.46–4.39 (m, 2H, C*H*Bz), 3.45–3.39 (m, 2H, $CONHCH_2CH_2CH_3$), 1.62–1.57 (m, 2H, $CONHCH_2CH_2CH_3$), 1.05–0.93 (m, 3H, $CONHCH_2CH_2CH_3$), -2.00- -2.02 (br s, 1H, ring N*H*), -3.60- -3.70 (dd, 2H, C*H*Bz).

**Mass spec:** MALDI-MS calculated for $C_{55}H_{45}N_5O$ $[M]^+$ 789.9628, found: 789.9661.

**Elem. Anal.**: Found: C; 83.0 %, H; 5.1 %, N; 8.2 %. Calc.: C; 83.6 %, H; 4.9 %, N; 8.9 %.

**5-[4-(*N*-(4-Sulphamoylphenethyl)benzamide)]-10,15,20-tri(4-*N*-methylpyridinium phenyl)-porphyrin tri-iodide, [H2TMePyP-ABS] (6.1)**

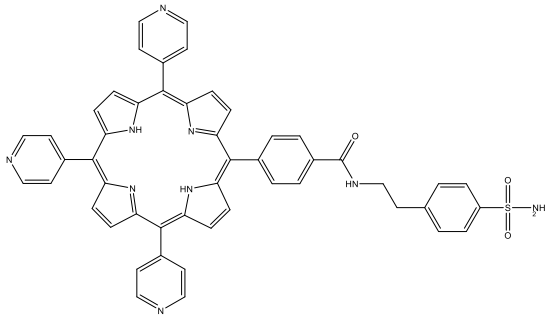

Compound **[$H_2$TPyP-ABS]** was synthesized employing general amide coupling method B. **6** (130 mg, 0.184 mmol), DIPEA (67.4 mg, 90.9 µL 0.522 mmol), 4-(2- aminoethyl)benzene sulphonamide (110 mg, 0.552 mmol), BOP (244 mg, 0.552 mmol), DMF (3 mL). **6.1** was purified via silica gel chromatography (2 to 8 % MeOH in CHCl3). Yield: 126 mg, 0.149 mmol, 81 %.

**$^1$H NMR (500 MHz, DMSO-$d_6$, 25 ºC)**: 9.08 (t, 1H, *J* = 5.4, CON*H*), 9.02 (m, 6H, C$H_{py}$), 8.88 (m, 8H, C$H_{pyrr}$), 8.29 (d, 2H, *J* = 8.3, Ar*H*), 8.27 (d, 2H, *J* = 8.3, Ar*H*), 8.25 (m, 6H, C$H_{py}$), 7.81 (d, 2H, *J* = 8.2, Ar*H*), 7.55 (d, 2H, *J* = 8.2, Ar*H*), 7.35 (s, 2H, $SO_2NH_2$), 3.68 (m, 2H, CONHC$H_2$CH$_2$), 3.07 (t, 2H, *J* = 7.1, CONHCH$_2$C$H_2$), -3.05 (s, 2H, ring N*H*).

**$^{13}$C NMR (125 MHz, DMSO-$d_6$, 25ºC)**: 166.9, 149.5, 149.0, 144.5, 144.3, 142.8, 134.9, 131.3 (broad) 129.9, 129.8, 126.6, 126.5, 120.8, 118.3, 118.1, 35.6, 25.6.

**Mass spec:** ESI-MS calculated for $C_{50}H_{37}ClN_9O_3S$ $[M + Cl]^-$ 878.2434, found: 878.2449.

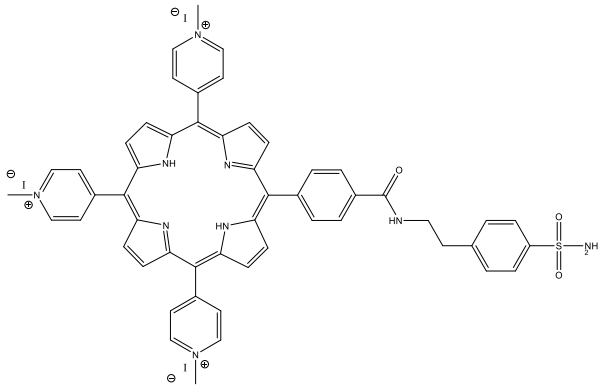

Compound **6.1** was synthesized employing the general alkylation method. **[$H_2$TPyP-ABS]** (65.0 mg, 0.077 mmol), MeI (109 mg, 47.9 µL, 0.77 mmol), DMF. Yield: 114 mg, 0.090 mmol, 92 %.

**$^1$H NMR (500 MHz, DMSO-$d_6$, 25ºC)**: 9.46 (m, 6H, C$H_{py}$), 9.11 (m, 8H, C$H_{pyrr}$), 9.02 (t, 1H, *J* = 5.4, CON*H*), 8.99 (m, 6H, C$H_{py}$), 8.32 (d, 2H, *J* = 8.7, Ar*H*), 8.30 (d, 2H, *J* = 8.8, Ar*H*), 7.81 (d, 2H, *J* = 8.3, Ar*H*), 7.56 (d, 2H, *J* = 8.4, Ar*H*), 7.34 (s, 2H, $SO_2NH_2$), 4.70 (m, 3x3H, 3xN-C$H_3$), 3.70 (m, 2H, CONHC$H_2$CH$_2$), 3.07 (t, 2H, *J* = 6.9, CONHCH$_2$C$H_2$), -3.06 (m, 1H).

**$^{13}$C NMR (125 MHz, DMSO-$d_6$, 25ºC)**: 166.2, 156.6, 156.5, 144.3, 144.2, 143.9, 143.1, 142.1, 134.4, 134.3, 132.1, 129.3, 126.0, 125.8, 124.1, 121.9, 115.4, 114.7, 114.5, 111.8, 47.9, 34.5, 25.3.

**Mass spec:** ESI-MS calculated for $C_{53}H_{44}N_9O_3S$ [M – 3I]$^{3+/3}$ 269.1143, found 269.1143, ESI-MS calculated for $C_{53}H_{44}N_9O_3S$ [M – 3I]$^{3+/2}$ 444.1717, found: 444.1708.

**HPLC:** (Method C) Rt = 12.22 min.

**Elem. Anal.**: Found: C; 50.3 %, H; 3.3 %, N; 9.8 %. Calc. [**6.1** + MeOH]: C; 49.9 %, H; 3.7 %, N; 9.7 %.

**5-[4-(*N*-(4-Sulphamoylphenethyl)benzamide)]-10,15,20-tri(4-*N*-methylpyridiniumyl phenyl)-porphyrin tri-chloride indium (III) chloride, [In(Cl)TMePyP-ABS] (6.2)**

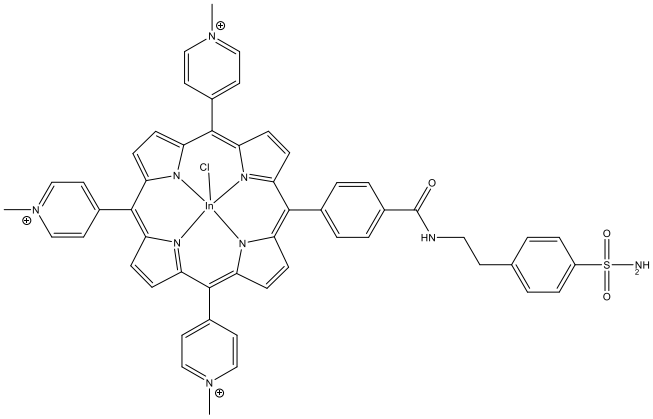

Compound **6.2** was synthesized employing general metal complexation method C. **6.1** (50.0 mg, 0.039 mmol), $InCl_3$ (17.4 mg, 0.079 mmol) in pH 4.5 NaOAc buffer (5 mL). Yield: 30.3 mg, 0.027 mmol, 68 %.

**$^1$H NMR (500 MHz, DMSO-*d*$_6$, 25 ºC)**: 9.41–9.67 (m, 6H, C*H*$_{py}$), 9.23–9.35 (br s, 4H C*H*$_{pyrr}$), 9.13–9.23 (br s, 3H, CON*H,* C*H*$_{pyrr}$), 9.02–9.11 (br s, 2H, C*H*$_{pyrr}$), 8.87–9.00 (br s, 6H, C*H*$_{py}$), 8.36 (d, 2H, *J* = 7.5, Ar*H*), 8.30 (d, 2H, *J* = 7.5, Ar*H*), 7.81 (d, 2H, *J* = 8.0, Ar*H*), 7.55 (d, 2H, *J* = 8.0, Ar*H*), 7.36 (s, 2H, $SO_2NH_2$), 4.66–4.87 (br s, 9H, 3x$CH_3$), 3.69 (m, 2H, CONHC$H_2$CH$_2$), 3.09–3.16 (t, 2H, *J* = 5.7, CONHCH$_2$C$H_2$).

**$^{13}$C NMR (75.5 MHz, DMSO-*d*$_6$, 25 ºC)**: 166.7, 156.6, 156.5, 147.8, 146.5, 146.4, 144.8, 144.3, 144.2, 142.9, 133.8, 133.3, 132.4, 132.3, 129.8, 126.2, 126.1, 117.3, 116.8, 48.1, 47.9, 35.1, 26.2.

**Mass Spectrum:** ESI-MS calculated for $C_{53}H_{42}ClInN_9O_3S$ [M – 3Cl]$^{3+/3}$ 344.7281, found 344.7298.

**HPLC:** (Method C) Rt = 12.05 min.

**5-[4-(*N*-3-(2-Nitroimidazol-1-yl)-propyl benzamide)]-10,15,20-tri(4-pyridyl)- porphyrin, [TPyP-2Nitim] (6.3)**

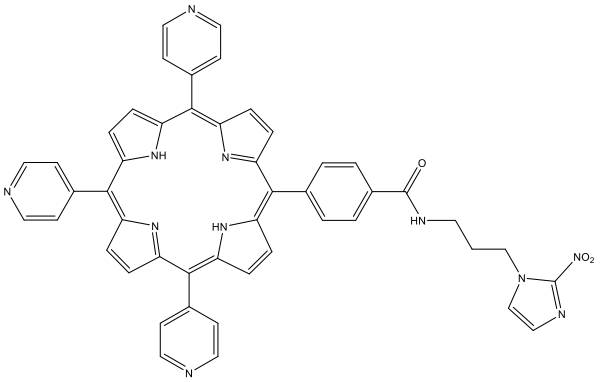

Compound **6.3** was synthesized employing general amide coupling method B. **6** (100 mg, 0.151 mmol), DIPEA (51.6 mg, 69.7 µL 0.400 mmol), **8** (38.0 mg, 0.181 mmol), BOP (90.0 mg, 0.195 mmol), DMF (2 mL). **6.3** was purified *via* silica gel chromatography (1 % to 7 % MeOH in $CHCl_3$). Yield: 84.7 mg, 0.104 mmol, 69 %.

**$^1$H NMR (300 MHz, DMSO-*d*$_6$, 25 ºC)**: 9.46 (d, 6H, *J* = 5.2, C*H*py), 9.05–9.23 (m, 8H, C$H_{pyrr}$), 8.95–9.04 (m, 6H, C$H_{py}$), 8.91 (t, 1H, *J* = 5.6, CON*H*), 8.31 (s, 4H, Ar*H*), 7.79 (s, 1H, C$H_{imid}$), 7.26 (s, 1H, C$H_{imid}$), 4.27 (t, 2H, *J* = 6.7, $CONHCH_2CH_2CH_2N_{imid}$), 3.35 (m, 2H, $CONHCH_2CH_2CH_2N_{imid}$), 2.18 (qt, 2H, *J* = 6.7, $CONHCH_2CH_2CH_2N_{imid}$), -3.05 (br. s, 2H, ring N*H*).

**$^{13}$C NMR (75.5 MHz, DMSO-*d*$_6$, 25 ºC)**: 166.4, 150.4, 148.82, 148.80, 148.3, 144.7, 143.6, 134.2, 134.1, 131.6,(broad), 129.2, 128.1, 127.9, 126.0, 120.2, 117.7, 117.4, 47.6, 36.5, 30.0.

**Mass spec:** ESI-MS calculated for $C_{48}H_{34}N_{11}O_3$ $[M - H]^-$ 812.2852, found: 812.2854.

**Elem. Anal.**: Found: C; 55.2 %, H; 3.3 %, N; 9.8 %. Calc.: C; 54.8 %, H; 3.2 %, N; 10.0 %.

**5-[4-(*N*-3-(2-Nitroimidazol-1-yl)-propyl benzamide)]-10,15,20-tri(4-methyl pyridinium)-porphyrin, [TMPyP-2Nitim] (6.4)**

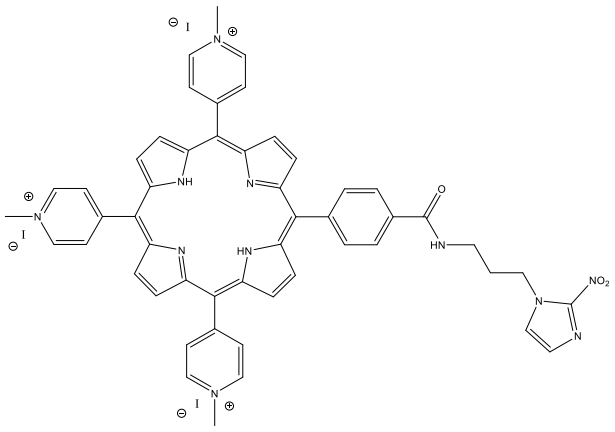

Compound **6.4** was synthesized employing the general pyridine alkylation method. **6.3** (60.0 mg, 0.046 mmol), MeI (65.3 mg, 28.6 µL, 0.46 mmol), DMF (5 mL). Yield: 50.2 mg, 0.040 mmol, 88 %.

**$^{1}$H NMR (500 MHz, DMSO-*d*$_6$, 25 ºC)**: 9.43–9.58 (m, 6H, C*H*$_{py}$), 9.06–9.26 (m, 8H, C*H*$_{pyrr}$), 9.00–9.06 (m, 6H, C*H*$_{py}$), 8.98 (t, 1H, *J* = 5.7, CON*H*), 8.37 (m, 4H, Ar*H*), 7.88 (d, 1H, *J* = 1.3, C*H*$_{imid}$), 7.28 (d, 1H, *J* = 1.3, C*H*$_{imid}$), 4.74 (m, 3x3H, 3x N-C*H*$_3$), 4.60 (t, 2H, *J* = 6.9, CONHCH$_2$CH$_2$C*H*$_2$N$_{imid}$), 3.51 (m, 2H, CONHC*H*$_2$CH$_2$CH$_2$N$_{imid}$), 2.22 (qt, 2H, *J* = 6.9, CONHCH$_2$C*H*$_2$CH$_2$N$_{imid}$), -3.02 (s, 2H, ring N*H*).

**$^{13}$C NMR (125 MHz, DMSO-*d*$_6$, 25 ºC)**: 166.3, 162.3, 156.52, 156.46, 144.7, 144.2, 143.1, 134.4, 134.2, 132.1, 131.5 (broad) 127.97, 127.95, 126.1, 121.9, 115.4, 114.8, 48.6, 47.5, 35.8, 30.8.

**Mass spec:** ESI-MS calculated for $C_{51}H_{44}N_{11}O_3$ $[M - 3I]^{3+/2}$ 428.6770, found: 428.6768.

**HPLC:** (Method C) Rt = 11.18 min.

**5-[4-(*N*-3-(2-Nitroimidazol-1-yl)-propyl benzamide)]-10,15,20-tri(4-methyl pyridinium)-porphyrin trichloride indium (III) chloride, [In(Cl)TMPyP-2Nitim] (6.5)**

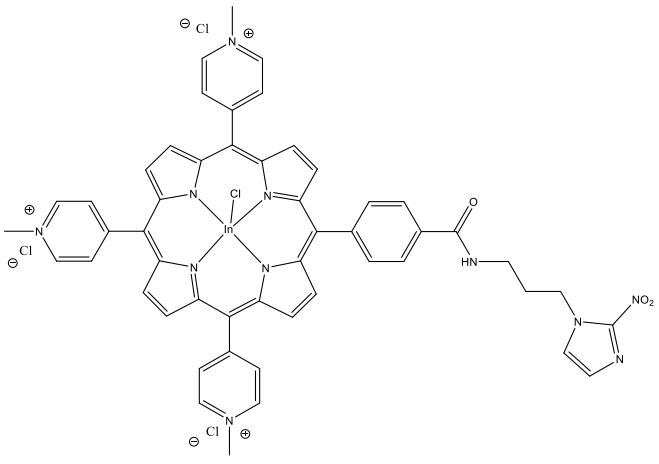

Compound **6.5** was synthesized employing general metalation method C. **6.4** (35.0 mg, 0.028 mmol), $InCl_3$ (12.5 mg, 0.056 mmol) in pH 4.5 NaOAc buffer (5 mL). Yield: 18.4 mg, 0.017 mmol, 59 %.

**$^1$H NMR (500 MHz, DMSO-*d*$_6$, 25 ºC)**: 9.53 (m, 6H, Ar*H*), 9.26 (m, 4H, C*H*$_{pyrr}$), 9.21 (d, 2H, *J* = 4.7, C*H*$_{pyrr}$), 9.13 (d, 2H, *J* = 4.7, C*H*$_{py}$), 8.94 (m, 6H, C*H*$_{py}$), 8.41 (d, 2H, *J* = 8.2, Ar*H*), 8.34 (d, 2H, *J* = 8.2, Ar*H*), 7.93 (s, 1H, C*H*$_{imid}$), 7.28 (s, 1H, C*H*$_{imid}$), 4.75 (m, 3x3H, 3xN-C*H*$_3$), 4.62 (t, 2H, *J* = 7.1, CONHCH$_2$CH$_2$C*H*$_2$N$_{imid}$), 3.50 (m, 2H, CONHC*H*$_2$CH$_2$CH$_2$N$_{imid}$), 2.17 (qt, 2H, *J* = 6.9, CONHCH$_2$C*H*$_2$CH$_2$N$_{imid}$).

**$^{13}$C NMR (125 MHz, DMSO-*d*$_6$, 25 ºC)**: 166.2, 156.56, 156.54, 148.3, 147.0, 146.7, 146.5, 144.7, 144.2, 134.5, 134.0, 133.4, 133.1, 132.8, 132.7, 132.4, 128.01, 127.95, 126.1, 116.3, 115.5, 48.4, 47.9, 35.8, 30.7.

**Mass spec:** ESI-MS calculated for $C_{51}H_{42}ClInN_{11}O_3$ $[M - 3Cl]^{3+/2}$ 502.6055, found: 502.6051.

**HPLC:** (Method C) Rt = 10.22 min.

**5-[4-(N-propyl benzamide)]-10,15,20-tri(4-pyridyl)-porphyrin, [TPyP-propyl]**

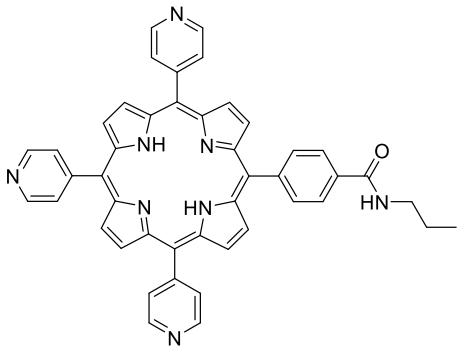


5-[4-(N-propyl benzamide)]-10,15,20-tri(4-pyridyl)-porphyrin was synthesized employing general amide coupling method B. 2.24 (75 mg, 0.113 mmol), DIPEA (38.7 mg, 52.3 µL 0.300 mmol), propylamine (7.97 mg, 8.04 µL, 0.135 mmol), BOP (67.5 mg, 0.146 mmol), CHCl3 (10 mL). 5-[4-(N-propyl benzamide)]-10,15,20-tri(4-pyridyl)-porphyrin was purified via silica gel chromatography (0 % to 5 % MeOH in $CHCl_3$). Yield: 65.2 mg, 0.093 mmol, 82 %.

**$^1$H NMR (300 MHz, DMSO-*d*$_6$, 25 ºC)**: 9.40 (d, 6H, *J* = 6.1, CH$_{py}$), 9.14 (m, 8H, CH$_{pyrr}$), 8.91 (m, 6H, CH$_{py}$), 8.65 (t, 1H, *J* = 5.5, CONH), 8.27 (d, 2H, J = 7.9, ArH), 8.15 (d, 2H, *J* = 8.1, ArH), 3.52 (m, 2H, CONHCH$_2$CH$_2$CH$_3$), 1.81 (m, 2H, CONHCH$_2$CH$_2$CH$_3$), 1.07 (t, 2H, *J* = 6.9, CONHCH$_2$CH$_2$CH$_3$), -2.95 (br s, 2H, ring NH).

**Mass Spectrum**: ESI-MS calculated for $C_{44}H_{35}N_8O$ $[M + H]^+$ 703.2928, found: 703.2935.

**5-[4-(Propyl benzamide)]-10,15,20-tri(4-methyl pyridinium)-porphyrin, [TMPyPpropyl] (6.6)**

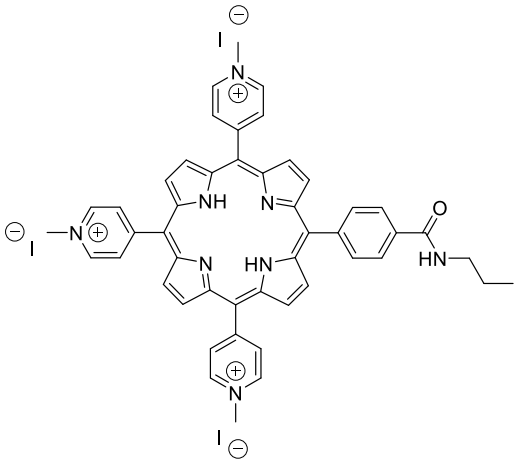

Compound 3.15 was synthesized employing the general pyridine alkylation method. 5-[4-(Npropylbenzamide)]-10,15,20-tri(4-pyridyl)-porphyrin (60.0 mg, 0.085 mmol), MeI (1.21 g, 528 µL, 8.50 mmol), DMF (5 mL). Yield: 91.1 mg, 0.081 mmol, 95 %.

**$^{1}$H NMR (300 MHz, DMSO-*d*$_6$, 25 ºC)**: 9.57 (m, 6H, $CH_{py}$), 9.18 (m, 8H, $CH_{pyrr}$), 8.97 (m, 6H, $CH_{py}$), 8.88 (t, 1H, *J* = 5.5, CONH), 8.37 (d, 2H, *J* = 7.7, ArH), 8.29 (d, 2H, *J* = 7.9, ArH), 4.69 (m, 3x3H, 3x N-CH3), 3.67 (t, 2H, *J* = 6.6, $CONHCH_2CH_2CH_3$), 1.92 (m, 2H, $CONHCH_2CH_2CH_3$), 1.10 (t, 3H, *J* = 6.7, $CONHCH_2CH_2CH_3$), -2.87 (s, 2H, ring NH).

**Mass spec:** ESI-MS calculated for $C_{48}H_{43}N_8O$ $[M - 3I]^{3+/2}$ 373.6772, found: 373.6794.

**HPLC:** (Method C) Rt = 10.25 min.

**3-(4-Nitroimidazol-1-yl) propanoic acid (10)**

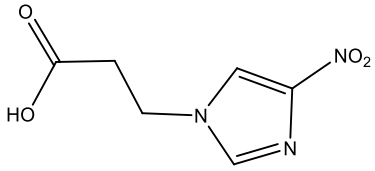

3-(4-Nitroimidazol-1-yl)propanoic acid was synthesized according to a literature procedure.[31] Aqueous 1 M NaOH (6 mL) was added dropwise over 15 min to a suspension of methyl-3-(4-nitroimidazol-1-yl) propanoate (250 mg, 1.254 mmol) in water (2 mL). After 20 min the solution was neutralized with aqueous 6 M HCl (1 mL). The precipitate was filtered and washed with ether to yield 3-(4-Nitroimidazol-1-yl) propanoic acid as a white solid. Yield: 507 mg, 2.74 mmol, 92 %.

**$^{1}$H NMR (300 MHz, DMSO-*d*$_6$, 25 ºC)**: δ 12.42 (s, 1H, COO*H*), 8.43 (d, 1H, *J* = 1.2, C*H*$_{imid}$), 7.85 (d, 1H, *J* = 1.3, C*H*$_{imid}$), 4.27 (t, 2H, *J* = 6.6, $NCH_2CH_2CO_2H$), 2.83 (2H, t, *J* = 6.7 Hz, $NCH_2CH_2CO_2H$).

**$^{13}$C NMR (75.5 MHz, DMSO-*d*$_6$, 25 ºC)**: δ 172.5, 147.6, 137.8, 120.4, 44.2, 35.0.

**Mass spec:** ESI-MS calculated for $C_6H_6N_3O_4$ $[M - H]^-$ 184.0364, found: 184.0352.

**3-(2-Nitroimidazol-1-yl) propanoic acid (11)**

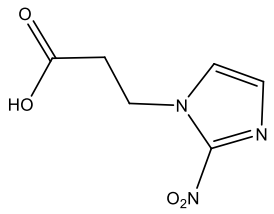

3-(2-Nitroimidazol-1-yl) propanoic acid was synthesized by an analogous route to 3-(4-Nitroimidazol-1-yl) propanoic acid. Methyl 3-(2-nitromidazol-1-yl) propanoate (300 mg, 1.50 mmol). Yield: 257 mg, 1.39 mmol, 93 %.

**$^1$H NMR (300 MHz, DMSO-*d*$_6$, 25 ºC)**: δ 7.62 (s, 1H, C*H*$_{imid}$), 7.12 (s, 1H, C*H*$_{imid}$), 4.51 (t, 2H, *J* = 6.7 Hz, $NCH_2CH_2COOMe$), 2.91 (t, 2H, *J* = 6.7 Hz, $NCH_2CH_2COOMe$).

**Mass spec:** ESI-MS calcd for $C_6H_6N_3O_4$ $[M + H]^+$ 184.0358, found: 184.0362.

**5-[4-(*2*-amino-propanamide)phenyl]-10,15,20-triphenyl-porphyrin, [$H_2$TPP-ala] (4.3)**

**a) 5-[4-(2-Boc-amino-propanamide)phenyl]-10,15,20-triphenyl-porphyrin, [$H_2$TPPala-Boc]**

5-(4-Aminophenyl)-10,15,20-triphenylporphyrin (115 mg, 0.183 mmol) was dissolved in DCM (15 mL) with DMAP (200 mg, 1.64 mmol) and Boc-alanine N-succinimidyl ester (200 mg, 0.70 mmol) and heated under reflux for 15 h at which point TLC ($CHCl_3$:MeOH, 95:5) indicated complete consumption of starting material. The solvent was removed under reduced pressure and the residue re-dissolved in $CHCl_3$. The solution was washed with water and brine and dried over anhydrous magnesium sulphate. The $CHCl_3$ was reduced to minimum volume under reduced pressure and the crude amide was purified by silica gel chromatography ($CHCl_3$:MeOH, 98:2) to give a purple solid on removal of solvent. Yield: 105 mg, 0.131 mmol, 72 %.

**$^1$H NMR ($CDCl_3$, 300 MHz, 20 ºC)**: 8.80 (d, 1H, *J* = 4.8, CON*H*), 8.77 (m, 8H, C*H*$_{pyrr}$), 8.14 (m, 6H, *o*-Ph), 8.11 (d, 2H, *J* = 8.4, Ar*H*), 7.86 (d, 2H, *J* = 8.4, Ar*H*), 7.69 (m, 9H, *m,p*-Ph), 4.42 (qt, 1H, *J* = 7.1 Hz, C*H*Me), 1.38 (s, 9H, tBu), 1.31 (d, 3H, *J* = 7.1, CH*CH*$_3$), -2.81 (s, 2H, ring N*H*).

**$^{13}$C NMR ($CDCl_3$, 75.5 MHz, 25 ºC)**: 181.4, 169.4, 141.5, 139.1, 136.7, 135.4, 135.1, 132.0 (broad), 128.2, 127.4, 121.9, 117.6, 79.2, 48.7, 28.6, 19.1.

**Mass spec:** ESI-MS calculated for $C_{52}H_{44}N_6O_3$ $[M + H]^+$ 801.3571, found: 801.3553.

**b) 5-[4-(*2*-Amino-propanamide)phenyl]-10,15,20-triphenyl-porphyrin, [$H_2$TPP-ala] (4.3)**

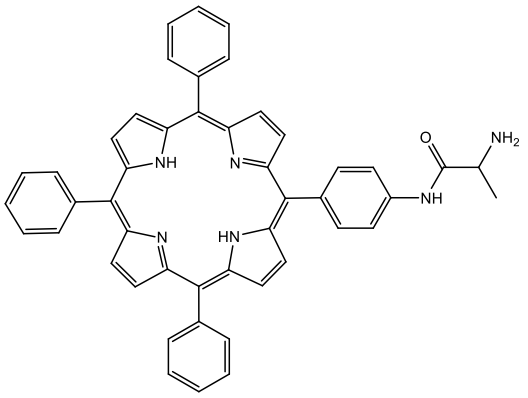

To a $CHCl_3$ (5 mL) solution of 5-[4-(*2-Boc*-amino-propanamide)phenyl]-10,15,20-triphenyl-porphyrin (105 mg, 0.131 mmol) is added TFA (1 mL) and the solution stirred overnight at rt. The solvent is removed under reduced pressure and the residue redissolved in DCM and the solution washed with water, saturated $Na_2HCO_3$ and brine and dried over anhydrous magnesium sulfate. The solvent was removed under reduced pressure to give a purple solid. Yield: 88.4 mg, 0.126 mmol, 96 %.

**$^1$H NMR (300 MHz, $CDCl_3$, 20 ºC)**: δ 9.80 (s, 1H, CON*H*), 8.78 (m, 8H, C$H_{pyrr}$), 8.11 (m, 6H, *o*-Ph), 8.05 (d, 2H, *J* = 8.3, Ar*H*), 7.91 (d, 2H, *J* = 8.3, Ar*H*), 7.64 (m, 9H, *m,p*-Ph), 3.71 (qt, 1H, *J* = 6.9 Hz, C*H*Me), 1.82 (s, 2H, N$H_2$), 1.47 (d, 3H, *J* = 6.8, CH$CH_3$), -2.92 (s, 2H, ring N*H*).

**$^{13}$C NMR (75.5 MHz, $CDCl_3$, 20 ºC)**: δ 170.1, 141.2, 139.5, 136.7, 135.2, 134.6, 132.4 (broad), 128.5, 127.3, 121.9, 117.9, 45.3, 17.8.

**Mass Spec:** ESI-MS calculated for $C_{47}H_{36}N_6O$ $[M + H]^+$ 701.3029, found: 701.2897.

**5-[4-(2-(3-(4-Nitroimidazol-1-yl)propanamido)propanamide)phenyl],10,15,20-triphenyl-porphyrin, [$H_2$TPP-ala-4Nitim] (4.4)**

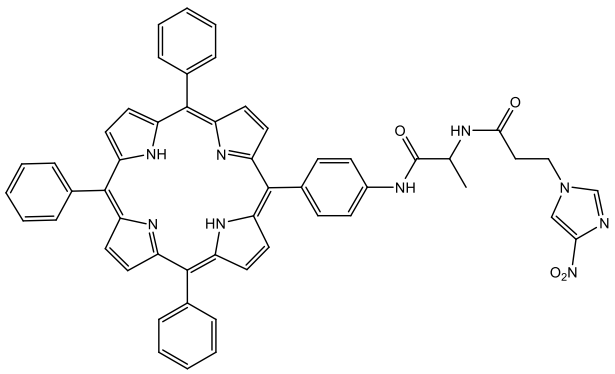

**10** (125 mg, 0.443 mmol) was added to a solution of porphyrin **4.3** (300 mg, 0.443 mmol) and $NEt_3$ (240 mg, 331 µL, 2.371 mmol) in DMF (4 mL) and heated under reflux for 16 h. The reaction mixture was cooled to rt and the DMF removed under reduced pressure. The residue was re-dissolved in $CHCl_3$ and the solution washed with water, brine and

dried over anhydrous magnesium sulfate. The $CHCl_3$ was reduced to minimum volume under reduced pressure and the product was purified by silica gel chromatograpy ($CHCl_3$/MeOH 19:1) to yield **4.4** as a purple solid. Yield: 285 mg, 0.328 mmol, 74 %.

**$^1$H NMR (500 MHz, DMSO-*d*$_6$, 25 ºC)**: δ 10.54 (s, 1H, CON*H*), 8.84 (m, 8H, C*H*$_{pyrr}$), 8.52 (d, 1H, *J* = 7.2, CON*H*CHMe), 8.38 (d, 1H, *J* = 1.3, C*H*$_{imid}$), 8.19 (m, 6H, *o-Ph*), 8.13 (d, 2H, *J* = 8.5, Ar*H*), 8.08 (d, 2H, *J* = 8.5, Ar*H*), 7.86 (d, 1H, *J* = 1.3, C*H*$_{imid}$) , 7.81 (m, 9H, *m,p*-Ph), 4.60 (qt, 1H, *J* = 7.0, $CH_3$C*H*NHCO), 4.38 (t, 2H, *J* = 6.6, NHCOCH$_2$C*H*$_2$N$_{imid}$), 2.85 (t, 2H, *J* = 6.5, NHCOC*H*$_2$CH$_2$N$_{imid}$), 1.43 (d, 3H, *J* = 7.1, C*H*$_3$), -2.88 (s, 2H, ring N*H*).

**$^{13}$C NMR (125 MHz, DMSO-*d*$_6$, 25 ºC)**: δ 172.1, 169.7, 147.8, 141.7, 139.4, 138.0, 136.5, 135.2, 134.7, 131.9 (broad), 128.5, 127.4, 122.2, 120.4, 118.1, 49.8, 44.3, 36.1, 18.6.

**Mass spec:** ESI-MS calculated for $C_{53}H_{42}N_9O_4$ $[M + H]^+$ 868.3360, found: 868.3358.

**HPLC** (Method A):$R_t$ = 10.47 min.

**Elem. Anal.**: Found: C; 73.5 %, H; 5.0 %, N; 14.1 %. Calc.: C; 73.3 %, H; 4.8 %, N; 14.5 %.

**5-[4-(2-(3-(2-Nitroimidazol-1-yl)propanamido)propanamide)phenyl]-10,15,20-triphenyl-porphyrin, [H$_2$TPP-ala-2Nitim] (4.5)**

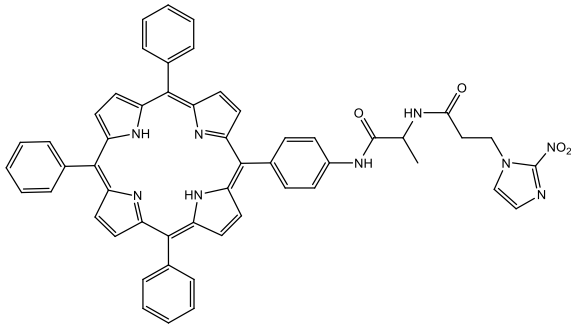


**11** (50.0 mg, 0.185 mmol) was added to a solution of porphyrin **4.3** (100 mg, 0.143 mmol) and $NEt_3$ (145 mg, 200 µL, 1.434 mmol) in DMF (5 mL) and heated under reflux for 16 h. The reaction mixture was cooled to rt and the DMF was removed under reduced pressure. The residue was re-dissolved in $CHCl_3$ and the solution washed with water, brine and dried over anhydrous magnesium sulfate. The $CHCl_3$ was reduced to minimum volume under reduced pressure and the product was purified by silica gel chromatography ($CHCl_3$/MeOH 19:1). **4.5** was recrystallized ($CHCl_3$/hexanes) to yield a purple solid. Yield: 98.1 mg, 0.113 mmol, 79 %.

**$^1$H NMR (500 MHz, DMSO-*d*$_6$, 25 ºC )**: δ 10.49 (s, 1H, N*H*COCH($CH_3$)), 8.85 (m, 8H, C*H*$_{pyrr}$), 8.48 (d, 1H, *J* = 7.2, $CH_3$CHN*H*), 8.20 (m, 6H, *o*-Ar*H*), 8.15 (d, 2H, *J* = 8.5, Ar*H*), 8.05 (d, 2H, *J* = 8.6, Ar*H*), 7.82 (m, 9H, *m, p*-Ar*H*), 7.60 (d, 1H, *J* = 1.0, C*H*$_{imid}$), 7.17 (d, 1H, *J* = 1.0, C*H*$_{imid}$), 4.65 (t, 2H, *J* = 6.7, NHCOCH$_2$C*H*$_2$N$_{imid}$), 4.57 (m, 1H, C*H*$CH_3$), 2.82 (t, 2H, *J* = 6.9, NHCOC*H*$_2$CH$_2$N$_{imid}$ ), 1.38 (d, 3H, *J* = 7.1, C*H*$_3$), -2.94 (s, 1H. ring N*H*).

**$^{13}$C NMR (125 MHz, DMSO-*d*$_6$, 25 ºC)**: 171.6, 169.2, 144.8, 141.2, 139.0, 136.0, 134.7, 134.2, 131.5 (broad), 128.1, 127.6, 127.0, 120.0, 117.6, 49.4, 45.9, 36.4, 24.8.

**Mass spec:** ESI-MS calculated for $C_{53}H_{41}NaN_9O_4$ $[M + Na]^+$ 890.3174, found: 890.3153.

**HPLC** (Method A): $R_t$ = 10.58 min.

**Elem. Anal.**: Found: C; 73.3 %, H; 5.2 %, N; 14.7 %. Calc.: C; 73.3 %, H; 4.8 %, N; 14.5 %.

**5-[4-(2-(3-(4-Nitroimidazol-1-yl)propanamido)propanamide)phenyl]-10,15,20-triphenyl-porphyrin gallium (III) chloride, [Ga(Cl)TPP-ala-4Nitim] (4.6)**

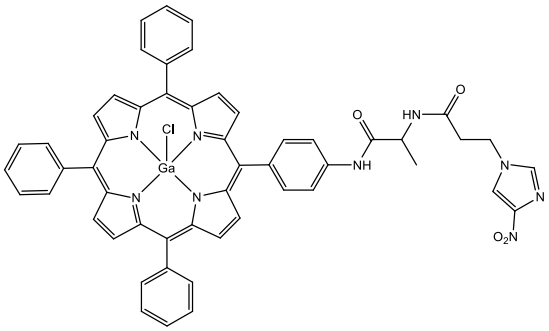


Compound **4.6** was synthesized employing general metal complexation method A. **4.4** (100 mg, 0.115 mmol), NaOAc (56.7 mg, 0.691 mmol), $GaCl_3$ (22.2 mg, 0.126 mmol), AcOH (10 mL). A maroon solid was obtained. Yield: 87.1 mg, 0.090 mmol, 78 %.

**$^1$H NMR (500 MHz, DMSO-*d*$_6$, 25 ºC)**: δ 10.53 (br s, 1H, CON*H*), 9.12–8.82 (m, 8H, C*H*$_{pyrr}$), 8.58 (br s, 1H, CON*H*) 8.39 (s, 1H, C*H*$_{imid}$), 8.29 (m, 7H, C*H*$_{imid}$, *o-Ph*), 7.96 (br. s, 2H, Ar*H*), 7.98 (br s, 2H, Ar*H*), 7.83 (m, 9H, *m-,p-Ph*), 4.56 (m, 1H, CONHC*H*Me), 4.37 (m, 2H, CONHC*H*$_2$CH$_2$N$_{imid}$), 2.82 (t, 2H, *J* = 6.3, CONHCH$_2$C*H*$_2$N$_{imid}$), 1.40 (d, 3H, *J* = 7.3, CONHCHC*H*$_3$).

**Mass spec:** ESI-MS calculated for $C_{53}H_{39}GaN_9O_4$ $[M - Cl]^+$ 934.2381, found: 934.2148.

**HPLC:** (Method A) $R_t$ = 9.71 min.

**Elem. Anal.**: Found: C; 66.2 %, H; 4.3 %, N; 12.8 %. Calc.: C; 65.6 %, H; 4.1 %, N; 13.0 %.

**5-[4-(2-(3-(4-Nitroimidazol-1-yl)propanamido)propanamide)phenyl]-10,15,20-triphenyl-porphyrin copper (II), [CuTPP-ala-4Nitim] (4.7)**

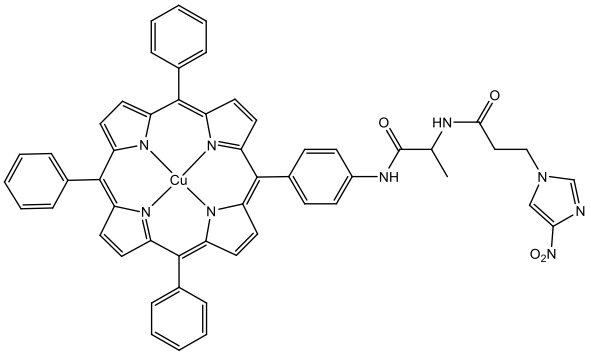

Compound **4.7** was synthesized employing general metal complexation method B. **4.4** (100 mg, 0.115 mmol), $Cu(OAc)_2 \cdot H_2O$ (65.8 mg, 0.330 mmol), DMF (10 mL). A red solid was obtained. Yield: 89.8 mg, 0.097 mmol, 84 %.

**Mass spec:** ESI-MS calculated for $C_{53}H_{39}CuNaN_9O_4$ $[M + Na]^+$ 951.2313, found: 951.2234.

**HPLC:** (Method A) $R_t$ = 10.23 min.

**Elem. Anal.**: Found: C; 68.9 %, H; 4.6 %, N; 13.2 %. Calc.: C; 68.5 %, H; 4.2 %, N; 13.6 %.

**5-[4-(2-(3-(2-Nitroimidazol-1-yl)propanamido)propanamide)phenyl]-10,15,20-triphenyl-porphyrin copper (II), [CuTPP-ala-4Nitim] (4.8)**

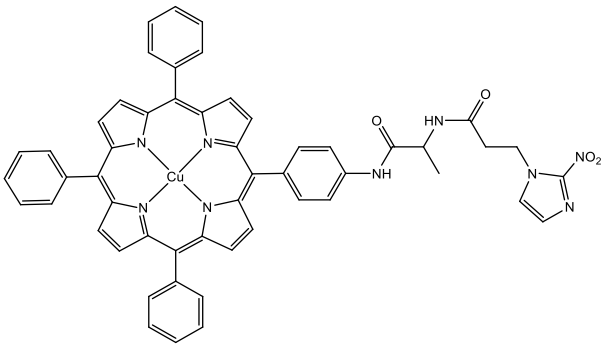

Compound **4.8** was synthesized employing general metal complexation method B. **4.5** (100 mg, 0.115 mmol), $Cu(OAc)_2 \cdot H_2O$ (65.8 mg, 0.330 mmol), DMF (10 mL). A red colored solid was obtained. Yield: 79.0 mg, 0.085 mmol, 74 %.

**Mass spec:** ESI-MS calculated for $C_{53}H_{38}CuN_9O_4$ $[M - H]^-$ 927.2348, found: 927.2342.

**HPLC** (Method A): $R_t$ = 10.31 min.

**Elem. Anal.**: Found: C; 68.1 %, H; 4.1 %, N; 13.6 %. Calc.: C; 68.5 %, H; 4.2 %, N; 13.6 %.

**Synthesis of the L-[7, 13]bombesin analogue**

a)

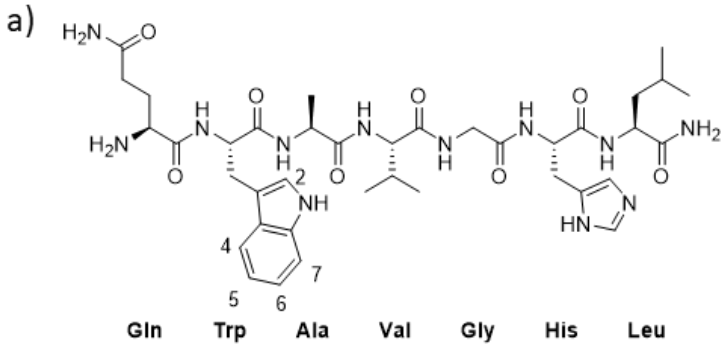


Fmoc-protected rink amide resin (1g, 0.5 mmol) was swelled in a peptide vessel for 20 min with DCM. This was subsequently deprotected using a solution of 20% piperidine in DMF, with deprotection confirmed by Kaiser-test. For the first step, three equivalents of the amino-acid (Fmoc-Leu-OH, 530 mg, 1.5 mmol) of HOBt (203 mg, 1.5 mmol) and of base N,N′-Diisopropylcarbodiimide (235 μL, 1.5 mmol) in DMF was added to the resin. This was to react for 90 minutes, followed by deprotection using 20% piperidine in DMF as confirmed by the Kaiser-test. Subsequent steps used three equivalents of amino acids, 1.9 equivalents of HOBt (360 mg) and 6 equivalents of N,N′-Diisopropylcarbodiimide and were followed by deprotection as described above. The amino acids were Fmoc-His(Trt)-OH (619.7 mg), Fmoc-Gly-OH (446 mg), Fmoc-Val-OH (509.1 mg),Fmoc-Ala-OH (467 mg), Fmoc-Trp(Boc)-OH (790 mg), Fmoc-Gln(Trt)-OH (916.05 mg), respectively. Finally the peptide was t-boc deprotected by stirring for three hours with a cocktail of 95% TFA, 2.5% TIS and 2.5% $H_2O$, with resin beads filtered and the solution collected. This was freeze-dried *in vacuo* and purified using semi-preparative HPLC yielding 60 mg of the desired peptide.

**Analytical HPLC:** Method F given above gave $R_t$ = 5.4 mins.

**ESI$^+$-TOF** ($CH_3OH$): m/z found: 405.2315 $[M+2H]^{2+}$, 809.4465 $[M+H]^+$; calculated for $C_{38}H_{56}N_{12}O_8$: 808.4344 Da.

**b)** Alternative synthesis of [7-13] bombesin.

The [7-13] fragment of bombesin was also synthesized by SPPS using a Biotage Initiator 2.5 microwave reactor and a Rink amide resin as a solid support (1.011 g, 0.60 mmol). First, the resin was swelled in dichloromethane and DMF. The deprotection of the resin was carried out in piperidine/DMF 1:4 in three cycles heating at 75 ºC for 10 minutes, 3 minutes and 3 minutes. The resin was washed between steps with dichloromethane and DMF. The coupling steps were carried out with an excess of the amino acid (1.79 mmol, 3 eq.), HATU (1.79 mmol, 3 eq.), HOBt (1.79 mmol, 3 eq.) in DIPEA (4.18 mmol, 7 eq.) and DMF (5 mL). The reaction mixture, once homogenized, was heated at 75 ºC for 10 minutes except in the case of His that was coupled at room temperature for 2 h. The deprotection after each coupling step was carried out in piperidine/DMF heating at 75 ºC for 10 minutes. The resin was washed with dichloromethane and DMF after each coupling and deprotection step and the efficiency of the coupling assessed by the Kaiser test using some resin beads. Finally, the cleavage of the peptide from the resin was performed using a cleavage cocktail containing TFA/phenol/$H_2O$/TIPS (88:5:5:2). The reaction mixture was stirred for 2.5 h at room temperature and the peptide

precipitated in cold diethyl ether and dried. The crude was purified by automated flash column chromatography using a C18 cartridge (method 1C) and lyophilized from acetic acid to yield a white solid.

**$^1$H NMR (500 MHz, $D_2O$, 25 ºC):** δ 8.51 (brs, 1H), 7.64 (d, *J* = 7.9 Hz, 1H), 7.51 (d, *J* = 8.2 Hz, 1H), 7.29 – 7.24 (m, 1H), 7.20 (brs, 1H), 7.17 (t, *J* = 7.6 Hz, 1H), 4.72 (t, *J* = 7.1 Hz, 1H), 4.65 (t, *J* = 7.2 Hz, 1H), 4.35 – 4.25 (m, 2H), 4.02 (t, *J* = 6.7 Hz, 1H), 3.99 – 3.89 (m, 3H), 3.36 – 3.20 (m, 2H), 3.20 – 3.11 (m, 2H), 2.40 (t, *J* = 7.5 Hz, 2H), 2.18 – 2.07 (m, 2H), 2.05 – 1.98 (m, 1H), 1.70 – 1.61 (m, 1H), 1.62 – 1.53 (m, 2H), 1.30 (d, *J* = 7.2 Hz), 0.97 (d, *J* = 6.7 Hz, 3H), 0.95 (d, *J* = 6.7 Hz, 3H), 0.92 (d, *J* = 5.7 Hz, 3H), 0.86 (d, *J* = 5.7 Hz, 3H).

HPLC method 1B described above showed R.T. 6.8 min.

**MS-ESI**: calculated for $C_{38}H_{56}N_{12}NaO_8$ $[M+Na]^+$: 831.4242; found: 831.4267.

**Preparation of L-[7,14]BBN peptides**

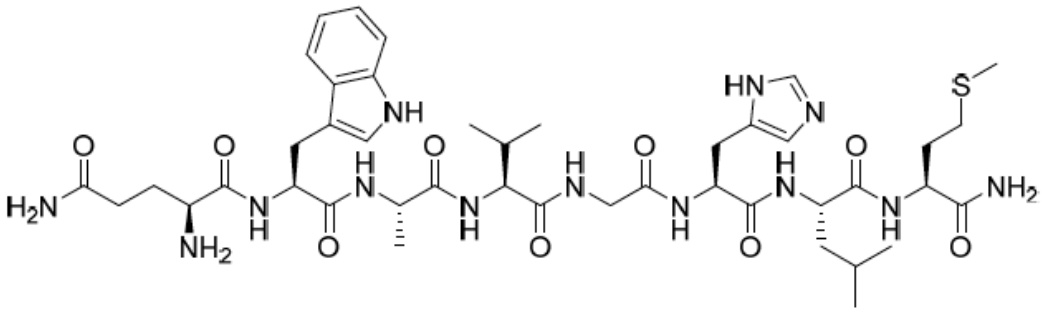


***BBN [7-14]-$NH_2$ & Cys-BBN [7-14]-$NH_2$***

Peptides **BBN [7-14]-$NH_2$**, and **Cys-BBN [7-14]-$NH_2$**, the cysteine functionalized analogue were both prepared by Fmoc solid-phase peptide synthesis on Rink Amide resin.

Once assembled, peptide **BBN [7-14]-$NH_2$** was retained in protected form on the resin until required for further elaboration. A small-scale cleavage was carried out upon *ca*. 20 mg of the peptide-resin to test the purity of the peptide. The cleavage was achieved by treatment of the resin with a mixture of TFA/TIS/$H_2O$/DTT (930:25:25:20) for 2.5 h. Treatment with TFA removes the peptide from the resin, generating a primary amide function at the C-terminus. TIS, $H_2O$ and dithiothreitol (DTT) were included as scavengers for the highly reactive carbocations generated during the acidolysis of the permanent Boc and trityl side chain protecting groups, which could otherwise react with sensitive amino acid residues such as Met and Trp. $H_2O$ and TIS are very efficient cation scavengers which are widely used in peptide chemistry in acid deprotection steps. *Note: The use of an additional sulphur- containing scavenger, namely DTT, is advisable when dealing with peptides which contain a Met residue, as this side chain is particularly sensitive to alkylation.*

Peptide **Cys-BBN [7-14]-$NH_2$** was prepared following the same procedure. In this case, after adding the N-terminal Cys residue, the peptide was directly cleaved from the resin as it would not be further functionalized. The mixture of scavengers had to be altered due to the presence of Cys, which also requires an efficient sulfur-containing cation scavenger, ethanedithiol (EDT). Therefore cleavage was achieved by treating the resin with TFA/TIS/$H_2O$/EDT (940:25:25:10) for 2.5 h, giving the expected fully deprotected peptide **Cys-BBN [7-14]-$NH_2$** in 58% yield after lyophilization. Analytical HPLC analysis of the crude peptide showed one major peak (Figure 17), so **Cys-BBN [7-14]-$NH_2$** was therefore deemed to be of sufficient purity for the subsequent ligation steps and was used without further purification.

**Synthesis of BBN(7-14): Gln-Trp-Ala-Val-Gly-His-Leu-Met-$NH_2$ (QWAVGHLM-$NH_2$)**

The peptide was assembled by Fmoc solid phase peptide synthesis on Rink Amide MBHA Resin (Novabiochem, 200-400 mesh, assumed 0.6 mmolg-1 loading) using an Activotec Activo-P11 automated peptide synthesiser, with a heated reactor. The first residue was attached to the resin manually as follows. The resin (250 mg, 0.15 mmol) was placed in a 10 mL plastic reactor, and was swollen in DCM and DMF (15 min each), and then the Fmoc protection was removed by treatment with 20% piperidine/DMF (2.5 mL, 5 + 15 min). After washing thoroughly with DMF to remove traces of piperidine, the deprotection was confirmed by a positive Kaiser test. Fmoc-Met-OH (251 mg, 0.59 mmol, 4 eq) in DMF (2.5 mL) was preactivated by treatment with *N,N´* -diisopropylcarbodiimide **(**DIC, 94 µL, 0.96 mmol, 6 eq.) and HOBt (81 mg, 0.59 mmol, 4 eq.). After 3 h, this solution was added to the deprotected resin, followed by DIPEA (159 µL, 0.96 mmol, 6 eq.) and the vessel was shaken for 45 min. The vessel was then transferred to the automated synthesiser, and the reaction vessel was fitted with a heating jacket (60°C). Subsequent Fmoc deprotection steps were performed using 20% piperidine/DMF (3 mL, 5 + 10 min). Amino acid couplings were performed with 3 eq. of Fmoc protected amino acid (Fmoc-Leu-OH, Fmoc-His(Trt)-OH, Fmoc-Gly-OH, Fmoc-Val-OH, Fmoc-Ala-OH, Fmoc-Trp-(Boc)-OH and Fmoc-Gln(Trt)-OH), 3 eq. of PyBop (0.15 M) and 6 eq. of DIEA (0.48 M) in DMF (total volume 4.3 mL). No final Fmoc deprotection step was performed to allow for subsequent elaboration of the peptide on the resin. The resin was washed with DMF, DCM, MeOH and $Et_2O$ and dried under vacuum to yield 374 mg of resin-bound **BBN(7-14)**. A small scale cleavage and deprotection was performed to check the quality of the peptide. Peptide resin (*ca.* 20 mg) was treated with TFA/TIS/$H_2O$/DTT (930:25:25:20, 0.8 mL) for 2.5 h. The resin beads were removed by filtration and the peptide was precipitated by addition of anhydrous $Et_2O$ (1 mL). The white precipitate was collected by centrifugation and washed with further $Et_2O$ (3 x 1.5 mL). The solvent was removed, and the precipitate was dissolved in 0.1% aq. TFA (0.25 mL) and 0.1% TFA/MeCN (0.75 mL) and analysed by HPLC. Rt (HPLC) = 5.87 min.

**MS-ESI**: calculated for $C_{43}H_{66}N_{13}O_9S$ $[M+H]^+$: 940.4827; found: 940.4791. Deviation: 3.83 ppm

**Synthesis of Cys-BBN(7-14)-$NH_2$: Cys-Gln-Trp-Ala-Val-Gly-His-Leu-Met-$NH_2$**

The synthesis of cysteine functionalized (7-14) bombesin was performed analogously to the preparation of **BBN(7-14)**, with an extra automated coupling with Fmoc-Cys(Trt)-OH. For this peptide a final Fmoc deprotection (3 mL, 5 + 15 min) was executed before removing the vessel from the synthesiser and collecting 405 mg of resin-bound **15**. The cleaving from the resin was accomplished by treatment with TFA/TIS/$H_2O$/EDT 940:25:25:10 (4 mL). After 2.5 h the resin beads

were removed by filtration and peptide **Cys-BBN(7-14)-$NH_2$** was precipitated in Et2O as above. Analytical HPLC showed the crude peptide to have predominantly a single peak, so **Cys-BBN(7-14)-$NH_2$** was used without further purification. The peptide was isolated as a TFA salt by dissolving in in 0.1% aq. TFA and 0.1% TFA/MeCN and lyophilized to give **Cys-BBN(7-14)-$NH_2$** as a fluffy white solid (111 mg, 58%); Rt (HPLC) = 5.99 min.

**MS-ESI**: calculated for $[M+H]^+$: 1043.4919; found: 1043.4938. Deviation: 1.82 ppm

**Synthesis of 11-azido undecanoyl-BBN(7-14)-$NH_2$**

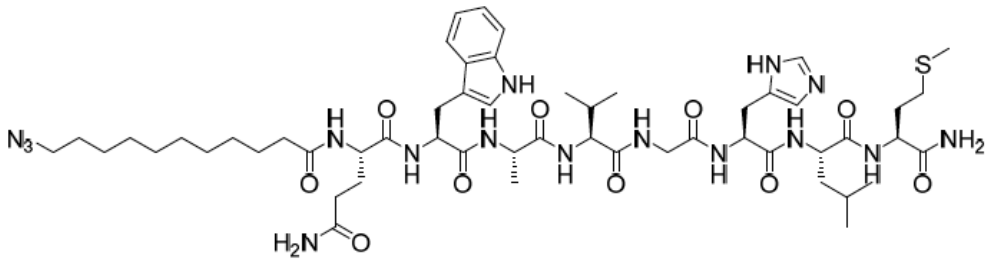

The acylation of the N-terminal amino acid was performed manually. Resin-bound **BBN[7-14]** (100 mg, X mmol) was swollen in DCM (2 mL, 2 x 1 min) before the Fmoc protecting group was removed as described in **BBN[7-14]**. The resin-bound peptide was then acylated with a solution of 11-azido undecanoic acid (66 mg, 0.29 mmol, 4 eq.), HATU (108 mg, 0.29 mmol, 3.98 eq.) and DIEA (76 µL, 0.43 mmol, 6 eq.) in DMF (3 mL) which had been preactivated for 5 minutes. The reaction mixture was shaken for 1 h, after which completion of the acylation was confirmed by a negative Kaiser test. The derivatized peptide **11-azido undecanoyl-BBN[7-14]-$NH_2$** was cleaved from the resin by treatment with TFA/$H_2O$/TIS/DTT/phenol 905:25:50:10:10 (2.5 mL) for 3 h, after which the peptide was precipitated from solution in $Et_2O$ as in **BBN[7-14]**, dissolved in 0.1% aq. TFA, filtered using a 0.2 µm syringe filter and purified by semi-prep HPLC. The purified peptide was lyophilized to give **11-azido undecanoyl-BBN[7-14]-$NH_2$** as a white solid (26 mg, 31 %); Rt (HPLC) = 8.44 min;

**MS-ESI**: calculated for $C_{54}H_{84}N_{16}NaOS$ $[M+Na]^+$: 1171.6175; found: 1171.6219. Deviation: 3.76 ppm

**4-oxo-4-((4-(10,15,20-triphenylporphyrin-5-yl)phenyl)amino) butanoic acid (4.9)**

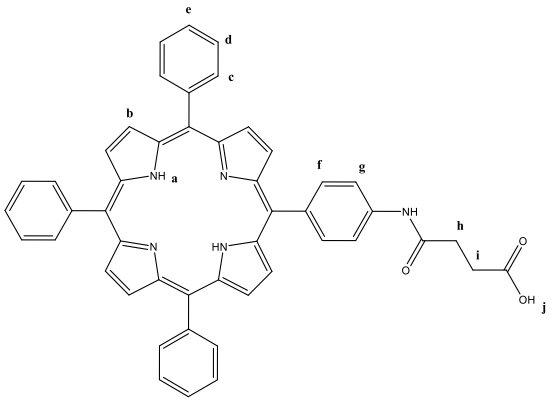

5-(4-aminophenyl)-10,15,20-triphenylporphyrin (Compound **4**; 20 mg, 31.7µmol) was added to TEA (6.6 µL, 47.6 µmol) in 1 mL $CHCl_3$ and stirred for 5 min. Succinic anhydride (4.76 mg, 47.6 µmol) was added and the reaction was stirred under $N_2$ for 3 hours. The solvent was removed under vacuum to give a red residue. 15.1 mg (65.3 %) was obtained.

**MS-ESI:** ESI$^+$ TOF$^+$ mode m/z calculated for: $C_{48}H_{35}N_5O_3$: 729.2740, found: 730.2844 [M+H].

**$^1$H NMR (500 MHz, $CDCl_3$, 298 K):** δ 8.86–8.84 (m, 8H, H**b**), 8.31 (s, 1H, H**j**), 8.22–8.19 (m, 6H, H**c**), 8.16 (d, *J* = 8.0 Hz, 2H, H**g**), 7.91 (d, *J* = 8.0 Hz, 2H, H**f**), 7.78–7.72 (m, 8H, H**d**/H**e**), 2.69–2.61 (m, 4H, H**h**/H**i**), 1.82 (s, 1H, NH), -2.78 (s, 2H, H**a**).

**$^{13}$C NMR (500MHz, $CDCl_3$):** 29.69 (succinic **C**), 126.65, 134.52 (aromatic **C**), 186.59 (**C**OOH).

**[7-13]bombesin-(4-(10,15,20-triphenylporphyrin-5-yl)phenyl) succinamide (4.10)**

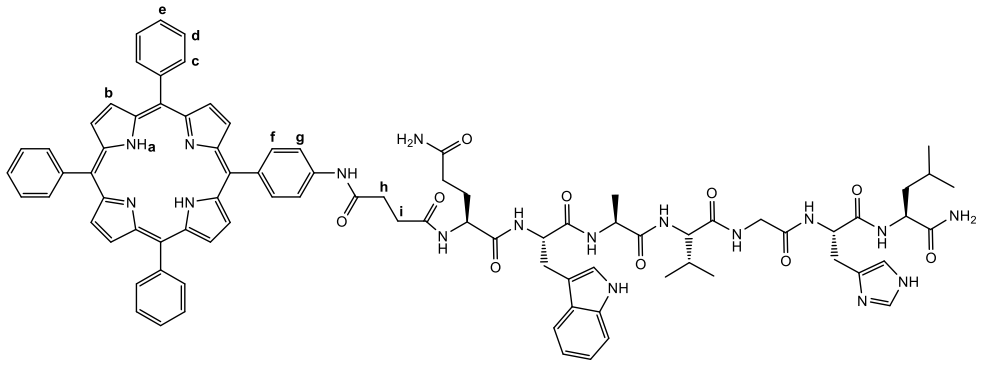


4-oxo-4-((4-(10,15,20-triphenylporphyrin-5-yl)phenyl)amino) butanoic acid (Compound **4.9**; 5.0 mg, 6.85 µmol), PyBOP (7.1 mg, 13.7 µmol) and DIPEA (2.63 µL, 15.1 µmol) were added to 1 mL DMF and stirred. After 30 min, [7-13]bombesin (5.5mg, 3.43 µmol) was added. The reaction was heated to 60 °C and left overnight (17 hours) before the temperature was increased to 75 °C. After 5 hours, the reaction was purified on HPLC semi-preparative column in 1 % TFA. The product was isolated as a green liquid due to the presence of TFA but turned purple upon drying then dissolving in DCM. The reaction was purified using semi preparative HPLC (1% TFA) and eluted at R.t. 21 minutes.
1.5 mg (18.8%) was obtained.

Separation method applied for this compound: Semi-preparative HPLC was performed on a *Dionex Ultimate 3000* system equipped with a *Thermo Fischer Rheodyne* 1000 µL sample loop and a *Macherey-Nagel Nucleodur HTech* C18 5 µm (250 x 21 mm) column with a flow rate of 4 mL min$^{-1}$. Mobile phase A was 0.1 % TFA in water, mobile phase B was 0.1% TFA in acetonitrile. The gradient for semi-preparative HPLC was T = 0 min, B = 5%; T = 1 min, B = 5%; T = 21 min, B = 95%; T = 23 min, B = 95%; T = 26 min, B = 5%. High resolution mass spectrometry (MS) analyses were performed using a mass spectrometer equipped with an electro-spray ion source (Bruker microTOF and MALDI-TOF with Linear and Reflectron analysers).
**MS-ESI:** positive mode ESI m/z calculated for $NaC_{86}H_{89}N_{17}O_{10}$ [M+Na]: 1542.6871, found: 1542.7059 [M+Na].
Deviation: 12.19 ppm.

**General EDC/HOBt coupling procedure**

The appropriate carboxylic acid was dissolved in anhydrous DMF at 0 °C. The resulting solution was treated with 1.2 mol eq. each of 1-ethyl-3-(3-dimethylaminopropyl)carbodiimide hydrochloride (EDC.HCl) and 1-hydroxybenzotriazole hydrate (HOBt). The solution was stirred for 45 min before adding the porphyrin-$NH_2$ derivative **4** (1.1 eq) and N,*N*-diisopropylethylamine (DIEA, 3 eq). The reaction was allowed to warm to room temperature and stirred overnight, with complete consumption of starting material generally observed after 18 h. Unless otherwise stated, the resulting solution was diluted with DCM (10 mL) and washed with $H_2O$ (10 mL), sat. $NaHCO_3$ (10 mL) and brine (10 mL), dried over $Na_2SO_4$ and concentrated to residue. The crude products were purified by flash chromatography

**3-(2,5-dioxo-2,5-dihydro-1H-pyrrol-1-yl)-N-(4-(10,15,20-triphenylporphyrin-5-yl)phenyl)propanamide (4.11)**

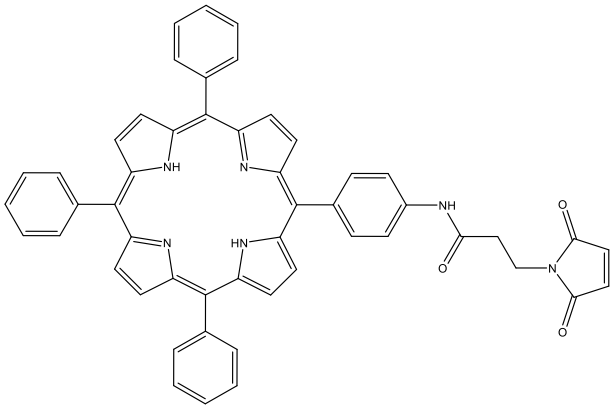


**4** (50 mg, 0.080 mmol), HOBt (13 mg, 0.095 mmol), 3-maleimidopropionic acid (16 mg, 0.095 mmol) and EDC.HCl (18 mg, 0.095 mmol) were dissolved in anhydrous DCM (5 mL) and stirred overnight at rt. Work-up was conducted according to the general procedure. Purification was achieved by flash chromatography, with DCM to elute unreacted 1, then DCM/MeOH 1% to elute 3. Removal of solvent *in vacuo* gave 3 as a shiny purple solid (45 mg, 73 %); Rf (DCM/MeOH 2%): 0.28; Rt (HPLC) = 10.63 min; UV-Vis: λmax (nm): 420, 516, 551, 592, 647.

**$^{1}$H NMR ($CDCl_3$):** δ 8.85–8.84 (m, 8H, β-pyrrole), 8.23–8.20 (m, 6H, Ar-H), 8.17 (d, 2H, *J* = 2.9 Hz maleimide,), 7.92 (d, 2H, *J* = 2.9 Hz), 7.80–7.73 (m, 10H, Ar-H), 6.80 (s, 1H, NHCO), 4.09 (t, 2H, *J* = 1.0 Hz, $CH_2$), 2.93 (t, 2H, *J* = 1.0 Hz $CH_2$), -2.78 (s, 2H, NH).

**$^{13}$C NMR ($CDCl_3$):** δ 170.59, 142.09, 135.05, 134.50, 134.29, 127.67, 126.64, 120.13, 118.10, 34.06.

**MS-ESI**: calculated for $C_{51}H_{37}N_6O_3$ $[M+H]^+$: 781.2922; found: 781.2923. Deviation: 0.13 ppm

**Thiol-maleimide ligation of 4.11 with Cys-BBN(7-14)-$NH_2$ (4.12)**

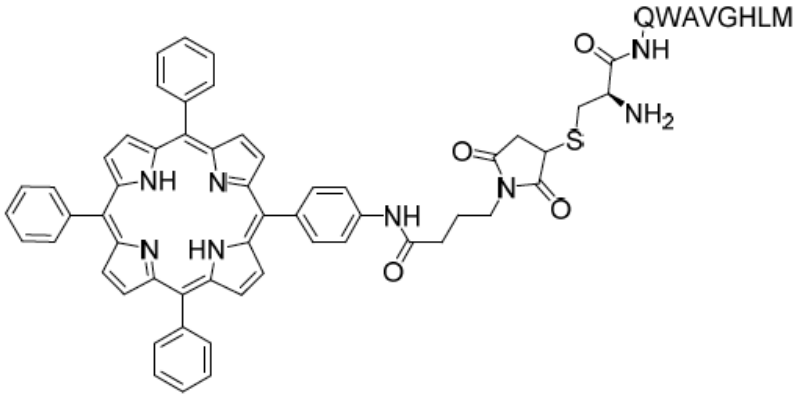


A solution of **4.11** (3.1 mg, 3.94 µmol)**, Cys-BBN(7-14)-$NH_2$** (5.0 mg, 3.94 µmol) and pyridine (64 µL, 200 eq.) in DMSO (1 mL) was stirred at r.t for 24 h. The resulting red solution was purified by semi-prep HPLC. The isolated conjugate was lyophilized to give **4.12** as a bright green solid (7 mg, 84 % yield); Rt (HPLC) = 8.41 min; UV-Vis: λmax (nm): 421, 517, 553, 591, 647.

**MS-ESI**: calculated for $C_{97}H_{108}N_{20}O_{13}S_2$ $[M+2H]^{2+}$: 912.8935, found: 912.9253. Deviation: 34.83 ppm

**Coupling of 4 with DBCO-acid (4.13)**

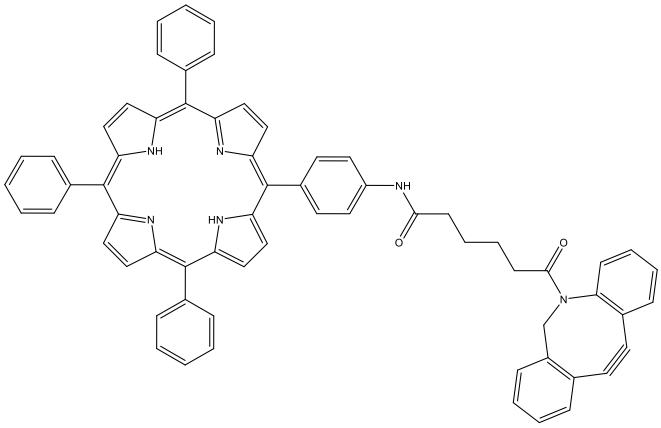


**4** (20.8 mg, 0.033 mmol), HOBt (4.9 mg, 0.036 mmol), dibenzocyclooctyne-acid (10.0 mg, 0.095 mmol), EDC.HCl (6.9 mg, 0.036 mmol) and DIEA (15.6 µL, 0.090 mmol) were dissolved in DCM (anhyd, 1 mL) and stirred at r.t overnight. Crude product was purified directly by flash chromatography, eluting remove unreacted **4** with DCM, then DCM/acetone 10 % to elute **4.13**. The red solution was concentrated, giving **4.13** as a purple solid (23 mg, 81 %); Rf (DCM/acetone 5 %) = 0.44; Rt (HPLC) = 11.98 min; UV-Vis: λmax (nm): 420, 516, 553, 594, 694.

**$^1$H NMR ($CDCl_3$):** δ 8.93 (s, 2H, β-pyrrole), 8.87 (s, 6H, β-pyrrole), 8,43 (s, 1H, NHCO), 8.25–8.17 (m, 10H, Ar-H), 7.96–7.92 (m, 2H, Ar-H), 7.78–7.74 (m, 10H, Ar-H), 7.46–7.29 (m, 8H, Ar-H (DBCO), 5.23 (d, *J* = 13.9 Hz, 1H), 3.72 (d, *J* = 13.9 Hz), 2.44–2.38 (m, 1H, CH), 2.34–2.28 (m, 1H, CH), 2.17–2.11 (m, 1H, CH), 2.02–1.95 (m, 1H, CH), 1.77–1.63 (m, 1H, CH) 1.51–1.42 (m, 1H, CH), 1.09–0.99 (m, 2H, $CH_2$), -2.73 (s, 2H, NH).

**MS-ESI**: calculated for $C_{65}H_{49}N_6O_2$: 945.3917, found: 945.3892 $[M+H]^+$. Deviation: 2.67 ppm

**SPAAC ligation of 4 with 11-azido undecanoyl-BBN[7-14]-$NH_2$ (4.14)**

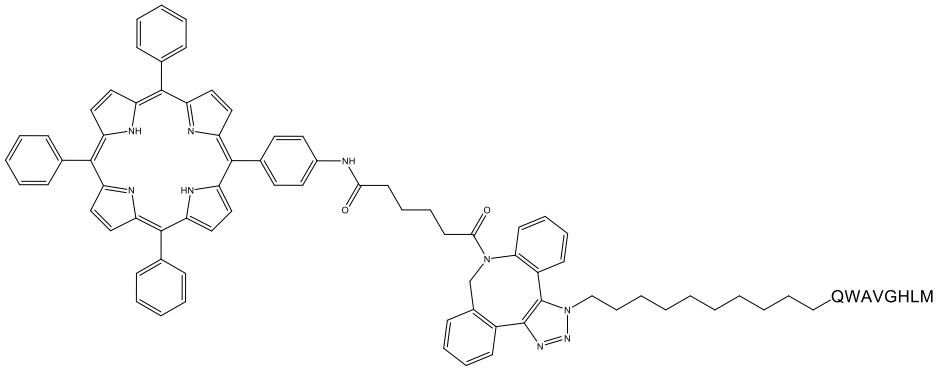


+ isomer

A solution of porphyrin **4.13** (3 mg, 3.83 µmol) and peptide **BBN(7-14*)*** (4 mg, 3.83 µmol) in DMSO (1 mL) was stirred at r.t for 24 h. The resulting red solution was purified by semi-preparative HPLC. The purified conjugate was lyophilized to give **4.14** as a bright green solid (7.8 mg, 86 %).

**Rt (HPLC)** = 10.08 min; UV-Vis: $\lambda_{max}$ (nm): 421, 515, 553, 592, 647.

**MS-ESI**: calculated for $C_{120}H_{133}N_{22}O_{12}NaS$ $[M+Na+H]^{2+}$: 1064.5040, found: 1064.0133.

3. NMR spectra

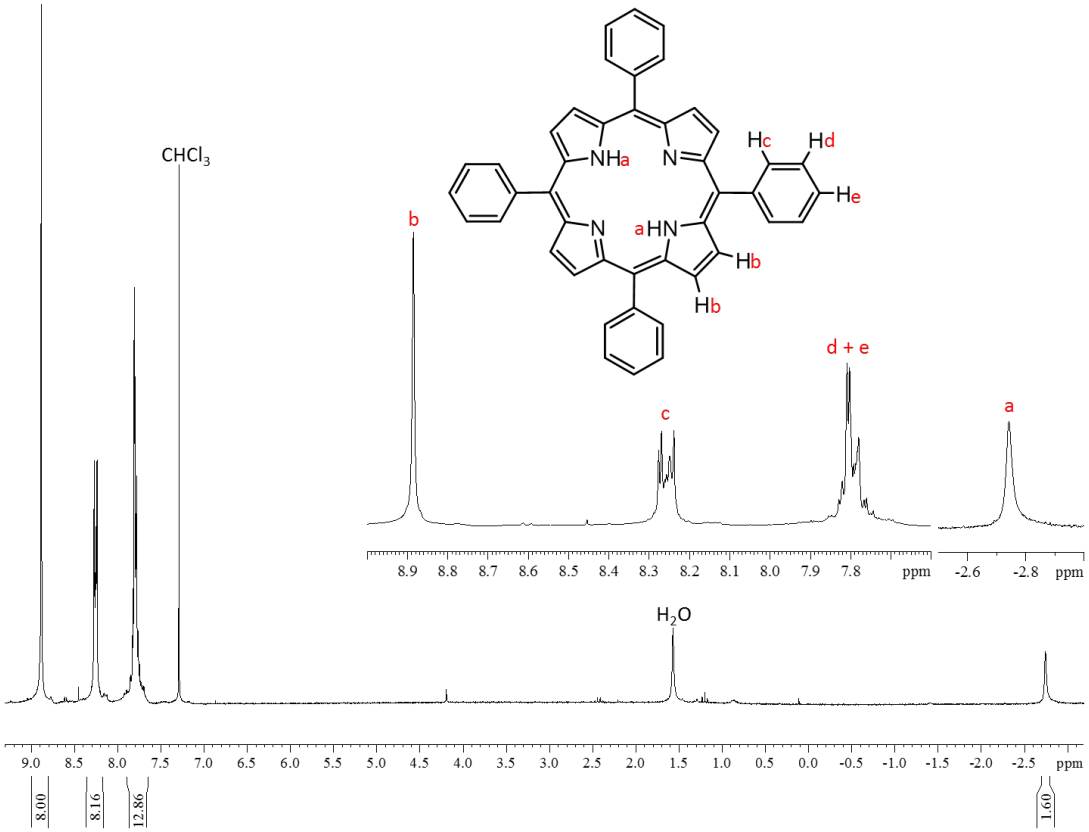


**Figure S1:** $^{1}$H NMR (300 MHz, 298 K, $CDCl_3$) of compound **1**.

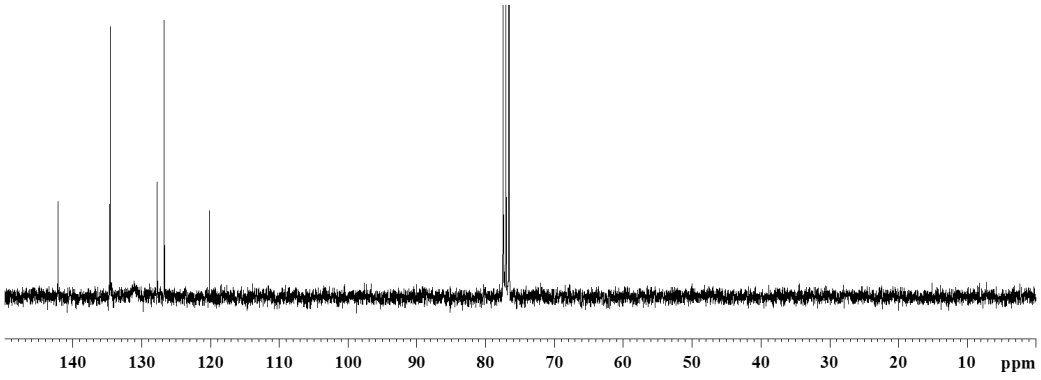


**Figure S2:** $^{13}$C NMR (125 MHz, 298 K, $CDCl_3$) of compound **1**.

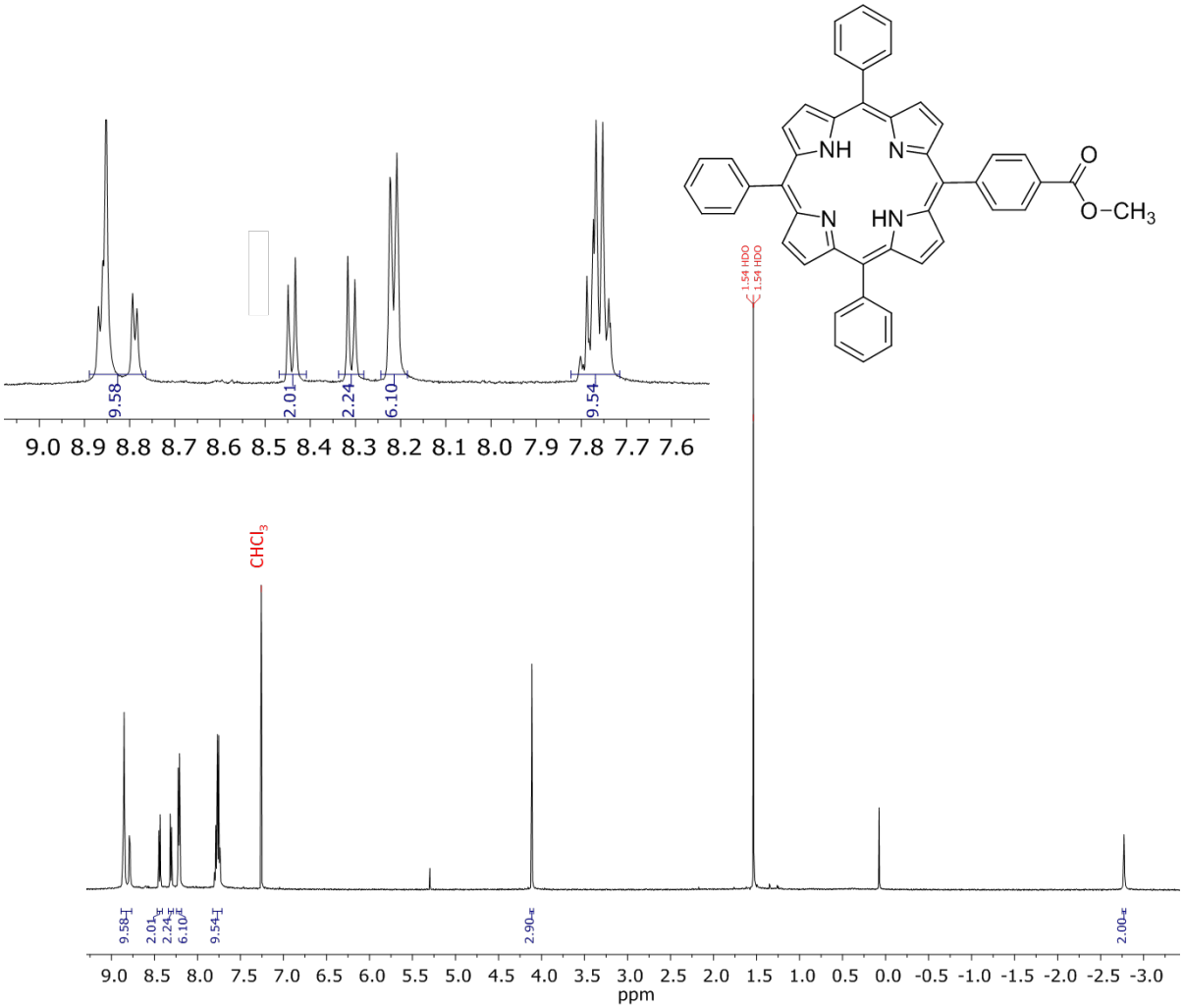


**Figure S3**: $^{1}$H NMR of compound **2** (500 MHz, 298 K, $CDCl_3$).

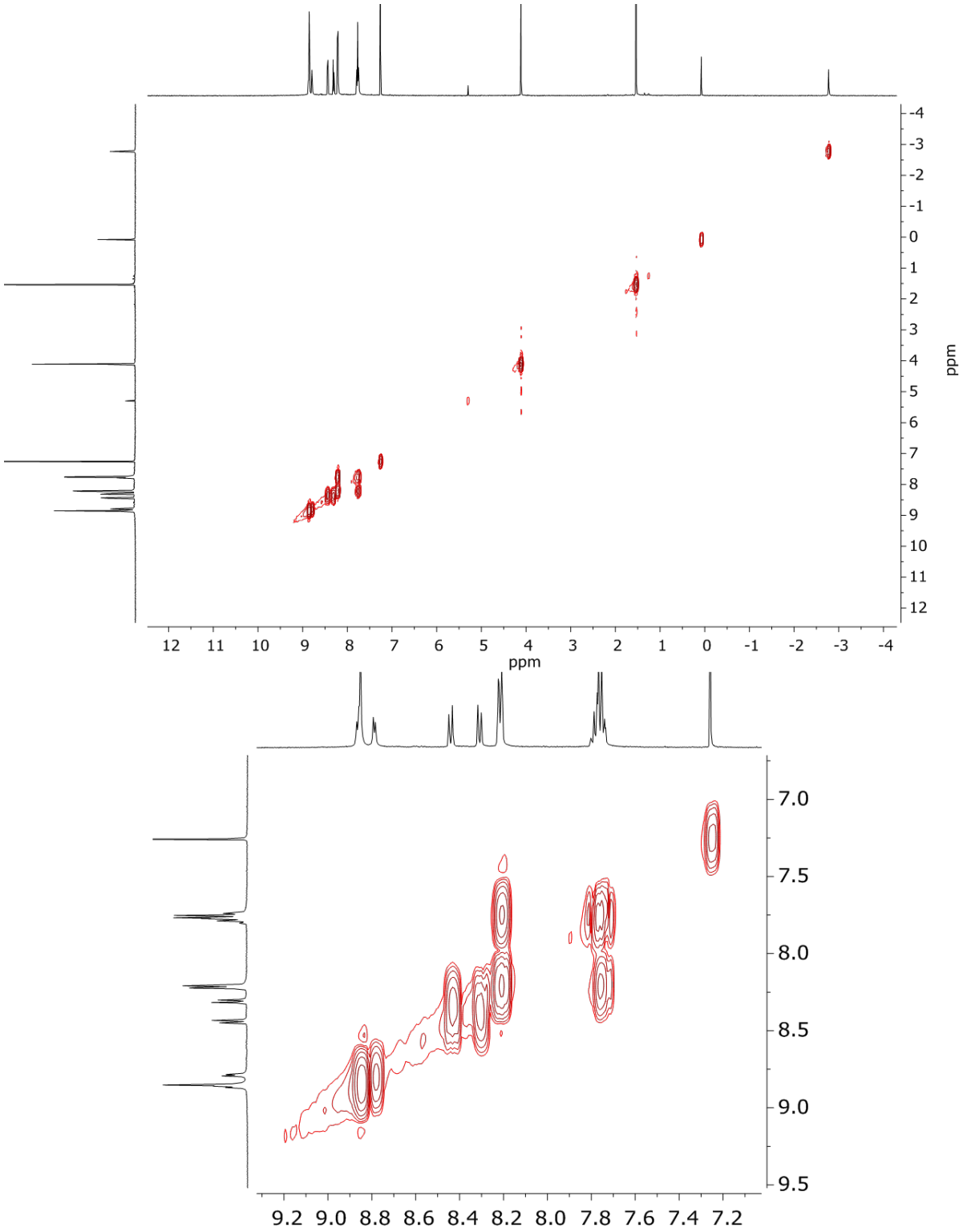


**Figure S4**: $^{1}$H-$^{1}$H COSY NMR of compound **2** (500 MHz, 298 K, $CDCl_3$), full spectra above, aromatic expansion below.

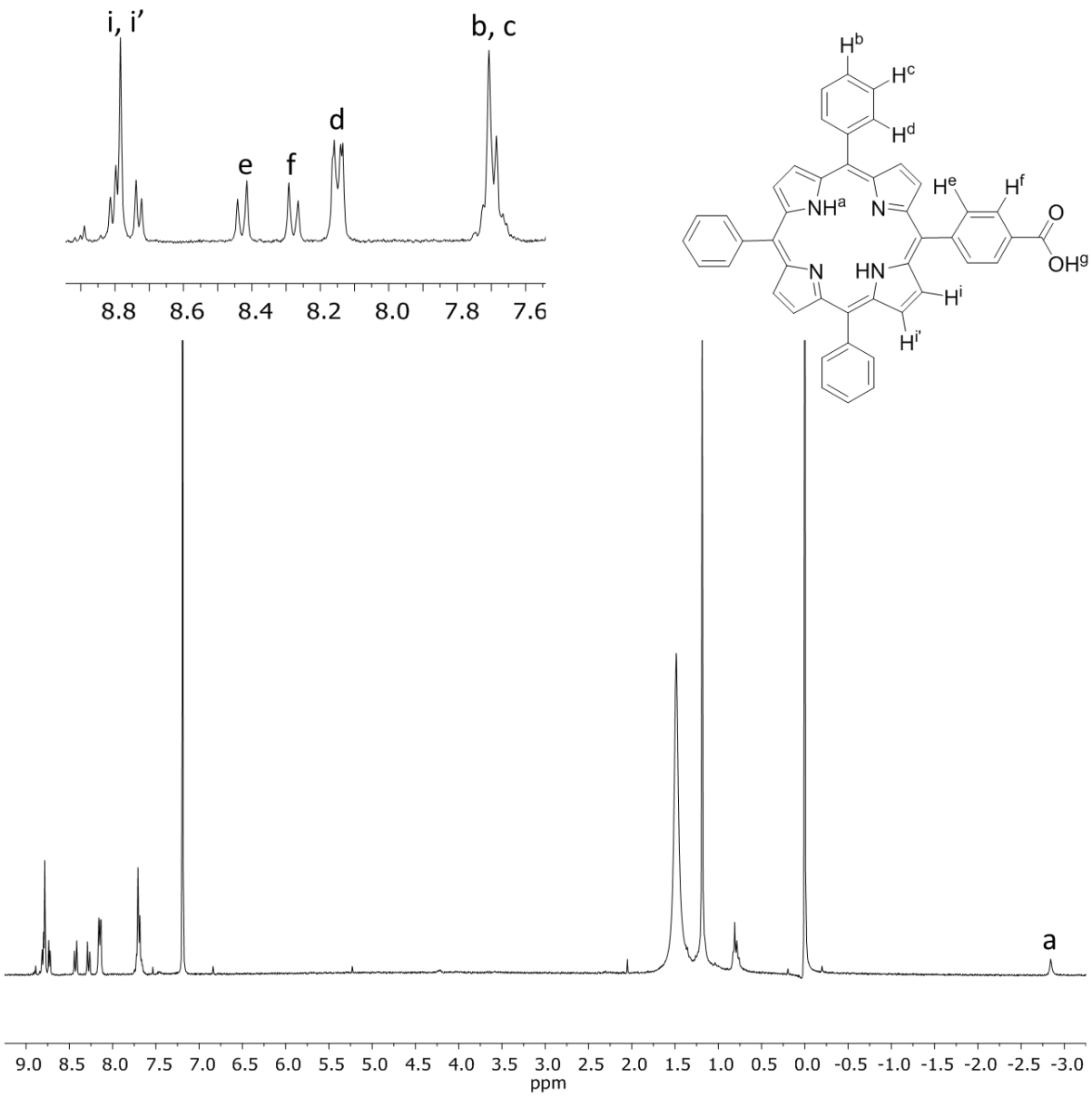


**Figure S5**: $^1$H NMR of compound **3** (500 MHz, 298 K, $CDCl_3$).

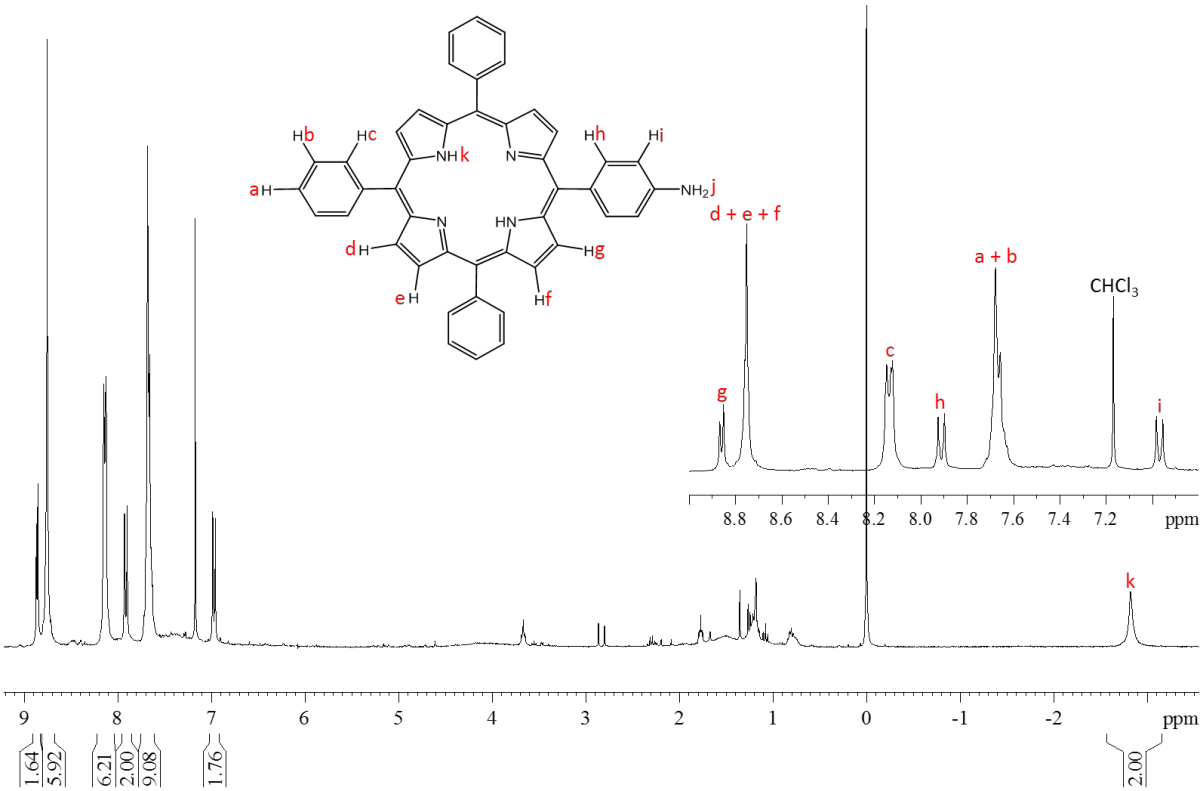


**Figure S6**: $^{1}$H NMR of compound **4** (500 MHz, 298 K, $CDCl_3$).

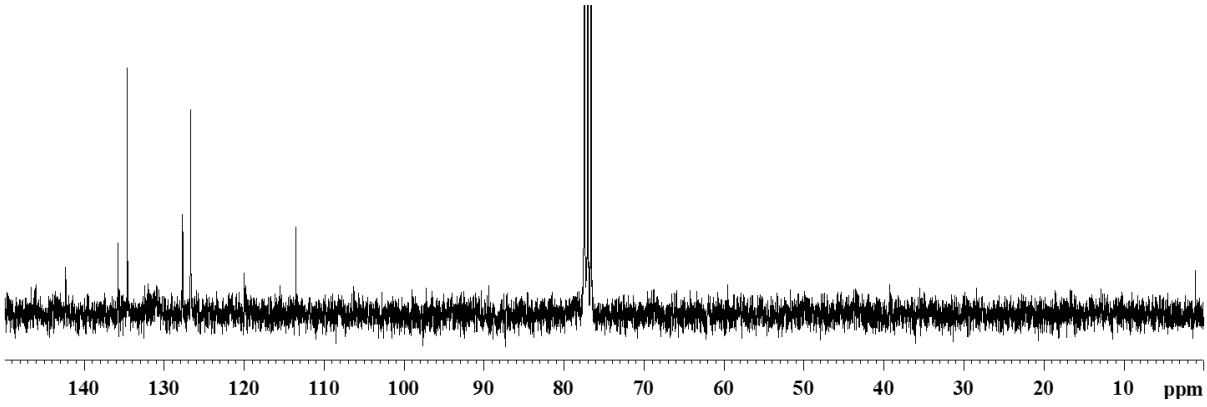


**Figure S7**: $^{13}$C NMR of compound **4** (125 MHz, 298 K, $CDCl_3$).

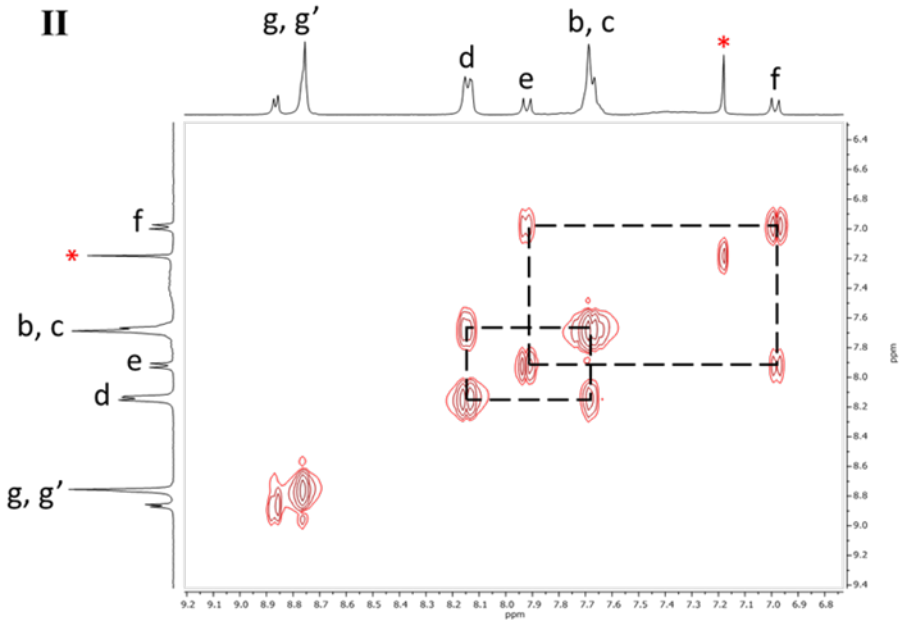


**Figure S8**: $^{1}H$-$^{1}H$ COSY NMR (500 MHz, 298 K, $CDCl_3$) of compound **4** aromatic region. * = $CHCl_3$ § = $CH_2Cl_2$.

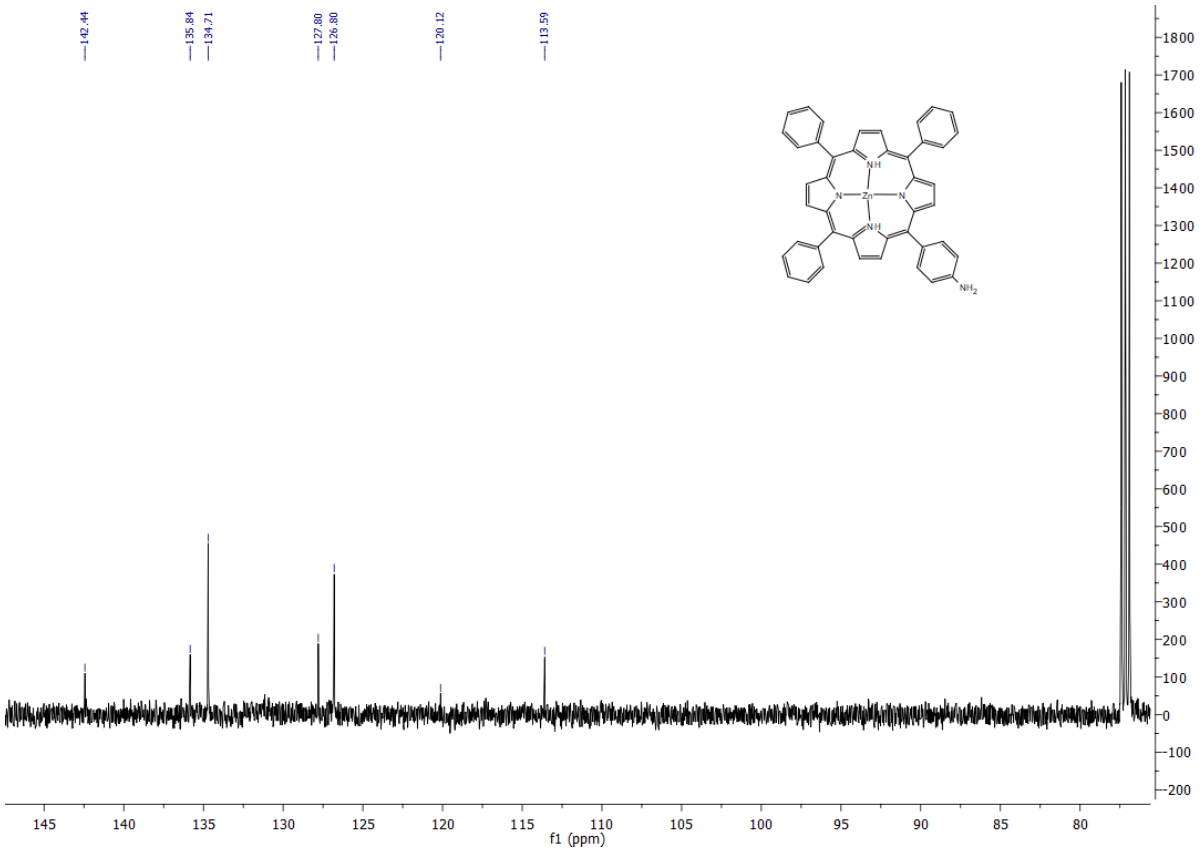


**Figure S9**: $^{13}C$ NMR spectrum ($CDCl_3$, 125.76 MHz) of compound **4.1**

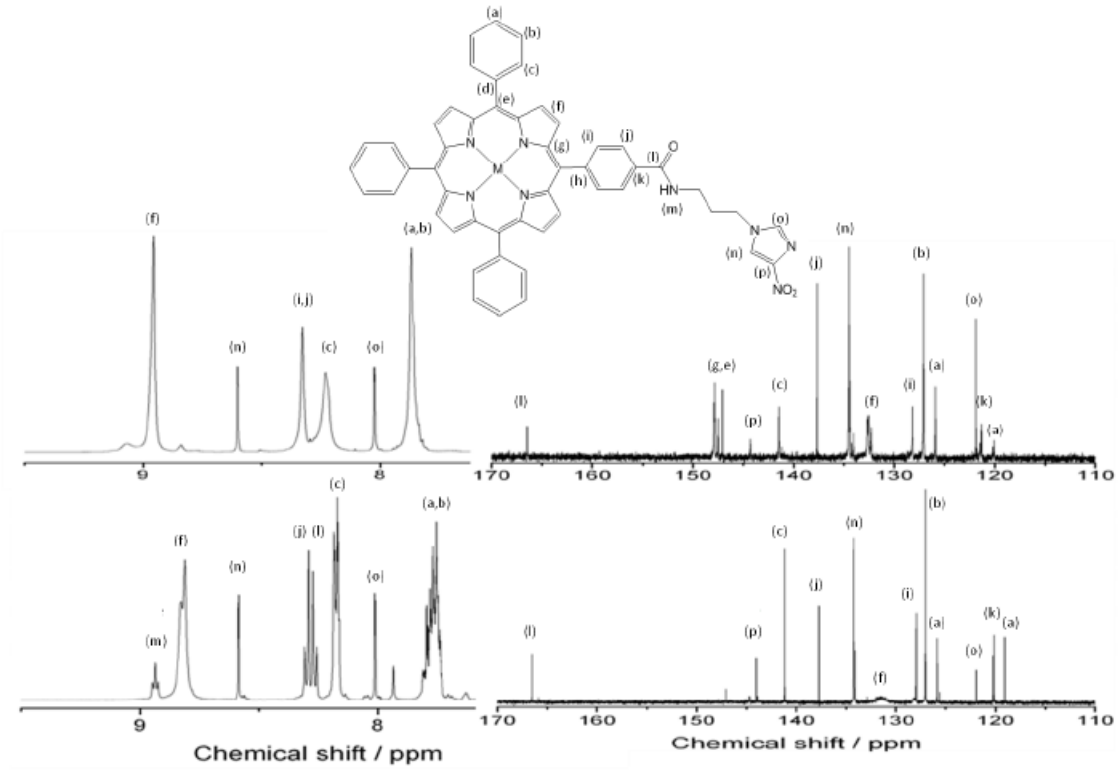


**Figure S10**: Stacked view of $^{1}H$ and $^{13}C$ NMR of **3.3** (bottom) and **3.6** (top) with selected assignments at 25 °C at 500 MHz

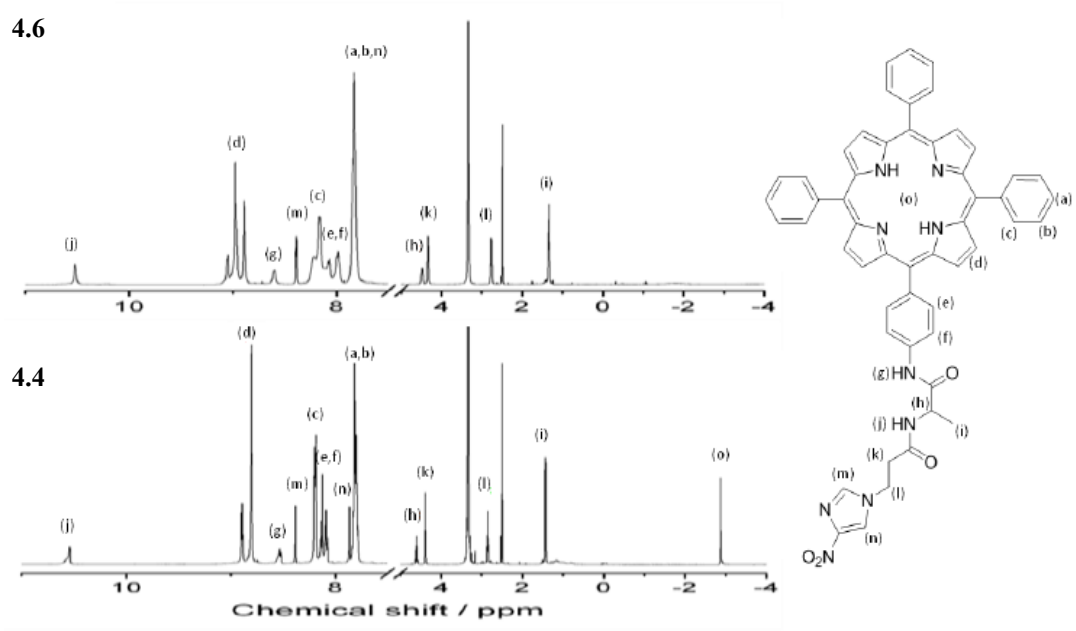


**Figure S11***:* $^{1}$H NMR of **4.4** (bottom) and **4.6** (top) in $d_6$-DMSO at 20 ºC at 500 MHz

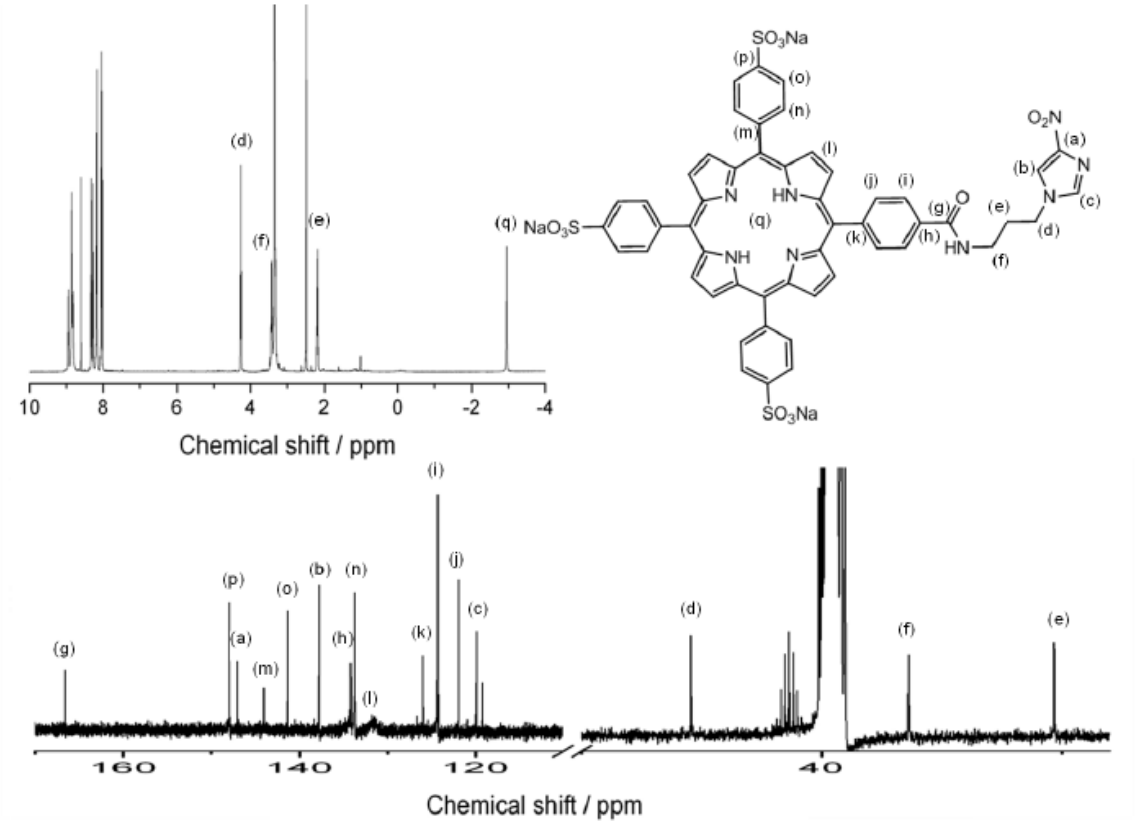


**Figure S12:** $^{1}$H and $^{13}$C NMR of **3.23** in $d^6$-DMSO at 20 °C at 500 MHz

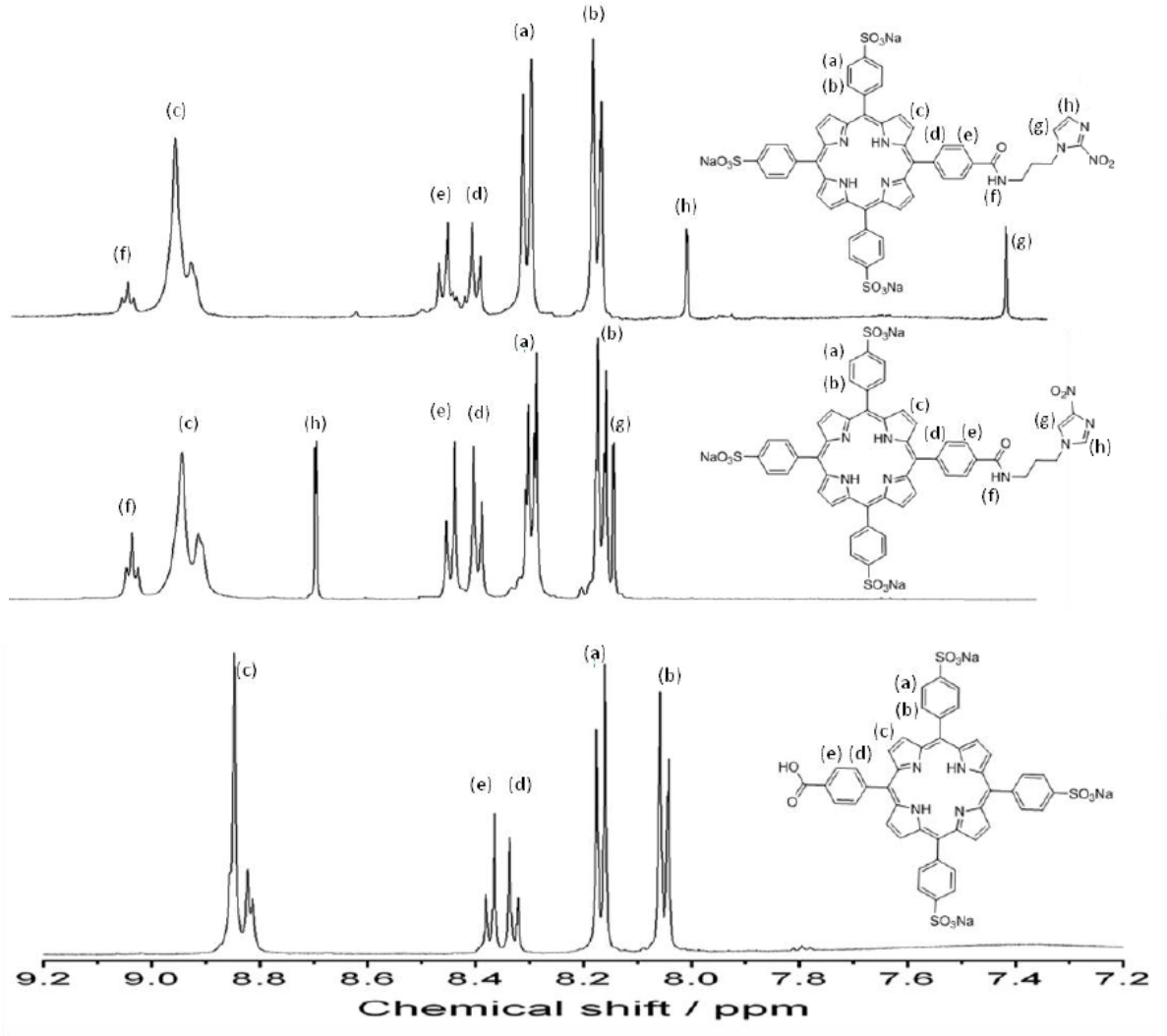


**Figure S13:** Stacked view of $^{1}$H NMR‟s of **3.23**, **3.22** and 5-(4-carboxyphenyl)-10,15,20-tri(*para*-phenyl-4-sulphonate)**,** all run in $d^{6}$-DMSO at 20 °C at 500 MHz

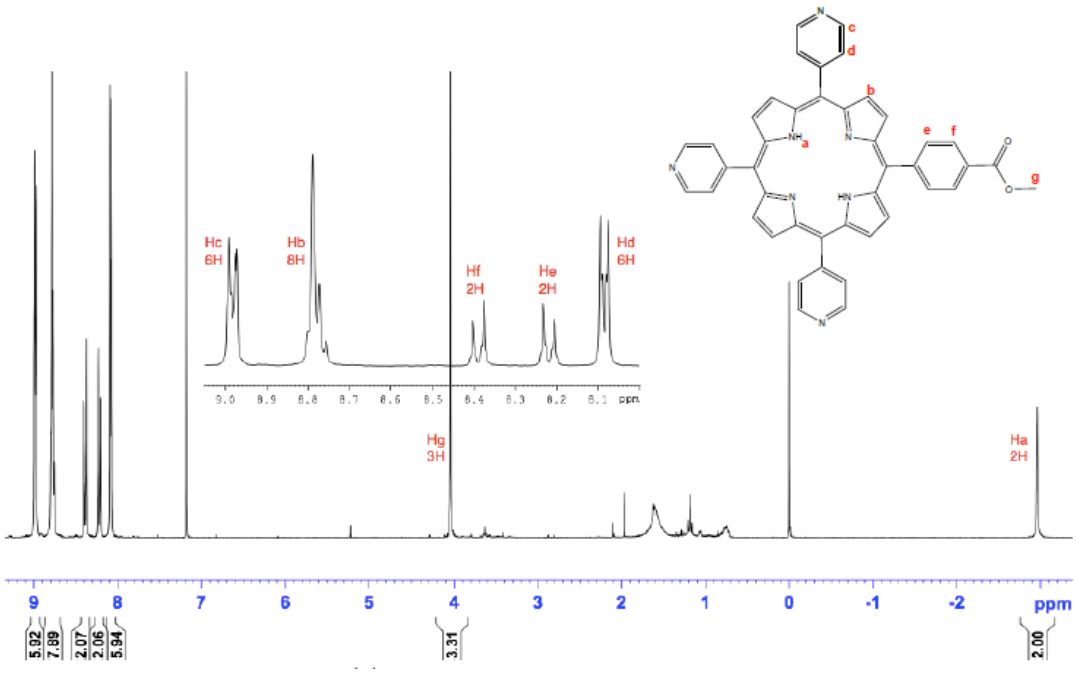


**Figure S14.** $^{1}$H NMR spectrum of porphyrin **5** (300 MHz, 298 K, $CDCl_3$)

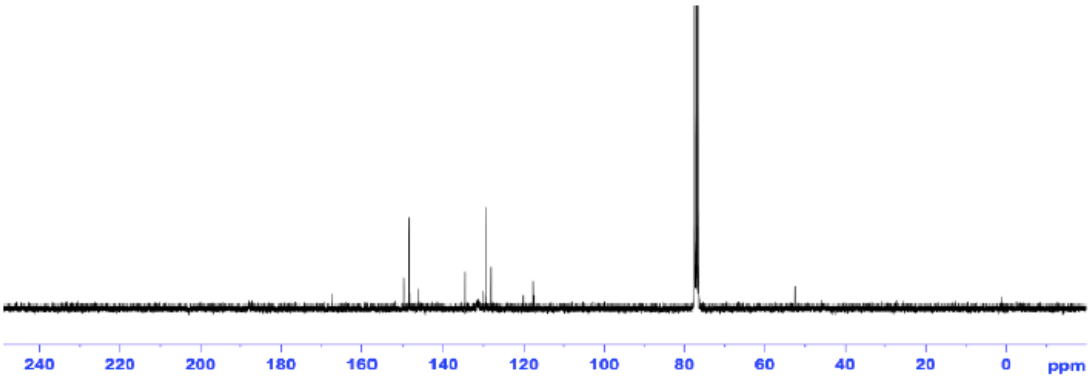


**Figure S15.** $^{13}$C NMR spectrum of porphyrin **5** (75.47 MHz, 298 K, $CDCl_3$)

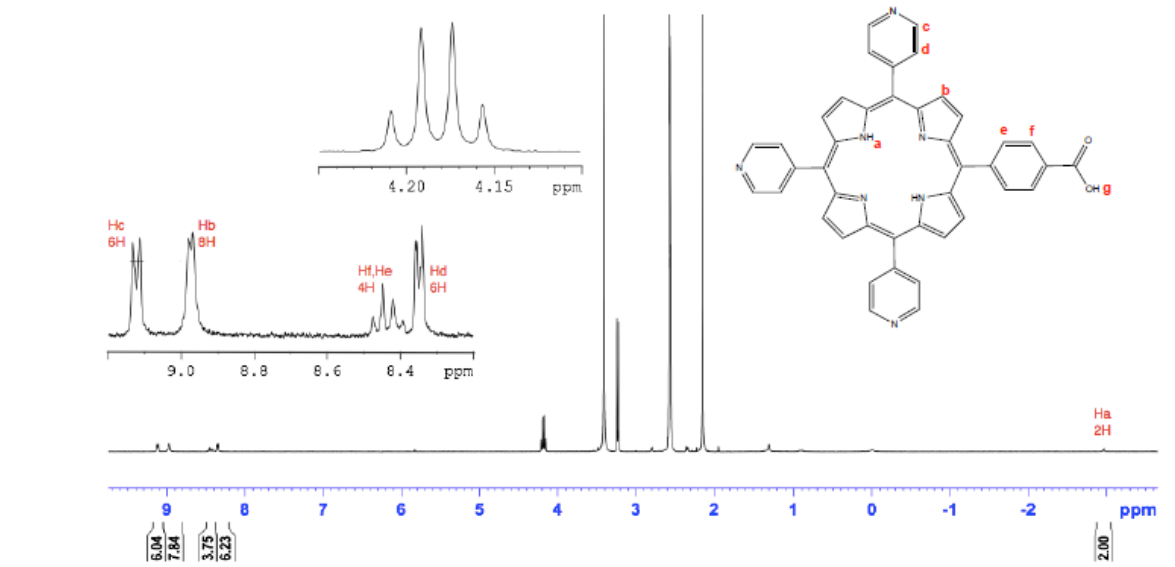


**Figure S16.** $^{1}$H NMR spectrum of porphyrin **6** (300 MHz, 298 K, DMSO)

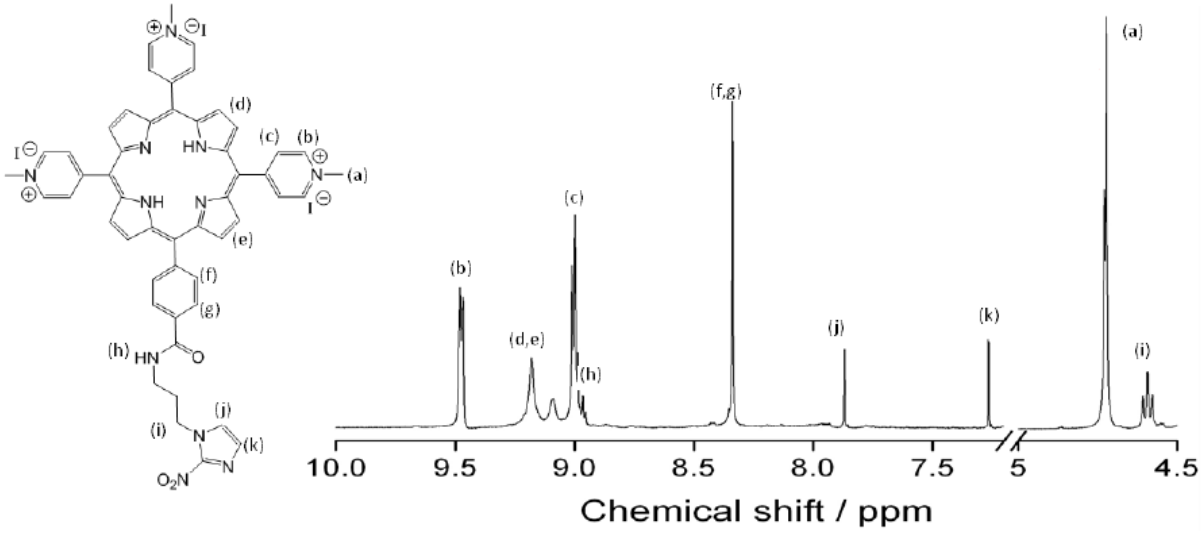

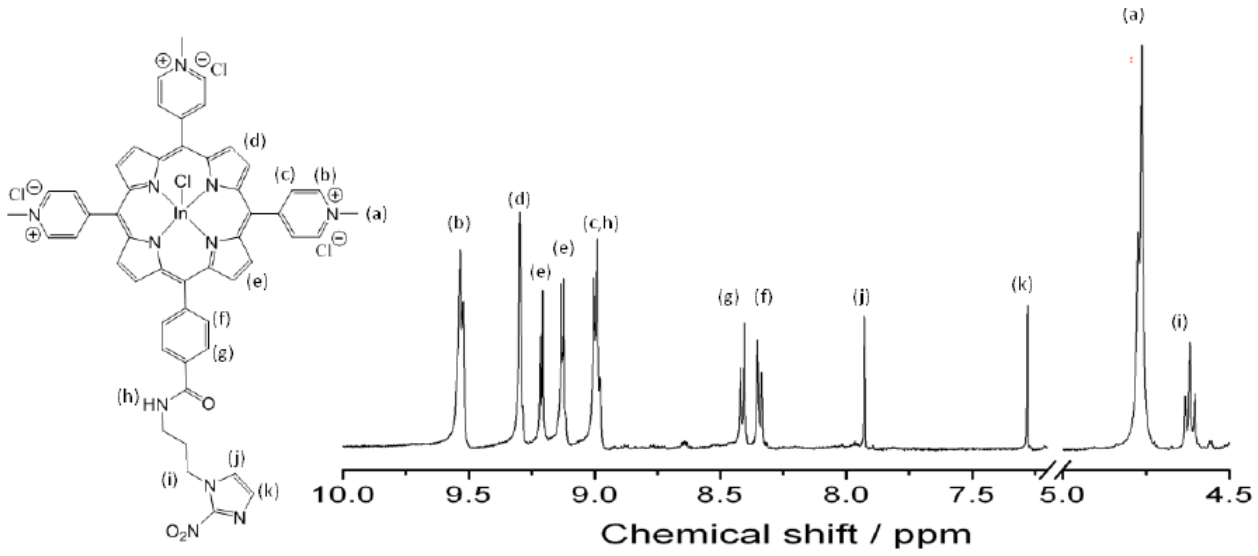


**Figure S17:** $^1$H NMR of **6.4** and **6.5** in *d6*-DMSO at 25°C at 500 MHz

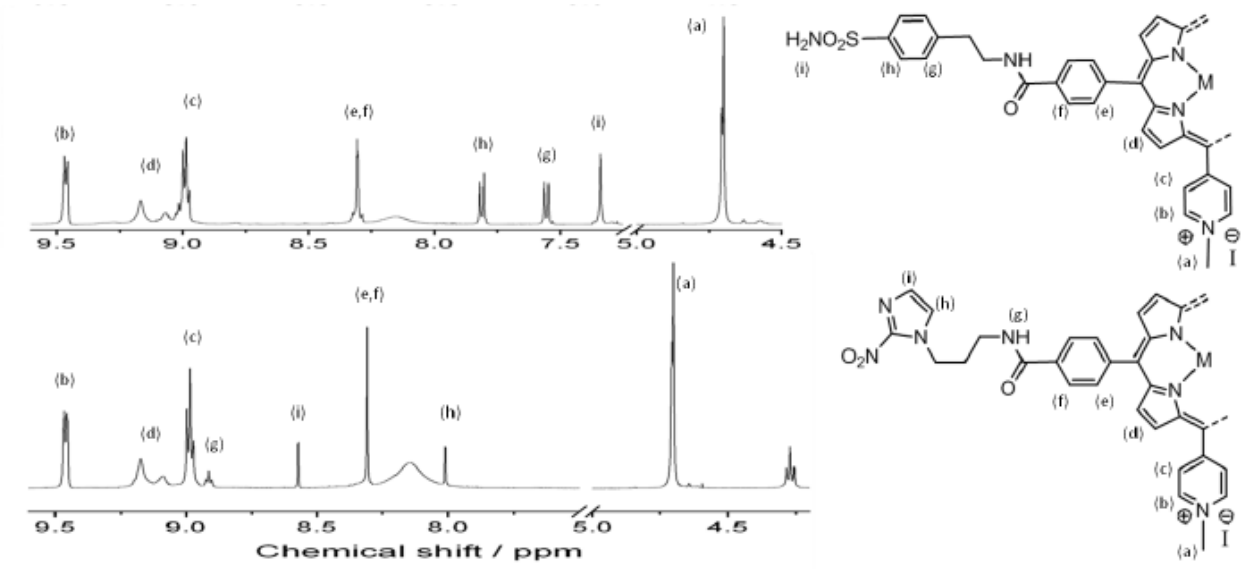


**Figure S18:** Stacked view of $^1$H NMR of **6.1** (top) and **6.4** (bottom) in $d^6$-DMSO at 25 °C at 500 MHz

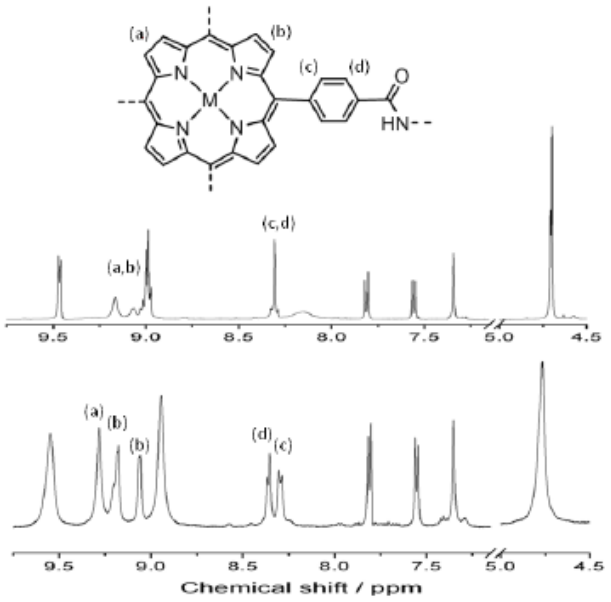


**Figure S19:** a) Stacked view of $^{1}$H NMR of **6.1** (top) and **6.2** (bottom) in $d^{6}$-DMSO at 25 °C at 500 MHz

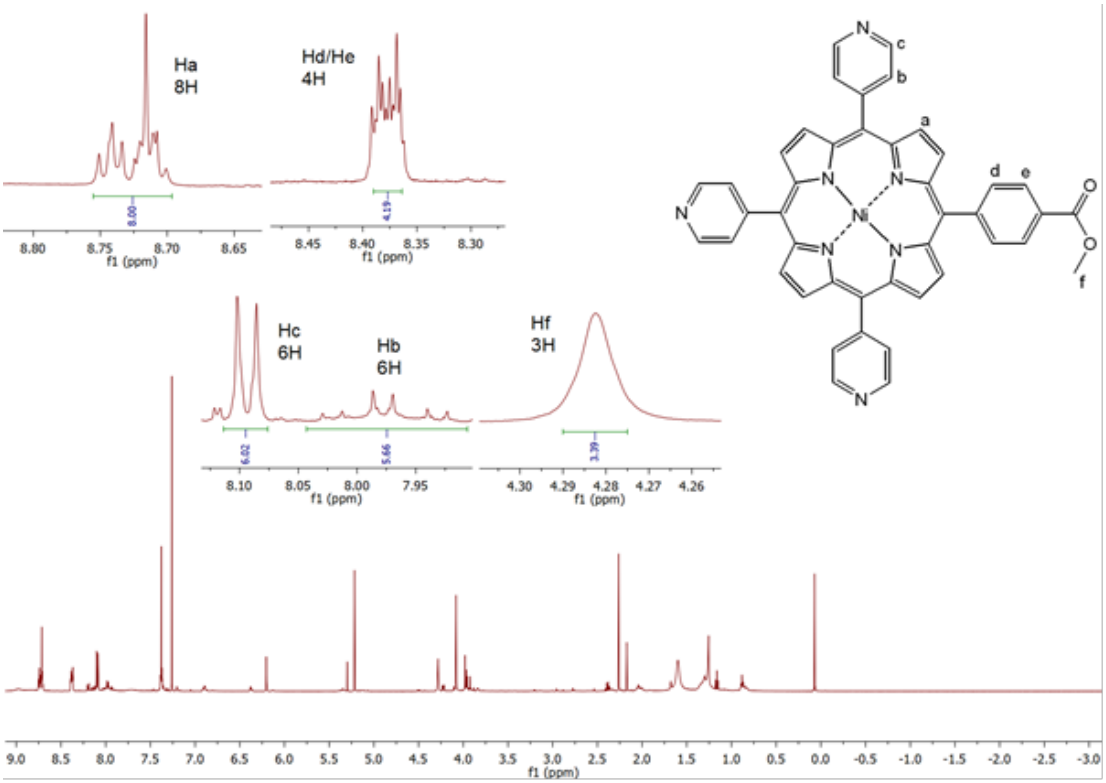


**Figure S20:** $^{1}$H NMR (500 MHz , 298 K, $CDCl_3$,) spectrum of compound **12**

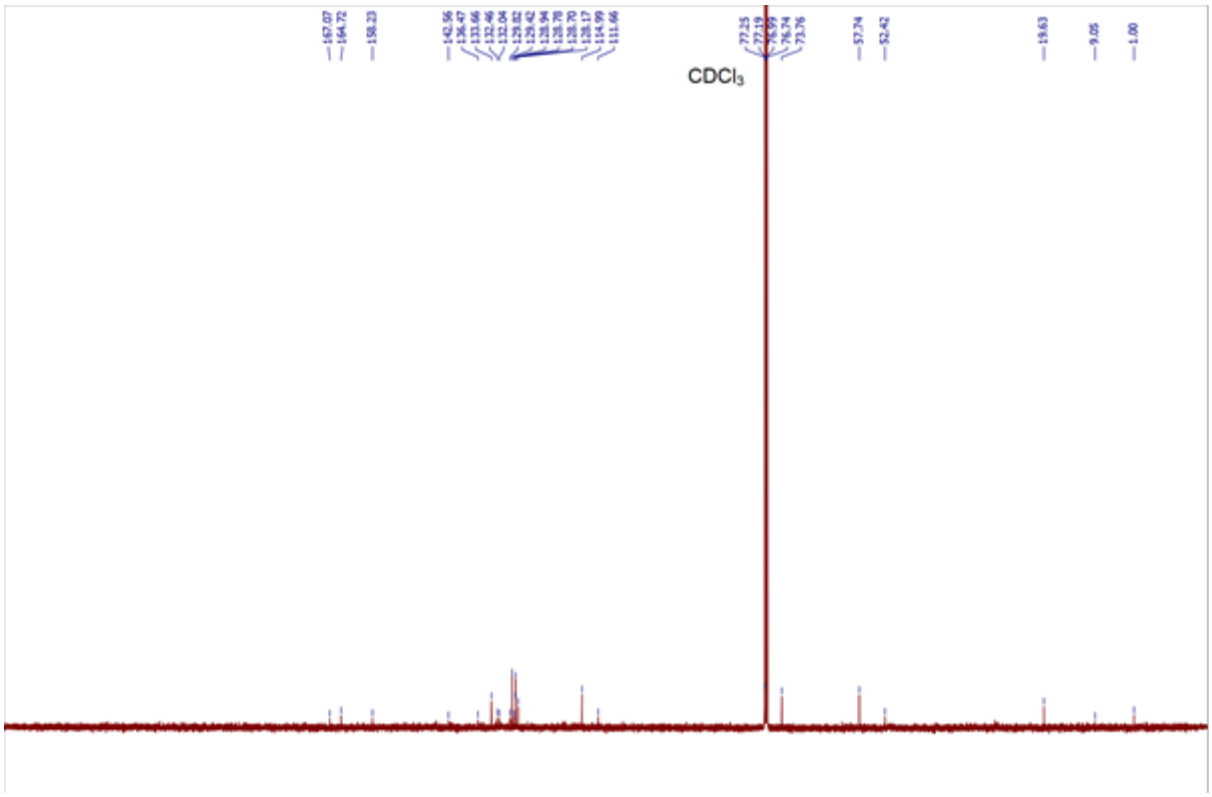


**Figure S21:** $^{13}C$ NMR (500 MHz , 298 K, $CDCl_3$,) spectrum of compound **12**

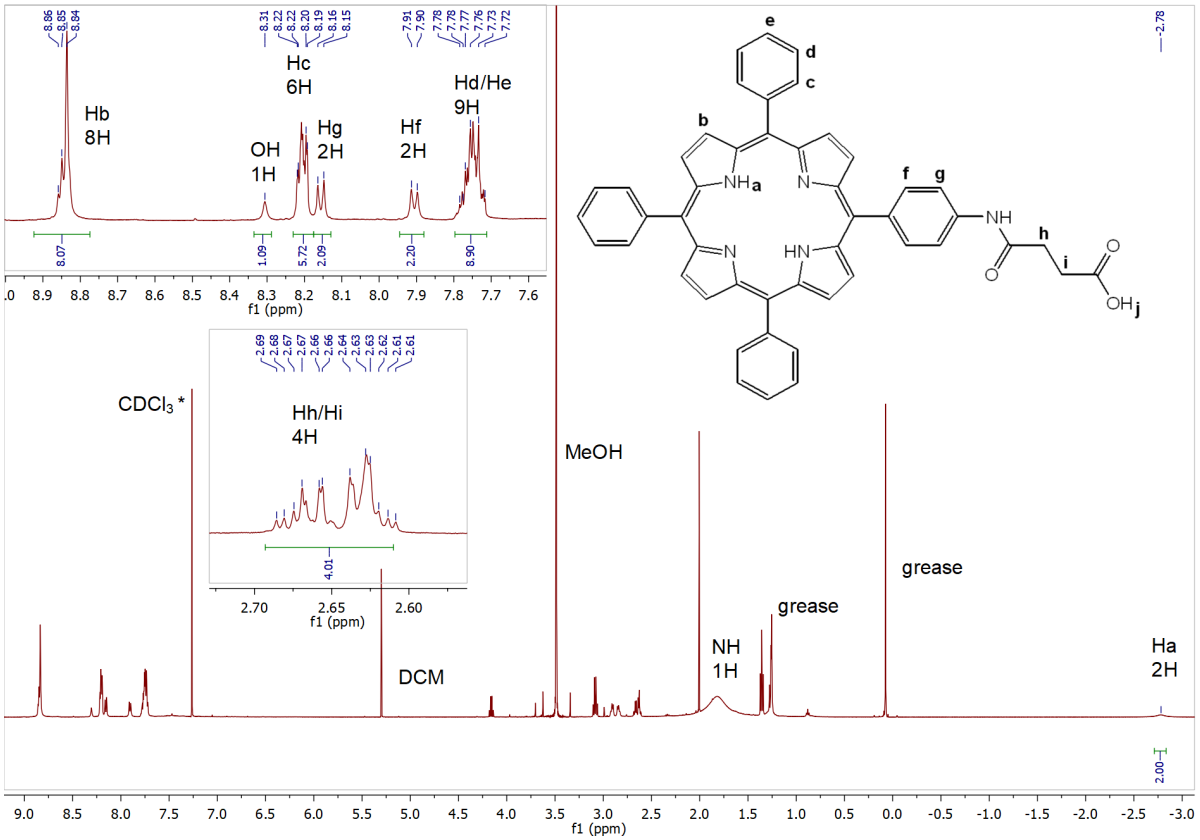


**Figure S22:** $^{1}H$ NMR (500 MHz , 298 K, $CDCl_3$,) spectrum of Compound **4.9**

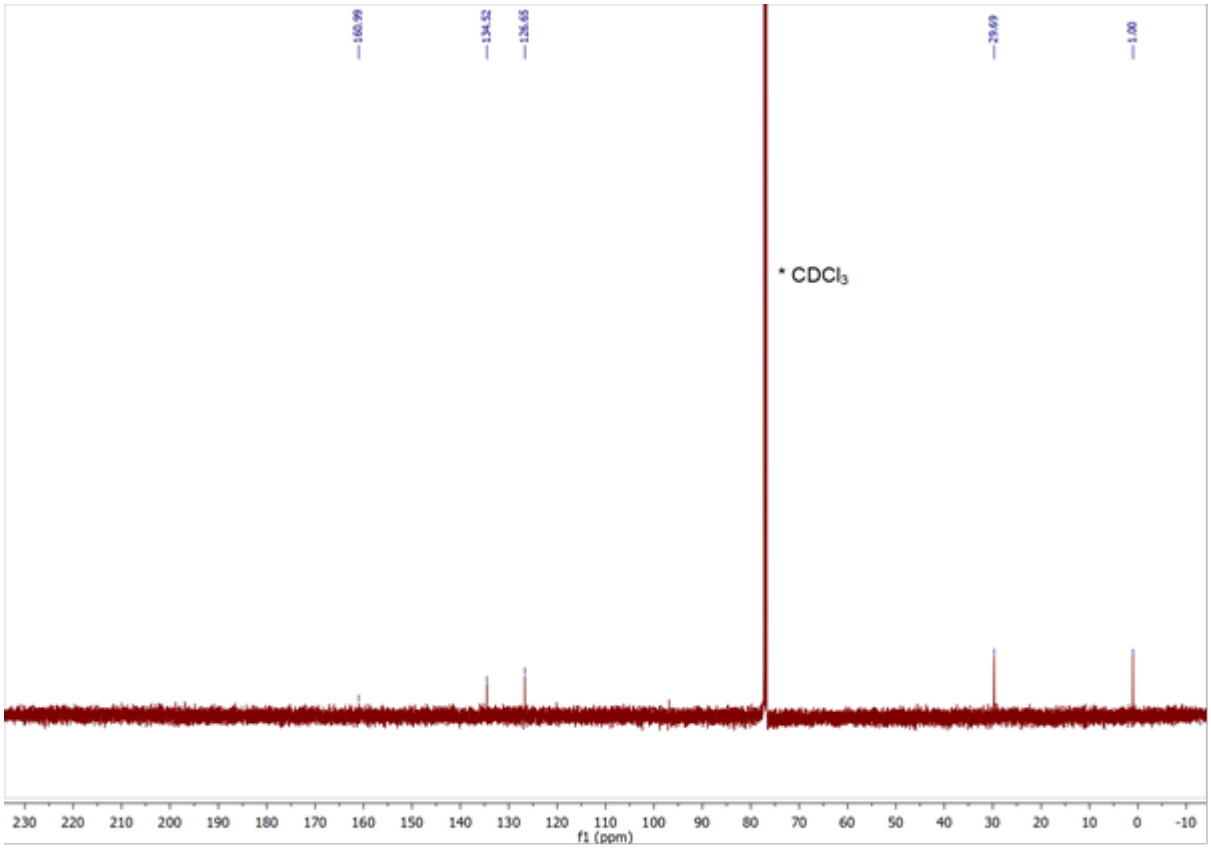


**Figure S23:** $^{13}C$ NMR ( MHz , 298 K, $CDCl_3$) spectrum of Compound **4.9**

4. ESI-MS spectra

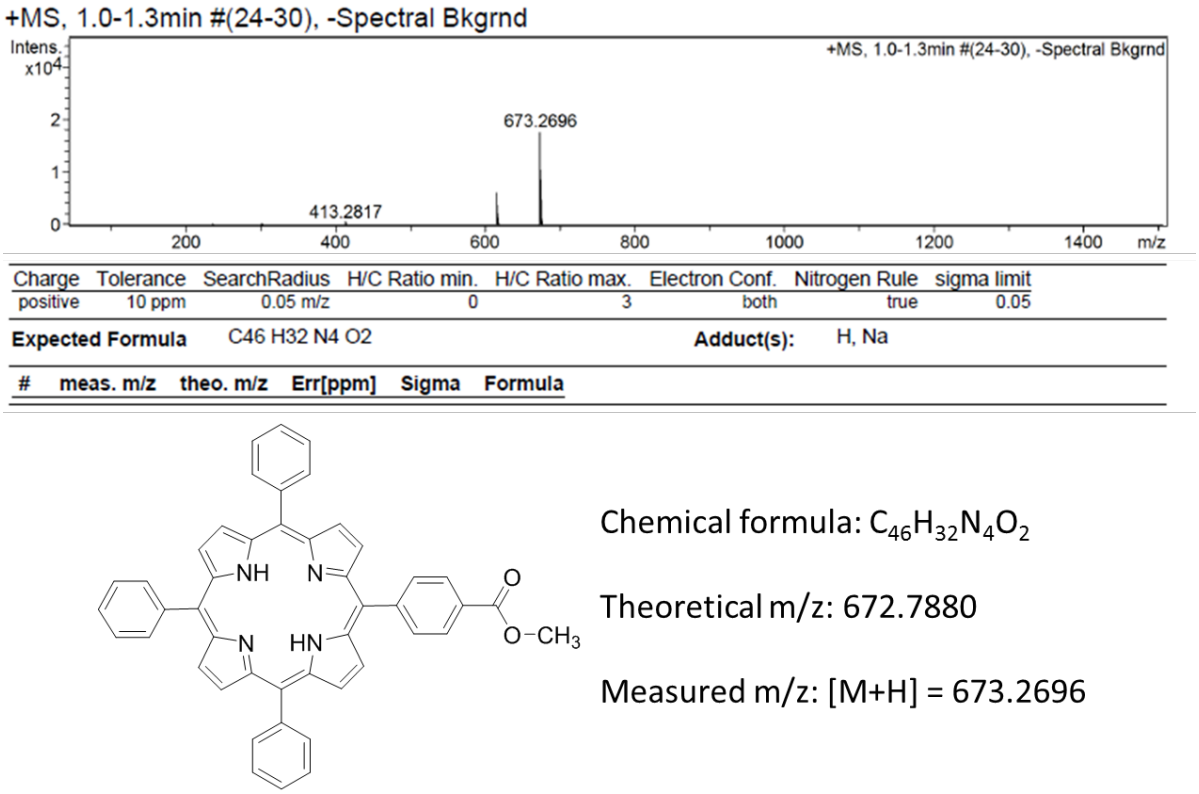


**Figure S24**: ESI/MS for compound **2**.

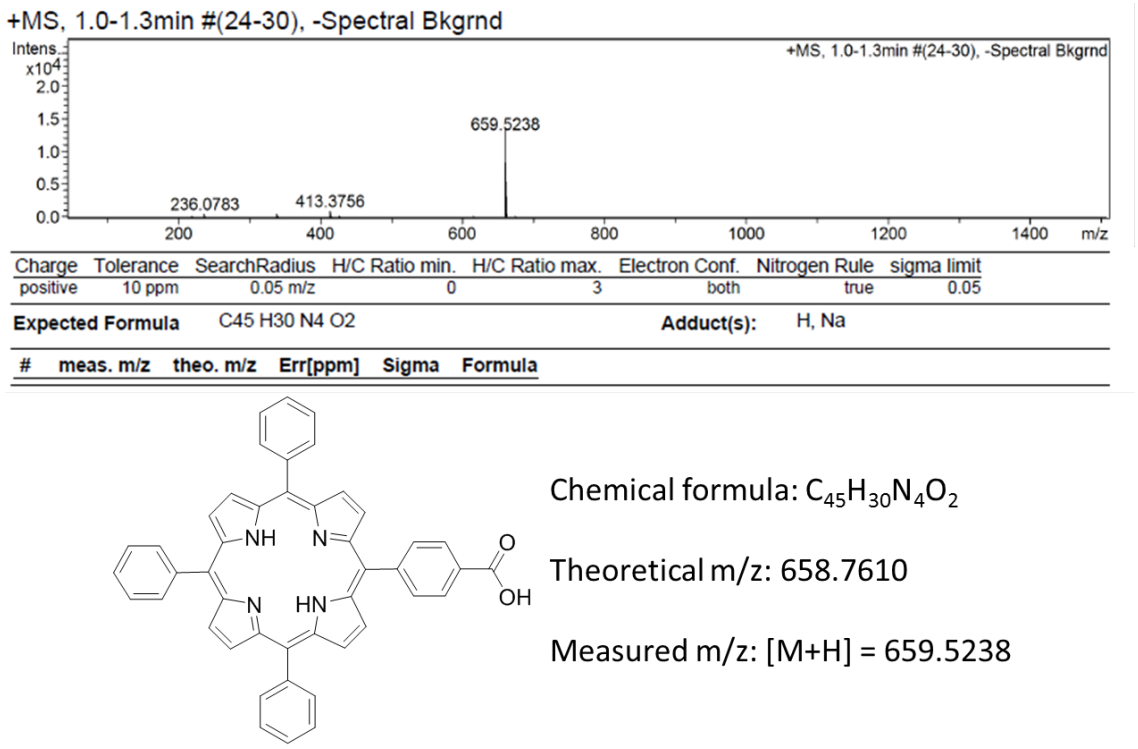


**Figure S25**: ESI/MS for compound **3**.

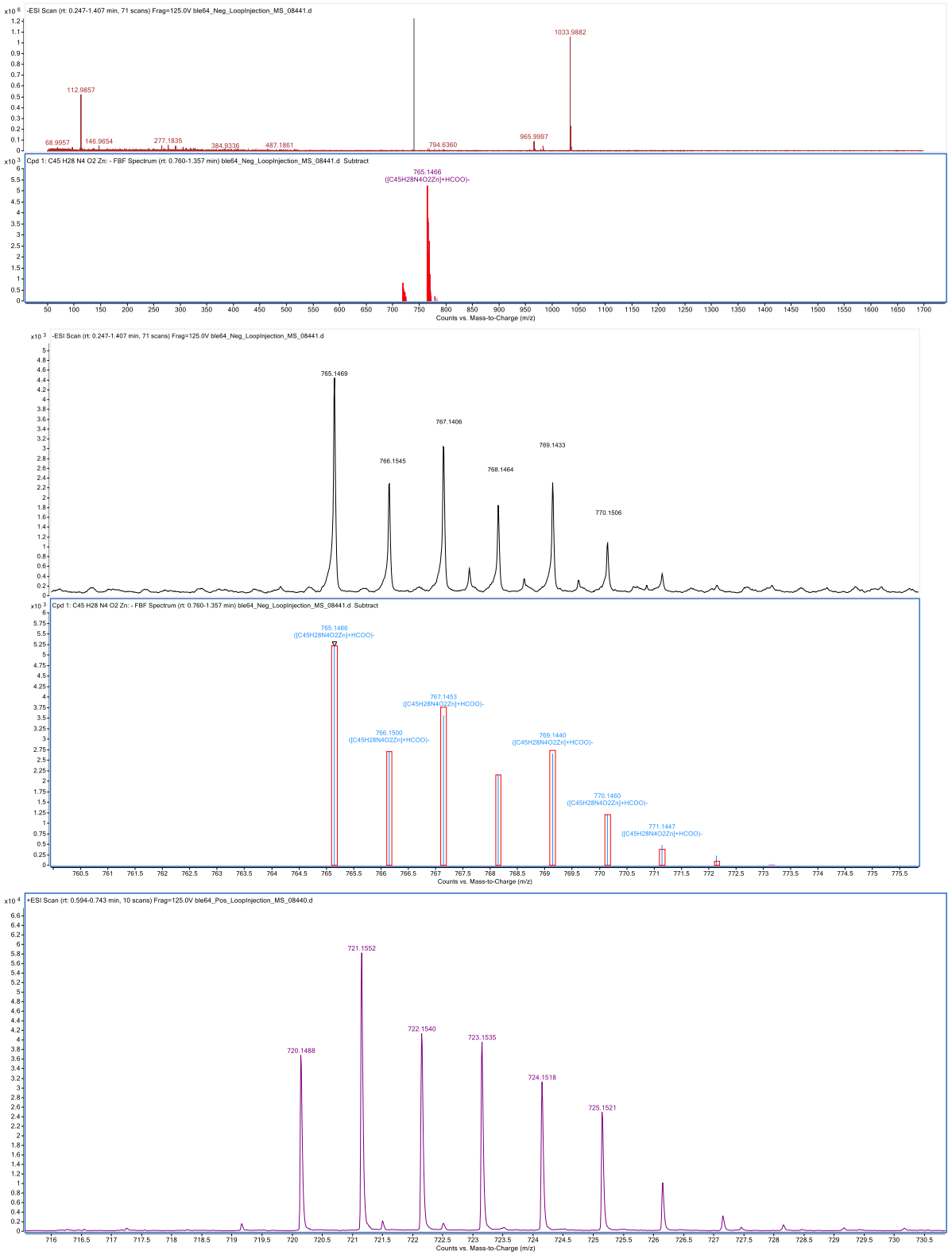


**Figure S26**: Compound **3.1** negative loop injection, full spectral window and observed spectra for [M]+HCOO$^-$ Theoretical = 765.1466, observed = 765.1469 with Zn isotope pattern [M-H] Observed = 721.1552 with Zn isotope pattern.

+MS, 1.0-1.3min #(47-60), -Spectral Bkgrnd

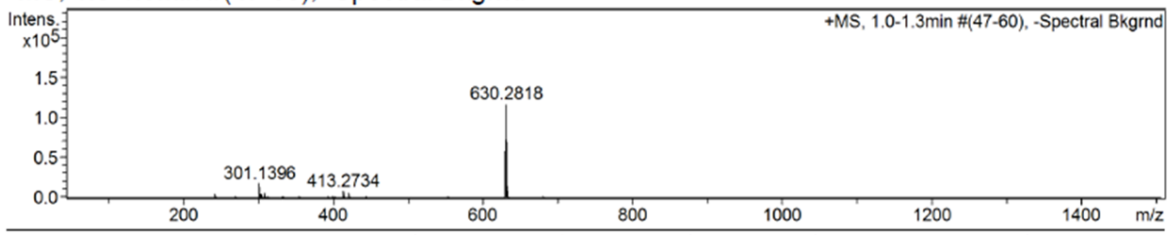


| Charge | Tolerance | SearchRadius | H/C Ratio min. | H/C Ratio max. | Electron Conf. | Nitrogen Rule | sigma limit |
|---|---|---|---|---|---|---|---|
| positive | 10 ppm | 0.05 m/z | 0 | 3 | both | true | 0.05 |

**Expected Formula** C44 H31 N5 **Adduct(s):** H, Na

| # | meas. m/z | theo. m/z | Err[ppm] | Sigma | Formula |
|---|---|---|---|---|---|

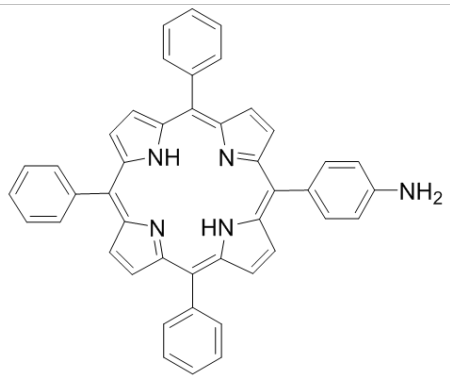


Chemical formula: $C_{44}H_{31}N_5$

Theoretical m/z: 629.7670

Measured m/z: [M+H] = 630.2818

**Figure S27**: ESI/MS for compound **4**.

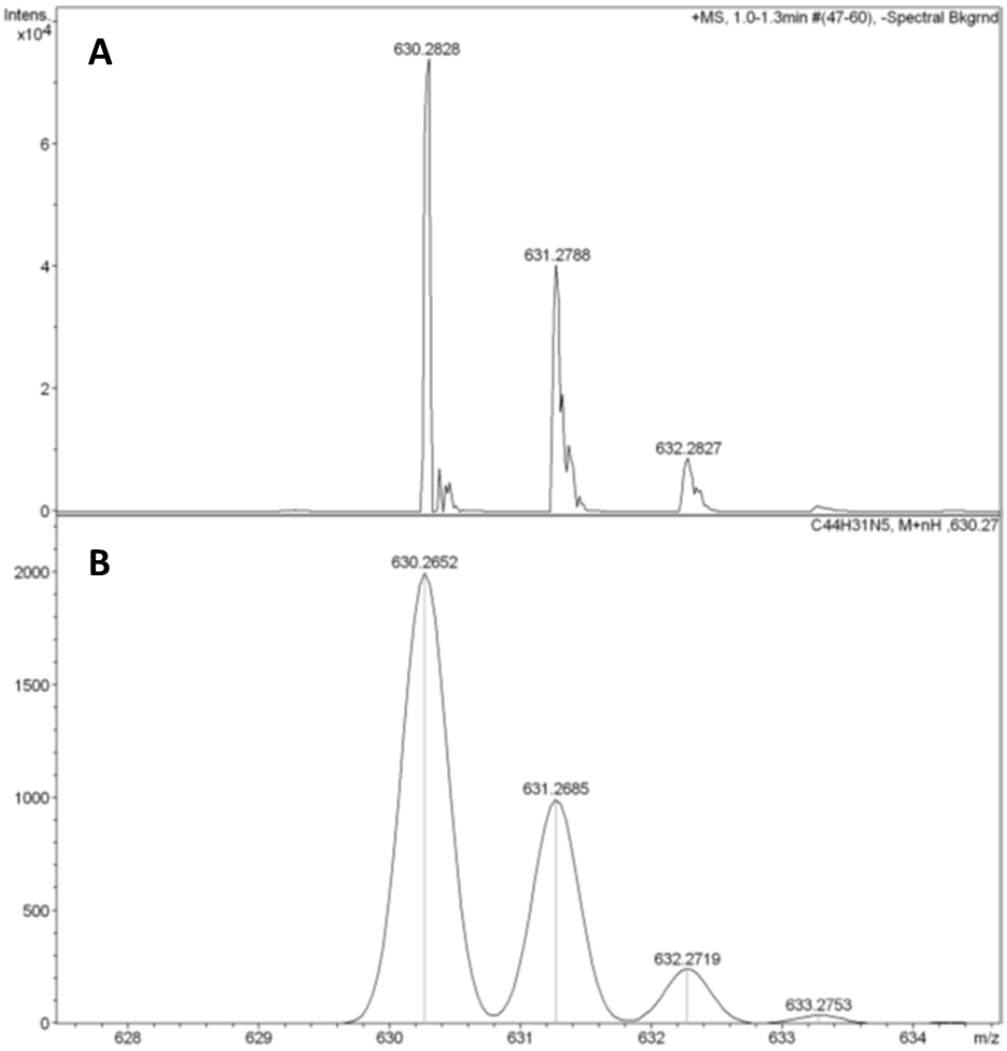


**Figure S28**: ESI-MS of unprotected porphyrin, compound **4**, showing observed (A) and theoretical (B) isotope patterns.

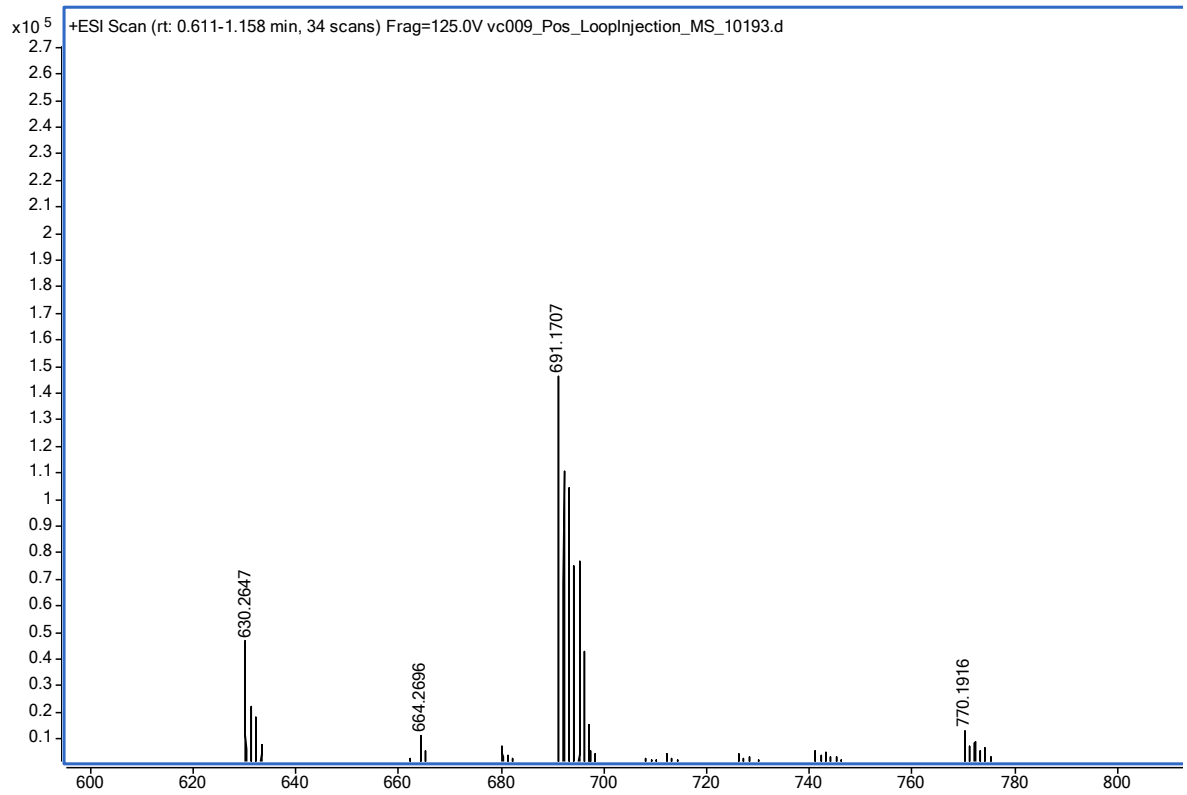
x10 5
+ESI Scan (rt: 0.611-1.158 min, 34 scans) Frag=125.0V vc009_Pos_LoopInjection_MS_10193.d
630.2647
664.2696
691.1707
770.1916

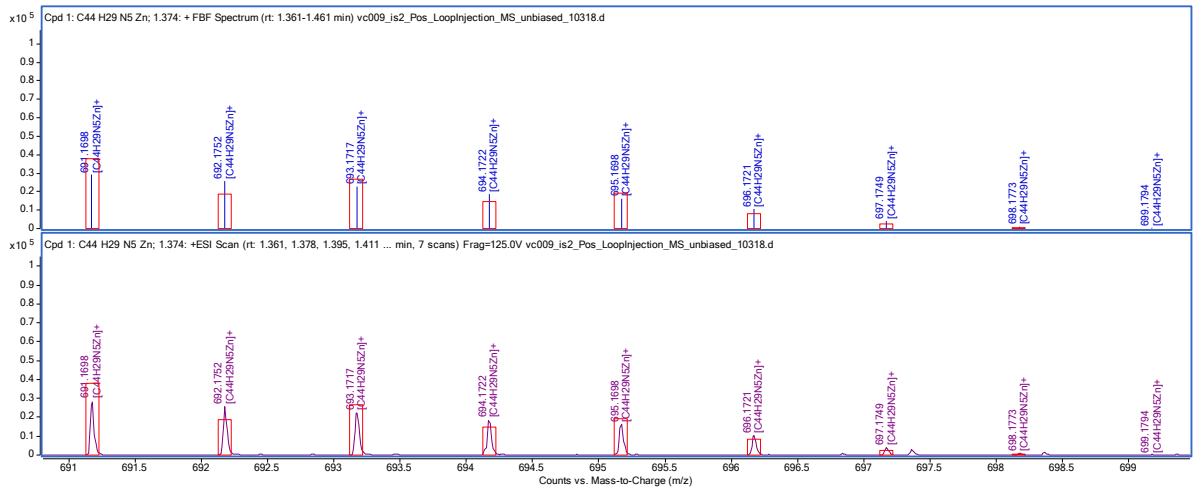
Cpd 1: C44 H29 N5 Zn; 1.374: + FBF Spectrum (rt: 1.361-1.461 min) vc009_is2_Pos_LoopInjection_MS_unbiased_10318.d
Cpd 1: C44 H29 N5 Zn; 1.374: +ESI Scan (rt: 1.361, 1.378, 1.395, 1.411 ... min, 7 scans) Frag=125.0V vc009_is2_Pos_LoopInjection_MS_unbiased_10318.d
Counts vs. Mass-to-Charge (m/z)

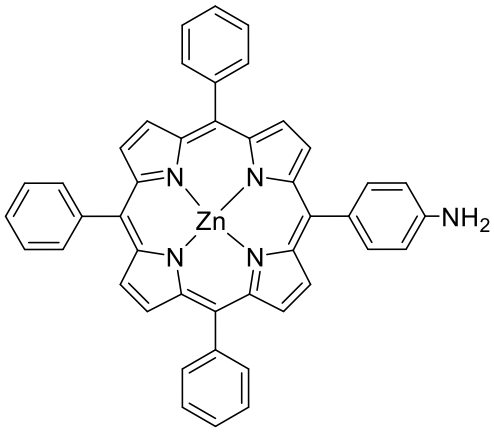


Chemical Formula: $C_{44}H_{29}N_5Zn$

Theoretical m/z: 691.1709

Observed m/z: [M+Z] = 691.1707

Deviation: 0.28 ppm

**Figure S29***: ESI-MS* of compound **4.1**

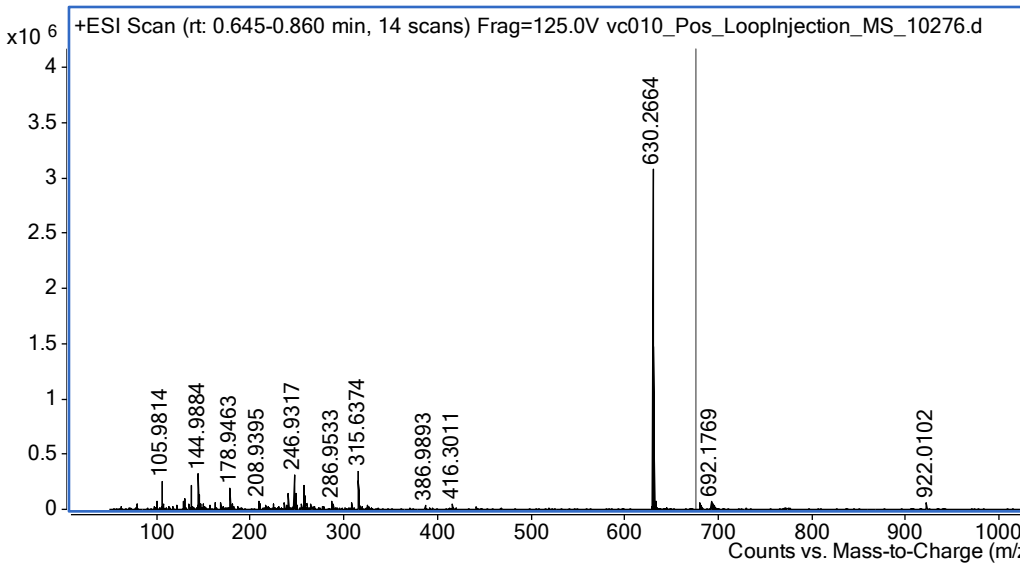
+ESI Scan (rt: 0.645-0.860 min, 14 scans) Frag=125.0V vc010_Pos_LoopInjection_MS_10276.d
x10 6
630.2664
692.1769
922.0102
105.9814
144.9884
178.9463
208.9395
246.9317
286.9533
315.6374
386.9893
416.3011
Counts vs. Mass-to-Charge (m/z)

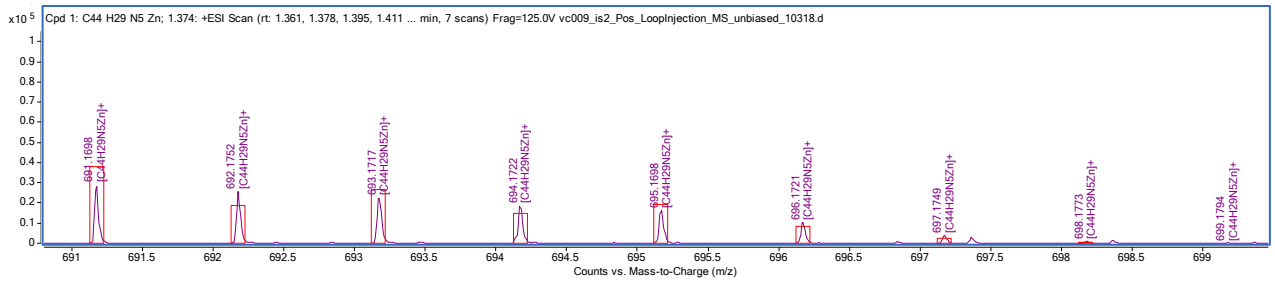
Cpd 1: C44 H29 N5 Zn; 1.374: +ESI Scan (rt: 1.361, 1.378, 1.395, 1.411 ... min, 7 scans) Frag=125.0V vc009_is2_Pos_LoopInjection_MS_unbiased_10318.d
x10 5
691.1698 [C44H29N5Zn]+
692.1752 [C44H29N5Zn]+
693.1717 [C44H29N5Zn]+
694.1722 [C44H29N5Zn]+
695.1698 [C44H29N5Zn]+
696.1721 [C44H29N5Zn]+
697.1749 [C44H29N5Zn]+
698.1773 [C44H29N5Zn]+
699.1794 [C44H29N5Zn]+
Counts vs. Mass-to-Charge (m/z)

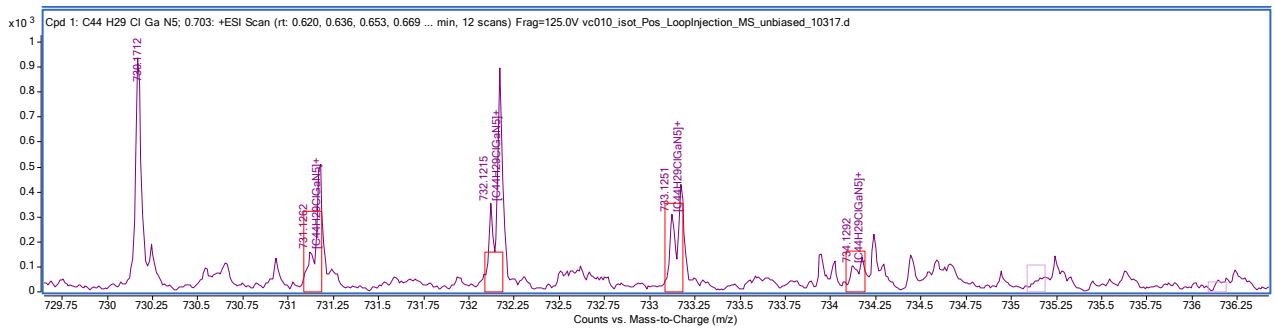
Cpd 1: C44 H29 Cl Ga N5; 0.703: +ESI Scan (rt: 0.620, 0.636, 0.653, 0.669 ... min, 12 scans) Frag=125.0V vc010_isot_Pos_LoopInjection_MS_unbiased_10317.d
x10 3
730.1712
731.1262 [C44H29ClGaN5]+
732.1215 [C44H29ClGaN5]+
733.1251 [C44H29ClGaN5]+
734.1292 [C44H29ClGaN5]+
Counts vs. Mass-to-Charge (m/z)

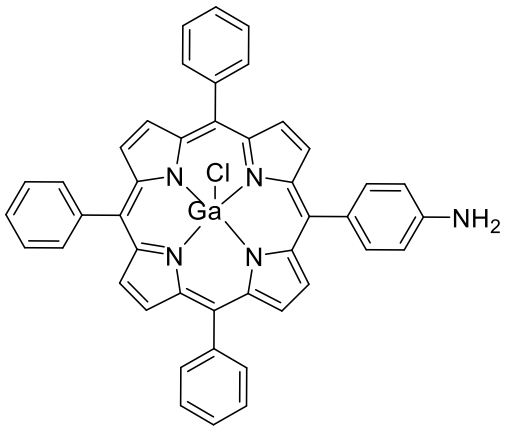


Chemical Formula: $C_{44}H_{29}ClGaN_5$

Measured m/z: $[M + H]^+ = 732.1262$

Theoretical m/z: 732.1446

Deviation: 24.99 ppm

**Figure S30**: ESI/MS calculated mass for compound **4.2**.

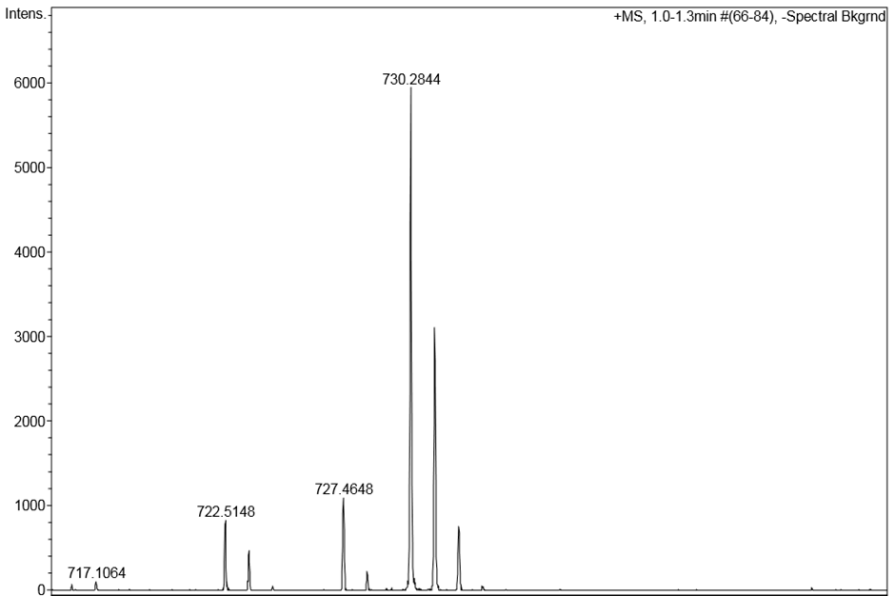

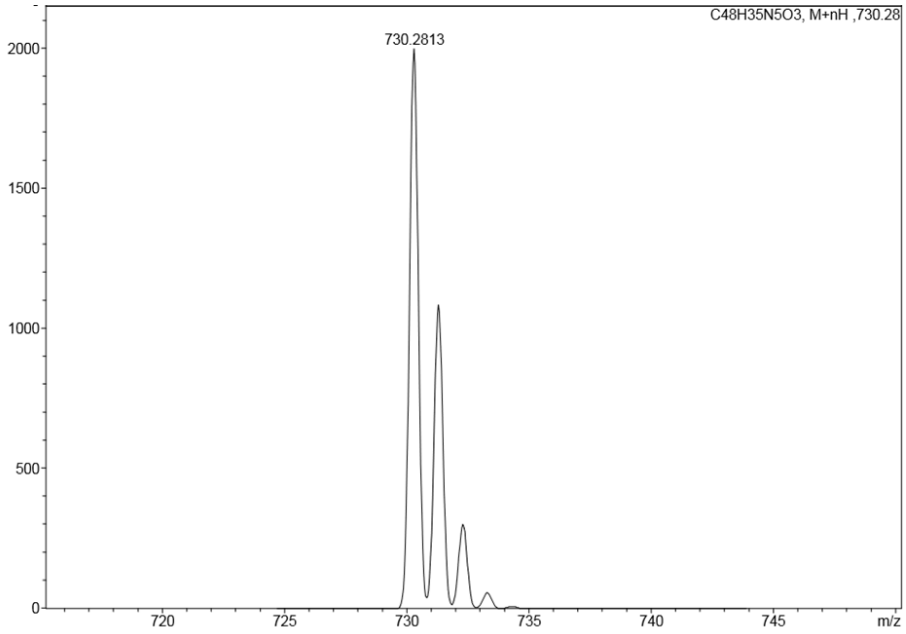


**Figure S31.** Expansion of the relevant peak in the $ESI^+$ $TOF^+$ mass spectroscopy of Compound **4.9.** Top: observed, bottom: predicted spectrum from chemical formula

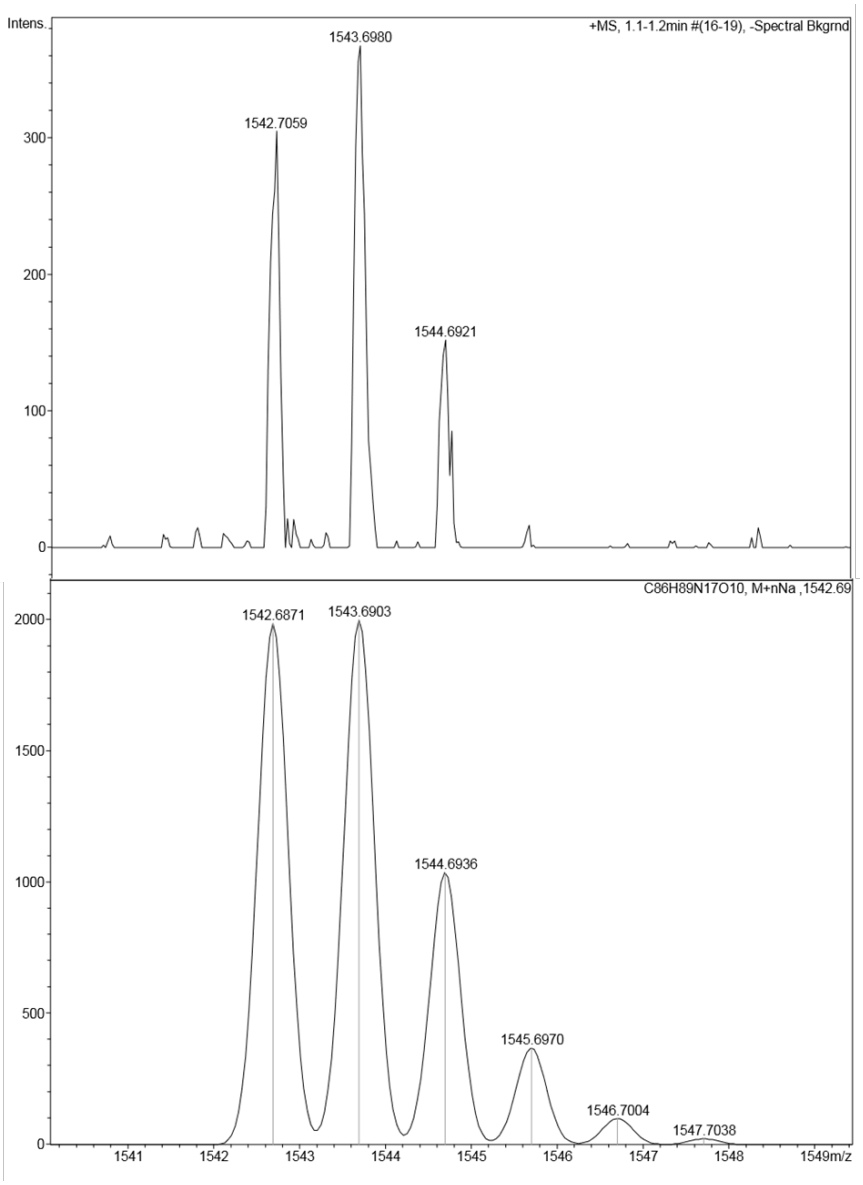


**Figure S32:** Expansion of the relevant peak in the $ESI^+$ $TOF^+$ mass spectroscopy Compound **4.10.** Top: observed, bottom: predicted spectrum from chemical formula.

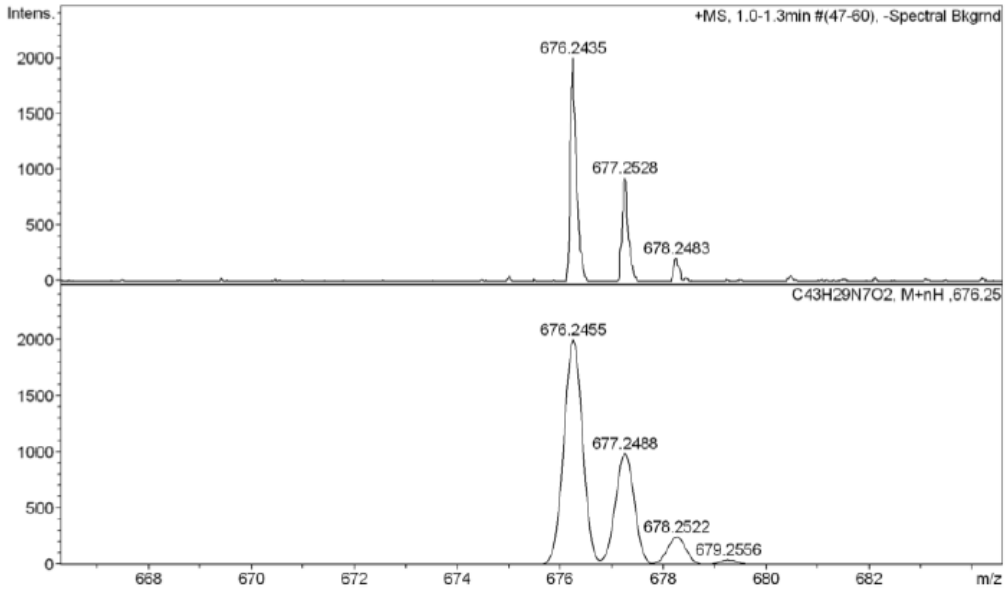


**Figure S33.** Expansion of the relevant peak in the ESI$^+$ mass spectrometry of mono-substituted porphyrin **5**: top: observed, bottom: predicted spectrum from chemical formula.

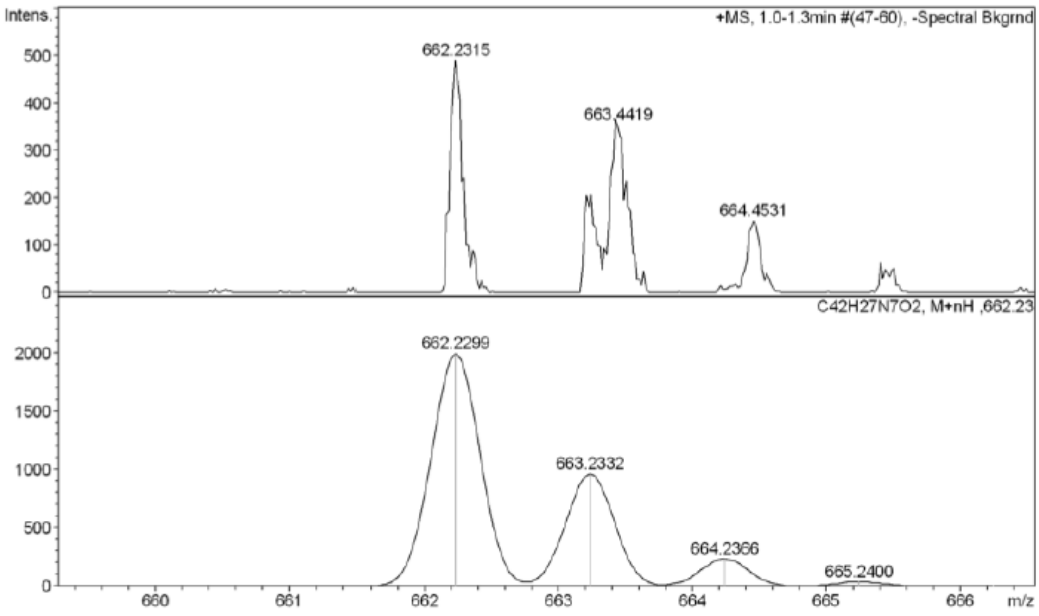


**Figure S34.** Expansion of the relevant peak in the ESI$^+$ mass spectrometry of porphyrin **6**: top:obsereved, bottom: predicted.

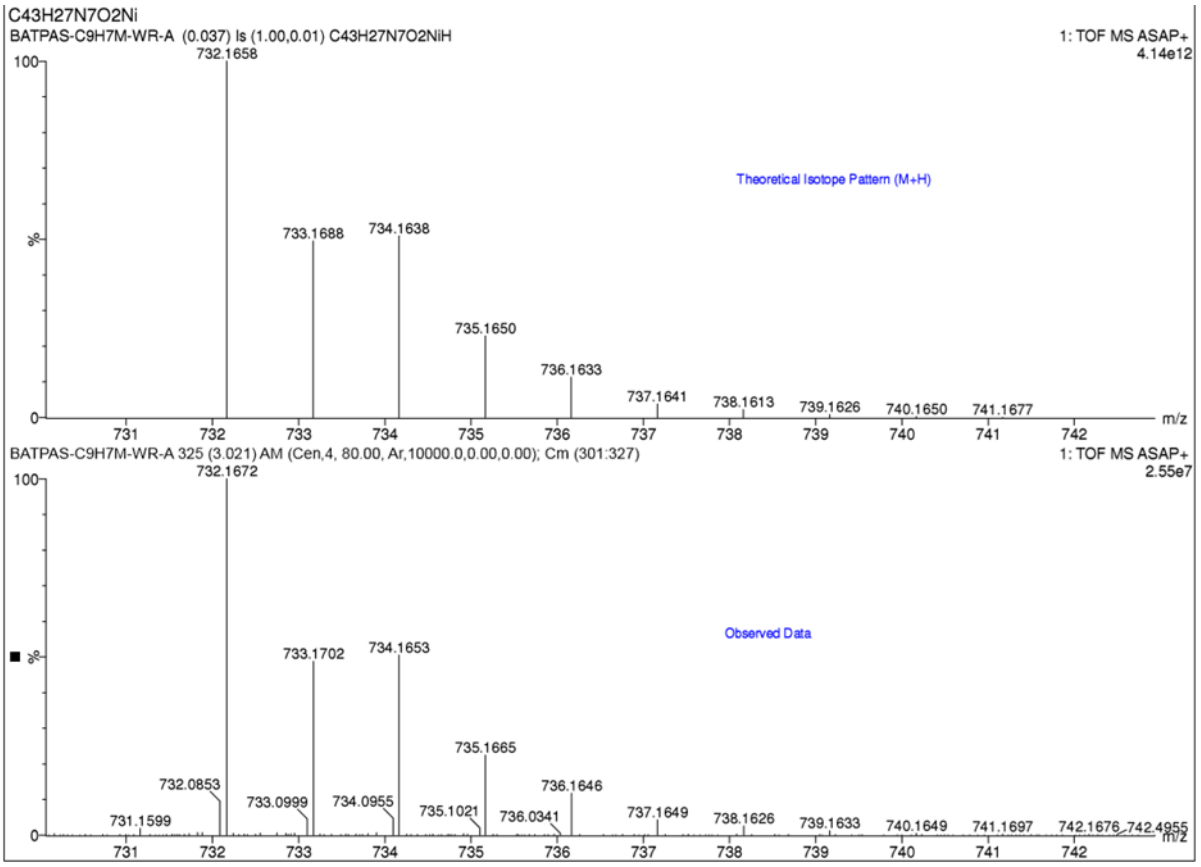


**Figure S35**. Expansion of the relevant peak in the ESI$^-$ TOF$^+$ mass spectroscopy of Compound **12.** Top: predicted spectrum from chemical formula, bottom: observed

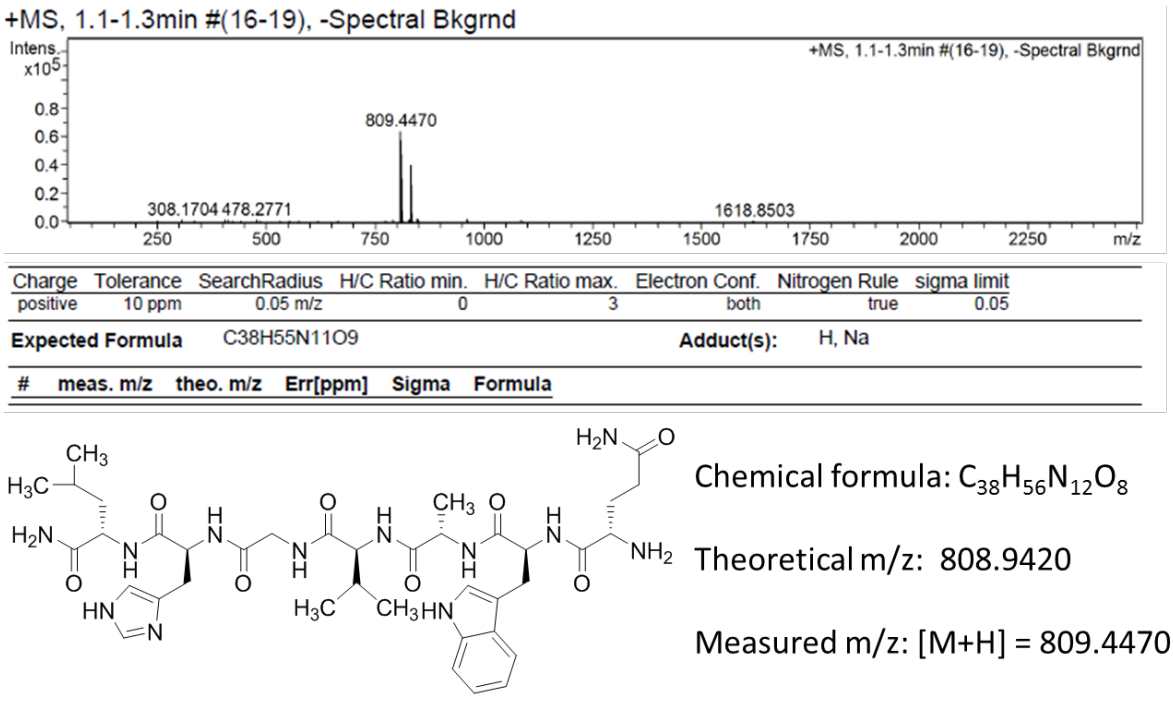


**Figure S36**: ESI/MS for compound **BBN**.

5. HPLC traces

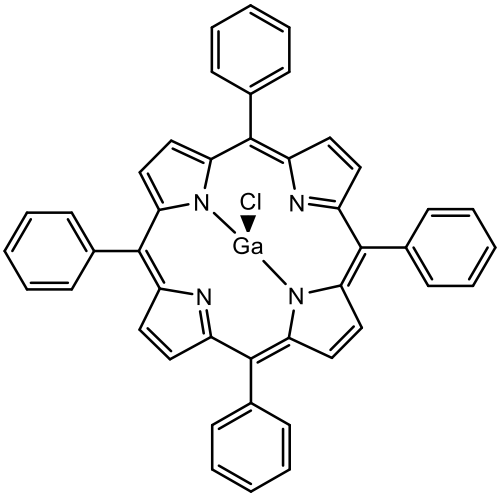


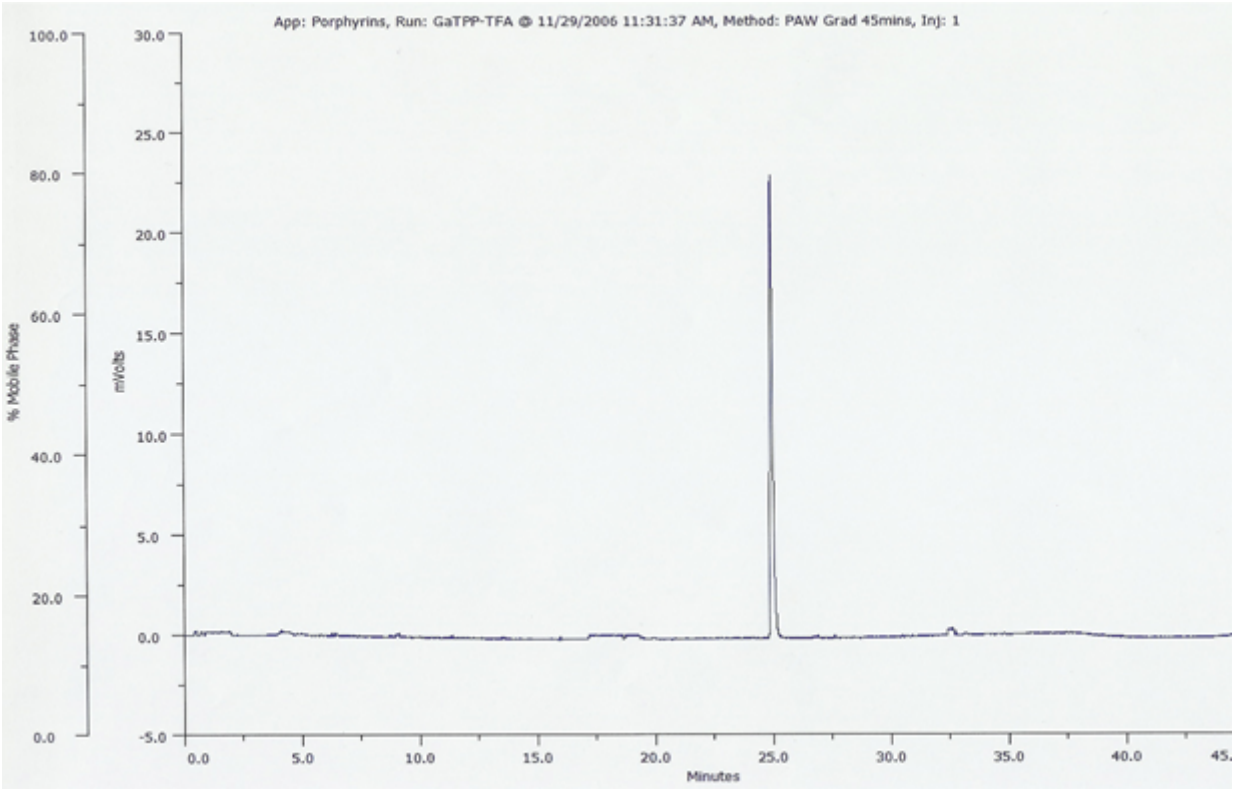

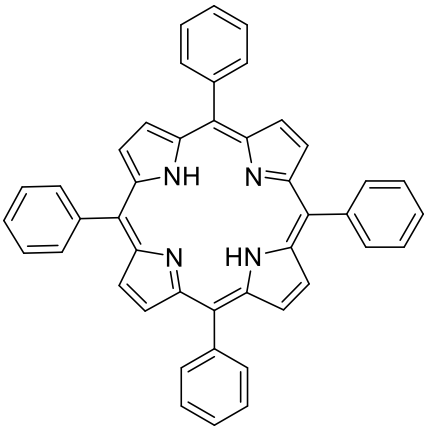


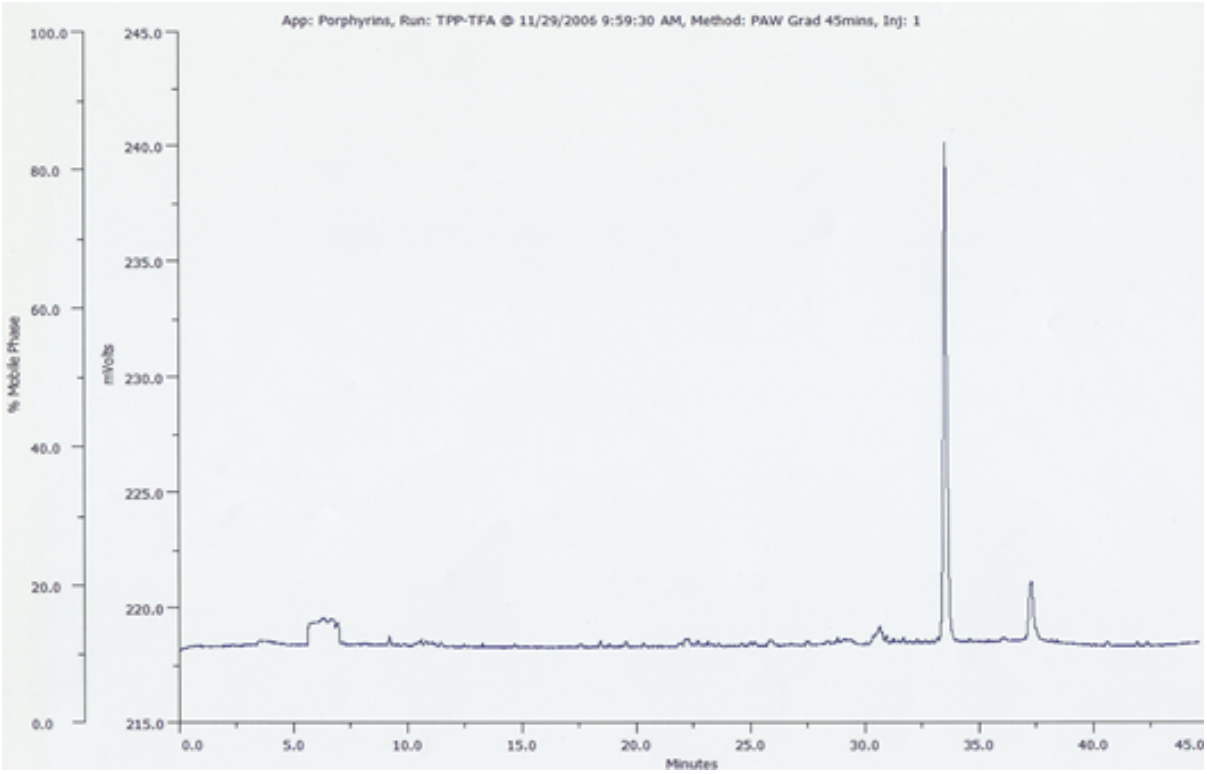


**Figure S37**: HPLC traces for Ga-TPP **1.1** (at the top) and TPP **1** (at the bottom).

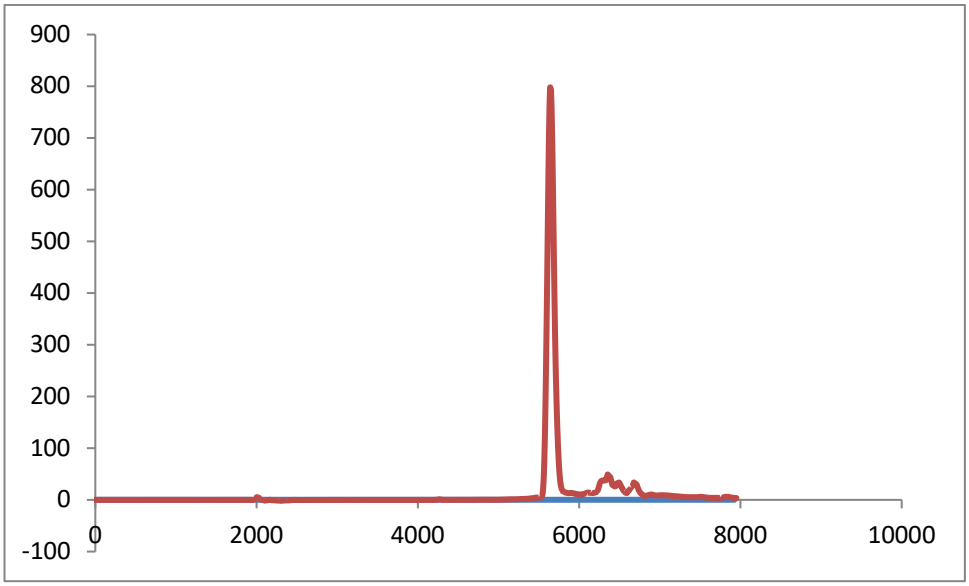


**Figure S38**: HPLC traces for compound **4.1**, 450 nm (MeCN, 2µM solution)

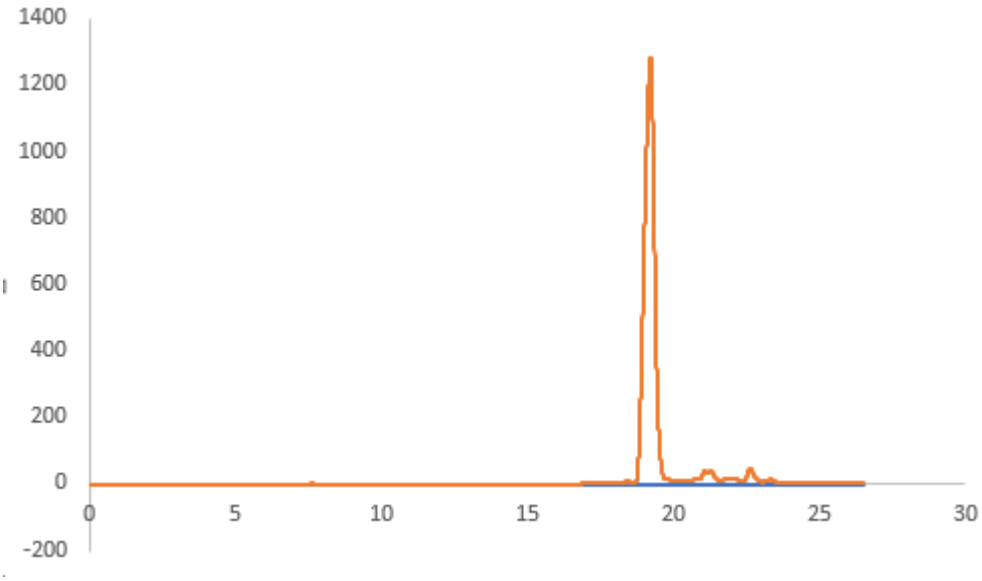


**Figure S39**: HPLC traces for compound **4.2**, 450 nm

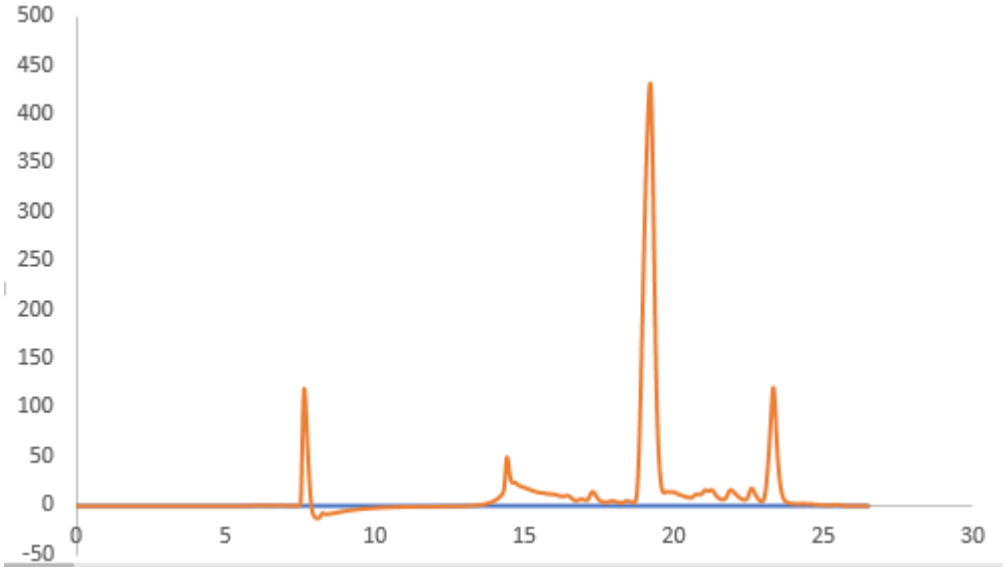


**Figure S40**: HPLC traces for compound **4.2**, 214 nm

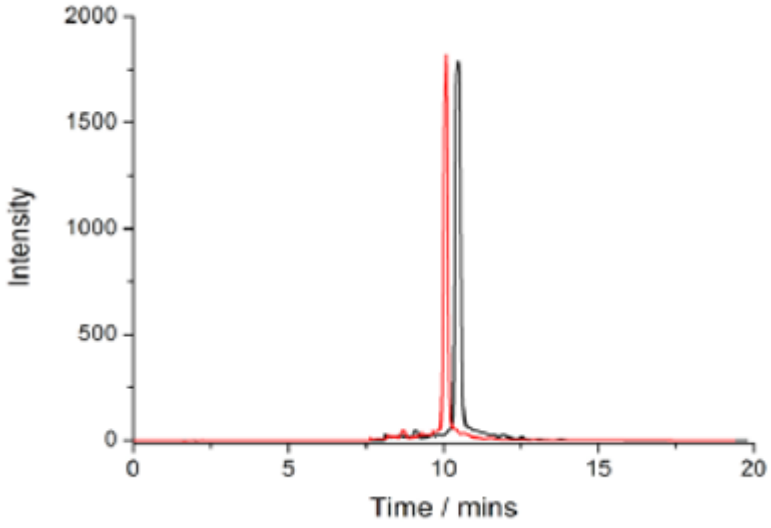


**Figure S41**: HPLC overlay of **6.1** (black) and **6.2** (red)

**Cys-BBN(7-14)-$NH_2$**

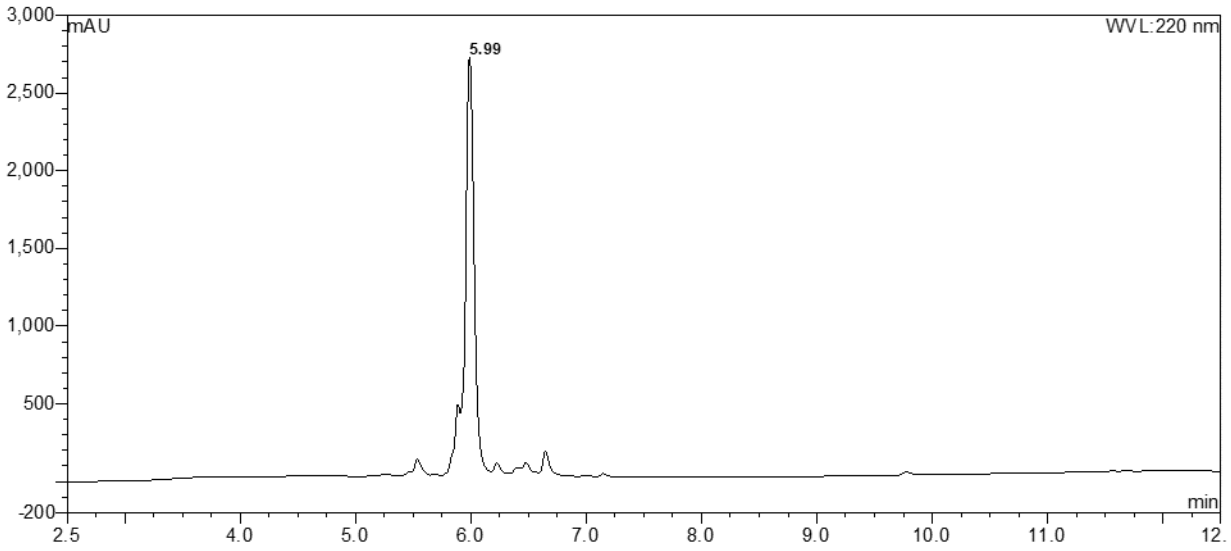


**Figure S42**: Analytical HPLC chromatogram of peptide **Cys-BBN(7-14)-$NH_2$**

**11-Azidoundecanoyl-BBN(7-14)-$NH_2$**

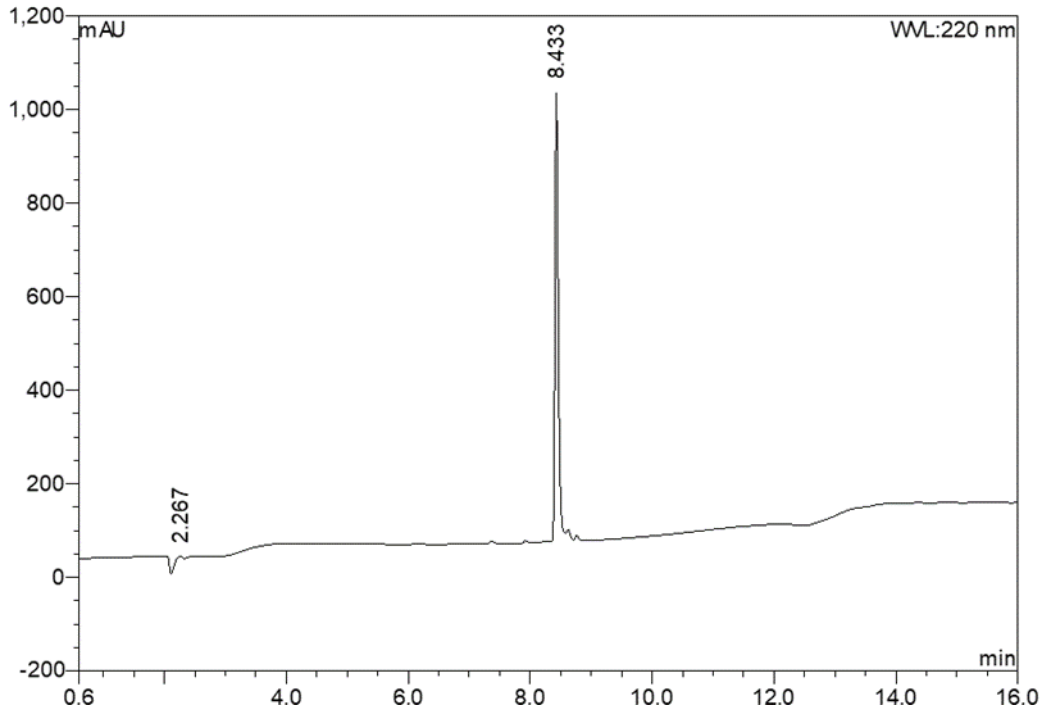


**Figure S43**: Analytical HPLC chromatogram of peptide **11-azidoundecanoyl-BBN(7-14)-$NH_2$**

**Thiol-maleimide conjugate BBN(7-14)-$NH_2$ (4.12)**

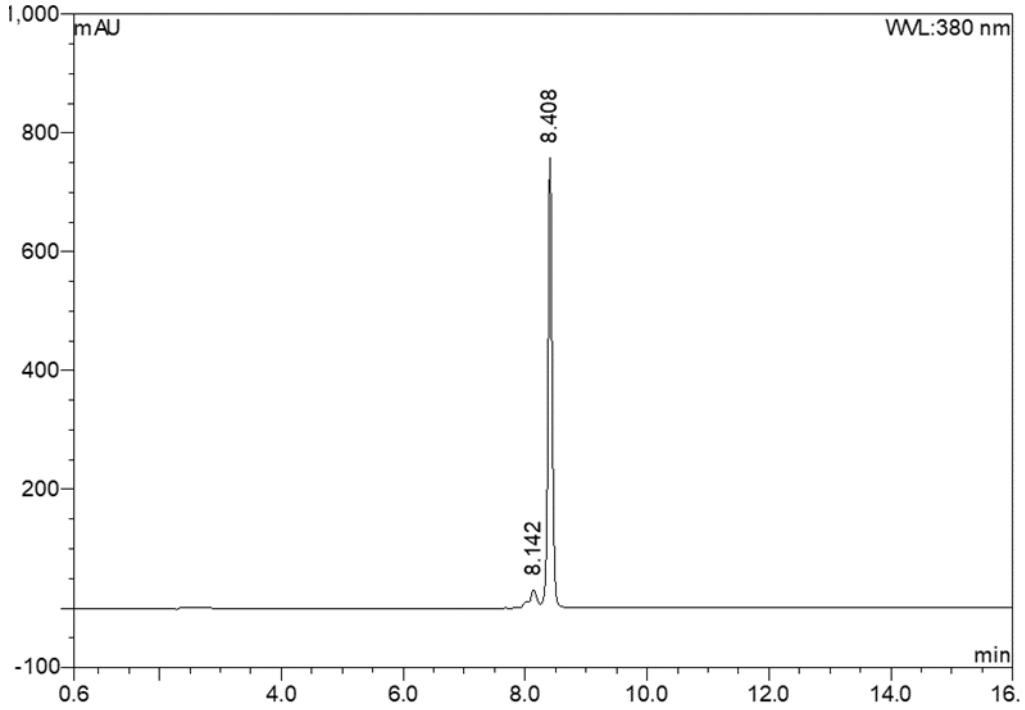


**Figure S44**: Analytical HPLC chromatogram of peptide-porphyrin conjugate (**4.12**)

**SPAAC conjugate BBN(7-14)-$NH_2$ (4.14)**

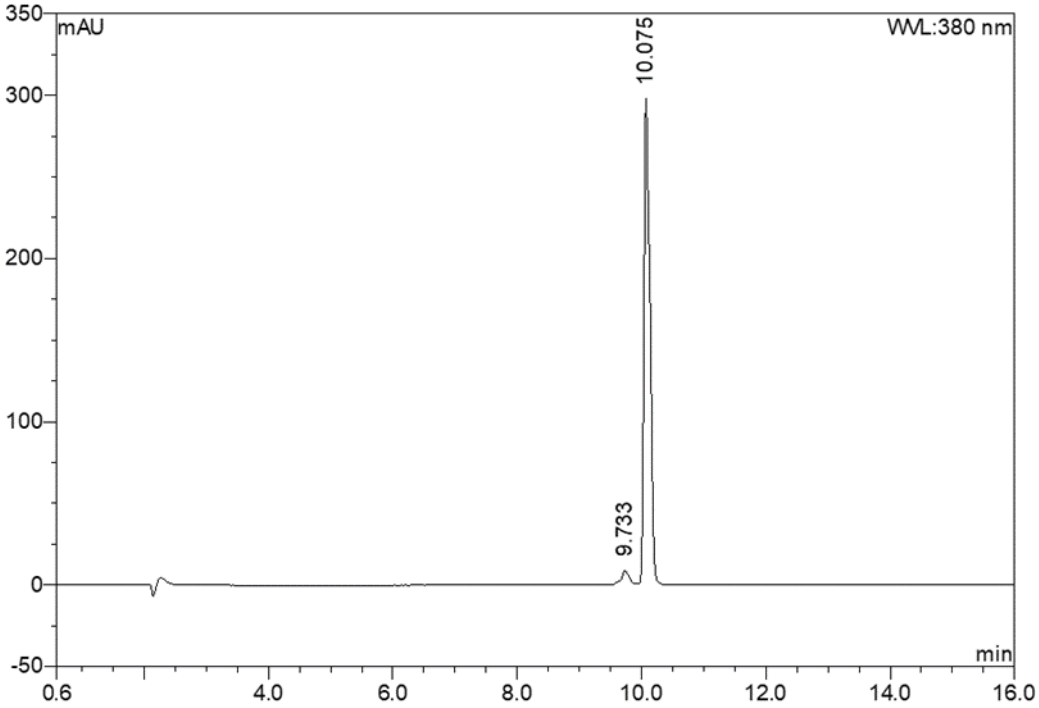


**Figure S45**: Analytical HPLC chromatogram of peptide-porphyrin conjugate (**4.14**)

6. UV-Vis spectroscopy

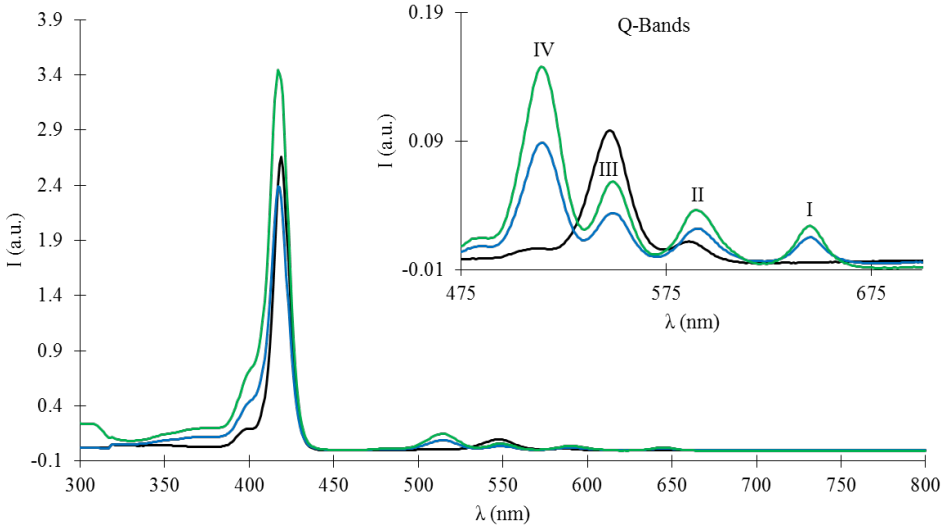


**Figure S46**: UV-Vis absorption spectra comparing compound **1.1** (black line) compound **3** (blue line) and compound **2** (green line) and expansion showing Q-bands (measured at 0.2 µM in DMF).

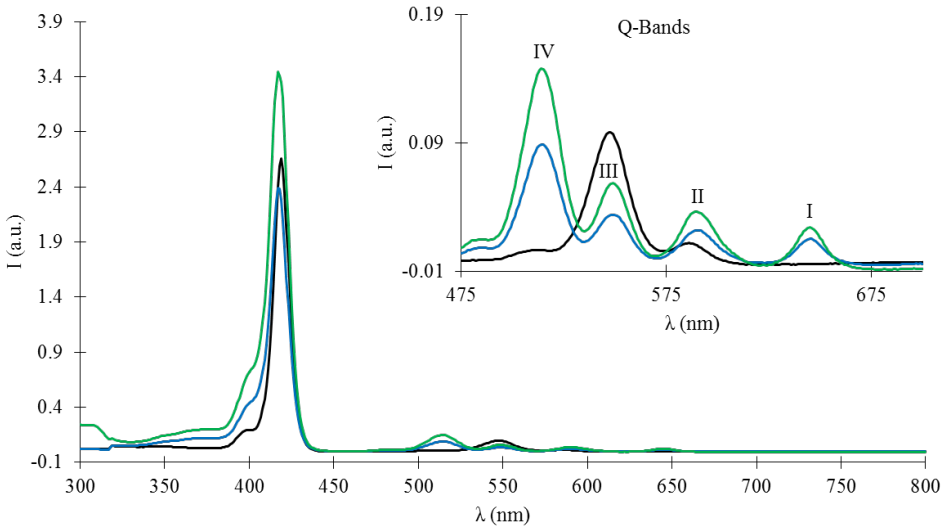


**Figure S47**: UV-Vis absorption spectra comparing compound **3.1** (ZnTPP-COOH, black line), compound **3** (TPP-COOH, blue line) and compound **2** (TPP-OMe, green line) and expansion showing Q-bands (measured at 0.2 µM in DMF).

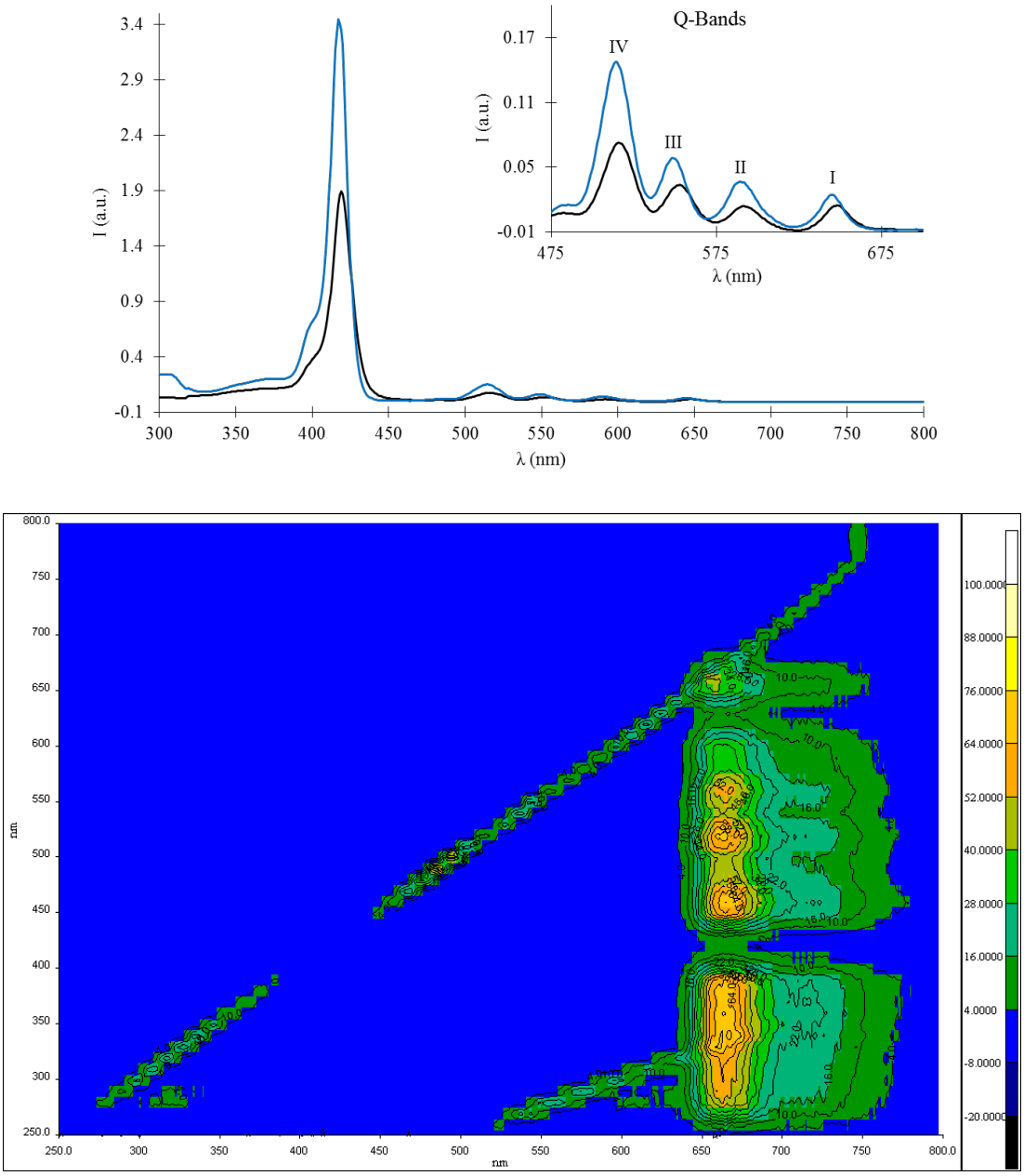


**Figure S48**: UV-Vis spectroscopy: overlay comparing compound **4**, TPP-$NH_2$ (black line) and compound **2**, TPP-OMe (blue line), expansion showing Q-bands ( spectra measured in 0.2 µM concentrations, DMF) and coppresponding excitation/emission profile recorded in DMSO 100µM.)

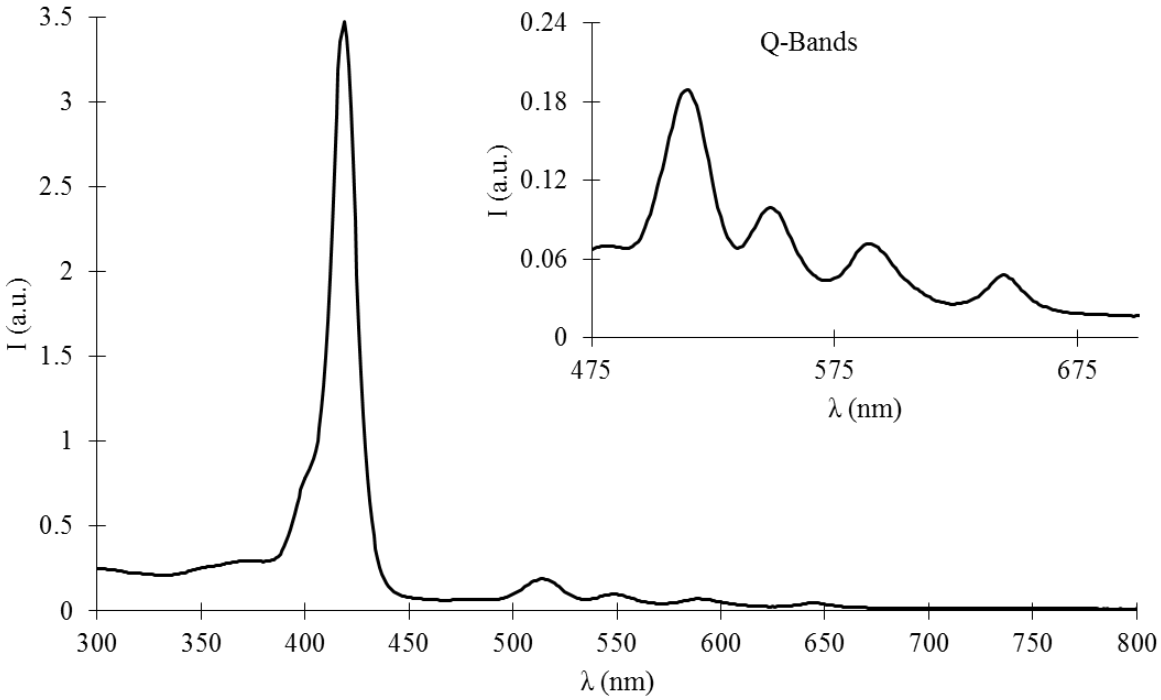


**Figure S49**: UV-Vis of compound **5**, showing expansions of Q-bands (0.2 μM , DMF).

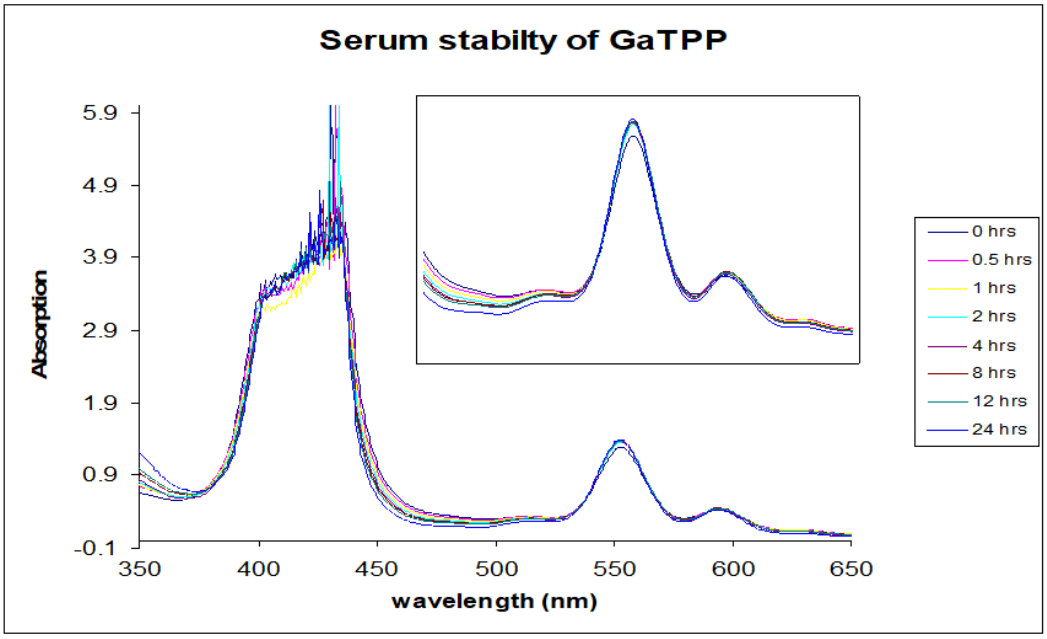


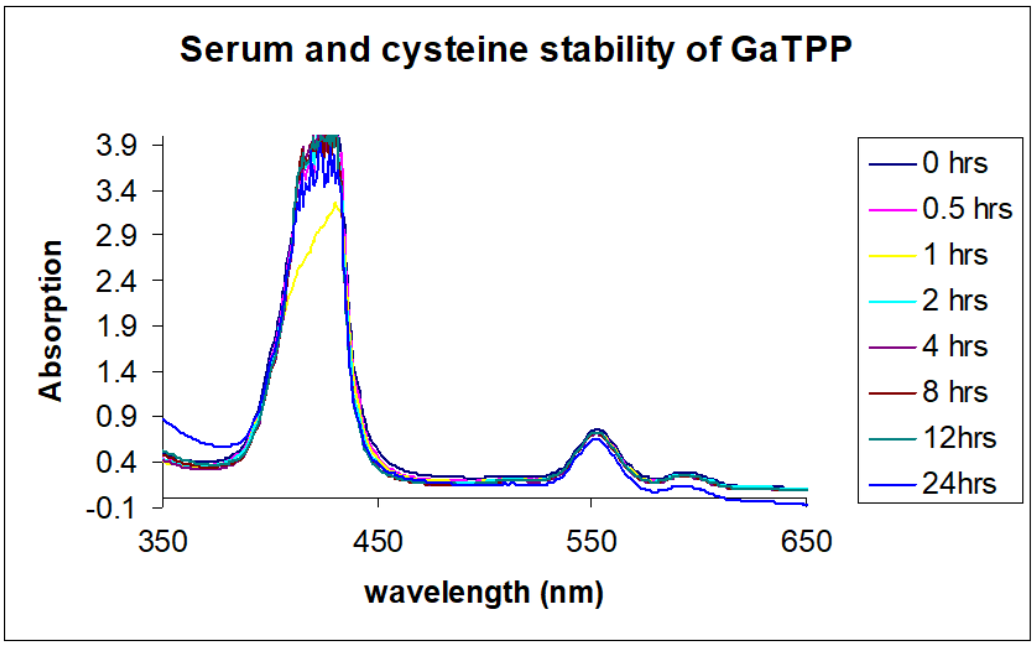


**Figure S50**: UV-Vis absorption spectra of compound **1.1**, and typical stability tests. A chloroform solution of compound 1 was incubated in foetal calf serum in the presence and absence of cysteine at 37 ℃ and the reaction followed by UV-Vis spectroscopy. The UV-Vis profiles suggest that the Ga-porphyrin is stable with limited loss of metal observed (7% decrease in peak intensity after 24h).

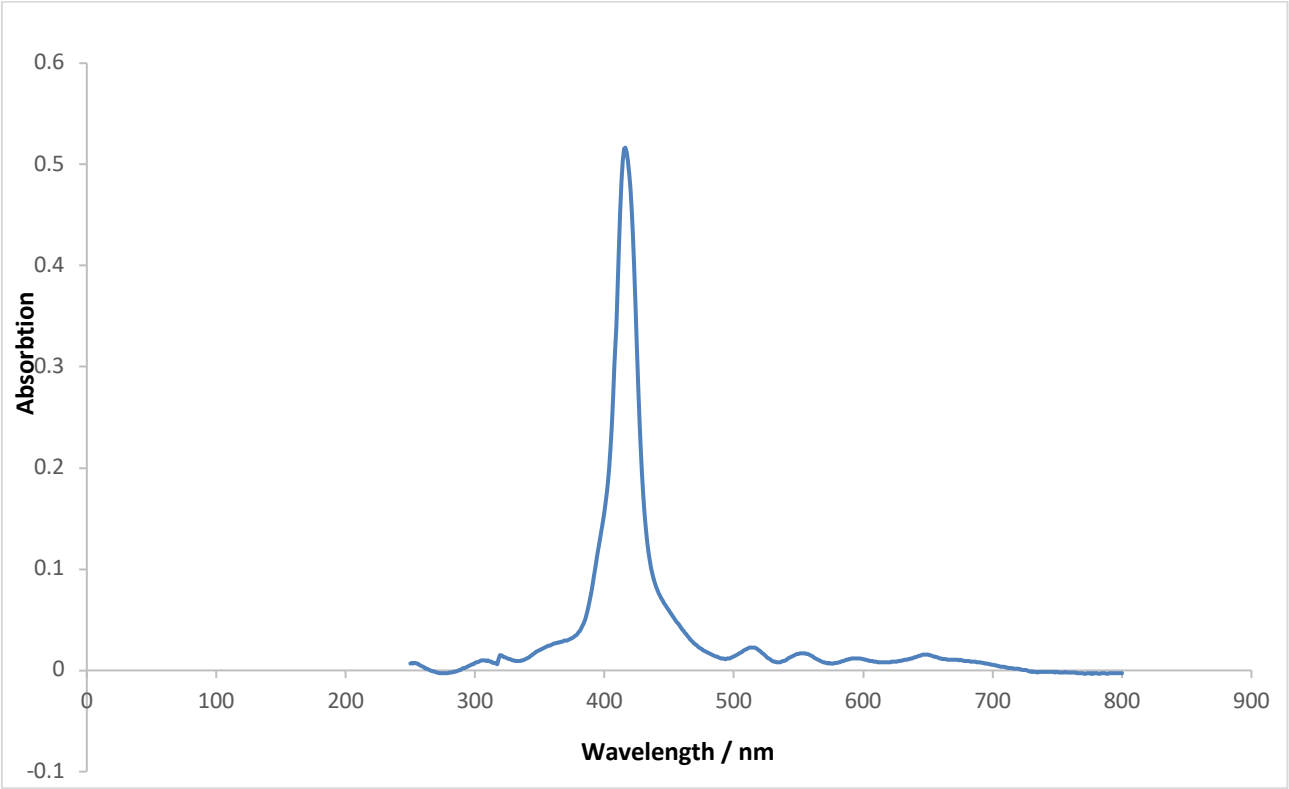


**Figure S51**: UV-Vis spectra of compound **4.2** ( 0.2 µM concentrations, DMF)

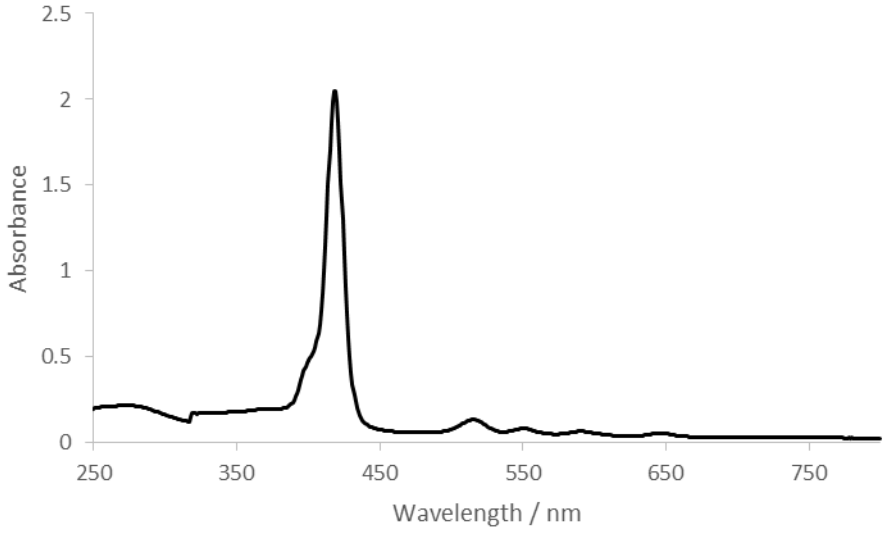


**Figure S52.** Absorbance spectrum for compound **4.9** (50 µM)

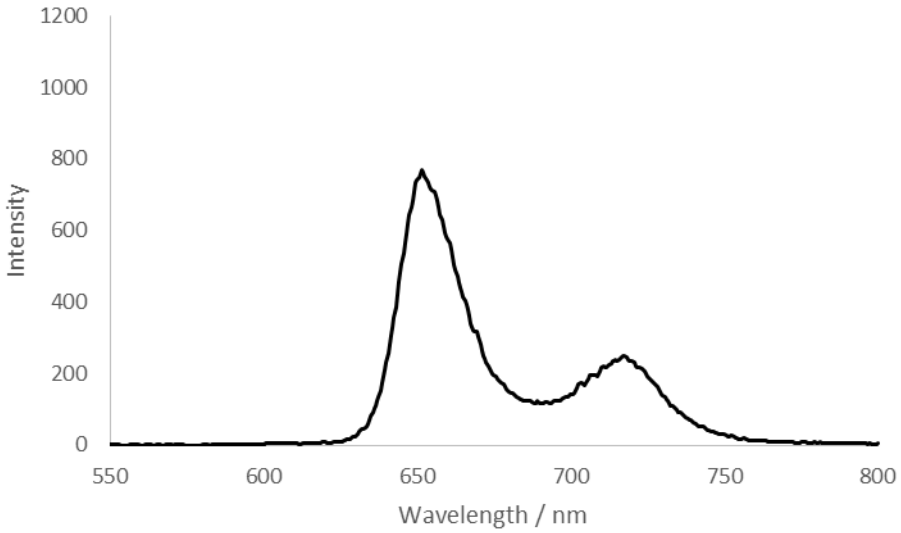


**Figure S53.** Emission spectrum of compound **4.9.** (50μM ) $\lambda_{ex}$ = 416 nm

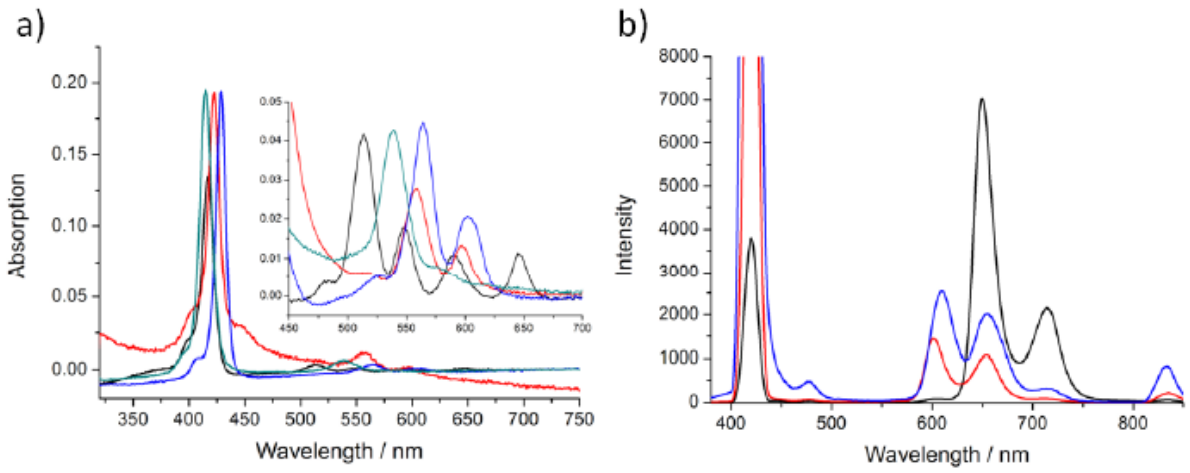


**Figure S54: a)** Overlay of UV-Vis absorption spectra for **3.16** (black)**, 3.17** (green)**, 3.18** (blue) and **3.19** (red) in DMF (all spectra measured at 2.0 μM) with expansion of the Q region (all spectra measured at 0.2 μM) inset**; b)** Overlay of fluorescence emission spectra of **3.16** (black)**, 3.18** (blue) and **3.19** (red) in DMF with λex at 420 nm (all spectra measured at 0.2 μM).

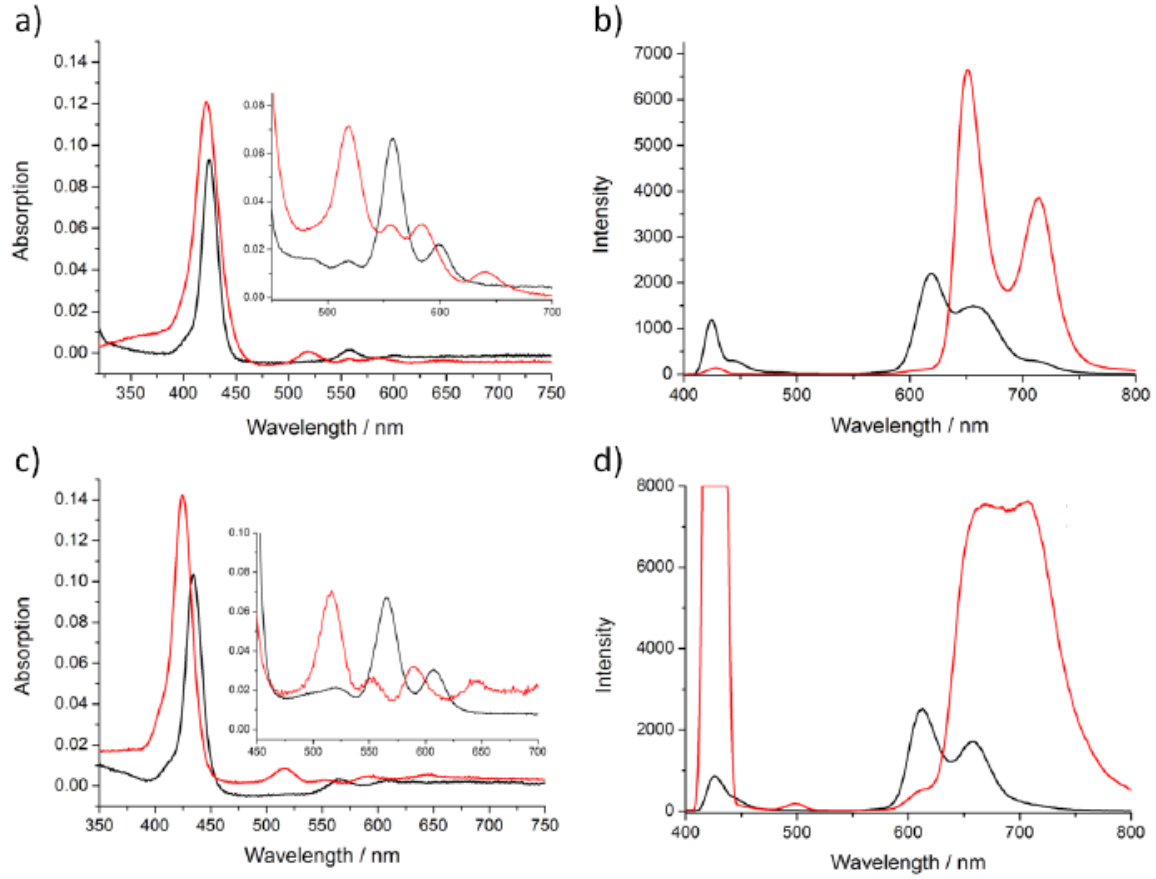


**Figure S55:** a) Overlay of UV-Vis spectra of **3.18** (red) and **3.19** (black) in DMSO(spectra measured at 2.0μM) with expansion of the Q region (spectra measured at 0.2 μM) inset; b) Overlay of fluorescence spectra of **3.18** (red) and **3.19** (black)with λex at 420 nm in DMSO(all spectra measured at 0.2 μM); c) Overlay of UV-Vis spectra of **3.18** (red) and **3.19** (black)in water (spectra measured at 2.0 μM) with expansion of the Q region (spectra measured at 0.2 μM) inset; d) Overlay of fluorescence spectra of **3.18** (red) and **3.19** (black) with λex at 420 nm in water (all spectra measured at 0.2 μM).

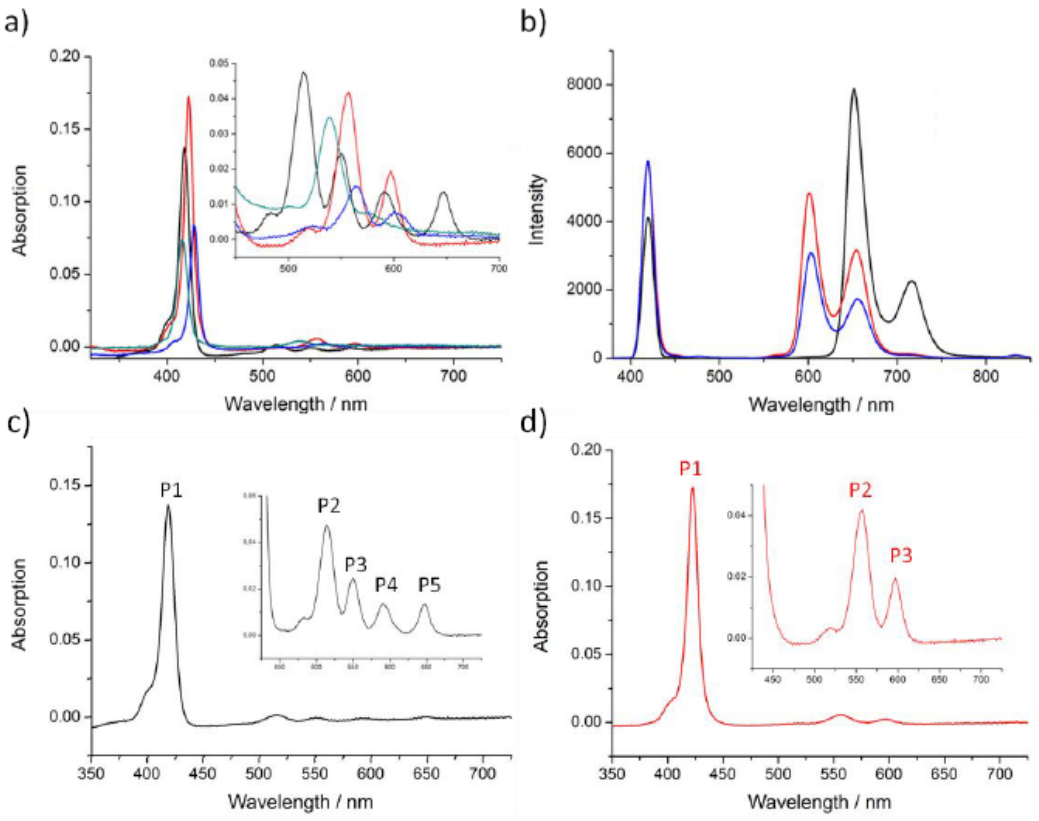


**Figure S56:** Overlay of UV-Vis spectra of **3.4** (black)**, 3.8** (red)**, 3.9** (blue) and **3.10** (green) (all spectra measured at 2.0μM) with expansion of the Q region (all spectra measured at 0.2 μM) inset; b) Overlay of fluorescence spectra of **3.4, 3.8** and **3.9** with λex at 418nm (all spectra measured at 0.2 μM); c) UV-Vis spectra of **3.4** with peak labelling; d) UV-Vis spectra of **3.8** with peak labelling.

**Table S1:** UV-Vis absorption wavelengths (nm) and respective molar extinction coefficients (in brackets) for compounds **3.3-3.10** and their respective quantum yields with $\lambda_{ex}$ at 418nm

| No. | Peak 1 | Peak 2 | Peak 3 | Peak 4 | Peak 5 | Φ |
|---|---|---|---|---|---|---|
| **3.3** | 419 (508960 ± 217) | 515 (20460 ± 290) | 550 (10780 ± 235) | 591 (6120 ± 541) | 647 (5800 ± 147) | 0.052 ± 0.003 |
| **3.4** | 417 (498210 ± 684) | 513 (18870 ± 1002) | 548 (8850 ± 562) | 590 (5560 ± 285) | 646 (5600 ± 307) | 0.053 ± 0.006 |
| **3.5** | 424 (398210 ±721) | 521 (4050 ± 220) | 5565 (18110 ± 225) | 599 (9850 ± 105) | - | 0.048 ± 0.009 |
| **3.6** | 428 (381450 ± 196) | 524 (6570 ± 475) | 562 (15480 ± 439) | 601 (5770 ± 590) | - | 0.042 ± 0.002 |
| **3.7** | 415 (354150 ± 1052) | 539 (17310 ± 324) | - | - | - | 0.001 ±0.0002 |
| **3.8** | 423 (429990 ±705) | 520 (4540 ± 143) | 557 (19610 ± 628) | 597 (9240 ± 411) | - | 0.044 ± 0.011 |
| **3.9** | 428 (400590 ± 470) | 524 (7850 ± 447) | 560 (17530 ± 95) | 603 (5940 ± 281) | - | 0.042 ± 0.007 |
| **3.10** | 416 (316820 ± 220) | 539 (14910 ± 178) | - | - | - | 0.000 ± 0.0001 |

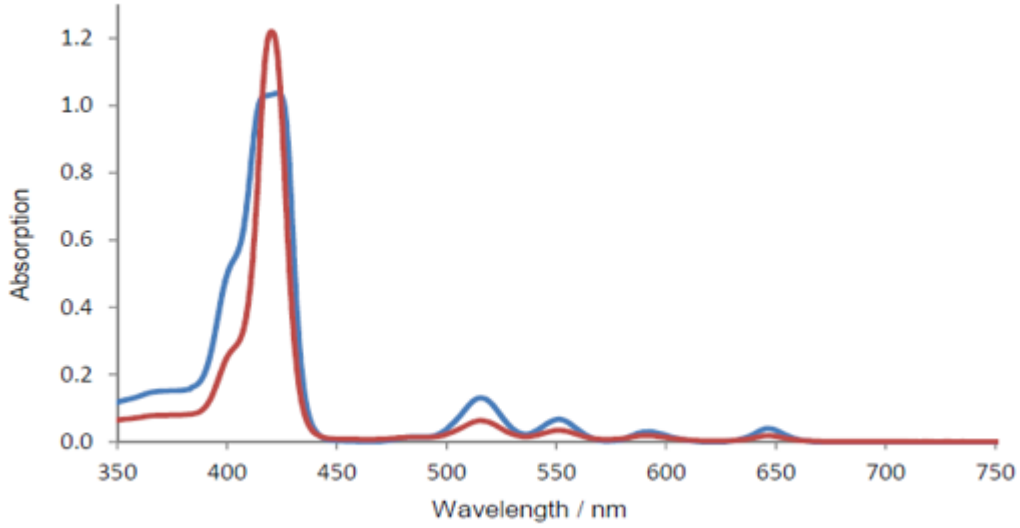


**Figure S57:** Overlaid absorption spectra of porphyrin conjugates **4.12** (in blue) and **4.14** (in red) in DMSO (2.0 μM) between 350-750 nm.

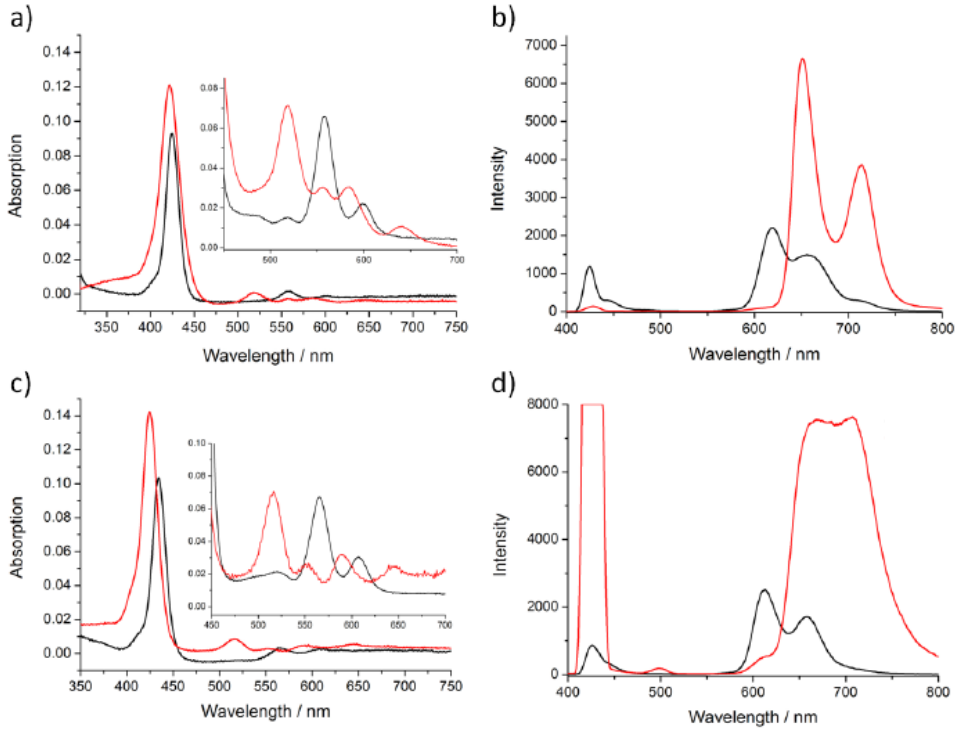


**Figure S58:** a) Overlay of UV-Vis spectra of **6.1** (red) and **6.2** (black) in DMSO(spectra measured at 2.0μM) with expansion of the Q region (spectra measured at 0.2 μM) inset; b) Overlay of fluorescence spectra of **6.1** (red) and **6.2** (black)with λex at 420 nm in DMSO(all spectra measured at 0.2 μM); c) Overlay of UV-Vis spectra of **6.1** (red) and **6.2** (black)in water (spectra measured at 2.0 μM) with expansion of the Q region (spectra measured at 0.2 μM) inset; d) Overlay of fluorescence spectra of **6.1** (red) and **6.2** (black) with λex at 420 nm in water (all spectra measured at 0.2 μM).

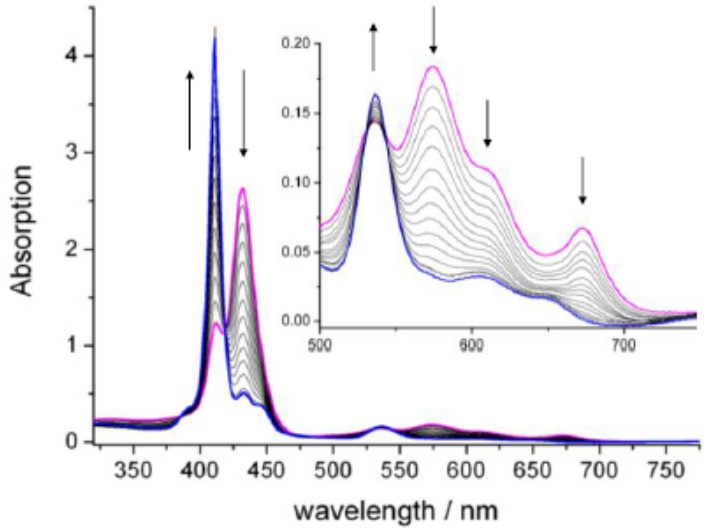


**Figure S59:** UV-Vis study on the addition of aliquots of copper chloride to **3.23**

Prior to the Cu(II) incorporation, the bead-activation of porphyrins was carried out using benzyl chloride functionalized polystyrene beads**.** Polystyrene-supported benzyl chloride was stirred with a 1:1 chloroform:methanol solution of **3.3** for 12 h. Filtration and washing yielded bright green beads (**4.8)**. Resuspension and reaction with a methanolic solution of copper chloride led to an immediate color change to give a pale pink solution which ESI-MS identified as the copper complex **3.7.**

HPLC and UV-Vis studies were used to further investigate the product. Figure S60 shows the UV/VIS absorption profile of the free ligand **3.3**, and the copper complex **3.7** synthesized by conventional means (Cu-P, blue line) or by activation with polystyrene supported benzyle chloride (CuP-beads, black line).

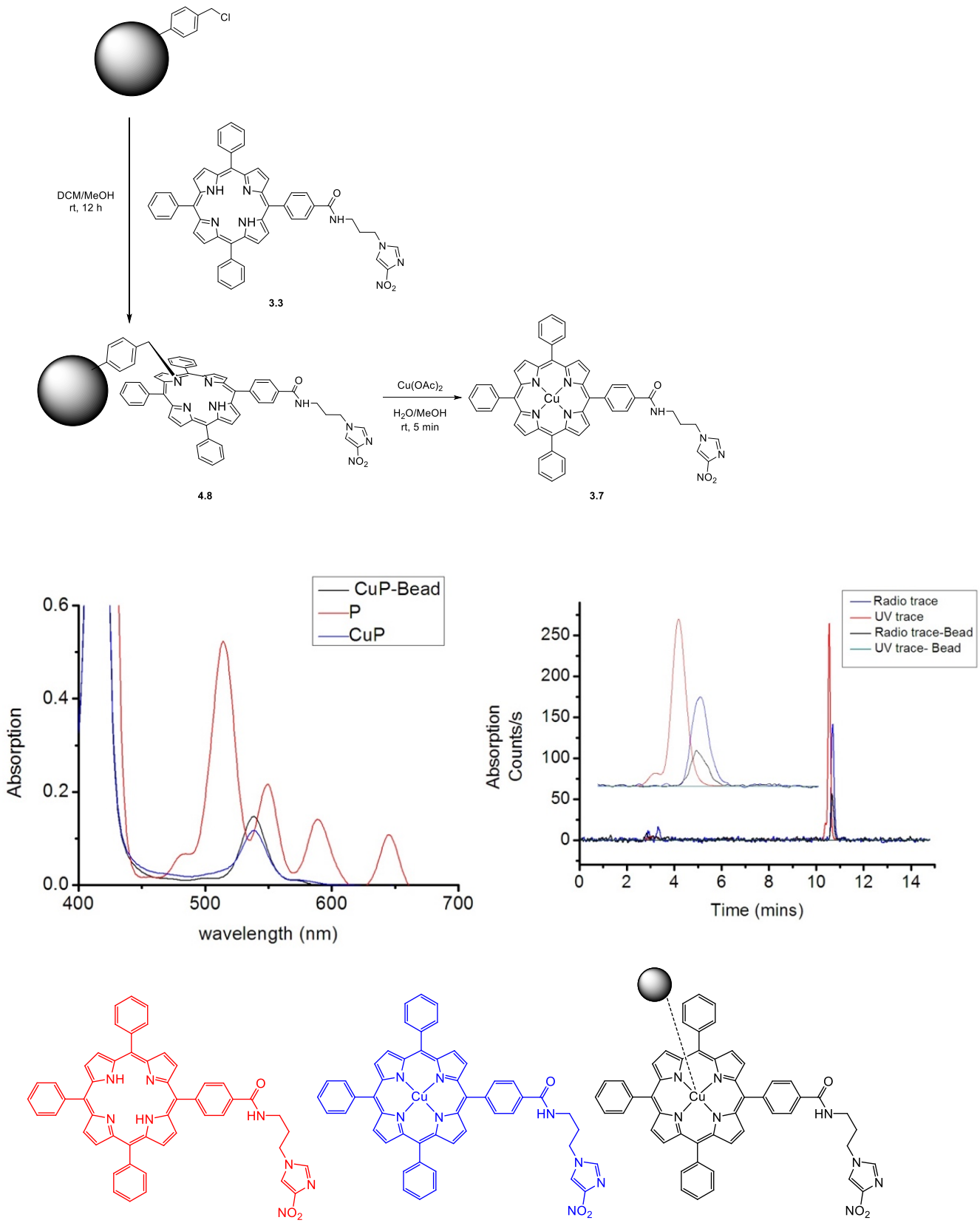


**Figure S60:** Above: Synthesis of copper complex **3.7** by polymer-supported benzyle chloride activation. Below: UV-Vis and HPLC analysis of copper complexation from a bead activated porphyrin: **3.7** synthesized via **4.8** (black), **3.3** (red) and **3.7** synthesized by conventional methods (blue). UV and radioHPLC traces after the [$^{64}$Cu]Cu(OAc)$_2$ treatment through the general radiolabelling procedure is included.

## *In vitro* kinetic stability tests

UV-Vis spectrophotometry was used as tool to assess the stability of the "cold" metal complexes prior to *in vitro* and *in vivo* radiolabelling studies. The gallium **3.8** and indium complexes **3.9** were initially dissolved in DMSO to give solutions of 200 μM and were diluted with phosphate buffered solution (PBS) to give a final concentration of 10 μM (final DMSO concentration 2.5 %). Solutions were incubated at 37 °C and followed by UV-Vis spectroscopy over 24 h as shown in Fig. S61 a) and b). For both **3.8** and **3.9** their absorption spectra show no sign of the formation of free ligand as would be indicated by the appearance of peaks at 515, 550, 590 and 647 nm, suggesting that the metal porphyrin complexes are stable with respect to loss of the metal ion on aqueous challenge. An analogous setup was followed for a serum protein challenge experiment, replacing the PBS with human serum albumin (HSA). Fig. S61 c) and d) again show no significant change in the complex integrity with no apparent change in the metal porphyrins' 'Q' band structure observed over time. While small changes in absorption maxima in the 'Q' band of each of the spectra are observed, this is attributed to binding interactions with the serum proteins and not as a result of loss of metal from the porphyrin cavity. By this simple assay protocol, gallium and indium porphyrin complexes are expected to be stable with respect to loss of metal, an important feature in the design of radiopharmaceuticals to ensure that non-target organ accumulation is minimized.

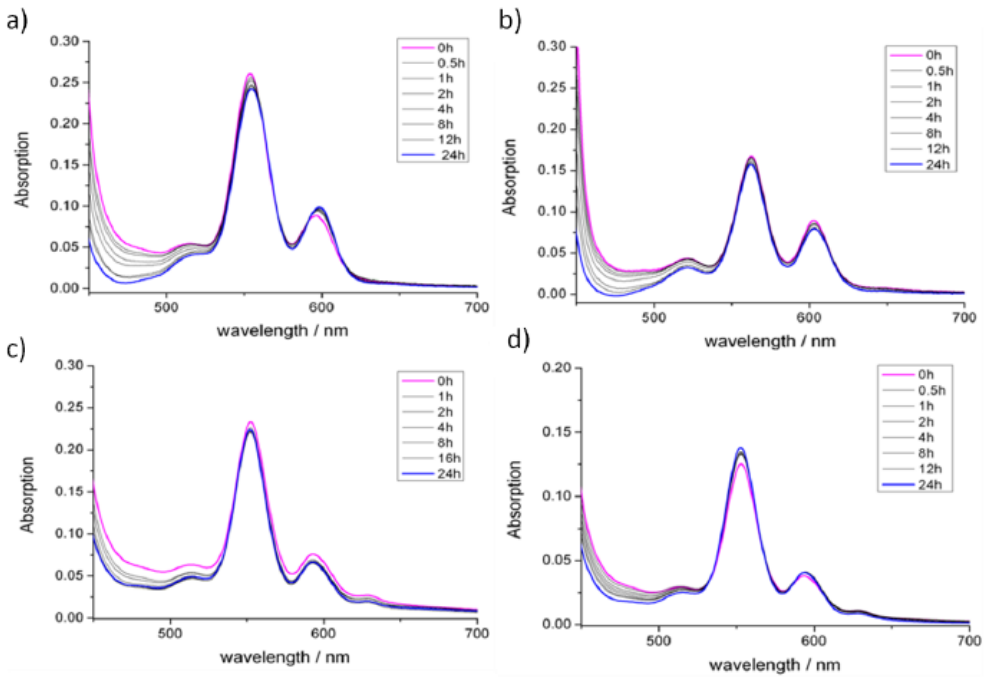


**Figure S61:** Comparison of UV-Vis spectra of **3.8** (a and c) and **3.9** (b and d) on aqueous (a and b) and serum challenges (c and d), respectively.

7. Cyclic Voltammetry

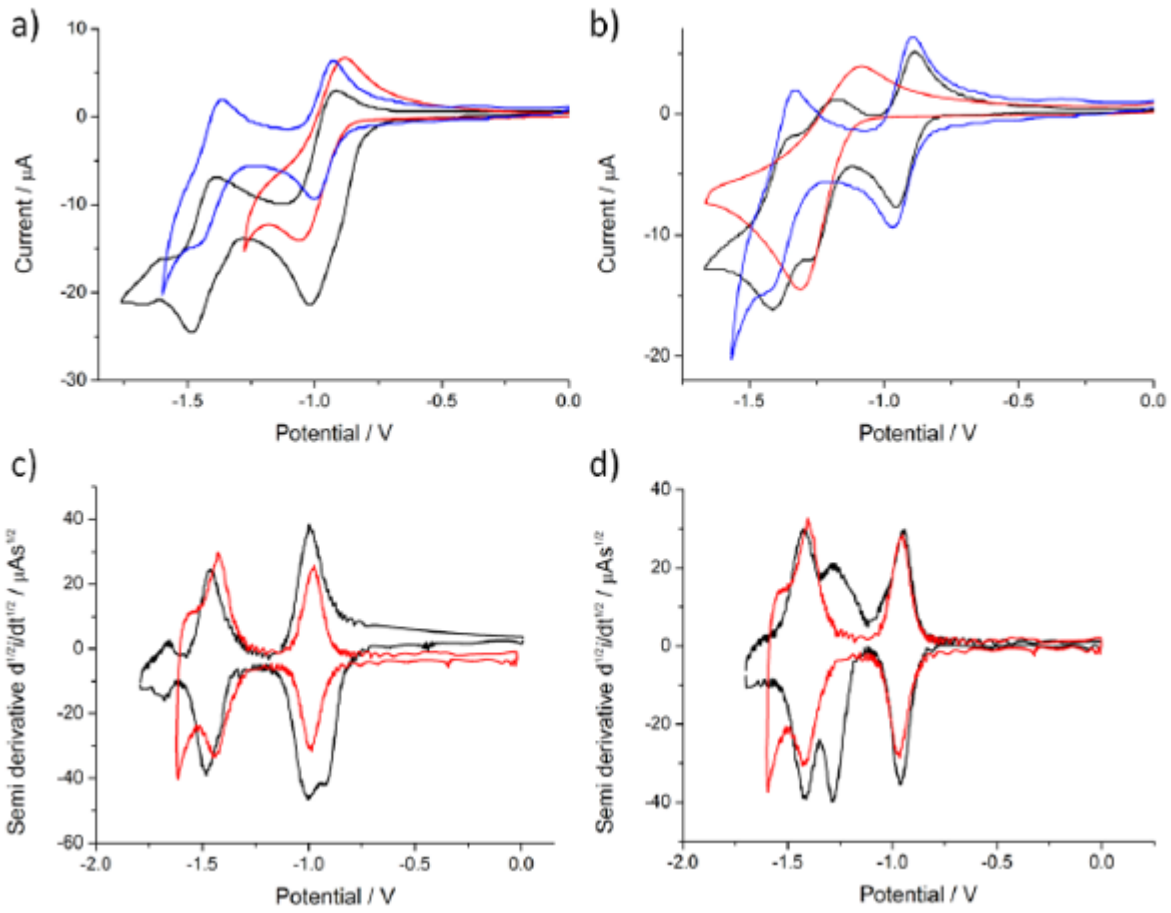


**Figure S62:** Comparison of cyclic voltammograms in DMF at 100 $mVs^{-1}$ a) **3.4** (black), **3.11** (blue) and 2-nitroimidazole (red); b) **3.3**, **3.11** (blue) and 4-nitroimidazole (red); c) semi derivative of **3.4** (black) and **3.11** (red); d) semi derivative of **3.3** (black) and **3.11** (red) all at 1mM, 298K, using a platinum disc working electrode

**Table S2:** Selected electrochemical parameters for **3.4**, 2-Nitromidazole and **3.11**

| Compound | E1/2 / V | ΔEp / V | $\lvert i_{pa}\rvert/\lvert i_{pc}\rvert$ | WHHM (cathodic) | WHHM (anodic) |
|---|---|---|---|---|---|
| **3.11** | -0.97 | 0.08 | 0.96 | 0.10 | 0.11 |
| 2-Nitim | -0.97 | 0.19 | 0.55 | 0.18 | 0.17 |
| **3.4** | -1.04 | 0.10 | 0.60 | 0.20 | 0.13 |

Reduction potentials are recorded at 1mM, in DMF at 298 K with a scan rate of 100 $mVs^{-1}$, using a platinum disc working electrode and a 0.1M tetrabutylammonium tetrafluoroborate electrolyte. For each couple six complete scan sweeps were recorded. Potentials listed are calculated from single one off measurements.

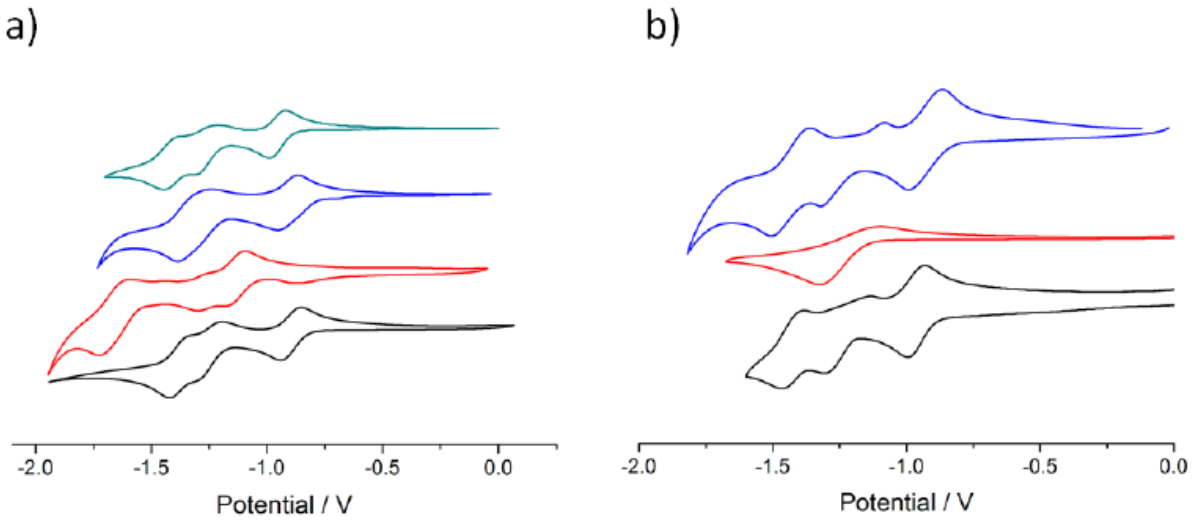


**Figure S63:** Overlay of cyclic voltammograms of a) **3.3** (black) with **3.5** (green), **3.6** (blue) and **3.7** (red); b) **4.4** (black) with **4.6** (blue) and 4-Nitim (red), all at 1mM, in DMF at 298K with a scan rate of 100 mVs-1, using a platinum disc working electrode.

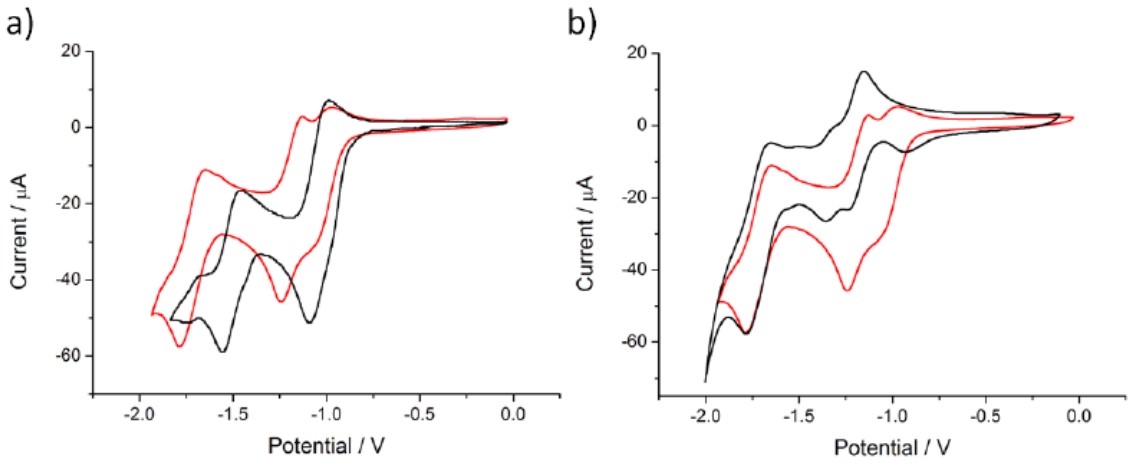


**Figure S64:** Overlay of cyclic voltammograms of a) **3.4** (black) and **3.10** (red) and b) **3.7** (black) and **3.10** (red) all at 1mM, in DMF at 298K with a scan rate of 100 mVs-1, using a platinum disc working electrode

**Table S3:** Electrochemical data for tetraphenyl porphyrin nitroimidazole conjugates

| Compound | E1/2 / V | ΔEp / V | E1/2 / V | ΔEp / V | E1/2 / V | ΔEp / V |
|---|---|---|---|---|---|---|
| **3.11** | -0.97 | 0.07 | -1.42 | 0.09 | - | - |
| **3.12** | -0.90 | 0.09 | -1.34 | 0.07 | - | - |
| **4-Nitim** | - | - | - | - | -1.25 | 0.22 |
| **2Nitim** | - | - | - | - | -0.97 | 0.18 |
| **4.4** | -1.02 | 0.06 | -1.48 | 0.09 | -1.28 | 0.18 |
| **4.5** | -1.04 | 0.10 | -1.51 | 0.10 | overlay | |
| **4.6** | -1.04 | 0.09 | -1.53 | 0.10 | -1.30 | 0.18 |
| **4.7** | -1.15 | 0.13 | -1.65 | 0.14 | -1.24 | 0.12 |
| **4.8** | -1.19 | 0.12 | -1.72 | 0.15 | -1.03 | 0.12 |
| **3.3** | -0.98 | 0.07 | -1.44 | 0.08 | -1.29 | 0.10 |
| **3.4** | -0.97 | 0.12 | -1.40 | 0.13 | overlay | |
| **3.5** | -0.99 | 0.10 | -1.53 | 0.10 | -1.35 | 0.12 |
| **3.6** | -1.13 | 0.09 | -1.65 | 0.13 | -1.26 | 0.07 |
| **3.7** | -0.91 | 0.09 | -1.31 | 0.14 | -1.31 | 0.14 |
| **3.8** | -0.96 | 0.11 | -1.49 | 0.10 | overlay | |
| **3.9** | -1.13 | 0.09 | -1.64 | 0.13 | -0.10 | 0.12 |
| **3.10** | -0.93 | 0.10 | -1.32 | 0.14 | -1.01 | 0.12 |

*Reduction potentials are recorded at 1mM, in DMF at 298 K with a scan rate of 100 $mVs^{-1}$, using a platinum disc working electrode and a 0.1M tetrabutylammonium tetrafluoroborate electrolyte. For each couple six complete scan sweeps were recorded. Potentials listed are calculated from single one-off measurements.

**Table S4:** Electrochemical parameters for **6.5** and **6.4***

| No. | Center | Ec /V | Ea /V | E ½ /V | ΔEp /V |
|---|---|---|---|---|---|
| **6.5** | Pyridinium | -0.61 | -0.50 | -0.56 | 0.11 |
| | Porphyrin I /Nitroimidazole | -0.97 | -0.84 | -0.92 | 0.10 |
| | Porphyrin II | -1.62 | -1.42 | -1.55 | 0.14 |
| **6.4** | Pyridinium | -0.62 | -0.53 | -0.57 | 0.11 |
| | Nitroimidazole | -0.92 | Not seen | - | - |
| | Porphyrin I | -1.06 | Not seen | - | - |
| | Porphyrin II | -1.48 | Not seen | - | - |
| | Porphyrin II | -1.48 | Not seen | - | - |

Reduction potentials are recorded at 1mM, in DMF at 298 K with a scan rate of 100 $mVs^{-1}$, using a platinum disc working electrode and a 0.1M tetrabutylammonium tetrafluoroborate electrolyte. For each couple six complete scan sweeps were recorded. Potentials listed are calculated from single one-off measurements

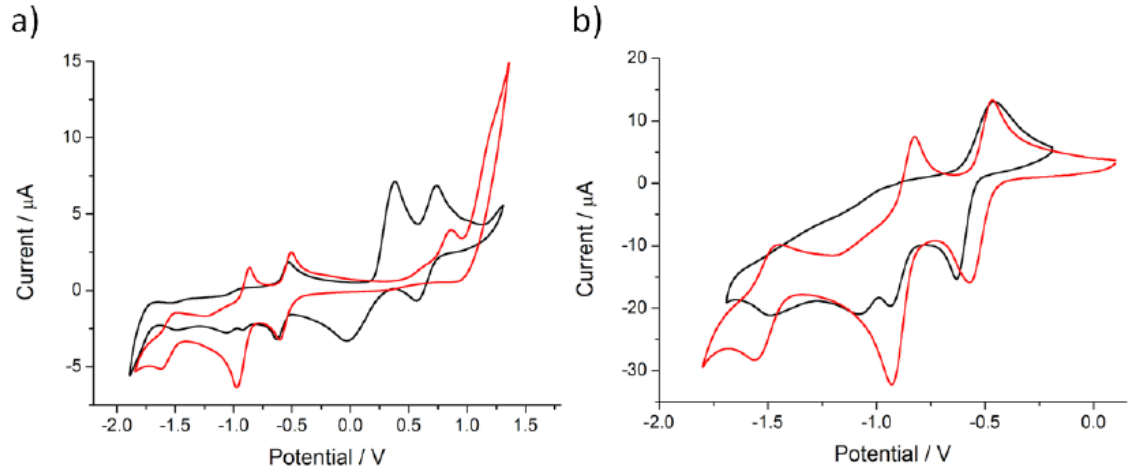


**Figure S65:** Cyclic voltammogram overlays of **6.4** (black) and **6.5** (red) for a) full wave and b) reduction couples all at 1mM, in DMF at 298K with a scan rate of 100 $mVs^{-1}$, using a platinum disc working electrode

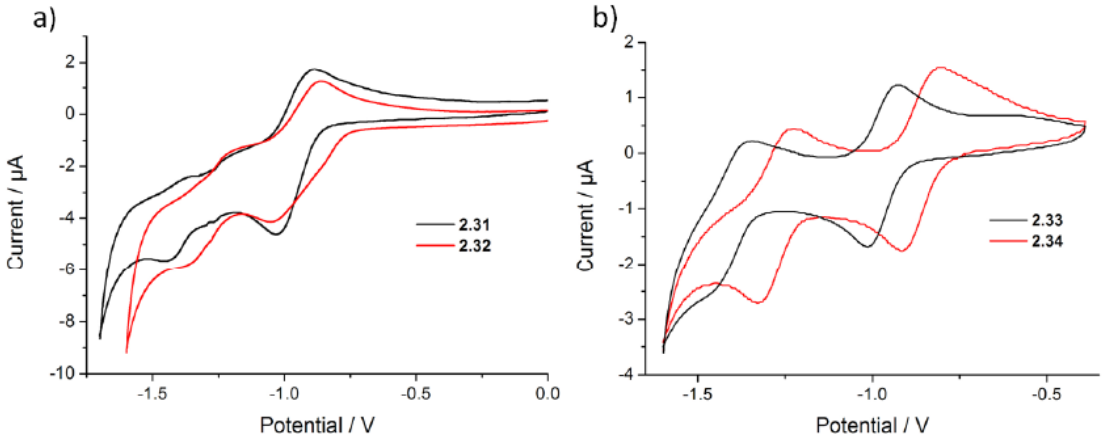


**Figure S66:** Overlay of cyclic voltammograms of sulphonated porphyrin derivatives a) **3.23** (black) and **3.24** (red); b) **3.14** (black) and **3.15** (red) all at 1mM, in DMF at 298K with a scan rate of 100 mVs-1, using a platinum disc working electrode

**Table S5:** Cyclic voltammetry parameters for sulphonated porphyrin derivatives*

| No. | E1/2 / V | ΔEp / V | E1/2 / V | ΔEp / V | E1/2 / V | ΔEp / V |
|---|---|---|---|---|---|---|
| **3.14** | -0.97 | 0.09 | -1.41 | 0.13 | - | - |
| **3.15** | -0.86 | 0.10 | -1.27 | 0.10 | - | - |
| **3.22** | -0.99 | 0.07 | -1.42 | 0.10 | -1.31 | 0.11 |
| **3.23** | -0.96 | 0.14 | -1.40 | 0.11 | overlay | |
| **3.24** | -0.96 | 0.19 | -1.29 | 0.17 | overlay | |
| **2-Nitim** | - | - | - | - | -0.97 | 0.18 |

*Reduction potentials are recorded at 1mM, in DMF at 298 K with a scan rate of 100 $mVs^{-1}$, using a platinum disc working electrode and a 0.1M tetrabutylammonium tetrafluoroborate electrolyte. For each couple six complete scan sweeps were recorded. Potentials listed are calculated from single one off measurements

8. Radiochemistry:

## *Gallium radiolabelling tests*

Experiments towards labelling several different porphyrins with gallium-68 were carried out. Different temperatures, solvents, pH values and purification/elution methods were tested to optimize the methodology. The table below gives an overview over the tested conditions. Radiochemical incorporation was low (ROI < 20 %) in all cases, and chromatographic elution of the gallium-68 labelled compounds over $C_{18}$-silica was not possible when unmodified TPP was used. Moreover, we found that in the case of unmodified [$^{68}$Ga]GaTPP multiple products were apparent, which may be the result of different counterions at the gallium center.

Purification of [$^{68}$Ga]**4.2** was successful. However, we found that the purified product, when loaded onto and eluted from a $C_{18}$-silica column once more still gave a signal for free gallium-68, potentially indicating low kinetic stability of the resulting complex.

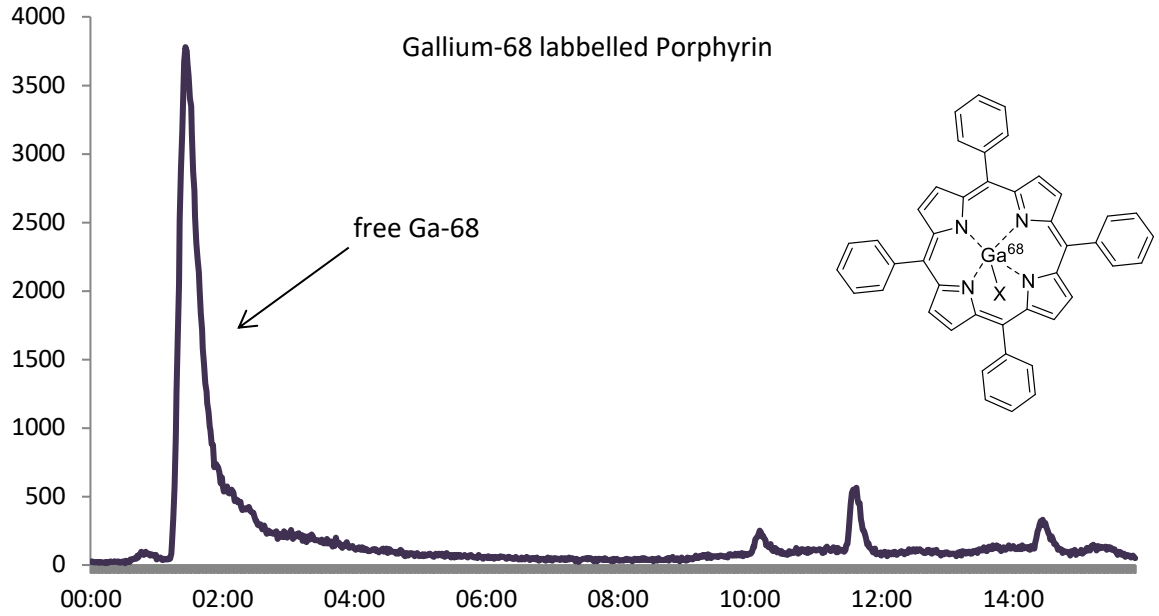


**Figure S67**: Radio chromatogram of compound [$^{68}$Ga]**1.1**.

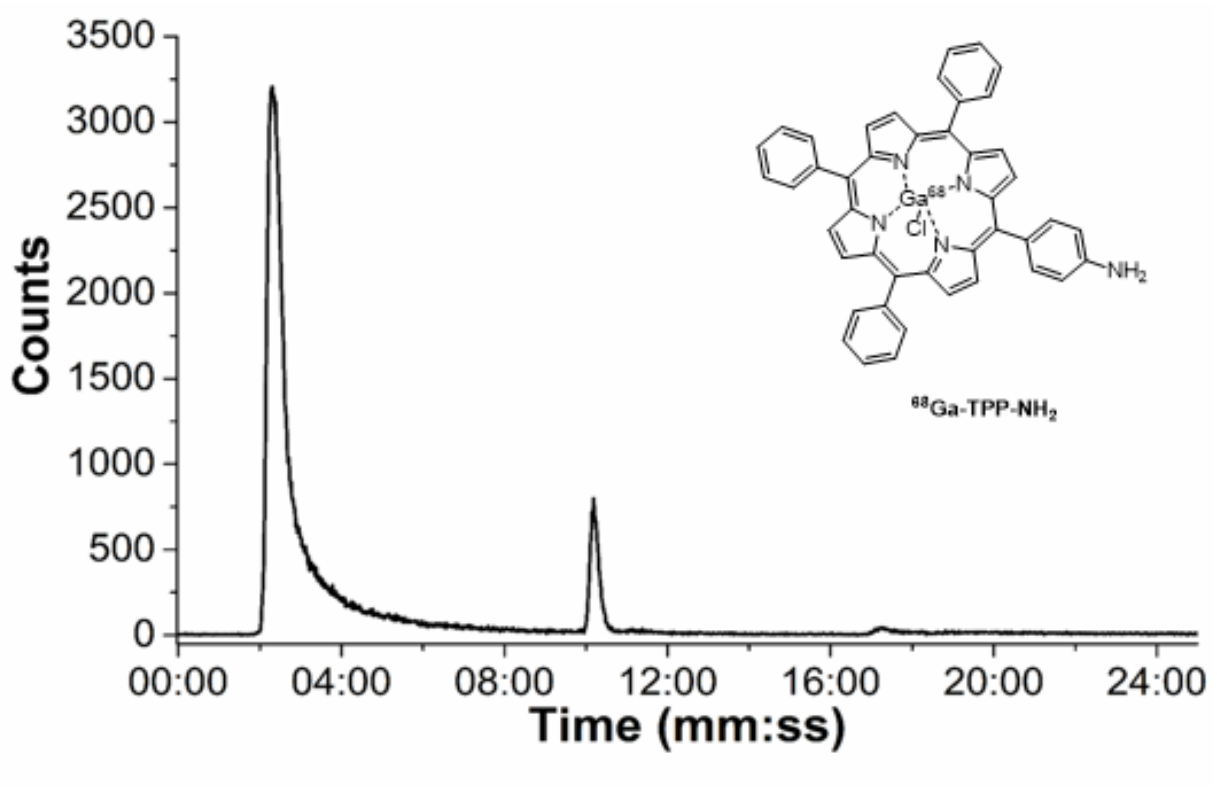


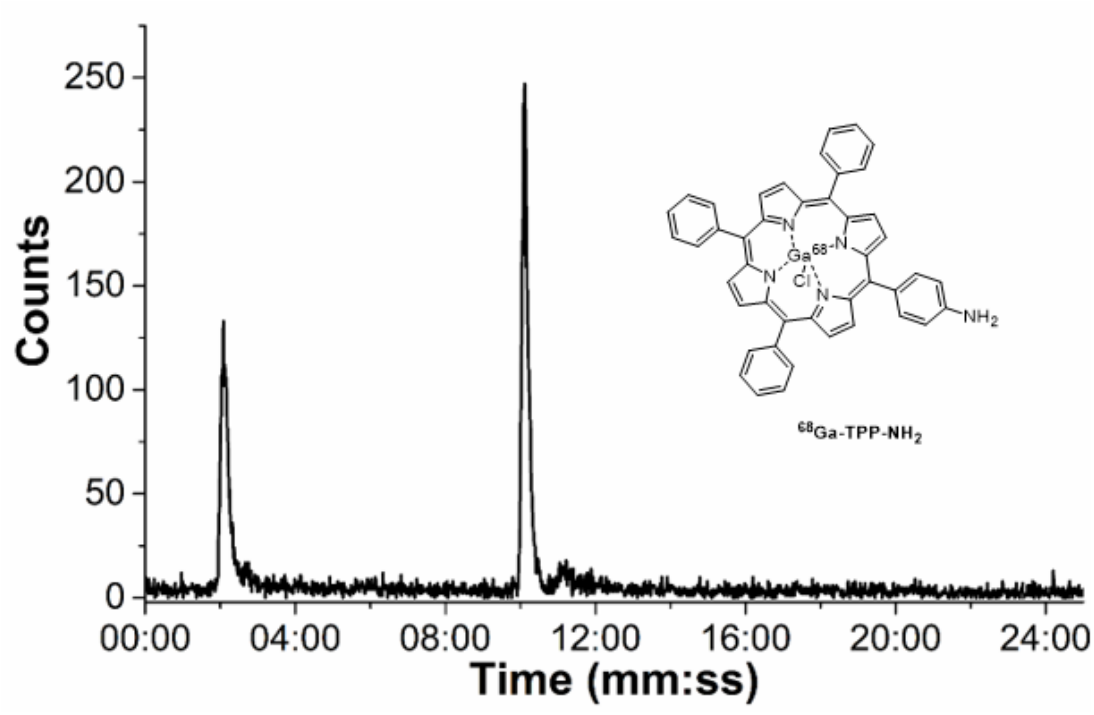


**Figure S68**: Radio chromatogram of compound [$^{68}$Ga]**4.2**, before (**top**) and after (**bottom**) chromatographic purification

## Indium-111 radiolabelling, lipophilicity and serum stability tests

The *in vivo* behaviour of the porphyrin conjugates was investigated to assess their pharmacokinetic properties, i.e. organ and tumour accumulation over time, route and rate of washout, and muscle and blood retention.. LogP's were measured accordingly by adding 0.5 MBq of the respective $^{111}$In labelled compound to a mixture of distilled water (0.5 mL) and of 1-octanol (0.5 mL) in an Eppendorf tube. The tube was vigorously vortexed over a period of 5 min and centrifuged for 5 min. Aliquots (50 μL) of both the aqueous and octanol layers were then collected in triplicate and the associated activity counted using a gamma counter. Compounds [$^{111}$In]**3.15**, [$^{111}$In]**6.6** and [$^{111}$In]**3.20** displayed logP values of -2.15, -2.24 and -2.12, suggesting that they were all strongly hydrophilic species. Serum binding studies were conducted for the indium labelled compounds to assess the extent of their binding to serum proteins and their stability over time. Human Serum Albumin binds a wide variety of drugs in the blood after administration, restricting the free concentration of them in plasma and as such affecting the drug pharmacokinetics and in vivo biodistribution. Each compound was incubated at a concentration of 0.5 MBq/ml in mouse serum (at 37 °C) over a 2 h period. Aliquots were removed in triplicate at 30, 60, 90 and 120 min. The protein in each aliquot was precipitated by addition to ethanol and isolated by centrifugation. The supernatant was removed to an Eppendorf tube and the pellet washed with ethanol, centrifuged again and separated. Protein binding was determined by measuring pellet and combined supernatant fractions. Despite the hydrophilic nature of the porphyrins, extremely high serum binding constants were measured for [$^{111}$In]**3.15**, [$^{111}$In]**6.6** and [$^{111}$In]**3.20** with greater than 95 % of the activity associated with human serum albumin proteins over all time points. This data is in agreement with that measured for the analogous tetra-sulphonylphenyl porphyrin and tetra-methylpyridinium porphyrin species [19, 49, 50], and with the work carried out by Nakijama et. al. which showed strong porphyrin association with transferrin, low density lipoproteins and with human serum albumin [51]. The strong protein binding affinity may in part explain the poor hypoxic selectivity of the nitroimidazole compound **3.24** and the poor selectivity of the sulphonamide compound **3.20** under *in vitro* conditions. If the porphyrin units are bound to proteins, then they may become trapped and unable to undergo reductive processes in hypoxic tissue or for specific receptor binding.

## Preliminary investigations into the biodistribution and imaging of Indium-111 labelled porphyrins

Biodistribution and Imaging studies in MKN45 gastric cancer tumor bearing mice were conducted at Barts and the London School of Medicine and Dentistry in the laboratory of Prof. Stephen Mather. All animal experiments were conducted in compliance with British Home Office regulations governing animal experimentation. Tumour xenografts were induced in female CD1 nude mice (Charles River) by subcutaneous injection of $5x10^6$ MKN45 cells, and the tumours were allowed to grow until they had reached a size greater than 12 mm (10–15 d). Imaging was performed using a NanoSPECT/CT small animal scanner (Bioscan). $^{111}$In-labelled porphyrins (0.05 mg of Porphyrin/ 20 MBq of $^{111}$In) were injected into the tail vein. SPECT/CT imaging was performed at 0, 3, 5, and 24 h post injection. The mice were anaesthetized with isoflurane (4% induction, 2% maintenance). A 36 pinhole collimator with 1.4 mm pinholes was used for the SPECT acquisitions. Count rates ranged between 50,000–100,000 for each of the 16 projections. Radionuclide images were reconstructed using proprietary HiSPECT (Bioscan) iterative reconstruction and were fused with CT images using proprietary InVivoScope (Bioscan) software. The mice were sacrificed by $CO_2$ euthanasia at either 5 or 24 h after injection. Tumours and other tissues (blood, stomach, spleen, liver, pancreas, kidneys, muscle, tail, heart, lungs, and intestines) were removed and weighed. The tissues were counted in a gamma-counter together with standards of known radioactivity, and the percentage injected dose per gram of tissue (%ID/g) was calculated by dividing the activity in the

tissue samples (gamma-counter) by the injected activity (dose calibrator). The unpaired t test (Excel; Microsoft) (significance level, 0.05) was used for statistical analysis.

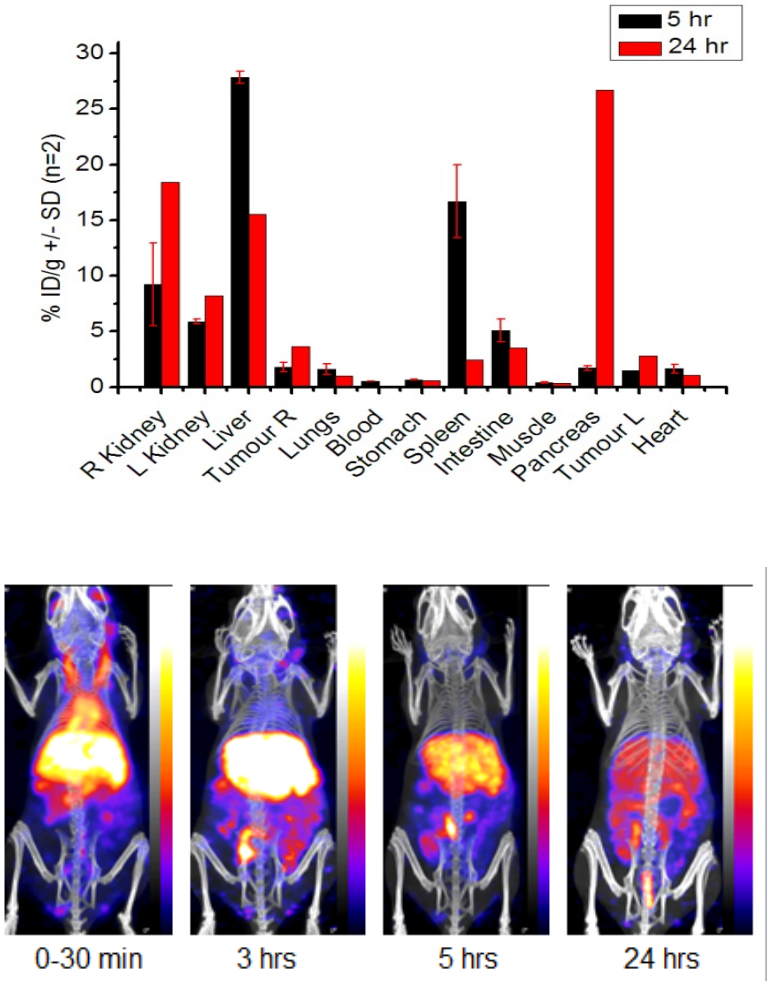


**Figure S69**: In vivo distribution studies of compound [$^{111}$In]**3.15**.

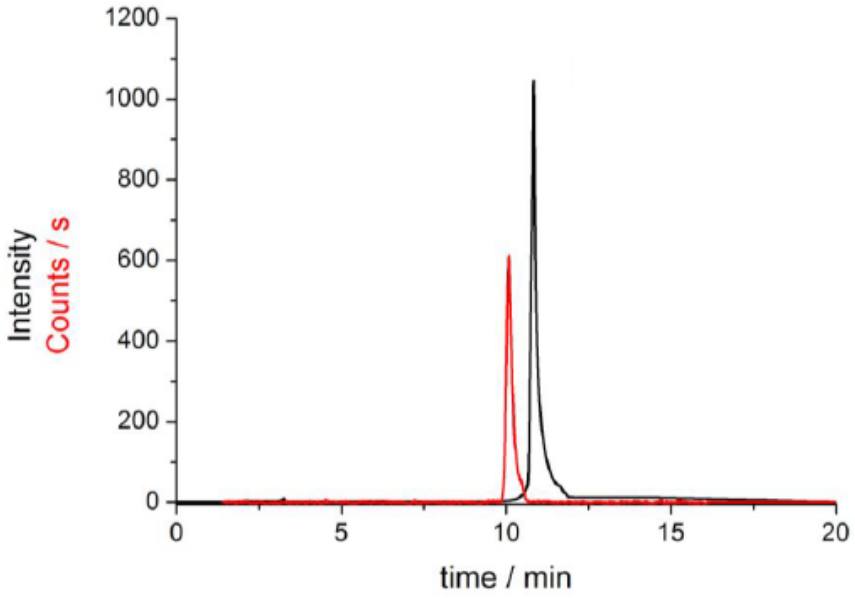


**Figure S70:** Overlay of UV-Vis HPLC trace of **3.23** (black) with radio-HPLC trace of [$^{111}$In]**3.24** (red)

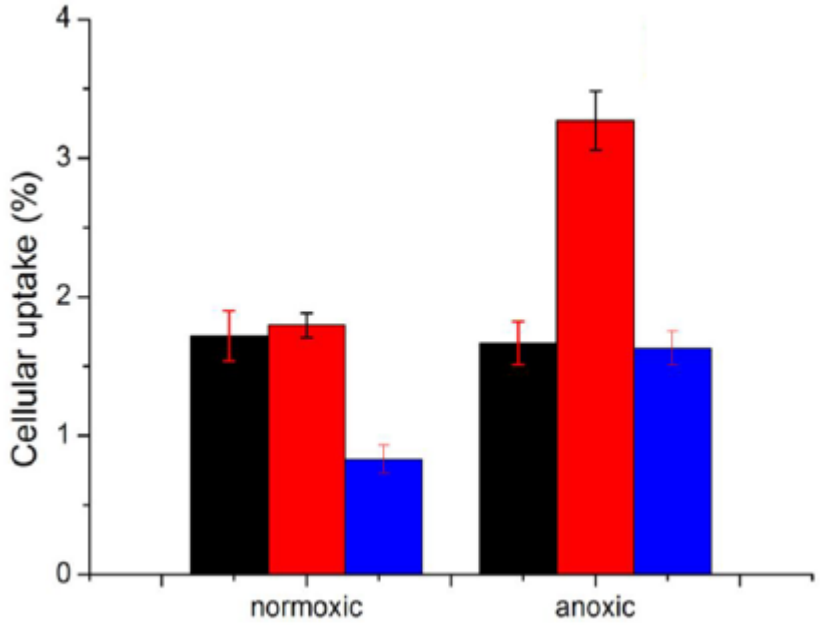


**Figure S71:** Uptake under different gas conditions of [$^{111}$In]**3.24** (red), [$^{111}$In]**3.15** (black) and [$^{18}$F]FMISO (blue).

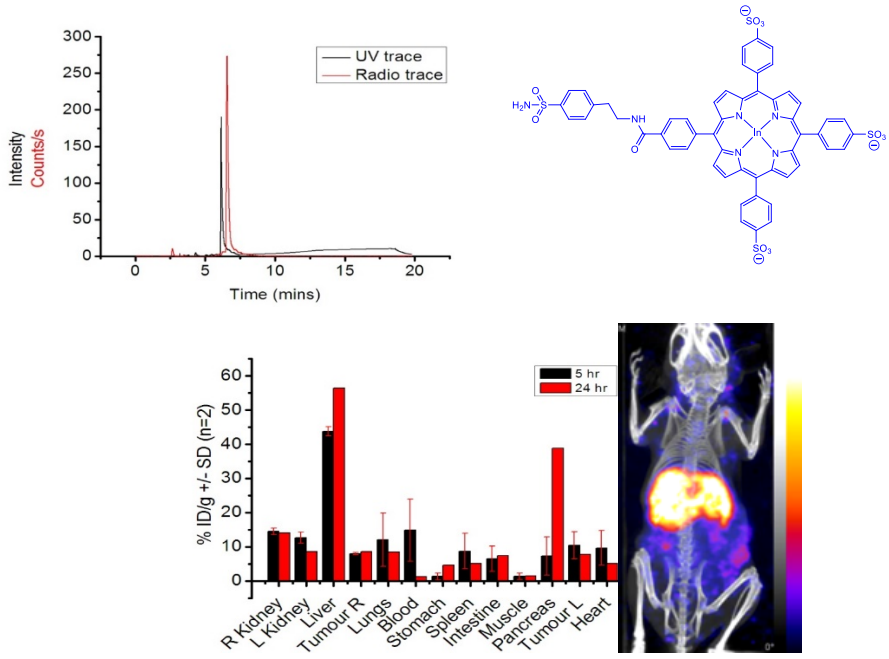


**Figure S72:** HPLC traces, biodistribution data of [$^{111}$In]**3.20** and SPECT image measured at 24 h of MKN45 tumor bearing mice injected with [$^{111}$In]**3.20**.

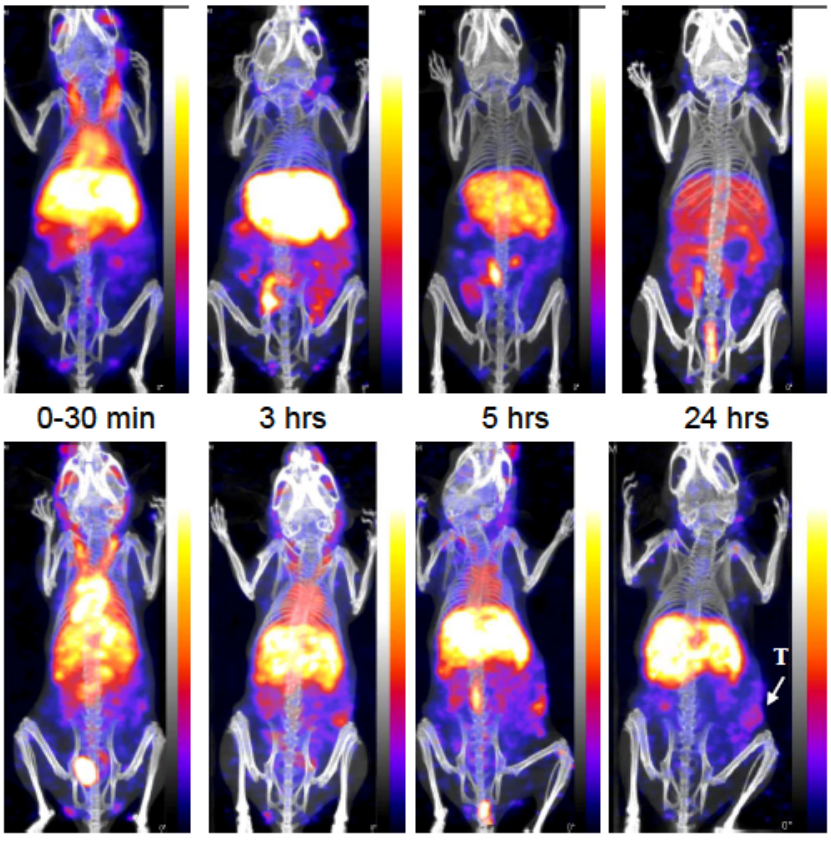


**Figure S73:** SPECT images measured at 30 min, 3, 5 and 24 h of MKN45 tumor bearing mice injected with [$^{111}$In]**3.15** (top row) and [$^{111}$In]**3.21** (bottom row). Tumor is marked „T“

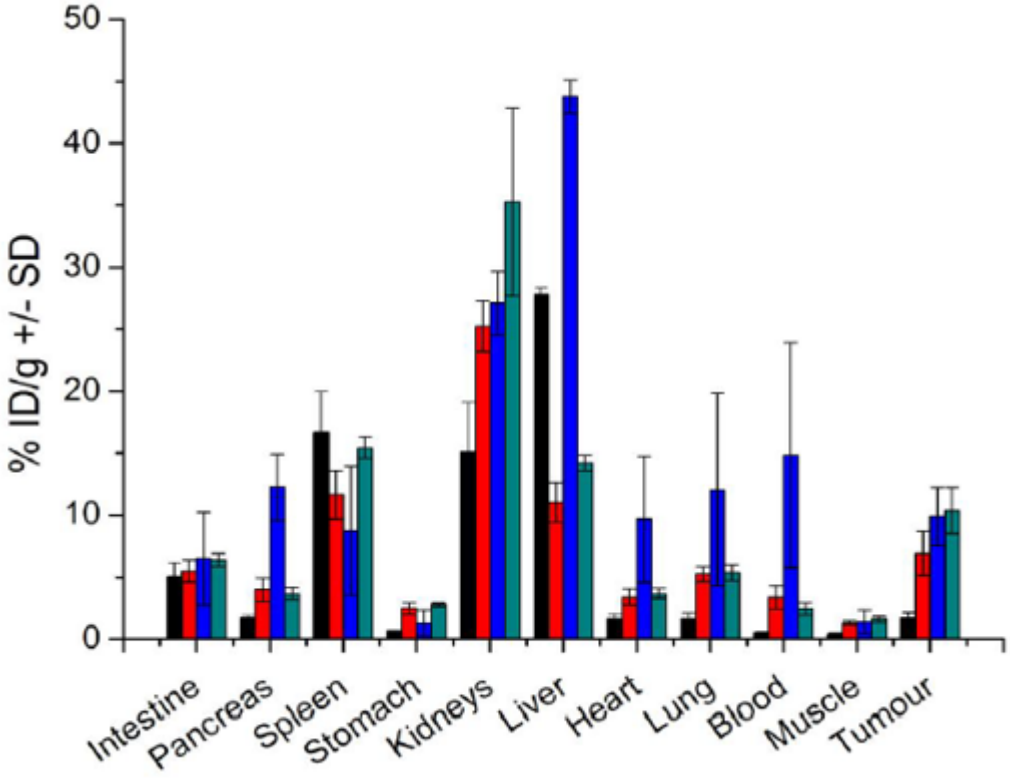


**Figure S74:** Biodistribution data for [$^{111}$In]**3.15** (black 5h, red 24 h) and [$^{111}$In]**3.21** (blue 5 h, green 24 h) at 5 h and 24 h for MKN45 tumor bearing mice

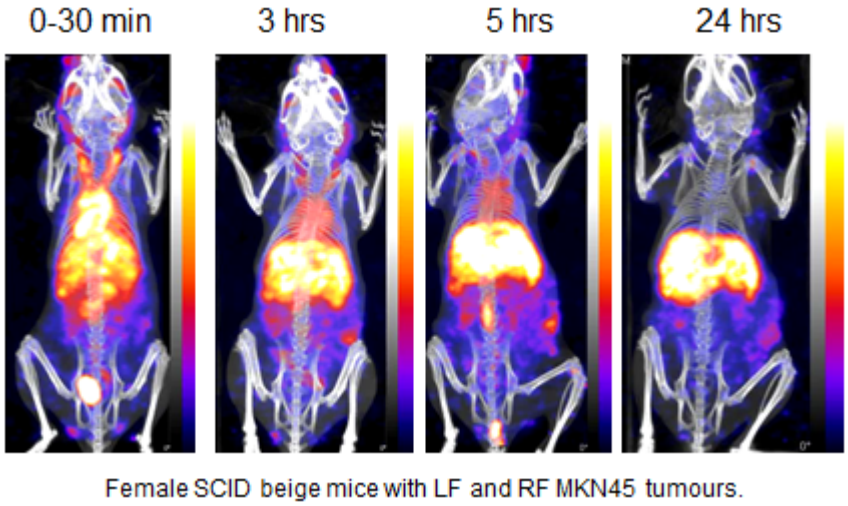


**Figure S75**: In vivo distribution studies of compound [$^{111}$In]**3.21**.

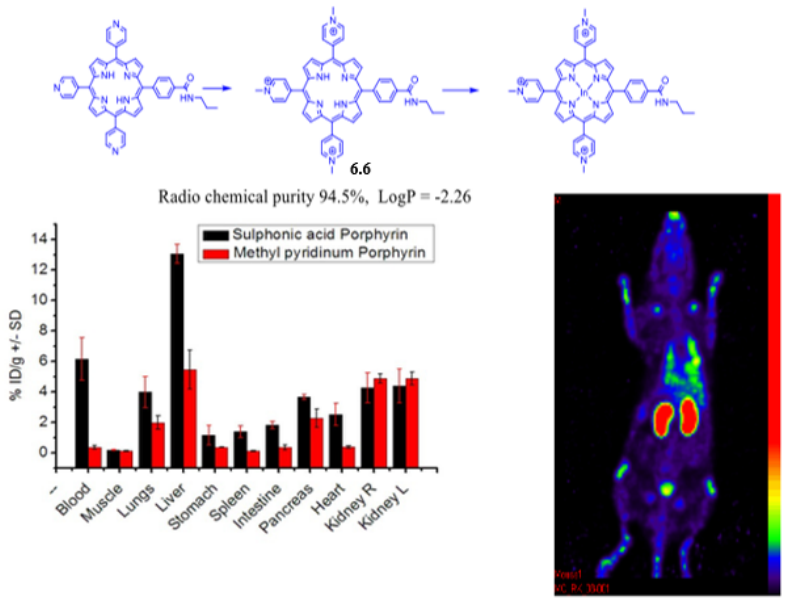


**Figure S76:** *In vivo* distribution of the polycationic compound [$^{111}$In]**6.6** and corresponding SPECT scan after 24 h.

9. Cellular imaging assays

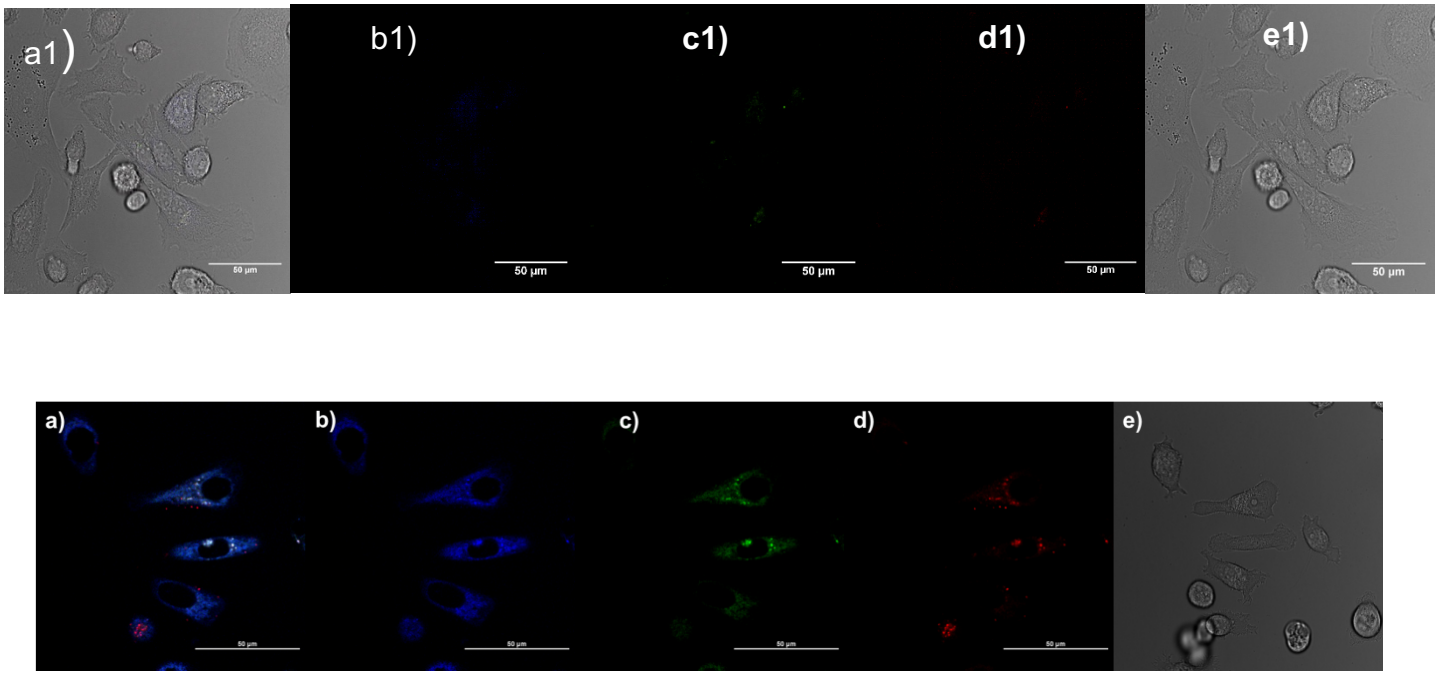


**Figure S77: Top row:** PC3 control experiments, excitation 405 nm; a1) overlay of blue-green-red channels; b1) blue channel (λem = 417-477 nm); c1) green channel (λem = 500-550 nm); d1) red channel (λem = 570-750 nm); e1) DIC.Scale bar: 50 µm; **Bottom row:** Uptake of TPP, compound 1, 10 microM conc., 1% DMSO, 16 h) incubation at 37 ˚C a) overlay of blue-green-red channels; b) blue channel (λem = 417-477 nm); c) green channel (λem = 500-550 nm); d) red channel (λem = 570-750 nm); e) DIC channel. Scale bar: 50 µm.

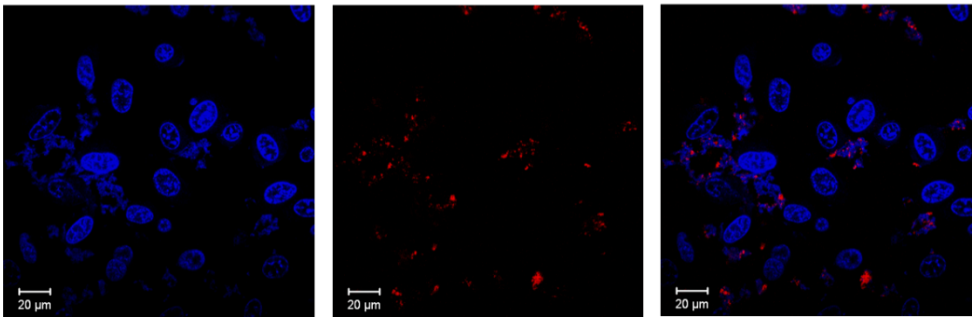


**Figure S78**: Confocal images of compound **2** (10 µM conc., 1% DMSO), Hoechst co-stained imaging, and corresponding overlays: PC-3 cells after incubation for 1h at 37 °C.

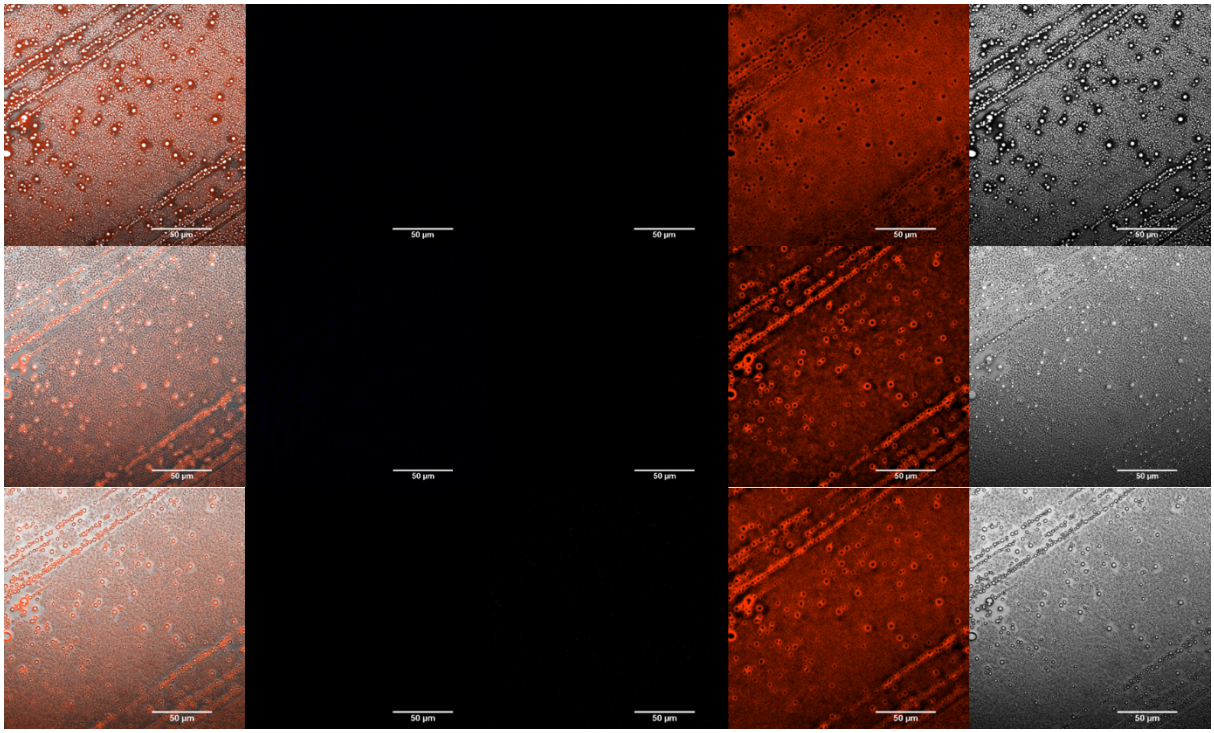

**Figure S79**: Single-photon laser-scanning confocal fluorescence imaging of compound **2** deposited on a borosilicate glass from 1mg/mL $CHCl_3$ solutions. Images show aggregation and stacking: overlapped micrographs of the DIC, blue, green and red channels (LHS stack) then in order from left to right stacked micrographs show: emissions in blue channel ($\lambda_{em}$ = 420–480 nm) green channel ($\lambda_{em}$ = 516–530 nm); red channel ($\lambda_{em}$ = 615–650 nm), also DIC channel (RHS stack , from $\lambda_{ex}$ = 405 nm). scale bar: 50 µm.

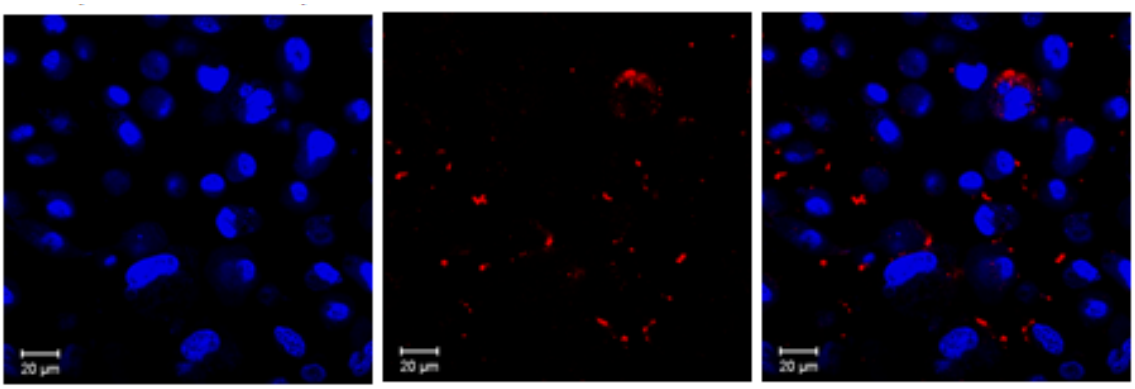

**Figure S80**. Confocal fluorescence images of compound **3** at 10μM solution in 1% DMSO and co-stained with Hoechst with PC-3 cells after incubation for 1h at 37 °C, and corresponding overlay.

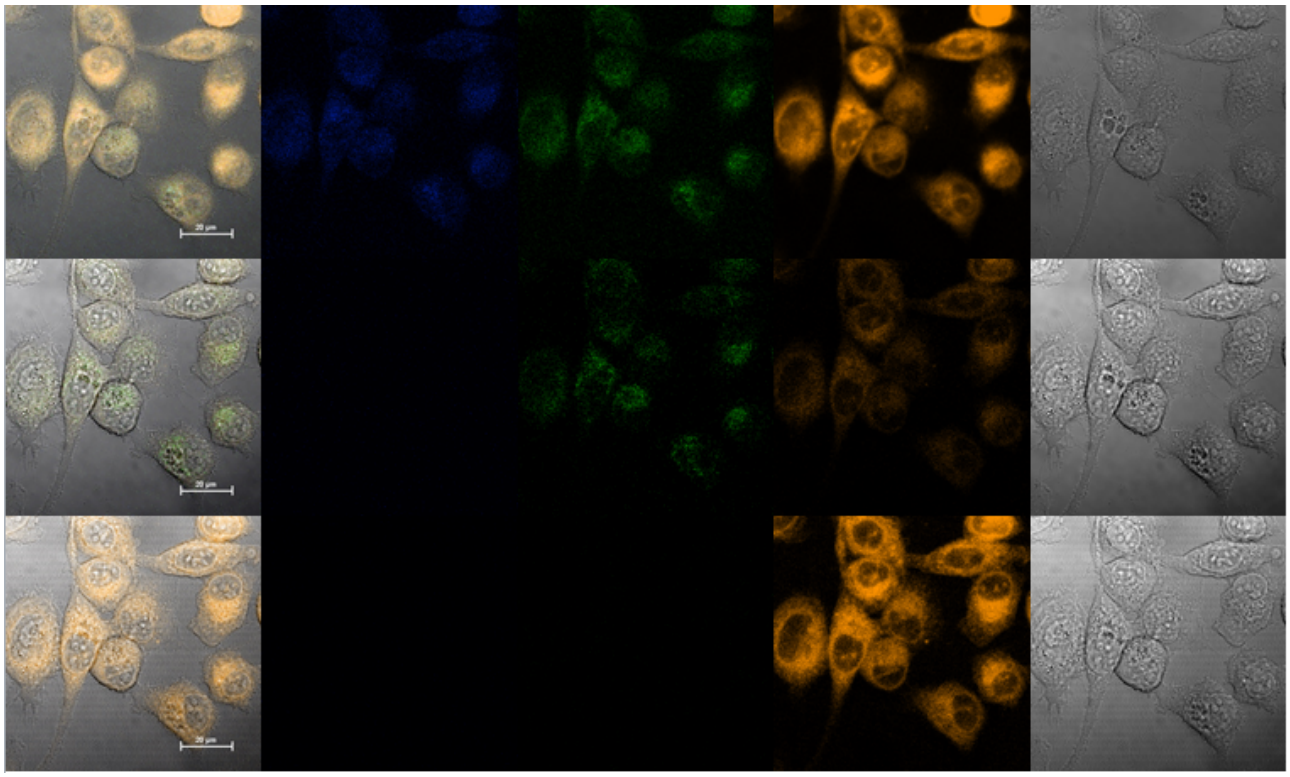

**Figure S81:** Single photon confocal microscopy images of **3** in PC3 20 min, 37 °C, 10μm conc (1% DMSO). where 1) 405, 2) 488 and 3) 561 nm excitation and corresponding emissions are: a) overlay of blue-green-red channels; b) blue channel (λem = 417-477 nm); c) green channel (λem = 500-550 nm); d) red channel (λem = 570-750 nm).

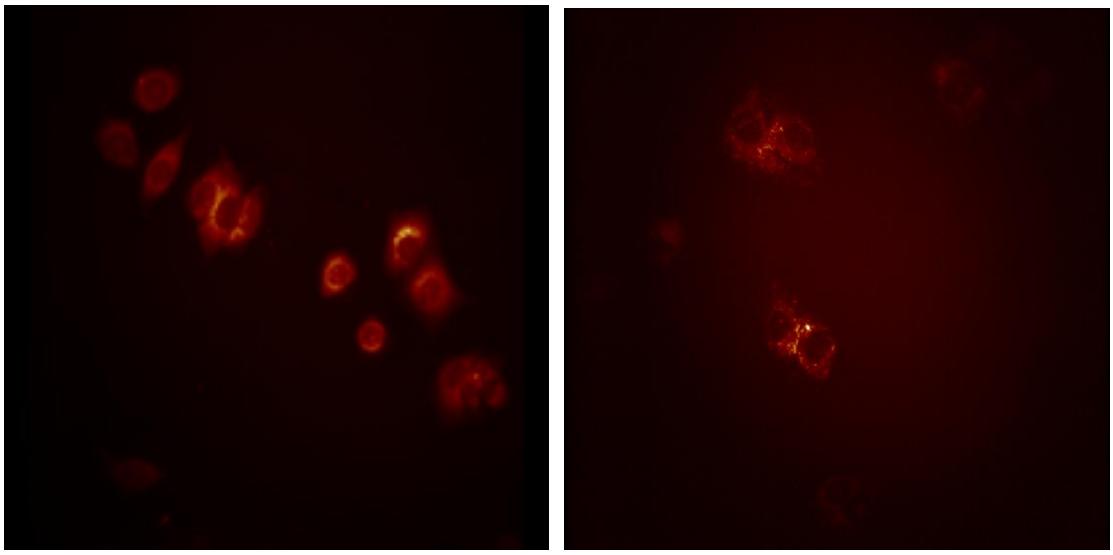

**Figure S82**. Epifluorescence imaging at the uptake of compound **1.1. (**GaClTPP, left) and Ga(Cl)TPPNH2 (4.2, right image) into HeLa cells (10µM, 37 °C 1 hr incubation with HeLa cells (ex = 405 nm, emission > 600 nm) indicated the localization of the porphyrin in regions of the cytoplasm.

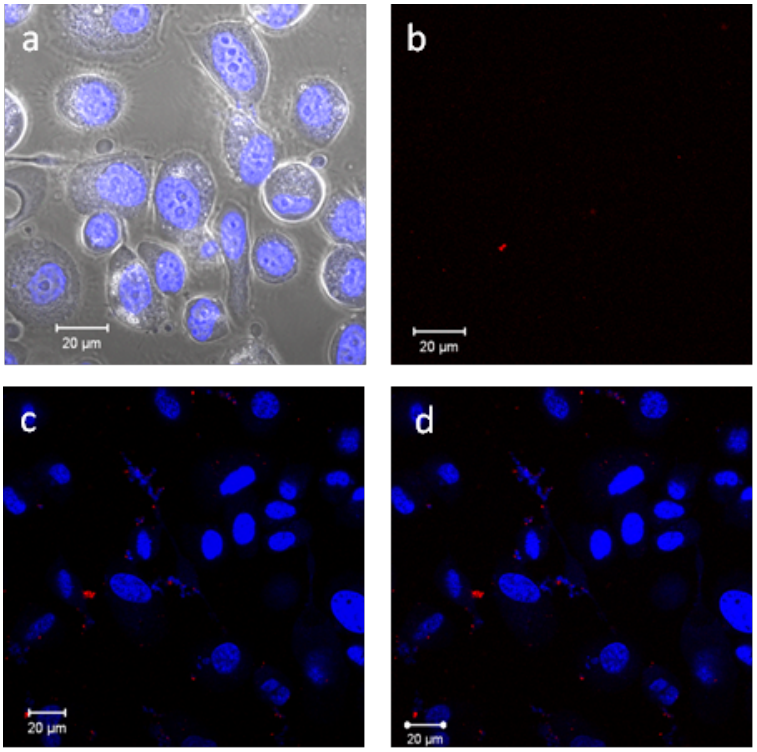


**Figure S83**: Confocal fluorescence imaging of the free base amino-porphyrin **4** in PC3 cells. Hoescht nuclear stain is in blue and porphyrin in red. All incubations were at 37 °C. a) cells treated only with Hoescht nuclear stain for 30 min. b) **4** 10µM 30 min. c) **4** 10 µM 1 h. d) **4** 100 µM 30 min

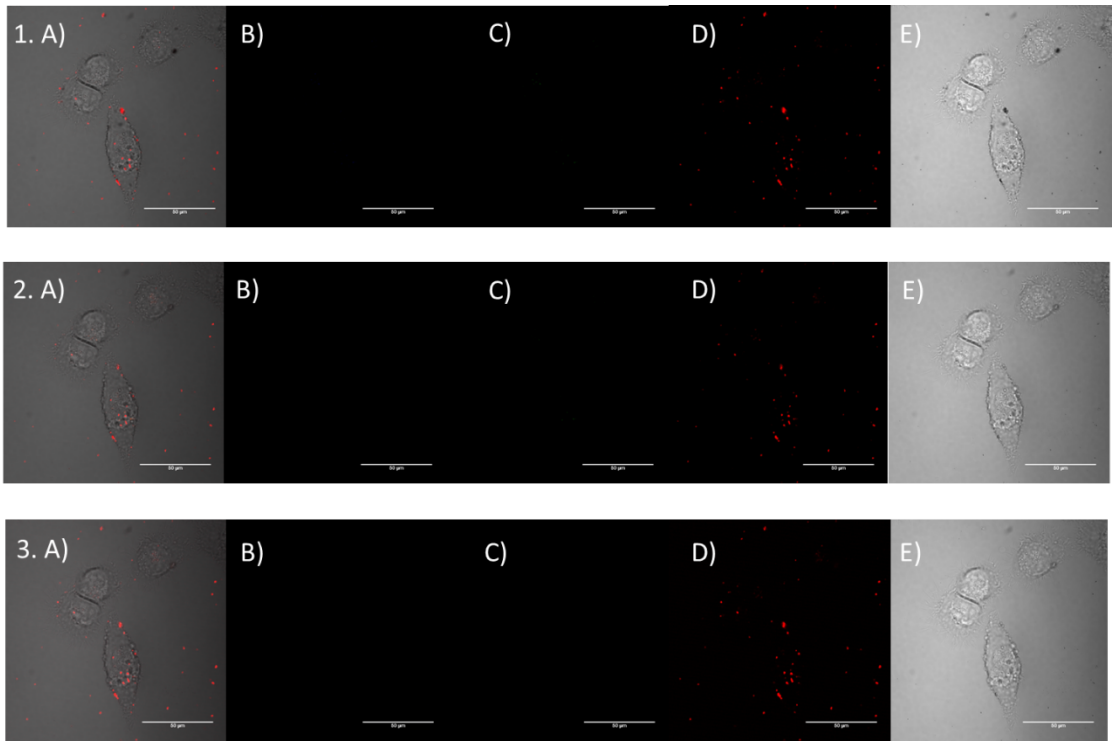


**Figure S84**: Confocal fluorescence images **4** 50 µM (1%DMSO): 20 min incubation, where 1) 405, 2) 488 and 3) 561 nm excitation and corresponding emissions are: a) overlay of blue-green-red channels; b) blue channel (λem = 417-477 nm); c) green channel (λem = 500-550 nm); d) red channel (λem = 570-750 nm).

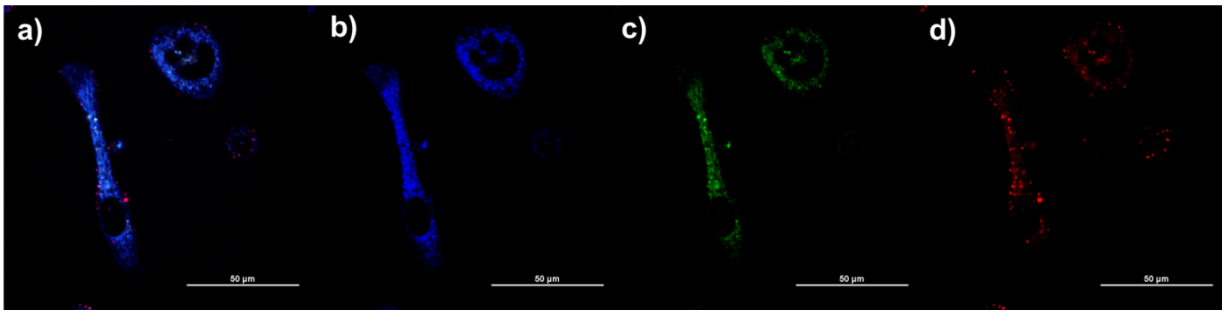


**Figure S85**: Confocal fluorescence images for compound **4,** incubated for 16 h, 10 µM conc (1%DMSO): a) overlay of blue-green-red channels; b) blue channel (λem = 417-477 nm); c) green channel (λem = 500-550 nm); d) red channel (λem = 570-750 nm).

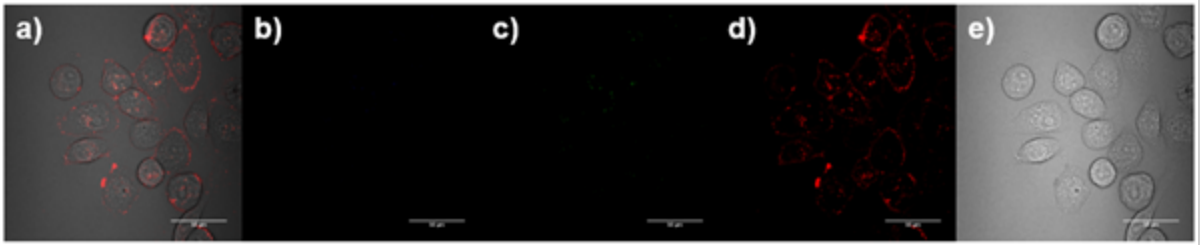


**Figure S86:** Confocal microscopy of 50 µM Compound **4.9** in 1 % DMSO serum free medium a) overlay of DIC-blue-green-red channels; b) Blue channel, λex =405 nm; c) Green channel, λex = 488 nm; d) Red channel, λex = 561 nm; e) DIC channel. Scale bar: 50 µm.

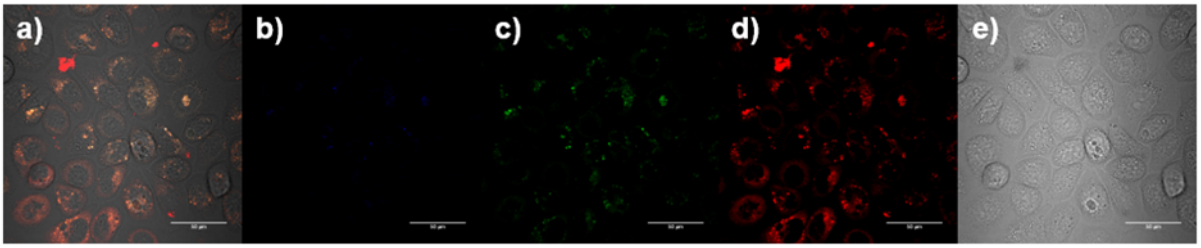


**Figure S87:** Confocal microscopy of 200 µM Compound **4.10** in 1 % DMSO serum free medium a) overlay of DIC-blue-green-red channels; b) Blue channel, λex =405 nm; c) Green channel, λex = 488 nm; d) Red channel, λex = 561 nm; e) DIC channel. Scale bar: 50 µm.

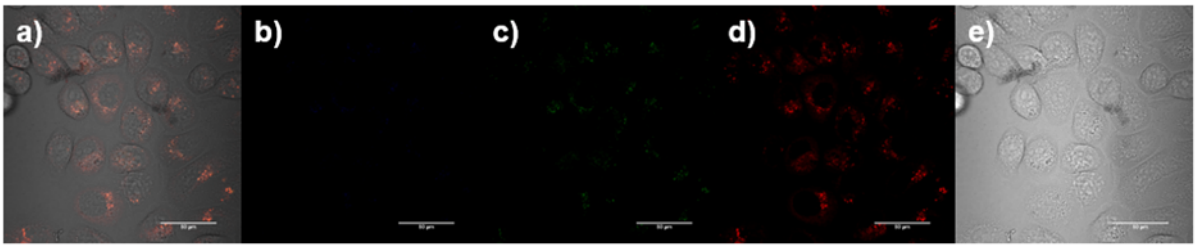


**Figure S88:** Confocal microscopy of 50 µM Compound 4.**12** in 1 % DMSO serum free medium a) overlay of DIC-blue-green-red channels; b) Blue channel, λex =405 nm; c) Green channel, λex = 488 nm; d) Red channel, λex = 561 nm; e) DIC channel. Scale bar: 50 µm.

## 10. Theoretical Modelling of Porphyrin-Metal Complexes and TDDFT calculations

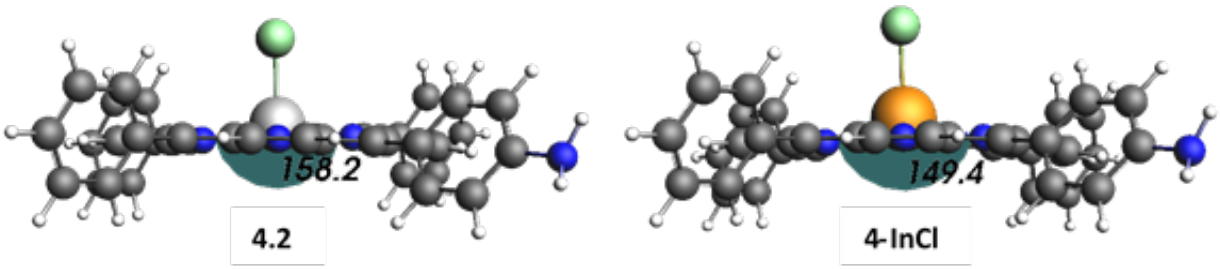


**Figure S89:** N-M-N angles of **4.2** and **4-InCl**, showing displacement of metal centers from the porphyrin plane. Note: the smaller N-M-N angle is depicted. Deviation from the larger N-M-N angle is 0.6° (Ga) or 0.5° (In).

A change in Mulliken charges (Table S6) is observed between the free base **4**, and the corresponding metal complexes. The following table compares the charge distributions of the porphyrin core, arbitrarily separating the porphyrin into three regions: the nitrogens (red), the adjacent pyrrole carbons (blue), and the carbophenyl bridges (green).

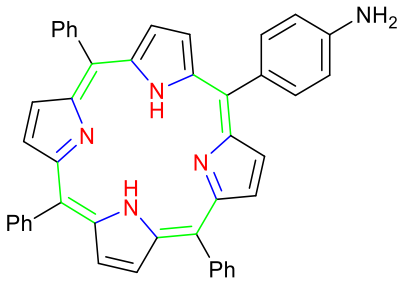


**Table S6**: Average Mulliken charges within the porphyrin framework

| Cmpd. | Mulliken Charge Nitrogens (red) | Mulliken Charge Adjacent Pyrrole C's (blue) | Mulliken Charge carbophenyl (green) |
|---|---|---|---|
| **4** | -0.499 (N) / 0.055 (NH) | 0.165 | - 0.027 |
| **4.1** | -0.498 | 0.192 | - 0.038 |
| **4.2 Cl** | - 0.595 | 0.209 | - 0.051 |
| **4.2-OAc** | - 0.604 | 0.209 | - 0.051 |
| **4–InCl** | - 0.598 | 0.180 | - 0.034 |

The COSMO surfaces of all compounds are depicted below (Fig. S90).

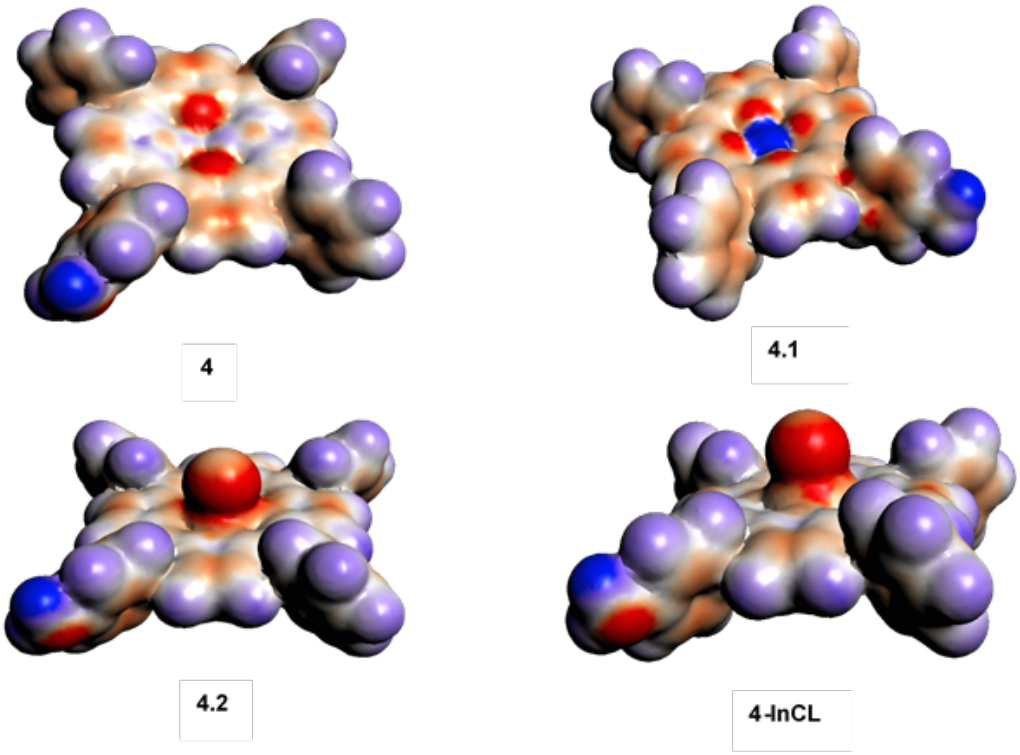


**Figure S90:** Overview over COSMO surfaces for **4** and metal complexes based on **4**.

Unlike other nitrogen-based conjugated systems, such as cyanines and the related phtalocyanines [39, 40], excitation energies were reasonably accurate and band-shapes well represented compared to the experimental results, at least for compounds based on 4. Using the *Davidson* algorithm, we found that the predicted transitions can be described accurately with the HOMO-2, HOMO-1, HOMO, LUMO and LUMO+1 orbitals. Noticeably, using the tight-binding (TB) approximation, led to more accurate prediction of the transition energy of the Soret band [41]. However, it relied mainly on orbital transitions involving the HOMO-4 orbital. The accuracy of Q-band transitions was not significantly affected by choosing the different TD-DFT protocol. Furthermore, calculations employing the TB approximation resulted in four Q-bands for all compounds. It was therefore disregarded. A comparison between the results obtained for **4** using either TDDFT+TB or TDDFT using the *Davidson* algorithm can be found in Table S7 and Fig. S91.

**Table S7**: Comparison of results obtained using either TD-DFT+TB or *Davidson* methodology. Experimental values obtained in DMF, taken from reference [42].

| Band | TDDFT+TB [nm] | Davidson Algorithm [nm] | Experiment [nm][41] |
|---|---|---|---|
| Soret | 407.9305<br>(+ bathochromic shoulder) | 477.2868 | 421 |
| Q-IV | 571.8343 | 560.9418 | 520 |
| Q-III | 593.0609 | 585.8144 | 560 |
| Q-II | 655.9561 | 670.9943 | 596 |
| Q-I | 693.5092 | 696.1933 | 656 |

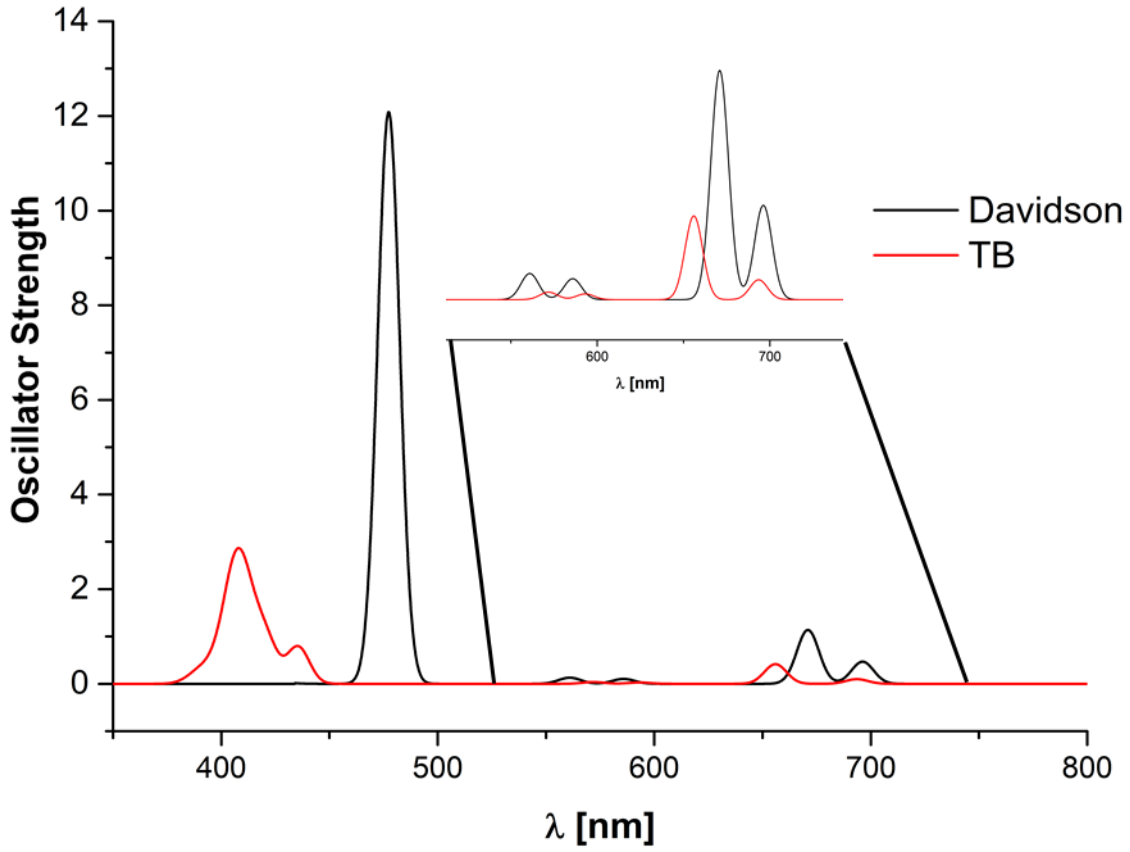


**Figure S91**: Comparison between TD-DFT results for **4**, using either tight-binding (TB) approximation or *Davidson* algorithm.

Transition energies and orbital contributions obtained using the Davidson algorithm are given in table 3. The number of bands was accurately predicted (Soret band, four Q-bands for **4**, Soret band, three Q-bands for **4.1**, **4.2** and 4-InCl). The Soret band showed the greatest deviation from experimental values and was predicted to have lower excitation energy compared to the experiment (ca. 0.35 eV). Fig. S91 shows a comparison between the calculated spectra.

**Table S8:** Transitions energies and orbital contributions of 4 and its derivatives, as determined by TD-DFT; a) main orbital transition; b) only contributions > 10% listed.

| Compound | Band | Transition Energy [eV/nm] | Orbital Transitions[a] | Orbital Contribution[b] |
|---|---|---|---|---|
| **4** | Soret | 2.5967 / 477.2868 | HOMO-2 → LUMO<br>HOMO-1 → LUMO+1<br>HOMO-2 → LUMO+1 | 56.2 %<br>15.4 %<br>13.1 % |
| | Q-IV | 2.2103 / 560.9418 | HOMO-1 → LUMO+1<br>HOMO-2 → LUMO | 61.7 %<br>24.1 % |
| | Q-III | 2.1164 / 585.8144 | HOMO-1 → LUMO<br>HOMO-2 → LUMO+1 | 71.5 %<br>16.8 % |
| | Q-II | 1.8479 / 670.9943 | HOMO → LUMO+1<br>HOMO-1 → LUMO+1 | 81.0 %<br>15.5 % |

| | | | | |
|---|---|---|---|---|
| | Q-I | 1.7809 / 696.1933 | HOMO → LUMO<br>HOMO-1 → LUMO | 83.7 %<br>11.7 % |
| **4.1** | Soret | 2.6223 / 472.8100 | HOMO-2 → LUMO+1<br>HOMO-1 → LUMO<br>HOMO → LUMO | 58.7 %<br>16.2 %<br>11.0 % |
| | Q-IV | 2.2298 / 556.0309 | HOMO-1 → LUMO+1<br>HOMO-2 → LUMO | 62.9 %<br>31.2 % |
| | Q-III | - | - | - |
| | Q-II | 1.9202 / 645.6708 | HOMO → LUMO+1<br>HOMO-1 → LUMO+1 | 83.4 %<br>12.5 % |
| | Q-I | 1.8892 / 656.2917 | HOMO → LUMO<br>HOMO-1 → LUMO | 80.5 %<br>15.3 % |
| **4.2** | Soret | 2.6160 / 473.9396 | HOMO-2 → LUMO+1<br>HOMO-1 → LUMO<br>HOMO-2 → LUMO | 50.6 %<br>15.6 %<br>15.1 % |
| | Q-IV | 2.1798 / 568.7839 | HOMO-1 → LUMO<br>HOMO-2 → LUMO+1 | 66.1 %<br>27.9 % |
| | Q-III | - | - | - |
| | Q-II | 1.8156 / 682.8842 | HOMO → LUMO+1 | 87.7 % |
| | Q-I | 1.7750 / 698.5098 | HOMO → LUMO<br>HOMO-1 → LUMO | 85.4 %<br>12.1 % |
| **4 – InCl** | Soret | 2.5841 / 479.7884 | HOMO-2 → LUMO<br>HOMO-1 → LUMO+1<br>HOMO-2 → LUMO+1 | 56.3 %<br>16.1 %<br>11.0 % |
| | Q-IV | 2.1471 / 577.4392 | HOMO-1 → LUMO<br>HOMO-2 → LUMO+1 | 70.5 %<br>22.7 % |
| | Q-III | - | - | - |
| | Q-II | 1.7679 / 701.2972 | HOMO → LUMO+1 | 88.4 % |
| | Q-I | 1.7167 / 722.2218 | HOMO → LUMO<br>HOMO-1 → LUMO | 85.6 %<br>11.7 % |

The metals (and where applicable the chloride counterion coordinated to it), do not appear to be involved in the electronic transitions. In fact, no significant difference between transitions is apparent. Fig. S92 gives an overview over all involved orbitals for **4** and **4-InCl.**

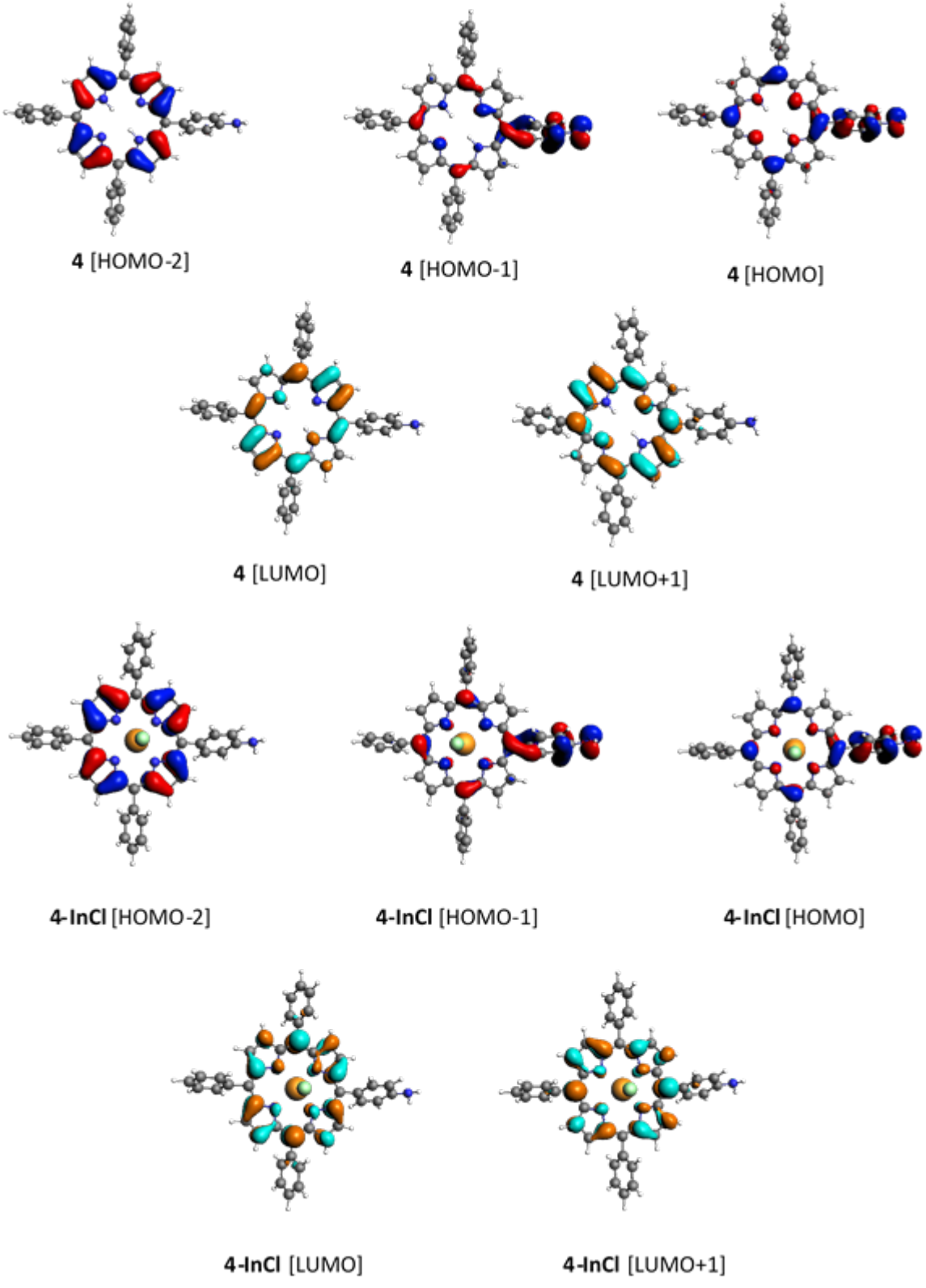


**Figure S92**: Overview over molecular orbitals involved in the excitation of **4** and **4-InCl** .Occupied molecular orbitals: red/blue, unoccupied molecular orbitals orange/cyan.

The calculations featuring **4.2-OAc** led to a slightly distorted structure, which led to additional excitation energies, presumably due to the reduction in symmetry.

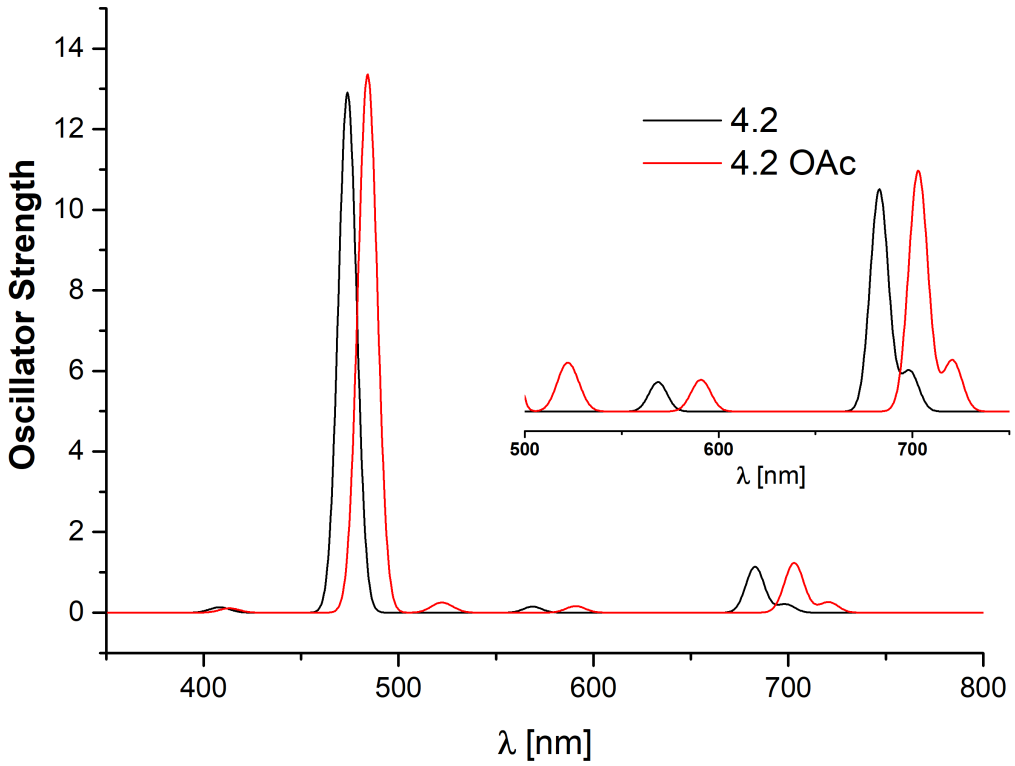


**Figure S93**: Comparison between TD-DFT results for **4.2 and 4.2-OAc**, showing an additional signal, as well as slight bathochromic shift for **4.2-OAc**

## 11. X-ray crystal data

A mixture of hexane:chloroform produced the crystal structure of TPP-$CO_2$Me (**2**). The crystal representation of compound **2** clearly displays the orientation of the external phenyl groups, perpendicular to the pyrrole ring of the porphyrin core, and the carbon-oxygen double bond of the methyl ester group in the plane of the aromatic group to which it is attached.

**Table S9:** Crystal data and structure refinement for compound **2**.

| | |
|---|---|
| Identification code | s19sip2 |
| Empirical formula | $C_{93}$ $H_{65}$ $Cl_3$ $N_8$ $O_4$ |
| Formula weight | 1464.88 |
| Temperature/ K | 150.00(10) |
| Wavelength/ Å | 1.54184 |
| Crystal system | Triclinic |
| Space group | P-1 |
| Unit cell dimensions: a/Å | 6.4382(5) |
| b/ Å | 12.7905(11) |
| c/ Å | 22.7905(12) |
| α/ ° | 96.4850(6) |
| β/ ° | 92.580(6) |
| γ/ ° | 104.284(8) |
| Volume/ $Å^3$ | 1801.9(2) |
| Z | 1 |
| Density (calculated) $Mg/m^3$ | 1.350 |
| Absorption coefficient/ $mm^{-1}$ | 1.650 |
| F(000) | 762 |
| Crystal size/ $mm^3$ | 0.497 x 0.201 x 0.059 |
| Theta range for data collection | 3.596 to 69.331 |
| Index ranges | -6<=h<=7, -15<=k<=15, -27<=l<=22 |
| Reflections collected | 10189 |
| Independent reflections | 6224 [R(int) = 0.0522] |
| Completeness to theta = 67.684° | 93.70% |
| Absorption correction | Semi-empirical from equivalents |
| Max. and min. transmission | 1.00000 and 0.39703 |
| Refinement method | Full-matrix least-squares on $F^2$ |
| Data / restraints / parameters | 6224 / 56 / 550 |
| Goodness-of-fit on $F^2$ | 1.026 |
| Final R indices [I>2sigma(I)] | R1 = 0.0792, wR2 = 0.2017 |

| | |
|---|---|
| R indices (all data) | R1 = 0.1048, wR2 = 0.2303 |
| Extinction coefficient | n/a |
| Largest diff. peak and hole/ e.Å$^{-3}$ | 0.544 and -0.309 |

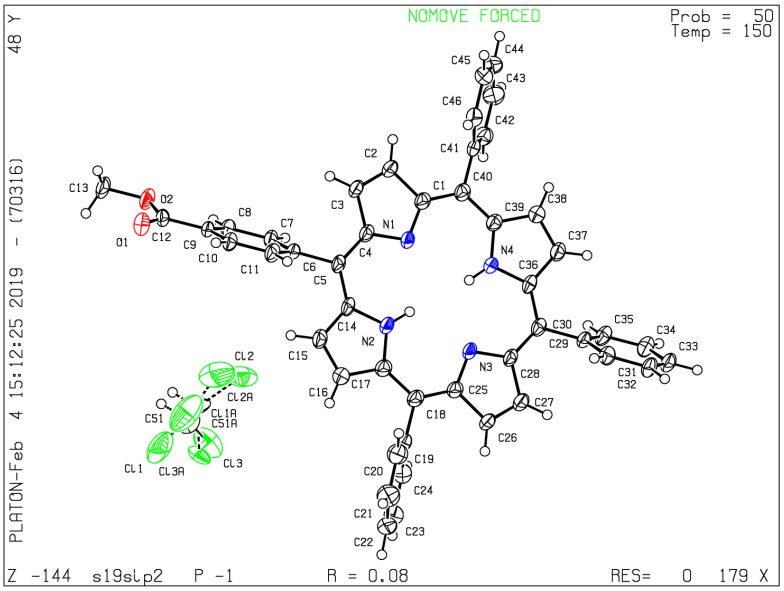


**Figure S94**: Crystal structure for compound **2** (generated from "checkcif").

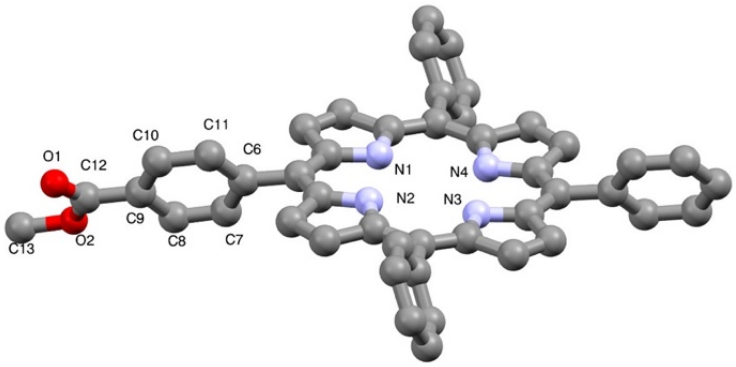


**Figure S95**: Molecular structure from single crystals X-ray diffraction for compound **2.**

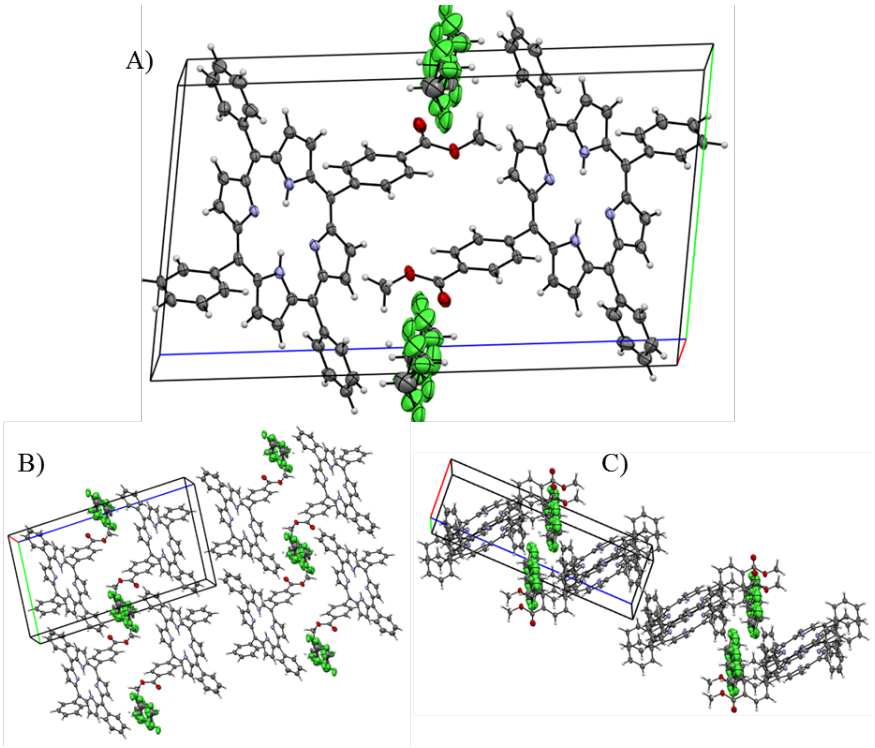


**Figure S96**: ORTEP representations of compound **2** showing A) unit cell, view along b axis, distance of 10.030 Å between porphyrin core planes, and B) and C) showing extended packing along b axis.

Crystals suitable for X-ray diffraction of the copper sulphonamide complex **3.17** were grown by the slow infusion of hexane into a solution of the complex in 1:1 chloroform:methanol. Data was collected using a synchrotron X-ray source.

Some relevant short interactions are displayed in the intramolecular network of the crystal structure of complex **3.17**. Packing involves H-bonding interactions between the amide oxygen and sulphonamide nitrogen (O(1)···N(6)* 2.829 Å). Longer range interactions including H-bonding interactions between the amide nitrogen and the sulphonamide oxygen (N(5)···O(3)* 3.133 Å) and T-type interactions between the phenyl groups and the tetrapyrrole ring on adjacent molecules (3.325 Å) are also present. The bond lengths in the sulphonamide unit are in accord with those for similar aromatic sulfonamide species [43].

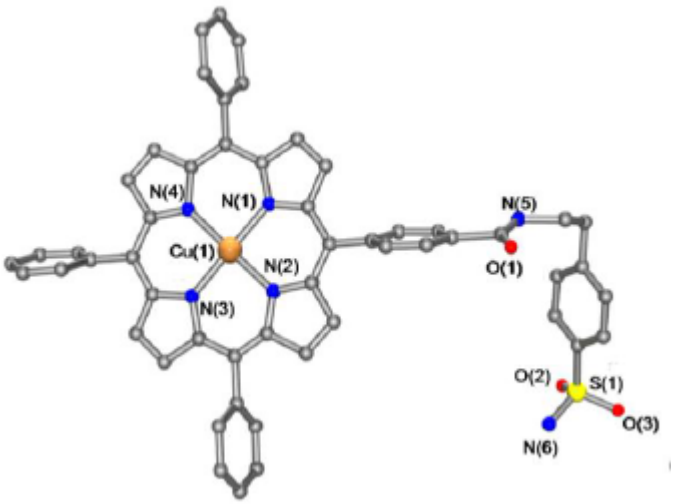


**Figure S97:** Ball and stick representations of the molecular structures of **3.17**

**Table S10:** Selected bond lengths (Å) and bond angles (θ) of **3.17**

| | | | |
|---|---|---|---|
| Cu(1)-N(1) | 2.019(7) | S(1)-O(3) | 1.463(17) |
| Cu(1)-N(2) | 1.984(7) | S(1)-O(2) | 1.451(17) |
| Cu(1)-N(3) | 1.990(7) | S(1)-N(6) | 1.57(2) |
| Cu(1)-N(4) | 2.000(8) | C(42)-C(45)-N(5) | 115(4) |
| C(45)-O(1) | 1.23(4) | C(42)-C(45)-O(1) | 110(3) |
| C(45)-N(5) | 1.14(4) | O(1)-C(45)-N(5) | 134(4) |

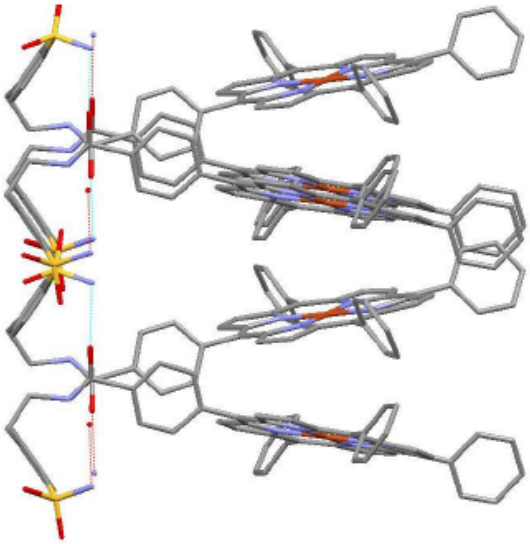

**Figure S98:** Fragment of the unit cell displaying some relevant short contacts in the intermolecular network (view over axis c) in the crystal structure of **3.17**. Color code: brown = Cu(II), blue = N, yellow = S, red = O, grey = C

Crystals of nitroimidazole compound **3.22** have been grown by the slow infusion of acetone into an aqueous THF solution (1:1 v/v THF:water). The crystals produced extremely weak X-ray diffraction patterns and a structure could only be solved when a synchrotron radiation source was used. The small crystal size, the large size of the unit cell and asymmetric unit, the weak scattering of the involved atoms and the extensive disorder of solvating water molecules made solving and refining this data set extremely challenging. Packing is dominated by H-bonding interactions with H- bonding evident between the imidazole nitrogen and amide NH group (N(5)-H(51)···N(8)"), and nitro group oxygen and amide NH group (N(5)-H(51)···O(3)") on two adjacent porphyrin conjugates with H-bonding length of 3.075 and 2.936 Å respectively (Fig. 7) and extensive H-bonding between the sulphonate oxygen atoms and solvent water molecules. Weak T-type or edge-face interactions are also present between phenyl rings and pyrrole groups of adjacent molecules, the partially positively charged hydrogen atom of one phenyl rings points perpendicular to the center of the aromatic plane of the pyrrole ring, at distances of between 3.505 and 3.695 Å.

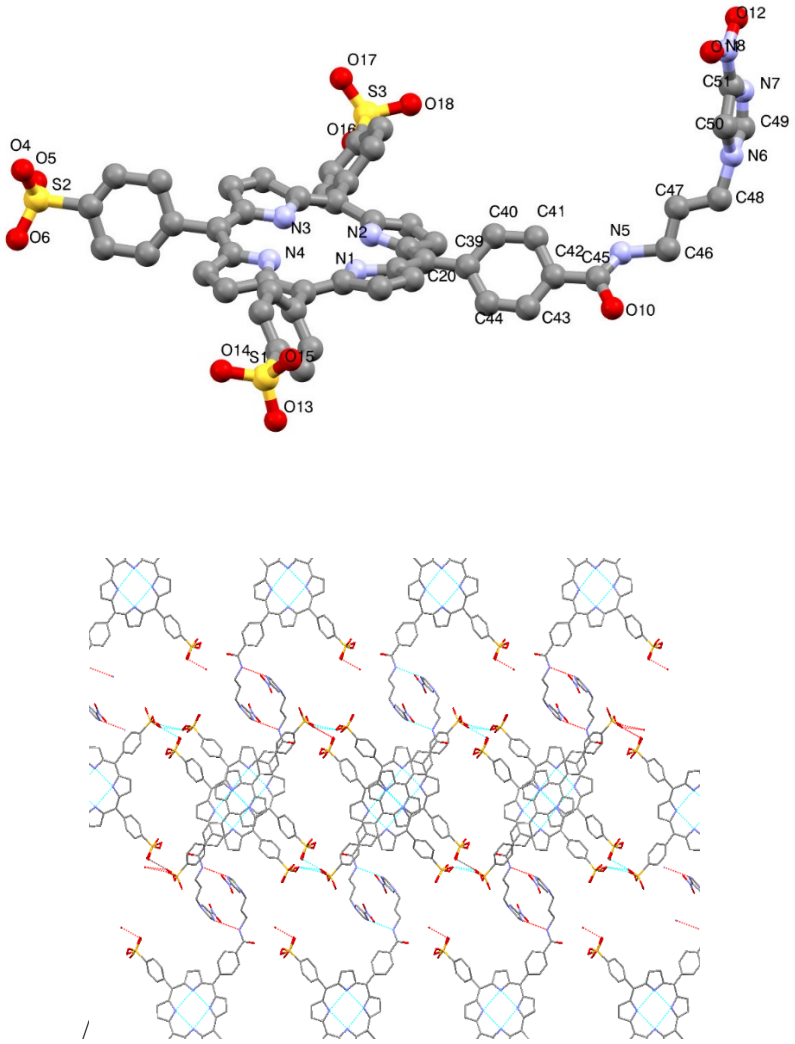


**Figure S99:** Molecular structure of compound **3.22** and its packing diagram showing H-bonding interaction between nitroimidazole group and amide NH and short-range interactions between sulphonate groups and solvent. Each sulphonate group has been modelled as disordered over 2 sites with 50 % occupancy each. Color code: blue = N, yellow = S, red = O, grey = C.

**Table S11**: Selected bond lengths (Å) and bond angles (θ) of **3.22**

| | | | |
|---|---|---|---|
| S(1)-C(24) | 1.781 (14) | C(45)-N(5) | 1.30 (3) |
| S(2)-C(30) | 1.792 (15) | N(5)-H---N(7)' | 3.099 |
| S(3)-C(36) | 1.760 (15) | C(42)-C(45)-N(5) | 122.0(2) |
| C(42)-C(45) | 1.45 (3) | C(42)-C(45)-O(10) | 117.6(19) |
| C(45)-C(10) | 1.29 (2) | O(10)-C(45)-N(5) | 121.2(2) |

Table S12. Crystal data and structure refinement for **compound 1.1.**

| | | |
|---|---|---|
| Identification code | ox024 | |
| Empirical formula | C46 H31 Ga N4 O2 | |
| Formula weight | 741.47 | |
| Temperature | 150(2) K | |
| Wavelength | 0.7848 Å | |
| Crystal system | Monoclinic | |
| Space group | $P2_1/n$ | |
| Unit cell dimensions | a = 10.573(2) Å | α= 90°. |
| | b = 15.905(3) Å | β= 92.02(3)°. |
| | c = 20.628(4) Å | γ= 90°. |
| Volume | 3466.8(12) $Å^3$ | |
| Z | 4 | |
| Density (calculated) | 1.421 $Mg/m^3$ | |
| Absorption coefficient | 1.090 $mm^{-1}$ | |
| F(000) | 1528 | |
| Crystal size | 0.100 x 0.030 x 0.020 $mm^3$ | |
| Theta range for data collection | 3.541 to 29.996°. | |
| Index ranges | -13<=h<=12, -16<=k<=20, -15<=l<=26 | |
| Reflections collected | 19430 | |
| Independent reflections | 7487 [R(int) = 0.0795] | |
| Completeness to theta = 28.091° | 99.6 % | |
| Absorption correction | Semi-empirical from equivalents | |
| Max. and min. transmission | 1.00 and 1.00 | |
| Refinement method | Full-matrix least-squares on $F^2$ | |
| Data / restraints / parameters | 7487 / 0 / 480 | |
| Goodness-of-fit on $F^2$ | 1.054 | |

| | |
|---|---|
| Final R indices [I>2sigma(I)] | R1 = 0.0576, wR2 = 0.1430 |
| R indices (all data) | R1 = 0.0762, wR2 = 0.1581 |
| Extinction coefficient | n/a |
| Largest diff. peak and hole | 0.469 and -0.626 e.Å$^{-3}$ |

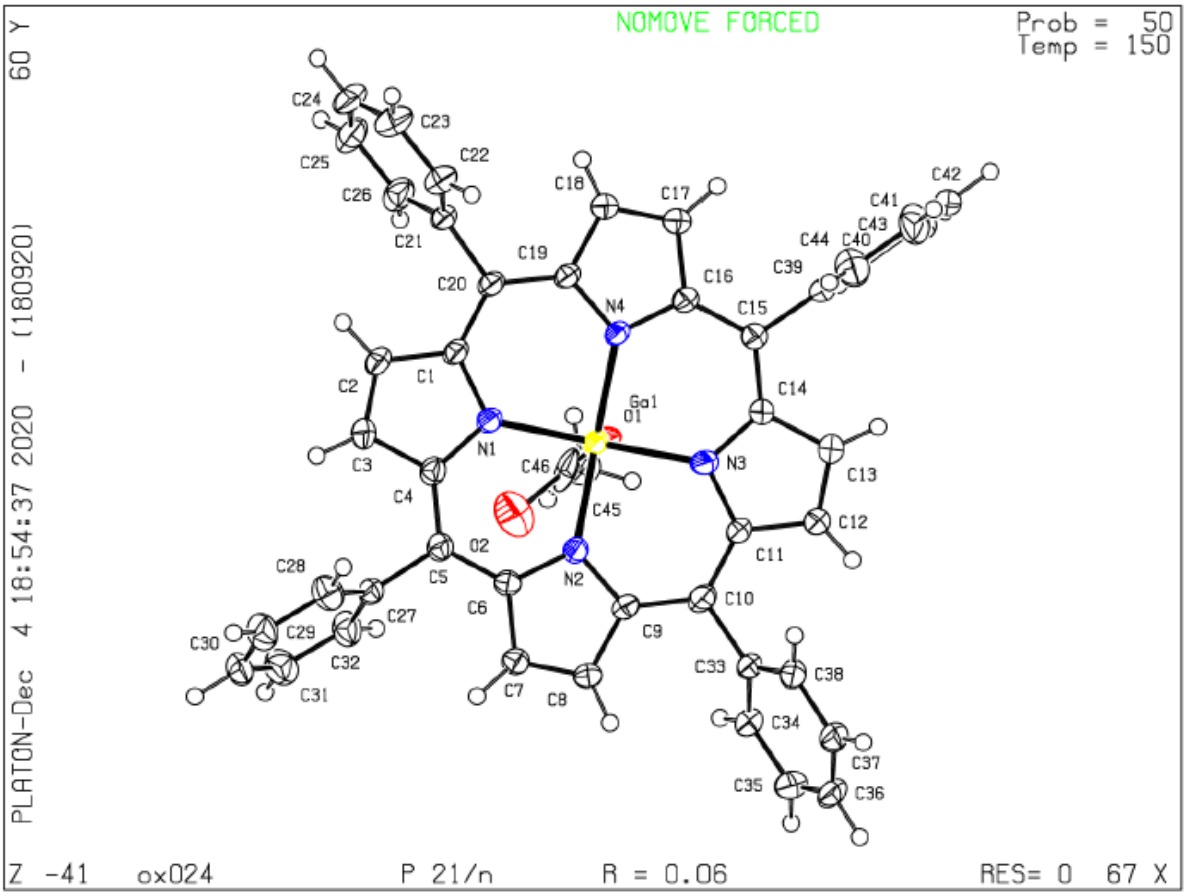

Table S13. Crystal data and structure refinement for Compound 3.22.

| | | |
|---|---|---|
| Identification code | ox118j | |
| Empirical formula | C53 H36.50 N8 Na O20 S3 | |
| Formula weight | 1224.57 | |
| Temperature | 150(2) K | |
| Wavelength | 0.6944 Å | |
| Crystal system | Monoclinic | |
| Space group | $P2_1/c$ | |
| Unit cell dimensions | a = 21.150(6) Å | ⟨= 90°. |
| | b = 8.234(2) Å | ®= 102.663(6)°. |
| | c = 36.277(10) Å | © = 90°. |
| Volume | 6164(3) $Å^3$ | |
| Z | 4 | |
| Density (calculated) | 1.320 $Mg/m^3$ | |
| Absorption coefficient | 0.190 $mm^{-1}$ | |
| F(000) | 2518 | |
| Crystal size | 0.200 x 0.020 x 0.010 $mm^3$ | |
| Theta range for data collection | 0.964 to 21.428°. | |
| Index ranges | -22<=h<=17, -8<=k<=8, -38<=l<=37 | |
| Reflections collected | 23289 | |
| Independent reflections | 7454 [R(int) = 0.1306] | |
| Completeness to theta = 21.428° | 99.0 % | |
| Absorption correction | Semi-empirical from equivalents | |
| Max. and min. transmission | 1.00 and 1.00 | |
| Refinement method | Full-matrix least-squares on $F^2$ | |
| Data / restraints / parameters | 7454 / 315 / 1007 | |
| Goodness-of-fit on $F^2$ | 1.097 | |
| Final R indices [I>2sigma(I)] | R1 = 0.1228, wR2 = 0.3093 | |
| R indices (all data) | R1 = 0.2588, wR2 = 0.3968 | |
| Extinction coefficient | n/a | |
| Largest diff. peak and hole | 0.697 and -0.482 e.$Å^{-3}$ | |

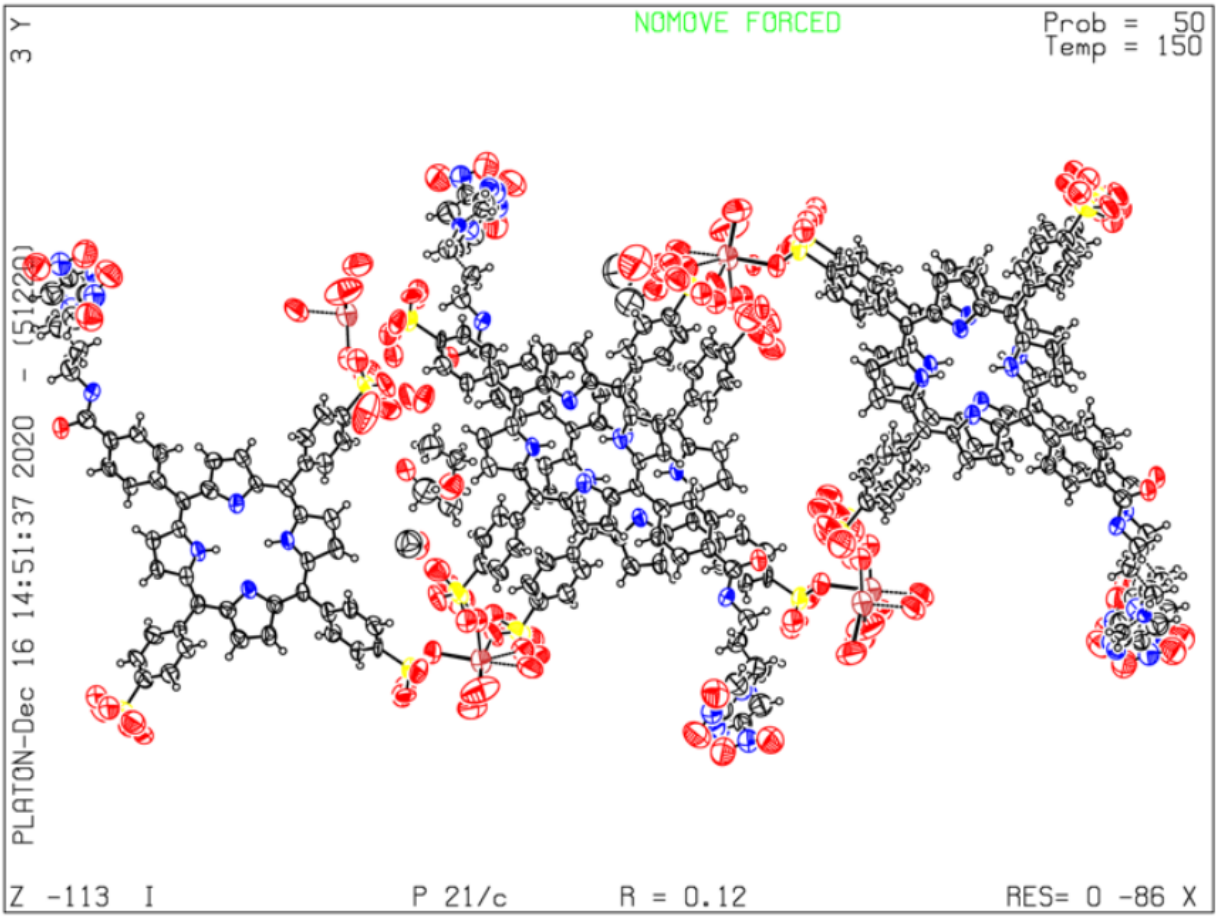


S14 Crystal data and structure refinement for Compound 3.17.

| | | |
|---|---|---|
| Identification code | bath723_sq | |
| Empirical formula | C51 H34 Cu N5.50 O2.50 S0.75 | |
| Formula weight | 851.42 | |
| Temperature | 150(2) K | |
| Wavelength | 0.6939 Å | |
| Crystal system | Monoclinic | |
| Space group | $P2_1/c$ | |
| Unit cell dimensions | a = 37.898(10) Å | a= 90°. |
| | b = 8.689(2) Å | b= 97.142(3)°. |
| | c = 14.905(4) Å | g = 90°. |
| Volume | 4870(2) $Å^3$ | |
| Z | 4 | |
| Density (calculated) | 1.161 $Mg/m^3$ | |
| Absorption coefficient | 0.490 $mm^{-1}$ | |
| F(000) | 1758 | |
| Crystal size | 0.070 x 0.050 x 0.050 $mm^3$ | |

| | |
|---|---|
| Theta range for data collection | 2.349 to 22.620°. |
| Index ranges | -41<=h<=41, -9<=k<=9, -16<=l<=16 |
| Reflections collected | 28422 |
| Independent reflections | 6905 [R(int) = 0.0713] |
| Completeness to theta = 22.620° | 99.3 % |
| Absorption correction | Semi-empirical from equivalents |
| Max. and min. transmission | 1.00 and 1.00 |
| Refinement method | Full-matrix least-squares on $F^2$ |
| Data / restraints / parameters | 6905 / 79 / 565 |
| Goodness-of-fit on $F^2$ | 1.061 |
| Final R indices [I>2sigma(I)] | R1 = 0.1168, wR2 = 0.2704 |
| R indices (all data) | R1 = 0.1471, wR2 = 0.2880 |
| Extinction coefficient | n/a |
| Largest diff. peak and hole | 0.898 and -2.688 e.Å$^{-3}$ |

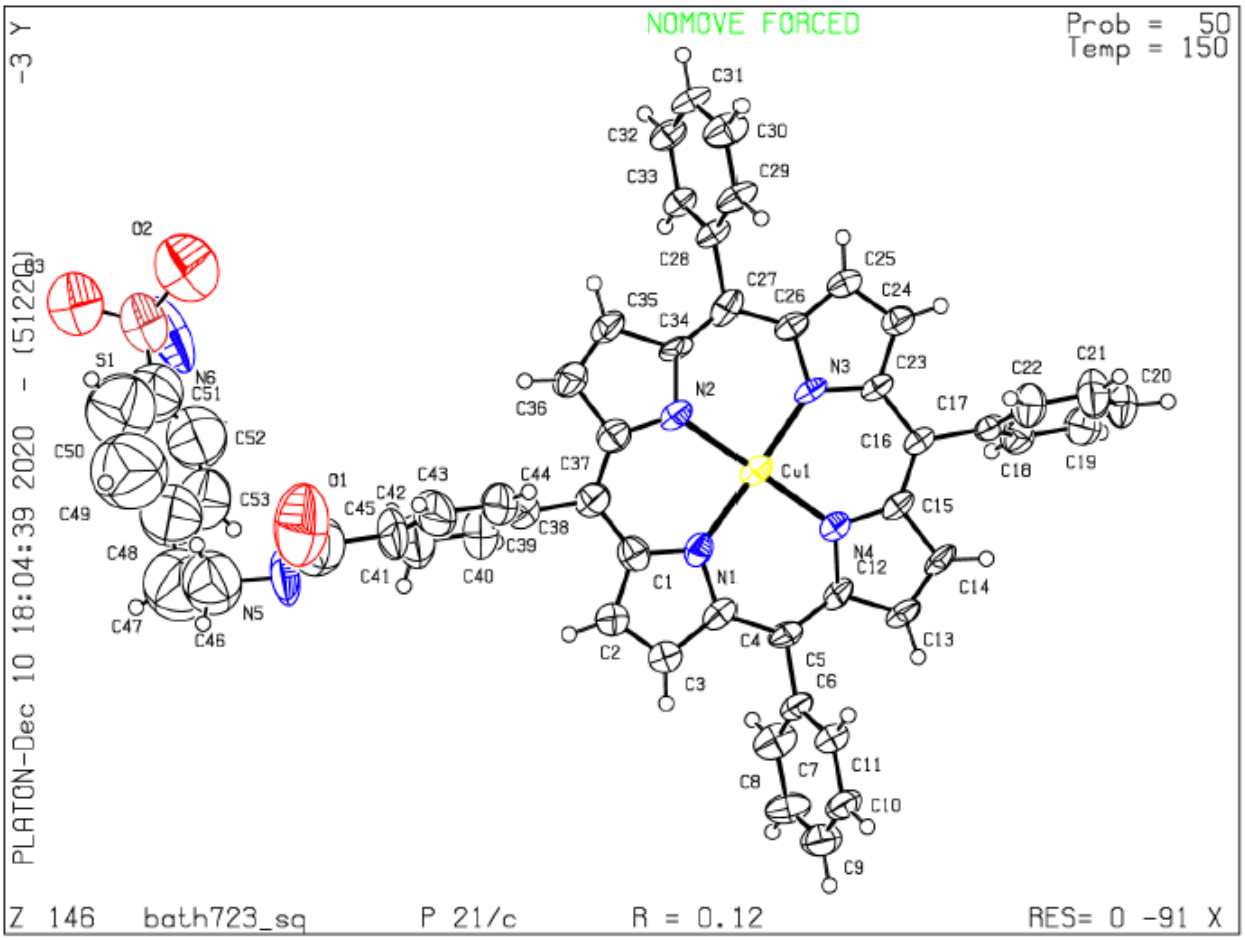

## References


[1] H.E. Gottlieb, V. Kotlyar, A. Nudelman, NMR chemical shifts of common laboratory solvents as trace impurities, J. Org. Chem., 62 (1997) 7512-7515.
[2] Mestrelab, www.mestrelab.com, last accessed 01/2021.
[3] G. te Velde, F.M. Bickelhaupt, E.J. Baerends, C. Fonseca Guerra, S.J.A. van Gisbergen, J.G. Snijders, T. Ziegler, Chemistry with ADF, Journal of Computational Chemistry, 22 (2001) 931-967.
[4] C.C. Pye, T. Ziegler, An implementation of the conductor-like screening model of solvation within the Amsterdam density functional package, Theoretical Chemistry Accounts, 101 (1999) 396-408.
[5] P. Rydberg, L. Olsen, The Accuracy of Geometries for Iron Porphyrin Complexes from Density Functional Theory, The Journal of Physical Chemistry A, 113 (2009) 11949-11953.
[6] E. Van Lenthe, E.J. Baerends, Optimized Slater-type basis sets for the elements 1–118, Journal of Computational Chemistry, 24 (2003) 1142-1156.
[7] E. van Lenthe, A. Ehlers, E.-J. Baerends, Geometry optimizations in the zero order regular approximation for relativistic effects, The Journal of Chemical Physics, 110 (1999) 8943-8953.
[8] E. van Lenthe, J.G. Snijders, E.J. Baerends, The zero-order regular approximation for relativistic effects: The effect of spin–orbit coupling in closed shell molecules, The Journal of Chemical Physics, 105 (1996) 6505-6516.
[9] S.K. Wolff, Analytical second derivatives in the Amsterdam density functional package, International Journal of Quantum Chemistry, 104 (2005) 645-659.
[10] A. Bérces, R.M. Dickson, L. Fan, H. Jacobsen, D. Swerhone, T. Ziegler, An implementation of the coupled perturbed Kohn-Sham equations: perturbation due to nuclear displacements, Computer Physics Communications, 100 (1997) 247-262.
[11] H. Jacobsen, A. Bérces, D.P. Swerhone, T. Ziegler, Analytic second derivatives of molecular energies: a density functional implementation, Computer Physics Communications, 100 (1997) 263-276.
[12] A. Rosa, E.J. Baerends, S.J.A. van Gisbergen, E. van Lenthe, J.A. Groeneveld, J.G. Snijders, Electronic Spectra of M(CO)6 (M = Cr, Mo, W) Revisited by a Relativistic TDDFT Approach, Journal of the American Chemical Society, 121 (1999) 10356-10365.
[13] S.J.A. van Gisbergen, J.G. Snijders, E.J. Baerends, Implementation of time-dependent density functional response equations, Computer Physics Communications, 118 (1999) 119-138.
[14] R. Rüger, E. van Lenthe, T. Heine, L. Visscher, Tight-binding approximations to time-dependent density functional theory — A fast approach for the calculation of electronically excited states, The Journal of Chemical Physics, 144 (2016) 184103.
[15] F.R.L. A. D. Adler, J. D. Finarelli, J. Goldmacher, J. Assour and L. Korsakoff, A Simplified Synthesis for meso-Tetraphenylporphin, J. Org. Chem., 32 (1967) 476.
[16] N. Swamy, D.A. James, S.C. Mohr, R.N. Hanson, R. Ray, An estradiol-porphyrin conjugate selectively localizes into estrogen receptor-positive breast cancer cells, Bioorganic & medicinal chemistry, 10 (2002) 3237-3243.
[17] R. Luguya, L. Jaquinod, F.R. Fronczek, M.G.H. Vicente, K.M. Smith, Synthesis and reactions of meso-(p-nitrophenyl)porphyrins, Tetrahedron, 60 (2004) 2757-2763.
[18] R. Dondi, E. Yaghini, K.M. Tewari, L. Wang, F. Giuntini, M. Loizidou, A.J. MacRobert, I.M. Eggleston, Flexible synthesis of cationic peptide-porphyrin derivatives for light-triggered drug delivery and photodynamic therapy, Organic & biomolecular chemistry, 14 (2016) 11488-11501.
[19] M. Balaz, A.E. Holmes, M. Benedetti, G. Proni, N. Berova, Porphyrin substituted phosphoramidites: new building blocks for porphyrin-oligonucleotide syntheses, Bioorganic & medicinal chemistry, 13 (2005) 2413-2421.
[20] M.P. Hay, W.R. Wilson, J.W. Moselen, B.D. Palmer, W.A. Denny, Hypoxia-selective antitumor agents. 8. Bis(nitroimidazolyl)alkanecarboxamides: a new class of hypoxia-selective cytotoxins and hypoxic cell radiosensitisers, Journal of medicinal chemistry, 37 (1994) 381-391.
[21] P.E. Fields, T.F. Gajewski, F.W. Fitch, Blocked Ras activation in anergic CD4+ T cells, Science, 271 (1996) 1276-1278.

[22] V.S. Gaware, M. Hakerud, K. Leosson, S. Jonsdottir, A. Hogset, K. Berg, M. Masson, Tetraphenylporphyrin tethered chitosan based carriers for photochemical transfection, Journal of medicinal chemistry, 56 (2013) 807-819.
[23] K.K. Pasunooti, J.-L. Song, H. Chai, P. Amaladass, W.-Q. Deng, X.-W. Liu, Synthesis, characterization and application of trans-D–B–A-porphyrin based dyes in dye-sensitized solar cells, Journal of Photochemistry and Photobiology A: Chemistry, 218 (2011) 219-225.
[24] M. Balaz, A.E. Holmes, M. Benedetti, G. Proni, N. Berova, Porphyrin substituted phosphoramidites: new building blocks for porphyrin-oligonucleotide syntheses, Bioorg. Med. Chem., 13 (2005) 2413-2421.
[25] I. Chambrier, C. Banerjee, S. Remiro-Buenamanana, Y. Chao, A.N. Cammidge, M. Bochmann, Synthesis of Porphyrin-CdSe Quantum Dot Assemblies: Controlling Ligand Binding by Substituent Effects, Inorganic chemistry, 54 (2015) 7368-7380.
[26] E. Barragán, B. Gordillo, G. Vargas, L. Velazco, The role of cobalt, copper, nickel, and zinc in the DNA replication inhibitory activity ofp-aminophenyl triphenylporphyrin, Applied Organometallic Chemistry, 18 (2004) 311-317.
[27] C. Wang, C.C. Wamser, NMR Study of Hyperporphyrin Effects in the Protonations of Porphyrins with 4-Aminophenyl and 4-Pyridyl Meso Substituents, The Journal of organic chemistry, 80 (2015) 7351-7359.
[28] J.P. Tome, M.G. Neves, A.C. Tome, J.A. Cavaleiro, M. Soncin, M. Magaraggia, S. Ferro, G. Jori, Synthesis and antibacterial activity of new poly-S-lysine-porphyrin conjugates, Journal of medicinal chemistry, 47 (2004) 6649-6652.
[29] S. Monge, J. Selambarom, J.P. Roque, A.A. Pavia, Synthesis of precursors of iodine-labeled multifunctional ligands containing 2-nitroimidazole for the detection of hypoxic tissues and/or tumors, Tetrahedron, 57 (2001) 9979-9987.
[30] M. Ma, L. Peng, C. Li, X. Zhang, J. Wang, Highly stereoselective [2,3]-sigmatropic rearrangement of sulfur ylide generated through Cu(I) carbene and sulfides, Journal of the American Chemical Society, 127 (2005) 15016-15017.
[31] Z. Li, T. Chu, X. Liu, X. Wang, Synthesis and in vitro and in vivo evaluation of three radioiodinated nitroimidazole analogues as tumor hypoxia markers, Nucl. Med. Biol., 32 (2005) 225-231.
[32] J.C. Roberts, S.L. Newmyer, J.A. Mercer-Smith, S.A. Schreyer, D.K. Lavallee, Labeling antibodies with copper radionuclides using N-4-nitrobenzyl-5-(4-carboxyphenyl)-10,15,20-tris(4-sulfophenyl) porphine, International journal of radiation applications and instrumentation. Part A, Applied radiation and isotopes, 40 (1989) 775-781.
[33] M.K. Bhalgat, J.C. Roberts, J.A. Mercer-Smith, B.D. Knotts, R.L. Vessella, D.K. Lavallee, Preparation and biodistribution of copper-67-labeled porphyrins and porphyrin-A6H immunoconjugates, Nuclear medicine and biology, 24 (1997) 179-185.
[34] D.K.W. Lavallee, A.; Diaz, A.; Battioni, J. P.; Mansuy, D., Efficient metalloporphyrin synthesis under mild conditions using *N*-benzyl porphyrins, Tetrahedron Lett., 217 (1986) 3521.
[35] D.K.M. Lavallee, D.; Battioni, J. P. , Research Corp. Technologies, Inc., USA, Application: US, (1988).
[36] C.H. Bedel-Cloutour, L. Mauclaire, A. Saux, M. Pereyre, Syntheses of functionalized indium porphyrins for monoclonal antibody labeling, Bioconjugate chemistry, 7 (1996) 617-627.
[37] J.C. Roberts, Y.E. Adams, D. Tomalia, J.A. Mercer-Smith, D.K. Lavallee, Using starburst dendrimers as linker molecules to radiolabel antibodies, Bioconjugate chemistry, 1 (1990) 305-308.
[38] M. Gandelman, K.M. Naing, B. Rybtchinski, E. Poverenov, Y. Ben-David, N. Ashkenazi, R.M. Gauvin, D. Milstein, A general method for preparation of metal carbenes via solution- and polymer-based approaches, Journal of the American Chemical Society, 127 (2005) 15265-15272.
[39] B. Le Guennic, D. Jacquemin, Taking Up the Cyanine Challenge with Quantum Tools, Accounts of Chemical Research, 48 (2015) 530-537.
[40] R.V. Belosludov, D. Nevonen, H.M. Rhoda, J.R. Sabin, V.N. Nemykin, Simultaneous Prediction of the Energies of Qx and Qy Bands and Intramolecular Charge-Transfer Transitions in Benzoannulated and Non-Peripherally Substituted Metal-Free Phthalocyanines and Their Analogues: No Standard TDDFT Silver Bullet Yet, The Journal of Physical Chemistry A, 123 (2019) 132-152.

[41] E. Hasegawa, J.-I. Nemoto, T. Kanayama, E. Tsuchida, Syntheses and properties of vinyl monomers containing a meso-tetraphenylporphin ring and their copolymers, European Polymer Journal, 14 (1978) 123-127.
[42] J.-I.N. E. Hasegawa, T. Kanayama and E. Tsuchida, Synthesis of a new iron(III) porphyrin acrylate-styrene copolymer and its catalysis for hydroxylation of cyclohexane, European Polymer Journal, 14 (1978) 123-127

[43] W.A. Siddiqui, S. Ahmad, H.L. Siddiqui, T. Hussain, M. Parvez, Synthesis and Crystal Structures of o-[(Phenyl/p-methoxyphenyl)carbamoyl]benzene Sulfonamides, Journal of Chemical Crystallography, 40 (2010) 116-121.